Synthesis, Structural, and Catalytic Studies of Palladium Amino Acid Complexes

David Bruce Hobart, Jr.

Dissertation submitted to the faculty of the Virginia Polytechnic Institute and State University in

partial fulfillment of the requirements for the degree of

Doctor of Philosophy

In

Chemistry

Joseph S. Merola

Paul A. Deck

Brian E. Hanson

Gary L. Long

Blacksburg, VA

Synthesis, Structural, and Catalytic Studies of Palladium Amino Acid Complexes

David Bruce Hobart, Jr.

ABSTRACT

Palladium(II) acetate and palladium(II) chloride react with amino acids in acetone/water to yield *cis* or *trans* square planar bis-chelated palladium amino acid complexes. The naturally occurring amino acids and some *N*-alkylated and substituted derivatives and homologs were evaluated as ligands. Thirty-eight amino acids in total were investigated as ligands. The formation of aquo complexes in water was observed and studied by ^{13}C NMR spectroscopy and modeled by DFT calculations. Each class of amino acid ligand is catalytically active with respect to the oxidative coupling of olefins and phenylboronic acids. Some enantioselectivity is observed and the formation of products not reported in other Pd(II) oxidative couplings is seen. Both activated and non-activated alkenes were oxidatively coupled to phenylboronic acids incorporating both electron-donating and electron-withdrawing groups. The crystal structures of nineteen catalyst complexes were obtained. The extended lattice structures arise from N-H••O or O••(HOH)••O hydrogen bonding. NMR, HRMS, FTIR, single crystal XRD, and powder XRD data are evaluated.

Acknowledgements

The very first person I want to acknowledge is my wife Mary. Without her love and support I would not be writing this, plain and simple. She took a chance and embarked on this crazy journey with me, pushing, prodding, and sometimes likely wanting to knock some sense into me and I simply wouldn't have been able to complete this without her. I really don't think there are words in any language that could adequately express my love, respect, gratitude, and admiration for her. To my sons, Tyler and Ethan, this is as much for you as it is for me, in the hopes that you'll see anyone can do anything they put their mind to.

There's a long list of immediate family I owe a debt of gratitude to as well for their support. My mom, Jane, and dad, Bruce - I love you. Thanks for your unconditional love and support these 45 years, and hopefully a lot more! Ann, Mike, and Clemens, my "second" parents, ditto to you. To my sister Amy and sister- and brothers-in-law Dawn, Mark and Patrick, I doubt you think you did much but believe me, you did. Thank you all for sticking by me through thick and thin.

Joe Merola, how can I ever thank you enough for taking a chance on a 38 year old grad student and giving me a chance to chase a dream? I'll spend the rest of my life paying that one back! To the rest of my committee, thanks for doing your best to turn me into a real scientist. Paul, for trying, and maybe even succeeding in getting me to write better. Brian, I'll bet most of our conversations probably seemed pretty innocuous to you but they always got me thinking about things in a way I hadn't before. Gary, you were a calm voice of reason and a great sounding board. I appreciate all of you more than you know. Karen Brewer, I wish you were still here to be my "committee mom".

TABLE OF CONTENTS

Chapter 1. Background and Literature Review

The study of transition metal complexes containing ligand sets that are biologically relevant is an area that is rapidly expanding. Biologically relevant ligands include such species as amino acids, peptides, and other inorganics (chloride ion, nitrous oxide, etc.). These types of complexes show a variety of potentially useful properties, from catalysis[1-9] to anti-cancer[10-102] and anti-microbial[103-140] activity. This dissertation describes the synthesis and structural chemistry of bis(amino acid) complexes of palladium. Potential catalytic, anti-microbial, and anti-cancer properties of these compounds are described.

1.1   Abbreviations Used Herein

NMG	*N*-methylglycine
DMG	*N,N*-dimethylglycine
PBA	Phenylboronic acid
CF$_3$-PBA	4-(trifluoromethyl)phenylboronic acid
OCH$_3$-PBA	4-(methoxy)phenylboronic acid
MT	Methyl tiglate

Table 1. Abbreviations

1.2 Mono-(Amino Acid) Complexes of Pd(II)

The simplest of the mono-amino acid complexes of palladium is $K[Pd(NH_2CH_2COO)Cl_2]$ (Figure 1) reported by Baidina.[141] This complex contains one (*N,O*) chelated glycine ligand, with chloride ligands occupying the remaining two coordination sites. The complex is prepared by reacting 1 equivalent of glycine with K_2PdCl_4 and a stoichiometric amount of base. The crystal structure was determined, with the complex crystallizing in the *Pbca* space group. Bond lengths and angles were as expected for a square planar complex. No other chemical data was presented for the compound.
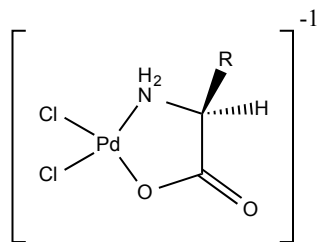
Figure 1. General structure of a mono-(amino acid) Pd(II) anion.

Mono-(alanine) complexes reported by Chernova show both (*N,O*) chelated and monodentate amino acid ligand coordination.[142] The dichloride and dibromide complexes, $K[Pd(NH_2CH(CH_3)COO)Cl_2]$ and $K[Pd(NH_2CH(CH_3)COO)Br_2]$, are identical in structure to the corresponding glycine complex reported by Baidina. The $Pd(NH_2CH(CH_3)COOH)_2Cl_2$ complex was prepared by treating Pd(II) chloride with a two-fold excess of alanine.

Vicol has prepared $K[Pd(Ala)Cl_2]$ and $K[Pd(Pro)Cl_2]$ as precursors to ternary Pd(II) amino acid complexes.[143,144] Ternary complexes are those in which two different amino acid ligands are coordinated to the metal and will be discussed later in this section.

McAuliffe[145] and Warren[146] have prepared the mono-chelated methionine palladium dichloride complex (Figure 2). Methionine coordinates in a bidentate (*S,N*) fashion through the thioether sulfur atom and amine nitrogen forming a six-membered chelate ring. Infrared spectroscopy shows a lower stretching frequency for the amine group, 3100-3250 cm^{-1} versus 3270-3410 cm^{-1} for the uncoordinated methionate. The carbonyl stretching vibration at 1720 cm^{-1} was given as evidence of non-coordination of the carboxylate group. Coordinated carboxylates typically show an asymmetric carbonyl stretch at 1580-1660 cm^{-1}.[145] The crystal structure was solved by Warren and clearly shows that chelation occurs through the sulfur and nitrogen atoms. Dimerization is noted to occur through intermolecular hydrogen bonding between the carboxyl groups.
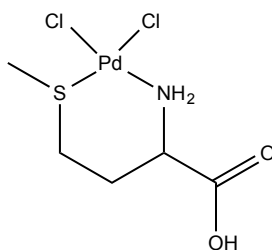
Figure 2. Dichloro-DL-methioninepalladium(II).

Two additional sulfur containing amino acids have been used to prepared mono-amino acid chelated palladium complexes. DL-Ethionine and S-methyl-L-cysteine complexes of palladium (Figure 3) were prepared.[147] Once again chelation was noted to occur in a bidentate fashion through the sulfur and nitrogen atoms. Infrared bands from 385-378 cm^{-1} were attributed to Pd-S stretching vibrations. As noted above, the carbonyl stretching frequency at 1737-1703 cm^{-1} indicates that the carboxylate group is not coordinated.
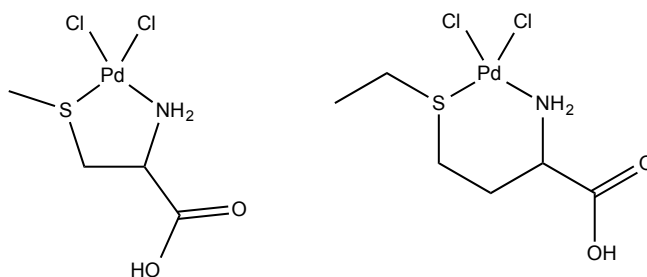
Figure 3. Pd(II) complexes of S-methyl-L-cysteine (left) and DL-ethionine (right).

1.3 Bis(Amino Acid) Complexes of Pd(II)

Unless otherwise noted, all bis(amino acid) complexes reported herein were synthesized according to the following general reaction scheme (Figure 4):
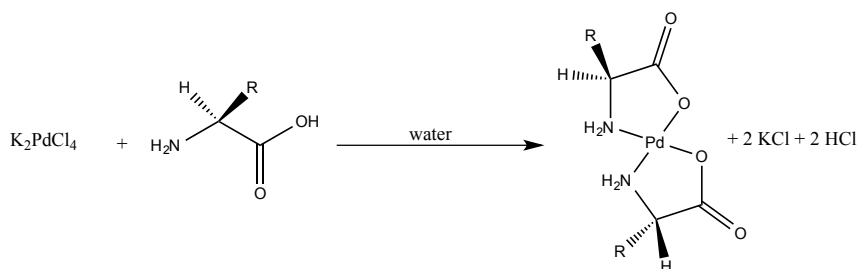
Figure 4. General reaction scheme for bis(amino acid) Pd(II) complexes. Note that the formation of *cis* or *trans* isomers is possible.

Baidina has reported the crystal structure of *cis*-Pd(Gly)$_2$. This complex crystallizes in the *C2/c* space group. No structural irregularities were noted, with the amine protons of one molecule hydrogen bonded to the carboxyl group of an adjacent molecule. Shestakova has reported the powder diffraction spectra of both *cis* and *trans* isomers of Pd(Gly)$_2$ (Figure 5), showing that they are different and represent differing crystallographic habits.[148]
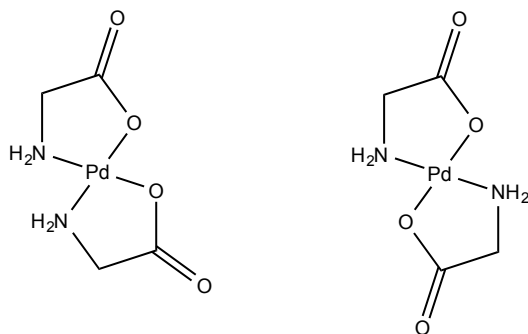
Figure 5. *Cis* and *Trans* isomers of Pd(Gly)$_2$.

In infrared spectral measurements of aqueous solutions of metal-amino acid chelates, Nakamoto[149] observed that the asymmetric carbonyl stretch of *trans*-Pd(Gly)$_2$ increased and the symmetric carbonyl stretch decreased in frequency as compared to glycine. This was taken as evidence of chelation of the carboxylate group, however no synthetic details or other explanation were given to account for their assignment of the *trans* isomer.

The crystal structure of *cis*-Pd(Val)$_2$ was reported[150] (Figure 6) with the molecule crystallizing in the P2$_1$2$_1$2$_1$ space group. Hydrogen atom positions were not determined, thus no intermolecular hydrogen bonding data are presented. The molecule is slightly distorted square planar, with N-Pd-O bond angles of ~83 degrees and O-Pd-O and N-Pd-N bond angles of ~96 degrees. The isopropyl side chains on the amino acid ligands lie above and below the square plane.
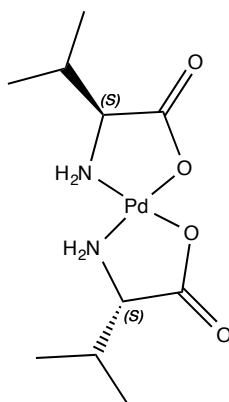
Figure 6. *Cis*-**Pd(Val)₂.**

The complex *cis*-Pd(Ser)$_2$ (Figure 7) was reported as a possible antitumor candidate by Vagg.[151] The crystal structure shows the compound to belong to the P2$_1$2$_1$2$_1$ space group. The molecular geometry is an irregular square planar arrangement with a small tetrahedral distortion at the chiral carbon of one of the ligands. The O-Pd-O bond angle of 94.2 degrees is significantly smaller than the N-Pd-N bond angle of 100.2 degrees, likely due to steric repulsion of the *cis* amine groups. Additionally, one of the amino acid ligands is essentially planar while the other is distorted from planarity. Intermolecular hydrogen bonding is quite evident in the molecule, with the four amine protons hydrogen bonded to three carboxylate and one hydroxyl oxygen atom on adjacent molecules and each hydroxyl proton hydrogen bonded to one carboxylate oxygen on adjacent molecules.
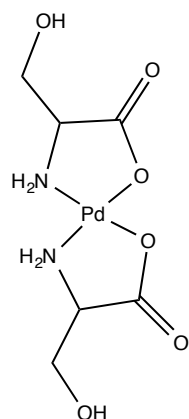
Figure 7. *Cis*-**Pd(Ser)$_2$.**

The bis-tyrosine palladium(II) complex has been reported[152] (Figure 8) and shows an interesting direct metal-side chain interaction. The compound exists in the *cis* conformation and crystallizes in the P2$_1$ space group. The phenol ring of one of the tyrosine ligands is directed in towards the metal center and lies in a plane parallel to the chelate plane. The other phenol ring of the second ligand is directed away from the metal center, however it does lie very close to the metal center of the adjacent molecule. The authors propose[153-155] that the aromatic ring in the tyrosine side chain appears to have some favorable interaction with the empty axial d-orbitals of the metal center that results in stabilization of this geometry.
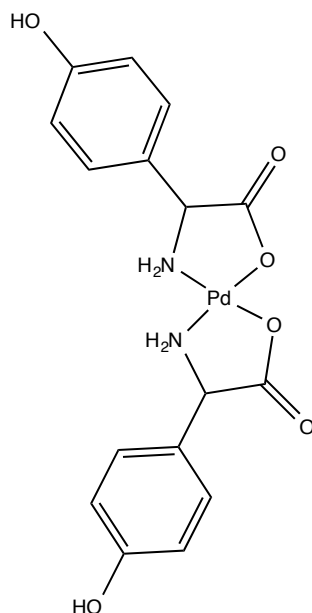
Figure 8. *Cis*-**Pd(Tyr)₂.**

A second bis-tyrosine palladium(II) crystal structure was reported by Jarzab[156], where there was no evidence of the metal-side chain interaction. This structure also crystallized in the $P2_1$ space group with *cis* square planar geometry. Unfortunately, no detailed synthetic details or crystallization parameters were given that may account for the two different crystal structures reported by these different groups.

Proline is an amino acid with the amine functionality contained in a five-membered ring. The bis(prolinato)palladium(II) complex (Figure 9) was first reported by Ito.[157] The compound forms with a *cis* arrangement of the amine groups and crystallizes in the $B22_12$ space group. The pyrrolidine rings of the ligands are arranged such that one is above and one is below the square plane of the complex. The rings are also puckered, with four of the five atoms lying in a plane while the fifth is bent out of the plane. Hydrogen bonding is evident. The amine proton is hydrogen bonded to the carboxyl oxygen of the adjacent molecule, resulting in parallel layers.
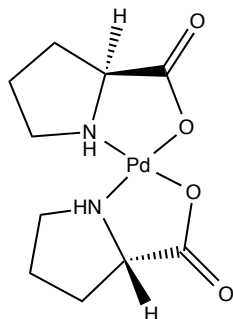
Figure 9. *Cis*-**Pd(Pro)$_2$.**

Chernova[158] has reported the crystal structure of bis(histidinato)Pd(II) (Figure 10). Histidine is unique in that it has both an imidazole ring and the possibility of coordination through any of three coordination sites: the amine group, the carboxylate group, and the nitrogen atom in the 3-position of the imidazole ring.
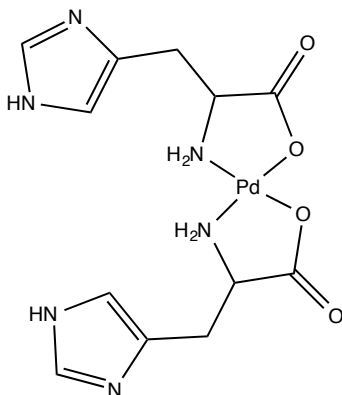
Figure 10. Proposed structure for bis-Pd(His)$_2$.

The complex was prepared by reacting PdCl$_2$ with two equivalents each of histidine and NaOH. Elemental analysis confirms the composition to be [Pd(His)$_2$]. Infrared spectroscopy was utilized to deduce the coordination geometry, however the data are not convincing. The lack of a strong absorption for the non-ionized carboxylate group would tend to indicate that the carboxyl group is ionized and is involved as one of the coordination sites. If this is the case, then the

amine nitrogen is likely the other coordination site, as coordination through either of the imidazole nitrogens would result in a seven or eight membered chelate ring.

A seven membered chelate ring is observed in bis(ornithinato)Pd(II) (Figure 11). Ornithine is an arginine derivative wherein the guanidinium group is replaced with an amino group. Nakayama[159] prepared bis(ornithinato)Pd(II) and obtained the crystal structure. In this case coordination to the metal is through both nitrogen atoms. The compound crystallizes in the $P2_12_12_1$ space group.
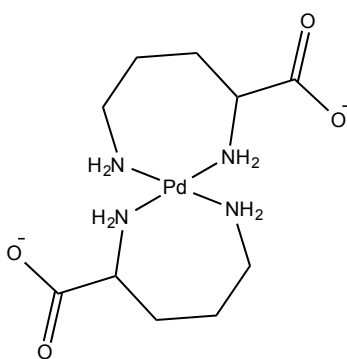
Figure 11. Bis(ornithinato)Pd(II), a unique seven membered chelate ring.

Bis(DL-isovaline)Pd(II) (Figure 12) was prepared by Boudreau and characterized by infrared spectroscopy.[160] Elemental analysis confirmed the composition of the complex. In an attempt to determine the stereochemistry of the complex, infrared absorption bands were analyzed. The asymmetric carboxylate stretch shifts to higher frequency while the symmetric stretch shifts to lower frequency, indicating that the carboxylate group is involved in chelation. The amine stretch similarly moves to higher frequency as compared to the unbound ligand, indicating coordination through the amine group. A band at 446 cm^{-1} is assigned to a Pd-N asymmetric stretch, and the lack of a symmetric stretch in this region leads the author to

conclude that the coordination geometry is *trans*. This does not seem unreasonable as steric hindrance may prevent formation of the *cis* isomer.
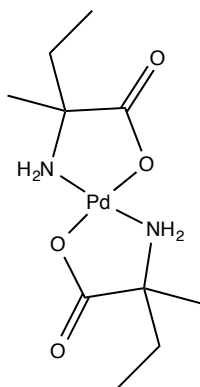
Figure 12. *Trans*-**Pd(isovalinate)₂.**

Amino acid amides are amino acids that have replaced the hydroxyl group of the carboxylic acid with an amine. Komorita[161,162] has prepared and characterized several bis(amino acid amide) palladium complexes (Figure 13) , including: *trans*-bis(glycine-amidato)Pd(II), *trans*-bis(L-alanine-amidato)Pd(II), *cis*-bis(L-alanine-amidato)Pd(II), *trans*-bis(L-leucine-amidato)Pd(II), and *cis*-bis(L-leucine-amidato)Pd(II). These amino acid amide complexes were prepared by stirring 1 equivalent of either palladium(II) chloride or potassium tetrachloropalladate(II) in water followed by addition of 2 equivalents of the amino acid amide. The products were a mixture of *cis* and *trans* isomers that were further separated by fractional crystallization from methanol/ether.
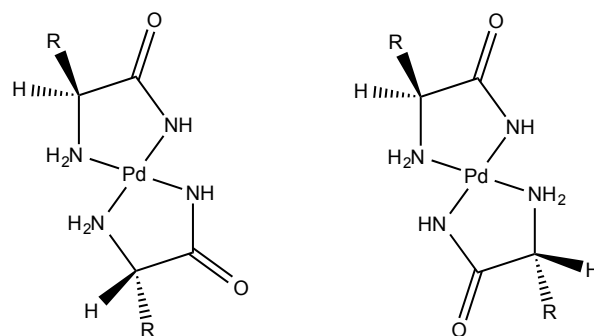
Figure 13. *Cis* (left) and *Trans* (right) isomers of a bis(amino acid amide) complex of Pd(II).

The circular dichroism (CD) spectra of the bis(amino acid amide) complexes were compared with the CD spectra of similar coordination compounds of known stereochemistry. In the case of *cis* stereochemistry there are four CD bands observed. The *trans* compounds show only three CD bands, and from these correlations the stereochemistry of the bis(amino acid amide) complexes was assigned. Infrared spectra were also obtained on these complexes. The intense carbonyl stretching band observed at about 1600 cm^{-1} indicated that coordination occurs through both nitrogen atoms and that the amide was not hydrolyzed during synthesis/workup.

1.4   Ternary Amino Acid Complexes of Pd(II)

Ternary (from the Latin *ternarius*, "composed of three items") amino acid complexes refer to those complexes in which the two chelated amino acid ligands are different, and both are coordinated to the same metal center (Figure 14).
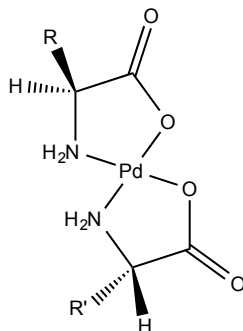
Figure 14. General structure of a ternary amino acid Pd(II) complex.

Three unique complexes of palladium with glycine ligands were reported by Shestakova.[163] In these complexes glycine was used as both a monodentate and chelating ligand. K[Pd(*N*-Gly)$_3$(H$_2$O)], K[Pd(*N*-Gly)$_2$(*N,O*-Gly)] and K$_2$[Pd$_2$(*N*-Gly)$_6$] were isolated. Infrared spectroscopy was used to identify the coordinated and non-coordinated carboxylate groups, with elemental analysis confirming the stoichiometry of the compounds. These compounds were prepared from a water solution of K$_2$PdCl$_4$, 1 M KOH, and glycine in a 1:4:4 molar ratio. Addition of 2 mol of HCl, cooling to 0 °C and filtering yielded K[Pd(*N*-Gly)$_3$(H$_2$O)]. Acetone was added to the remaining mother liquor, and K[Pd(*N*-Gly)$_2$(*N,O*-Gly)] was precipitated and filtered. Finally dimethylglyoxime was added and K$_2$[Pd$_2$(*N*-Gly)$_6$] was isolated.

Baidina also reported a ternary glycine complex of palladium, *trans*-[Pd(Gly)(GlyH)Cl] in which the nitrogen atom of the non-chelated glycine is *trans* to the (*N,O*) chelated glycine nitrogen atom.[164] The crystal structure was determined, clearly showing the arrangement of the amino acid ligands around the metal center.

Following on to their previously discussed mono-amino acid complexes, Vicol has synthesized [Pd(Ala)(Gly)], [Pd(Ala)(Val)], [Pd(Ala)(Pro)], and [Pd(Pro)(Val)].[165] The mono-coordinated complex is reacted with one equivalent of the second amino acid to yield the ternary

13

complexes. Elemental analysis confirms the composition of the complexes. Shifts in the IR spectra of these complexes confirm that chelation occurs through the carboxylate and amine moieties resulting in the formation of five-membered rings. UV-Vis spectroscopy was utilized to study the $d \rightarrow d$ transitions of these compounds, yielding the conclusion that they are indeed square planar d^8 complexes.[166]

Sullivan prepared dipeptide complexes of palladium and examined the CD spectra of each.[167] Complexes were synthesized by $CsCO_3$ neutralization of a solution containing a 1:1 molar ratio of $PdCl_2$ and either (Gly-S-Ala) or (S-AlaGly). Precipitation and recrystallization from ethanol, acetone and water yielded Cs[Pd(Gly-S-Ala)Cl] and Cs[Pd(S-AlaGly)Cl] respectively. The circular dichroism spectra show three spin-allowed circular dichroism bands corresponding to the A and E electronic transitions. The circular dichroism spectra showed remarkable consistency between the complexes, and the authors note that the use of circular dichroism to investigate metal coordination in chiral metal compounds required extreme caution.

1.5 Hydrogen Bonding Interactions of Pd(II) Amino Acid Complexes

There is comparatively little information in the open literature regarding the intermolecular hydrogen bonding of bis(amino acid)palladium(II) complexes. Yamauchi[168] has studied the ligand-ligand interactions of ternary amino acid complexes of palladium by circular dichroism and ^{1}H NMR spectroscopy. They report that the circular dichroism $\Delta\varepsilon$ values for these compounds are additive with respect to the individual $\Delta\varepsilon$ values for the component amino acids. These values can be calculated and the observed differences between $\Delta\varepsilon_{meas}-\Delta\varepsilon_{calc}$ are indicative

14

of the degree of ligand-ligand interaction. Examining the ^{1}H NMR coupling constants also

yields data on ligand-ligand interactions. There are three staggered rotational isomers about each

C_α-C_β bond (Figure 15). If hydrogen bonding interactions are present, there should be a preferred

conformation which can be predicted based on the coupling constants.
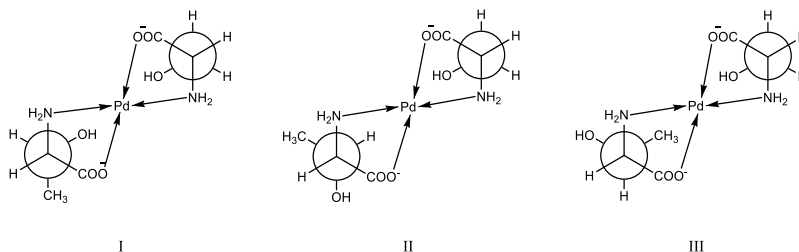
Figure 15. Newman projections of the three rotational isomers of a hypothetical Pd(Ser)(Thr) complex.

Odani[169] used similar analyses to determine the hydrogen bonding interactions between

palladium complexes of histidine with glycine, alanine, valine, serine, threonine, homoserine,

asparagine, or glutamine as the second amino acid ligand. The observed differences in $\Delta\varepsilon_{meas}$-

$\Delta\varepsilon_{calc}$ for histidinate complexes with a non-polar secondary amino acid ligand (glycine, alanine,

valine) are small, indicating that side chain interactions are small. On the other hand, $\Delta\varepsilon_{meas}$-

$\Delta\varepsilon_{calc}$ differences for polar side-chain amino acid ligands (serine, threonine, homoserine,

asparagine, glutamine) are larger, indicating that side chain interactions between the histidine

carboxylate and the amine or hydroxyl groups of the secondary amino acid ligand are present. If

L-histidine methyl ester is substituted in these complexes for histidine, the carboxylate group is

then blocked from participating in ligand-ligand interactions and the $\Delta\varepsilon_{meas}$-$\Delta\varepsilon_{calc}$ differences are

again small. This is taken as direct evidence that the carboxylate group is involved in the ligand-

ligand interactions and that these interactions are responsible for the magnitude of the differences seen in $\Delta\varepsilon$.

1.6   Biological Activity of Pd(II) Amino Acid Complexes

Cisplatin (*cis*-diamminedichloroplatinum(II)) has long been regarded as one of the best anti-tumor compounds available. There is considerable interest in determining if analogous palladium complexes might provide similar anti-tumor[10-64,66-102] or antimicrobial[103-140] activity, with well over 100 peer-reviewed papers published in the scientific literature in the last 5 years alone.

With respect to Pd(II)-amino acid complexes in particular, several examples from the literature show that these types of complexes are also active against a variety of microorganisms and cancer cell lines.[170] In 1977, Charleston reported the antitumor activity of several amino acid chelates of palladium. Induction of filamentous growth in E. coli was taken as a measure of antitumor activity, with the L-glutamic acid and L-serine complexes noted as more effective than the glycine complex.[171] Puthraya[172,173] prepared several ternary amino acid complexes with Pd(bipy)Cl$_2$ and tested their activities against L1210 lymphoid leukemic, P388 lymphocytic leukemic, Sarcoma 180, and Ehrlich ascites tumor cells, with ID50 values lower than those reported for cisplatin. This group has also studied similar compounds that utilize the phenanthroline ligand in place of bipyridine, with cisplatin-like activity against P388 lymphocytic cells reported for the [Pd(phen)(Gly)]$^+$ and [Pd(phen)(Val)]$^+$ complexes.[174] Also reporting on [Pd(phen)(AA)]$^+$ complexes is the Lin group.[175] They show antitumor activities against the S-180 animal tumor line for the [Pd(phen)(lys)]Cl, [Pd(phen)(arg)]Cl and

[Ph(phen)(pro)]Cl complexes. Paul[176] reports the synthesis, cytotoxicity, and DNA binding ability of [Pd(dipy)(Gly)]Cl and [Pd(dipy)(Ala)]Cl, where dipy is 2,2'-dipyridylamine. The complexes were tested for cytotoxicity against P388 lymphocytic leukemia cells. The alanine complex shows an ID_{50} value (10.5 μM) that is lower than that of cisplatin, however the ID_{50} value for the glycine complex (>100 μM) was higher than that of cisplatin. DNA binding studies were carried out using calf-thymus DNA. A decrease in the UV absorption maximum at 315 nm indicated binding of the complex to DNA. DNA binding is reversible and is therefore non-covalent in nature. Changing the ionic strength of the buffer medium results in recovery of the complex and implies that ionic and/or hydrogen bonding interactions are responsible for the DNA binding ability of these complexes. Diaminosuccinic acid and its diethyl ester derivative have been complexed with Pd(II) and the resulting compounds show anti-tumor activity.[177] Both complexes chelate to the metal center in a *cis* fashion with two chloride ligands. Structural characterization was carried out by X-ray crystallography. Anti-tumor activity was tested against MDA-MB468 (breast carcinoma) and HL-60 (leukemia) cancer cell lines. In both cases, the ID_{50} values for both complexes was approximately 4 μM (range 3.93 to 4.72 μM). Both complexes showed slightly better activity against the MDA-MB468 cell line. The proposed mechanism of action for these complexes is that they induce conformational changes in the DNA structure of the cell. The chemotherapeutic agent levamisole ((*S*)-6-Phenyl-2,3,5,6-tetrahydroimidazo[2,1-*b*][1,3]thiazole) has been used to prepare ternary Pd(II) complexes with L-alanine, L-phenylglycine, L-phenylalanine, L-valine, L-methionine, and L-proline.[178] The methionine and proline complexes were noted to induce new cell forms in *Saccharomyces cerevisiae* cells. Offiong has prepared palladium(II) complexes of glycine derivatized by imine formation with *o*-hydroxyacetophenones.[179] These complexes show powerful activity against

Ehrlich ascites tumor cells. Azomethines prepared by the condensation of 2-acetylfluorene and 4-acetylbiphenyl with glycine, alanine, valine, and leucine have been used as ligands for Pd(II) complexes and their antibacterial, antifungal, and insecticidal activities have been determined.[180] These complexes were active against both gram-positive and gram-negative bacteria as well as fungi from *Aspergillus*, *Fusarium*, and *Rhizopus* genera. Interestingly, these compounds also show insecticidal activity against *Helicoverpa armigera*, a major pest towards cotton. Amino acid dianions generated by tosylation of the amino acid amine terminus have been prepared by Li[181] and have shown cytotoxicity against HL-60, Bel-7402, BGC-823, and KB cell lines. The cytotoxicity of these compounds is less than that of cisplatin. Al-Fregi[182] has reported two amino acid Pd(II) chelates that shows significant antibacterial activity. The complexes, (cyclohexane-1,4-diyldimethanamine)Pd(II)glutamate and (cyclohexane-1,4-diyldimethanamine)Pd(II)aspartate were tested against eight gram positive bacterial strains. Both complexes showed cytotoxic activity, with the aspartate complex the better of the two. In both cases the amino acid ligand contains a dicarboxylic acid moiety and chelation to the metal center is via an (*O,O*) attachment. Minimum inhibitory concentrations were on the order of 500 µg/mL. The cell membranes of these bacteria contain mucopolysaccharides and proteins with a lesser amount of phospholipids, and the authors conclude that the cell wall makeup allows for enhanced permeability of the complexes into the cell.

1.7   Catalytic Activity of Palladium Complexes

Palladium-catalyzed C-C couplings are ubiquitous in modern synthetic chemistry, and there are many fine reviews describing both the significance and scope of these reactions.[1-9] The

2010 Nobel Prize in Chemistry was awarded to Heck, Nigishi, and Suzuki for their efforts in this area.[183] Some of the more significant examples are briefly discussed below.

The Heck[184] reaction (Figure 16) is the coupling of an aryl halide with an alkene to form a substituted alkene.
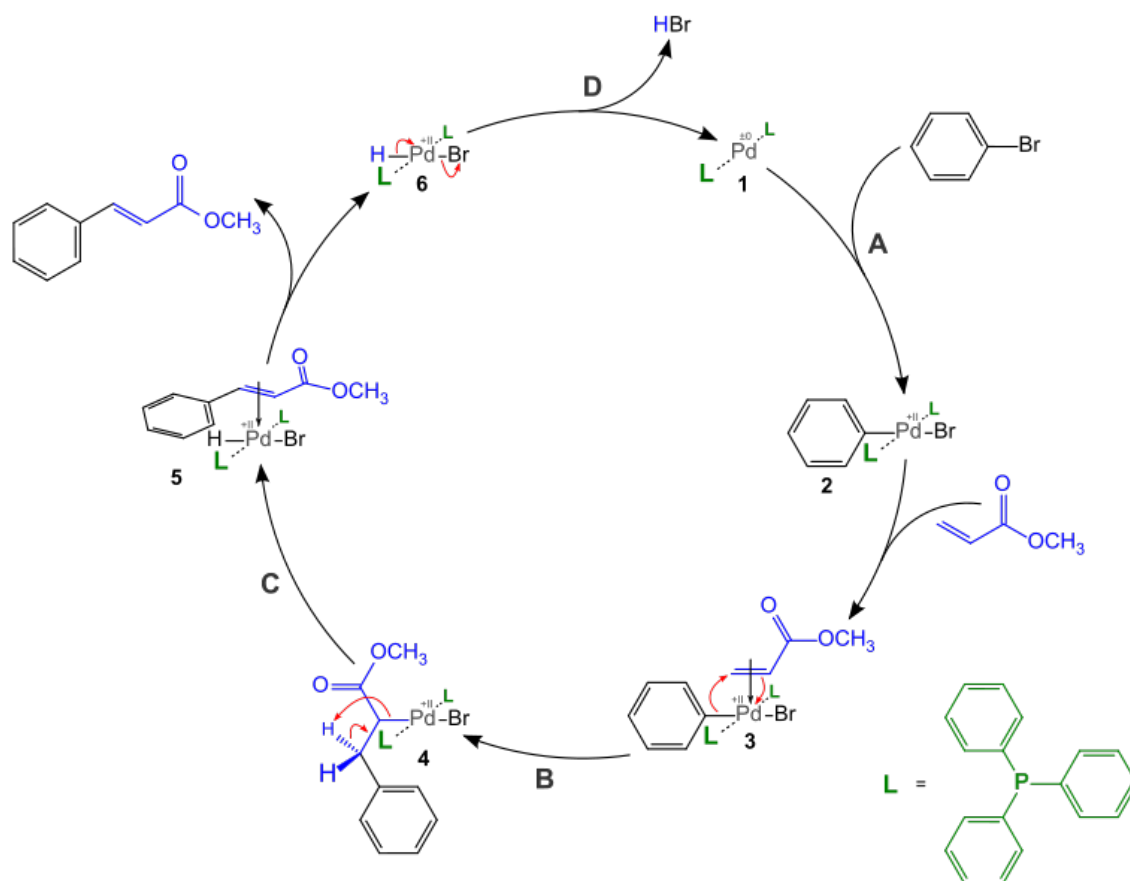
Figure 16. Mechanism of the Heck Reaction between bromobenzene and methyl acrylate. ["Heck Reaction Mechanism," Axel Müller, Wikimedia Commons, used under a CC BY 3.0 de. Retrieved from http://tinyurl.com/haqcgxs on 03/27/2016.]

The Heck reaction is stereoselective, with *trans* selectivity most commonly seen. The reaction is used in the synthesis of polymers, natural products, pharmaceuticals, and many asymmetric syntheses. Part of its versatility stems from the fact that the reaction is extremely tolerant to the presence of various functionalities on the substrate materials, such as amino, hydroxy, aldehyde, ketone, carboxy, ester, cyano and nitro groups.

The Suzuki[185] reaction (Figure 17) is similar to the Heck reaction, and is the coupling between an aryl- or vinyl-boronic acid with an aryl- or vinyl-halide.
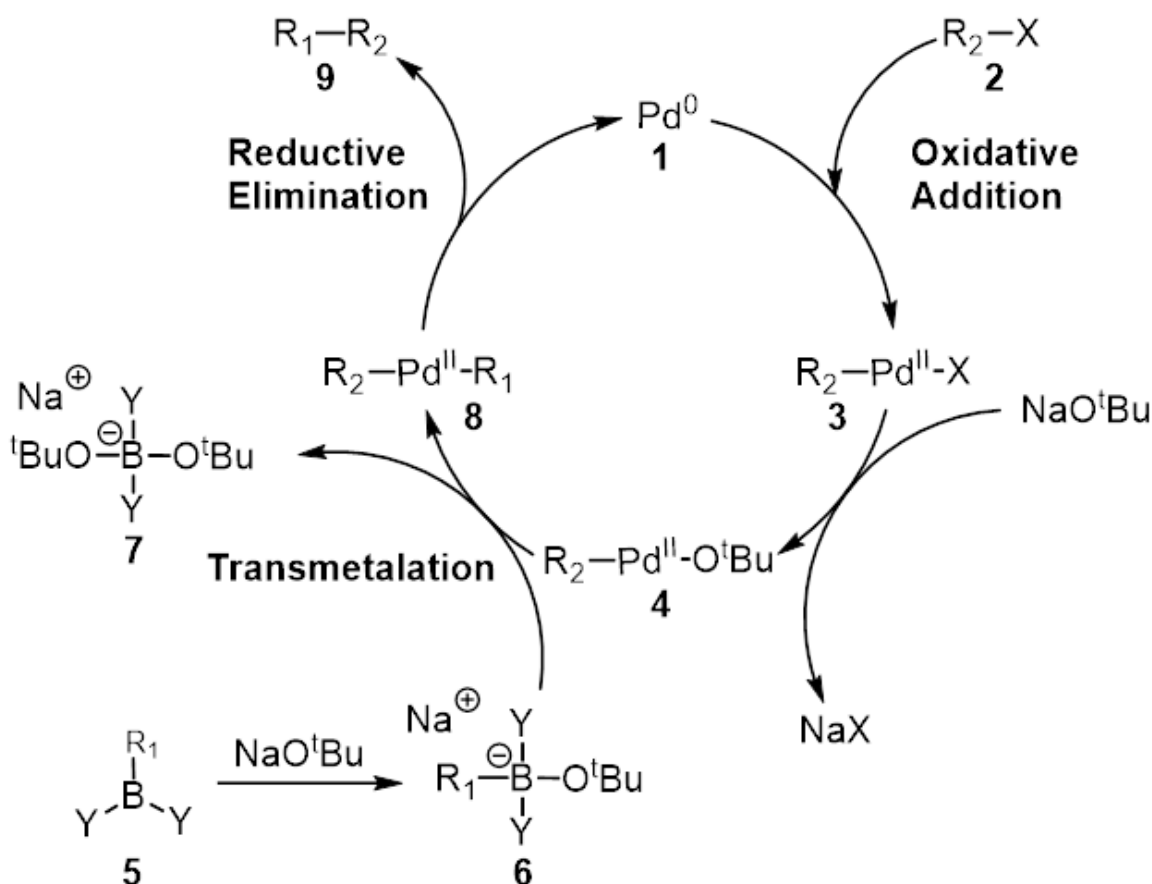
Figure 17. Mechanism of the Suzuki coupling reaction. ["Suzuki Coupling Full Mechanism 2," Wikimedia Commons, used under a CC BY-SA 3.0. Retrieved from http://tinyurl.com/jdqswk3 on 03/27/2016.]

The reaction is widely used to synthesize poly-olefins, styrenes, and substituted biphenyls, and has been extended to incorporate alkyl bromides. The reaction also works with triflates (OTf) instead of halides. Boronic esters and organotriflates may be used instead of boronic acids.

The Sonogashira[186] cross-coupling forms a carbon–carbon bond between a terminal alkyne and an aryl or vinyl halide, and differs from the above examples in that copper(I) iodide is used as a co-catalyst. It is amenable to mild conditions: room temperature, aqueous media, and

mild bases are not uncommon. It has been employed in pharmaceuticals, natural products, organic materials, and nanomaterials.

Some other less well-known palladium catalyzed cross couplings include the Stille[187] coupling of organohalides and organotin reagents, the Hiyama[188] coupling of organohalides and organosilicons, the Buchwald-Hartwig[189] amination, and the Heck-Matsuda[190] reaction of arenediazonium salts with alkenes.

1.7.1   Oxidative Coupling via Pd(II) Species

Oxidation reactions are some of the most utilized reactions in modern synthetic chemistry, and transition metal catalyzed oxidations are well known.[191] Palladium(II) oxidative catalysis is a growing field[191-196], and some of the more recent developments are discussed in this section.

Reactions such as the Heck, Suzuki, and Sonogashira couplings are known to proceed via Pd^0 species, with oxidative addition/reductive elimination yielding the desired products. Oxidative palladium(II) catalysis differs in that it utilizes molecular oxygen to regenerate the active catalyst in palladium(II) catalyzed coupling reactions. There are two proposed mechanisms for the catalytic cycle. In the first (Figure 18, Pathway A) reductive elimination of HX from complex **1** yields a Pd^0 species which is then oxidized by η^2-molecular oxygen. An initial protonation yields the Pd^{II} hydroperoxide species **4**, and a second protonation generates H_2O_2 and regenerates the catalyst. In the second proposed mechanism (Figure 18, Pathway B), molecular oxygen directly inserts into the palladium-hydride bond to generate the Pd^{II} hydroperoxide species **5**. Protonation again yields H_2O_2 and regenerates the catalyst. Note that

between the two proposed pathways, species **4** and **5** are indistinguishable, the difference between the two pathways being whether molecular oxygen inserts directly into a Pd-H bond or instead re-oxidizes the metal after a reductive elimination. Experimental evidence suggests that both pathways are possible and that the pathway observed for a catalytic system is dependent on catalyst structure and/or substrate conditions.[197-203]
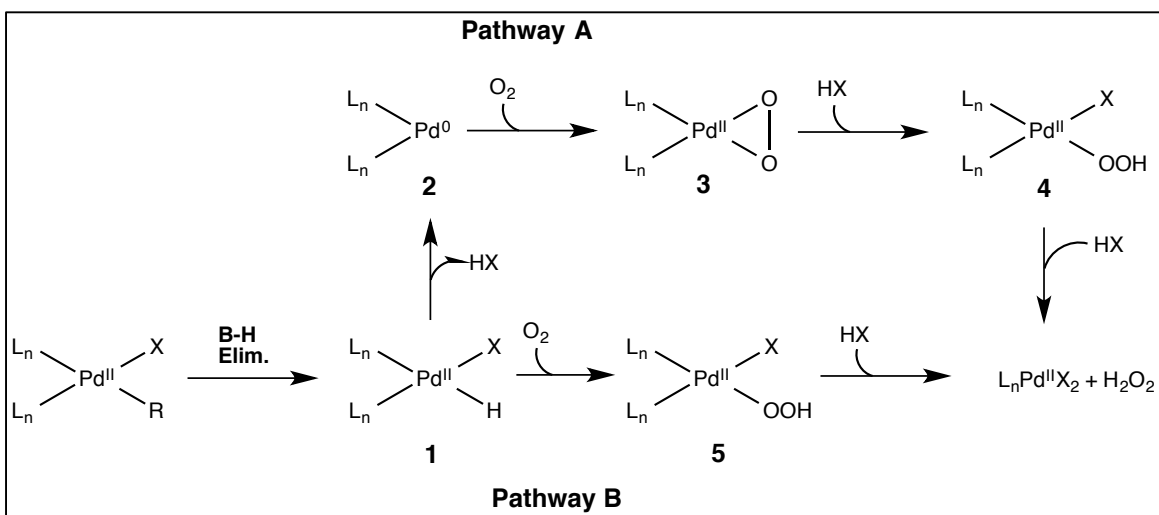
Figure 18. Proposed mechanistic pathways for Pd(II) oxidative catalysis.

There are many different types of coupling reactions noted to proceed via palladium(II) oxidative catalysis. There are hundreds of examples in the current literature of carbon-carbon[184,192,195,204-221], carbon-oxygen[222-229], carbon-nitrogen[229-237], carbon-sulfur[224,238,239] and carbon-phosphorous[8] couplings that are catalyzed by palladium(II) oxidative catalysis. These coupling reactions are used in the manufacture of many pharmaceuticals, natural products, fine chemicals, and polymers. In addition, palladium catalysts are known for their functional group tolerance, mild reaction conditions, and their low sensitivity to air and water. Pairing these advantages with an

abundant and easily accessible oxidant source shows the great utility and economic benefit that these systems can provide.

1.7.2 Base-free Heck-type Oxidative Coupling

Typical palladium-catalyzed cross-coupling reactions employ a base to facilitate the reaction. The role of the base is complex, with recent evidence suggesting that it is integral to several steps in the overall mechanism. Amatore[240] has shown that OH^- plays a positive role in the transmetalation step by formation of the reactive *trans*-$[ArPd(OH)(PPh_3)_2]$ species over the non-reactive *trans*-$[ArPdX(PPh_3)_2]$ intermediate. Hydroxide ion also promotes the reductive elimination of the biaryl product from $[PdL_2Ar_2]$. On the other hand, the presence of base can also have a negative impact on the cross-coupling of arylboronic acids. The Ar-$(B(OH)_3)^-$ anion is unreactive toward transmetalation, and as a result the base concentration must be carefully adjusted and controlled to balance the positive and negative influences on the overall reaction mechanism. Lima[241] found quite the opposite with non-aromatic boronic acids, whereby the R-$(B(OH)_3)^-$ anion was more reactive towards transmetalation. The examples cited here serve to display the complex and sometime competing role that the base plays in these cross-coupling reactions.

Given the complexity of the base's influence on the reaction mechanism and the fact that a stoichiometric amount of base must be added (compared to the alkyl/aryl halide used) it is clear that a base-free palladium-catalyzed cross-coupling system would be of great utility. There are several examples of base-free systems in the literature. Some of these systems merely utilize a boronate salt as the starting material, effectively moving the formation of the Ar-$(B(OH)_3)^-$ anion required for transmetalation outside of the catalytic cycle.[242] By far the more interesting

examples utilize a nitrogen-containing moiety on the ligand which can act as a base during the reaction. Iranpoor[243] reports a Pd(II) system that is base-free and utilizes a diazadiphosphetidine ligand to couple aryl halides in water. Wang[244] developed a polystyrene-imobilized Pd(II) catalyst with a phenanthroline ligand for the cross-coupling of arylboronic acids with olefins. Suleiman[245] has investigated a dinuclear Pd(II) complex with chelating diimine ligands and bridging diphosphines for the base-free coupling of arylboronic acids and olefins. Kantam[246] and Lindhardt[247] have opted for a slightly different approach. These groups use simple Pd(II) salts as the palladium source to cross-couple heteroaromatic halides with aryl olefins and disubstituted alkynes with electron-deficient alkenes, respectively. Taken as a whole, it is clear that base-free coupling conditions can be achieved with careful consideration of both substrate and/or ligand types.

1.7.3   Homocoupling in Palladium Catalysis

In the palladium-catalyzed cross coupling of aryboronic acids and olefins, one of the possible reaction products is the coupled biaryl. This reaction is known to occur and, depending on the goal of the synthetic methodology, may be viewed as either the desired reaction or an undesired side reaction. The mechanism of biaryl formation[198] involves formation of a peroxo complex $(\eta^2\text{-}O_2)PdL_2$ that forms an adduct with one equivalent of arylboronic acid (Figure 19). A second arylboronic acid molecule enters the cycle and results in the formation of an $ArPd(OH)L_2$ species, which is in turn transmetalated by yet another arylboronic acid to the Ar_2PdL_2 species. Reductive elimination of the biaryl followed by coordination of $\eta^2\text{-}O_2$ regenerates the original peroxo complex and starts the cycle anew. This catalytic cycle holds true for nucleophilic arylboronic acids and requires the presence of an oxidant, in this case

dioxygen. This methodology has proven successful for many biaryl couplings, including indole boronic acids[231], halogenated boronic acids[248], as well as many "normal" aryl and alkyl boronic acids.[211,248-252]

In some cases the formation of homocoupled products is undesirable. In this case there are two major ways to eliminate homocoupling. The first, and perhaps simplest, is to exclude dioxygen from the reaction and run the reaction anaerobically.[253] This can be problematic in practice, as the dioxygen is catalytic in the mechanism and its total exclusion is often unachievable. In the case of an oxidative coupling, exclusion of dioxygen is obviously not feasible and a second method must be considered. Proper ligand selection and/or design can be employed to prevent formation of the η^2-peroxo intermediate. Successful suppression of homocoupling has been observed by Hsu[254] by utilizing chelated bipyridine ligands to suppress the formation of the peroxo intermediate. Abnormal N-heterocyclic carbine ligands were prepared and used by Xu[255] to cross-couple aryl halides with aryl boronic acids. It is suggested that abnormal NHC ligands sterically inhibit the formation of the peroxo species. Yu[256] has successfully cross-coupled aryl silanes and aryl boronic acids in high yield with a simple palladium acetate/BINAP catalyst system (3% BINAP) that significantly reduces the formation of homocoupled products.

Pd⁰L₄ L = PPh₃
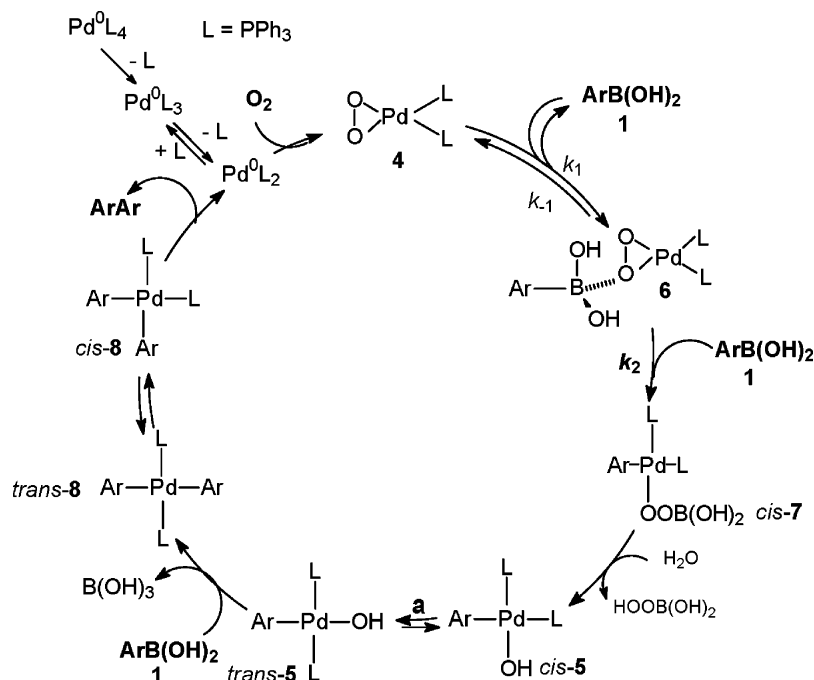
Figure 19. **Mechanism of Pd(II) catalyzed Arylboronic Acid Homocoupling. [Reprinted (adapted) with permission from "Mechanism of the Palladium-Catalyzed Homocoupling of Arylboronic Acids: Key Involvement of a Palladium Peroxo Complex", Adamo, C.; Amatore, C.; Ciofini, I.; Jutand, A.; Lakmini, H. Copyright (2006) American Chemical Society.]**

1.7.4 Multiple Insertion Reactions in Palladium Catalysis

The Heck-type cross-coupling of an arylboronic acid with an alkene results in the formation of a substituted alkene as the product. It is conceivable that the product alkene can itself undergo a further coupling reaction with another arylboronic acid molecule to generate a second product species. Despite this possibility, there are an extremely limited number of these multiple couplings reported in the literature. Pryjomska-Ray[257] has reported such a second coupling product in the cross coupling reaction between butyl acrylate and bromobenzene. The reaction system is base-free and conducted in molten tetrabutylammonium bromide. The primary product, butyl cinnimate, undergoes a second arylboronic insertion at the alkene to generate butyl-3,3-diphenyl acrylate (Figure 20).

26
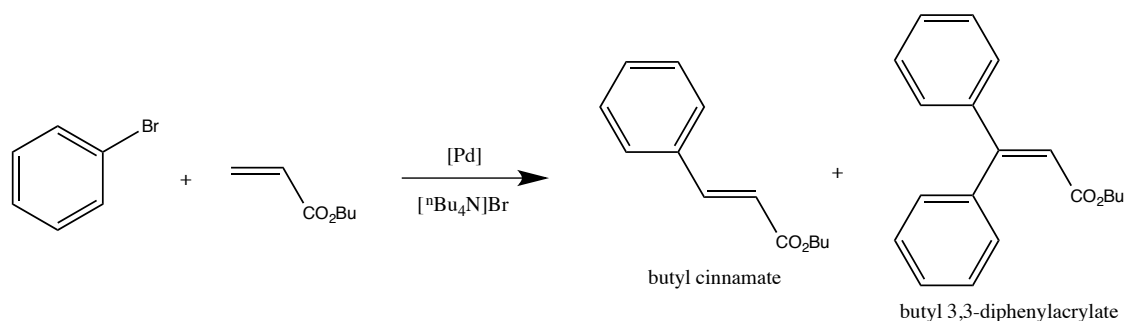
Figure 20. Multiple Insertion of Bromobenzene to Butyl Acrylate

1.8   REFERENCES

(1)   Al-Hassan, M. I. *Journal of the College of Science, King Saud University* **1988**, *19*, 137.

(2)   Beletskaya, I. P. *Journal of Organometallic Chemistry* **1983**, *250*, 551.

(3)   Hao, S.-l.; Zhang, Z.-p.; Liu, C.-l. *Gaofenzi Tongbao* **2011**, 1.

(4)   Lipshutz, B. H.; Abela, A. R.; Boskovic, Z. V.; Nishikata, T.; Duplais, C.; Krasovskiy, A. *Topics in Catalysis* **2010**, *53*, 985.

(5)   Mentzel, U. V.; Tanner, D.; Tonder, J. E. *Dansk Kemi* **2006**, *87*, 38.

(6)   Murahashi, S.-i. *Kagaku to Kogyo (Tokyo, Japan)* **2011**, *64*, 26.

(7)   Negishi, E.-i.; Wang, G.; Rao, H.; Xu, Z. *Journal of Organic Chemistry* **2010**, *75*, 3151.

(8)   Schwan, A. L. *Chemical Society Reviews* **2004**, *33*, 218.

(9)   Wang, N. *Youji Huaxue* **2011**, *31*, 1319.

(10)   Abdel Ghani, N. T.; Mansour, A. M. *Spectrochimica Acta, Part A: Molecular and Biomolecular Spectroscopy* **2011**, *81*, 529.

(11)   Abdel Ghani, N. T.; Mansour, A. M. *Inorganica Chimica Acta* **2011**, *373*, 249.

(12)   Abdel Ghani, N. T.; Mansour, A. M. *Journal of Molecular Structure* **2011**, *991*, 108.

(13)   Abdel Ghani, N. T.; Mansour, A. M. *European Journal of Medicinal Chemistry* **2012**, *47*, 399.

(14)   Abdel-Ghani, N. T.; Mansour, A. M. *Journal of Coordination Chemistry* **2012**, *65*, 763.

(15)   Alexandru, M.-G.; Cirkovic Velickovic, T.; Krstic, M.; Hrubaru, M.-M.; Draghici, C. *Journal of Molecular Structure* **2013**, *1041*, 55.

(16)   Alie El-Deen, A. A.; El-Askalany, A. E.-M. E.; Halaoui, R.; Jean-Claude, B. J.; Butler, I. S.; Mostafa, S. I. *Journal of Molecular Structure* **2013**, *1036*, 161.

(17)   Ari, F.; Aztopal, N.; Icsel, C.; Yilmaz, V. T.; Guney, E.; Buyukgungor, O.; Ulukaya, E. *Bioorganic & Medicinal Chemistry* **2013**, *21*, 6427.

(18)   Aryanpour, N.; Mansouri-Torshizi, H.; Nakhjavan, M.; Shirazi, F. H. *Iranian Journal of Pharmaceutical Research* **2012**, *11*, 689.

(19)   Balboa, S.; Carballo, R.; Castineiras, A.; Gonzalez-Perez, J. M.; Niclos-Gutierrez, J. *Polyhedron* **2013**, *50*, 512.

(20)   Barra, C. V.; Rocha, F. V.; Gautier, A.; Morel, L.; Quilles, M. B.; Carlos, I. Z.; Treu-Filho, O.; Frem, R. C. G.; Mauro, A. E.; Netto, A. V. G. *Polyhedron* **2013**, *65*, 214.

(21)   Barra, C. V.; Rocha, F. V.; Netto, A. V. G.; Frem, R. C. G.; Mauro, A. E.; Carlos, I. Z.; Ananias, S. R.; Quilles, M. B. *Journal of Thermal Analysis and Calorimetry* **2011**, *106*, 489.

(22)   Beresneva, T.; Mishnev, A.; Jaschenko, E.; Shestakova, I.; Gulbe, A.; Abele, E. *ARKIVOC (Gainesville, FL, United States)* **2012**, 185.

(23)   Campanella, N. C.; Demartini, M. d. S.; Torres, C.; Tonon de Almeida, E.; Gouvea, C. M. C. P. *Genetics and Molecular Biology* **2012**, *35*, 159.

(24)   Chardon, E.; Puleo, G. L.; Dahm, G.; Fournel, S.; Guichard, G.; Bellemin-Laponnaz, S. *ChemPlusChem* **2012**, *77*, 1028.

(25)   Chellan, P.; Shunmoogam-Gounden, N.; Hendricks, D. T.; Gut, J.; Rosenthal, P. J.; Lategan, C.; Smith, P. J.; Chibale, K.; Smith, G. S. *European Journal of Inorganic Chemistry* **2010**, 3520.

(26)   Chiririwa, H.; Moss, J. R.; Hendricks, D.; Meijboom, R.; Muller, A. *Transition Metal Chemistry (Dordrecht, Netherlands)* **2013**, *38*, 165.

(27)   Curcic, M. G.; Stankovic, M. S.; Mrkalic, E. M.; Matovic, Z. D.; Bankovic, D. D.; Cvetkovic, D. M.; Dacic, D. S.; Markovic, S. D. *International Journal of Molecular Sciences* **2012**, *13*, 2521.

(28)   de Souza, R. A.; Stevanato, A.; Treu-Filho, O.; Netto, A. V. G.; Mauro, A. E.; Castellano, E. E.; Carlos, I. Z.; Pavan, F. R.; Leite, C. Q. F. *European Journal of Medicinal Chemistry* **2010**, *45*, 4863.

(29)   Deepthi, S. B.; Trivedi, R.; Sujitha, P.; Kumar, C. G.; Sridhar, B.; Bhargava, S. K. *Journal of Chemical Sciences (Bangalore, India)* **2012**, *124*, 1405.

(30)   El-Sherif, A. A. *Journal of Coordination Chemistry* **2011**, *64*, 2035.

(31)   Elsayed, S. A.; Jean-Claude, B. J.; Butler, I. S.; Mostafa, S. I. *Journal of Molecular Structure* **2012**, *1028*, 208.

(32)   Gao, E.; Liu, F.; Zhu, M.; Wang, L.; Huang, Y.; Liu, H.; Ma, S.; Shi, Q.; Wang, N. *Journal of Enzyme Inhibition and Medicinal Chemistry* **2010**, *25*, 557.

(33)   Gao, E.; Zhu, M.; Liu, L.; Huang, Y.; Wang, L.; Shi, C.; Zhang, W.; Sun, Y. *Inorganic Chemistry* **2010**, *49*, 3261.

(34)   Gao, E.-J.; Wang, K.-H.; Zhu, M.-C.; Liu, L. *European Journal of Medicinal Chemistry* **2010**, *45*, 2784.

(35)   Gao, E.-j.; Wang, L.; Zhu, M.-c.; Liu, L.; Zhang, W.-z. *European Journal of Medicinal Chemistry* **2010**, *45*, 311.

(36)   Gao, E.-J.; Zhu, M.-C.; Huang, Y.; Liu, L.; Liu, H.-Y.; Liu, F.-C.; Ma, S.; Shi, C.-Y. *European Journal of Medicinal Chemistry* **2010**, *45*, 1034.

(37)   Gao, E. J.; Liu, L.; Zhu, M. C.; Huang, Y.; Guan, F.; Gao, X. N.; Zhang, M.; Wang, L.; Zhang, W. Z.; Sun, Y. G. *Inorganic Chemistry* **2011**, *50*, 4732.

(38)   Guerrero, E.; Miranda, S.; Luttenberg, S.; Frohlich, N.; Koenen, J.-M.; Mohr, F.; Cerrada, E.; Laguna, M.; Mendia, A. *Inorganic Chemistry* **2013**, *52*, 6635.

(39)   Guney, E.; Yilmaz, V. T.; Ari, F.; Buyukgungor, O.; Ulukaya, E. *Polyhedron* **2011**, *30*, 114.

(40)   Hegazy, W. H.; Al-Faiyz, Y. S. *Medicinal Chemistry Research* **2014**, *23*, 518.

(41)   Hernandez, W.; Paz, J.; Carrasco, F.; Vaisberg, A.; Manzur, J.; Spodine, E.; Hennig, L.; Sieler, J.; Beyer, L. *Zeitschrift fuer Naturforschung, B: A Journal of Chemical Sciences* **2010**, *65*, 1271.

(42)   Icsel, C.; Yilmaz, V. T.; Ari, F.; Ulukaya, E.; Harrison, W. T. A. *European Journal of Medicinal Chemistry* **2013**, *60*, 386.

(43) Illan-Cabeza, N. A.; Garcia-Garcia, A. R.; Martinez-Martos, J. M.; Ramirez-Exposito, M. J.; Moreno-Carretero, M. N. *Journal of Inorganic Biochemistry* **2013**, *126*, 118.

(44) Jevtic, V. V.; Pesic, M.; Radic, G. P.; Vukovic, N.; Sukdolak, S.; Klisuric, O.; Podolski-Renic, A.; Tanic, N.; Trifunovic, S. R. *Journal of Molecular Structure* **2013**, *1040*, 216.

(45) Kalaivani, P.; Prabhakaran, R.; Dallemer, F.; Poornima, P.; Vaishnavi, E.; Ramachandran, E.; Padma, V. V.; Renganathan, R.; Natarajan, K. *Metallomics* **2012**, *4*, 101.

(46) Kalaivani, P.; Prabhakaran, R.; Ramachandran, E.; Dallemer, F.; Paramaguru, G.; Renganathan, R.; Poornima, P.; Vijaya Padma, V.; Natarajan, K. *Dalton Transactions* **2012**, *41*, 2486.

(47) Karakuecuek-Iyidogan, A.; Tasdemir, D.; Oruc-Emre, E. E.; Balzarini, J. *European Journal of Medicinal Chemistry* **2011**, *46*, 5616.

(48) Kaushal, R.; Kumar, N.; Kaushal, R.; Awasthi, P. *International Journal of Current Research and Review* **2011**, *3*, 15.

(49) Khan, H.; Badshah, A.; Murtaz, G.; Said, M.; Zia ur, R.; Neuhausen, C.; Todorova, M.; Jean-Claude, B. J.; Butler, I. S. *European Journal of Medicinal Chemistry* **2011**, *46*, 4071.

(50) Kontek, R.; Matlawska-Wasowska, K.; Kalinowska-Lis, U.; Kontek, B.; Ochocki, J. *Acta Poloniae Pharmaceutica* **2011**, *68*, 127.

(51) Krogul, A.; Cedrowski, J.; Wiktorska, K.; Oziminski, W. P.; Skupinska, J.; Litwinienko, G. *Dalton Transactions* **2012**, *41*, 658.

(52) Lawson, M.; Hamze, A.; Peyrat, J.-F.; Bignon, J.; Dubois, J.; Brion, J.-D.; Alami, M. *Organic & Biomolecular Chemistry* **2013**, *11*, 3664.

(53) Lease, N.; Vasilevski, V.; Carreira, M.; de Almeida, A.; Sanau, M.; Hirva, P.; Casini, A.; Contel, M. *Journal of Medicinal Chemistry* **2013**, *56*, 5806.

(54) Lin, J. M.; Prakasha Gowda, A. S.; Sharma, A. K.; Amin, S. *Bioorganic & Medicinal Chemistry* **2012**, *20*, 3202.

(55) Long, R.; Mao, K.; Ye, X.; Yan, W.; Huang, Y.; Wang, J.; Fu, Y.; Wang, X.; Wu, X.; Xie, Y.; Xiong, Y. *Journal of the American Chemical Society* **2013**, *135*, 3200.

(56) Ma, L.; Zhang, J.; Zhang, F.; Chen, C.; Li, L.; Wang, S.; Li, S. *Journal of Coordination Chemistry* **2012**, *65*, 3160.

(57) Ma, T.; Chen, W.; Zhang, G.; Yu, Y. *Journal of Combinatorial Chemistry* **2010**, *12*, 488.

(58) Maia, P. I. d. S.; Graminha, A.; Pavan, F. R.; Leite, C. Q. F.; Batista, A. A.; Back, D. F.; Lang, E. S.; Ellena, J.; Lemos, S. d. S.; Salistre-de-Araujo, H. S.; Deflon, V. M. *Journal of the Brazilian Chemical Society* **2010**, *21*, 1177.

(59) Matesanz, A. I.; Hernandez, C.; Rodriguez, A.; Souza, P. *Journal of Inorganic Biochemistry* **2011**, *105*, 1613.

(60) Matesanz, A. I.; Leitao, I.; Souza, P. *Journal of Inorganic Biochemistry* **2013**, *125*, 26.

(61) Miklasova, N.; Fischer-Fodor, E.; Loennecke, P.; Tomuleasa, C. I.; Virag, P.; Perde Schrepler, M.; Miklas, R.; Silaghi Dumitrescu, L.; Hey-Hawkins, E. *European Journal of Medicinal Chemistry* **2012**, *49*, 41.

(62) Montagner, D.; Marzano, C.; Gandin, V. *Inorganica Chimica Acta* **2011**, *376*, 574.

(63) Motswainyana, W. M.; Onani, M. O.; Madiehe, A. M. *Polyhedron* **2012**, *41*, 44.

(64) Motswainyana, W. M.; Onani, M. O.; Madiehe, A. M.; Saibu, M.; Thovhogi, N.; Lalancette, R. A. *Journal of Inorganic Biochemistry* **2013**, *129*, 112.

(65) Mylonas, S.; Caranikas, S.; Polissiou, M.; Hatzigiannakou, A.; Tsiftsoglou, A.; Christou, I. *Met. Ions Biol. Med., Proc. Int. Symp., 1st* **1990**, 357.

(66) Nadeem, S.; Bolte, M.; Ahmad, S.; Fazeelat, T.; Tirmizi, S. A.; Rauf, M. K.; Sattar, S. A.; Siddiq, S.; Hameed, A.; Haider, S. Z. *Inorganica Chimica Acta* **2010**, *363*, 3261.

(67)   Nguyen, H. H.; Le, C. D.; Pham, C. T.; Trieu, T. N.; Hagenbach, A.; Abram, U. *Polyhedron* **2012**, *48*, 181.

(68)   Pathak, T. P.; Gligorich, K. M.; Welm, B. E.; Sigman, M. S. *Journal of the American Chemical Society* **2010**, *132*, 7870.

(69)   Polyanskaya, T. V.; Kazhdan, I.; Motley, D. M.; Walmsley, J. A. *Journal of Inorganic Biochemistry* **2010**, *104*, 1205.

(70)   Prabhakaran, R.; Kalaivani, P.; Poornima, P.; Dallemer, F.; Huang, R.; Vijaya Padma, V.; Natarajan, K. *Bioorganic & Medicinal Chemistry* **2013**, *21*, 6742.

(71)   Queiroz, M.-J. R. P.; Calhelha, R. C.; Vale-Silva, L. A.; Pinto, E.; Sao-Jose Nascimento, M. *European Journal of Medicinal Chemistry* **2010**, *45*, 5732.

(72)   Ramachandran, E.; Kalaivani, P.; Prabhakaran, R.; Rath, N. P.; Brinda, S.; Poornima, P.; Padma, V. V.; Natarajan, K. *Metallomics* **2012**, *4*, 218.

(73)   Ramachandran, E.; Senthil Raja, D.; Bhuvanesh, N. S. P.; Natarajan, K. *Dalton Transactions* **2012**, *41*, 13308.

(74)   Ramachandran, E.; Senthil Raja, D.; Rath, N. P.; Natarajan, K. *Inorganic Chemistry* **2013**, *52*, 1504.

(75)   Ratcliff, J.; Durham, P.; Keck, M.; Mokhir, A.; Gerasimchuk, N. *Inorganica Chimica Acta* **2012**, *385*, 11.

(76)   Rocha, F. V.; Barra, C. V.; Mauro, A. E.; Carlos, I. Z.; Nauton, L.; El Ghozzi, M.; Gautier, A.; Morel, L.; Godoy Netto, A. V. *European Journal of Inorganic Chemistry* **2013**, *2013*, 4499.

(77)   Sabounchei, S. J.; Shahriary, P.; Gholiee, Y.; Salehzadeh, S.; Khavasi, H. R.; Chehregani, A. *Inorganica Chimica Acta* **2014**, *409*, 265.

(78)   Saeidifar, M.; Mansouri-Torshizi, H.; Palizdar, Y.; Divsalar, A.; Saboury, A. A. *Nucleosides, Nucleotides & Nucleic Acids* **2013**, *32*, 366.

(79)   Schulz, J.; Renfrew, A. K.; Cisarova, I.; Dyson, P. J.; Stepnicka, P. *Applied Organometallic Chemistry* **2010**, *24*, 392.

(80)   Segapelo, T. V.; Lillywhite, S.; Nordlander, E.; Haukka, M.; Darkwa, J. *Polyhedron* **2012**, *36*, 97.

(81)   Shen, C.; Xia, H.; Yan, H.; Chen, X.; Ranjit, S.; Xie, X.; Tan, D.; Lee, R.; Yang, Y.; Xing, B.; Huang, K.-W.; Zhang, P.; Liu, X. *Chemical Science* **2012**, *3*, 2388.

(82)   Shi, C.-Y.; Gao, E.-J.; Ma, S.; Wang, M.-L.; Liu, Q.-T. *Bioorganic & Medicinal Chemistry Letters* **2010**, *20*, 7250.

(83)   Silva, T. M.; Andersson, S.; Sukumaran, S. K.; Marques, M. P.; Persson, L.; Oredsson, S. *PLoS One* **2013**, *8*, e55651.

(84)   Stringer, T.; Hendricks, D. T.; Guzgay, H.; Smith, G. S. *Polyhedron* **2012**, *31*, 486.

(85)   Sun, Y.-g.; Sun, D.; Yu, W.; Zhu, M.-c.; Ding, F.; Liu, Y.-n.; Gao, E.-j.; Wang, S.-j.; Xiong, G.; Dragutan, I.; Dragutan, V. *Dalton Transactions* **2013**, *42*, 3957.

(86)   Tanaka, M.; Kataoka, H.; Yano, S.; Ohi, H.; Kawamoto, K.; Shibahara, T.; Mizoshita, T.; Mori, Y.; Tanida, S.; Kamiya, T.; Joh, T. *BMC Cancer* **2013**, *13*, 237.

(87)   Tolstorozhev, G. B.; Skornyakov, I. V.; Pekhnio, V. I.; Kozachkova, A. N.; Sharykina, N. I. *Journal of Applied Spectroscopy* **2012**, *79*, 453.

(88)   Trost, B. M.; Dong, G. *Journal of the American Chemical Society* **2010**, *132*, 16403.

(89)   Tsekova, D.; Gorolomova, P.; Gochev, G.; Skumryev, V.; Momekov, G.; Momekova, D.; Gencheva, G. *Journal of Inorganic Biochemistry* **2013**, *124*, 54.

(90)   Ulukaya, E.; Ari, F.; Dimas, K.; Ikitimur, E. I.; Guney, E.; Yilmaz, V. T. *European Journal of Medicinal Chemistry* **2011**, *46*, 4957.

(91)   Ulukaya, E.; Frame, F. M.; Cevatemre, B.; Pellacani, D.; Walker, H.; Mann, V. M.; Simms, M. S.; Stower, M. J.; Yilmaz, V. T.; Maitland, N. J. *PLoS One* **2013**, *8*, e64278.

(92)   Vazquez, J.; Bernes, S.; Sharma, P.; Perez, J.; Hernandez, G.; Tovar, A.; Pena, U.; Gutierrez, R. *Polyhedron* **2011**, *30*, 2514.

(93)   Vranec, P.; Potocnak, I.; Sabolova, D.; Farkasova, V.; Ipothova, Z.; Pisarcikova, J.; Paulikova, H. *Journal of Inorganic Biochemistry* **2014**, *131*, 37.

(94)   Wang, C.-H.; Shih, W.-C.; Chang, H. C.; Kuo, Y.-Y.; Hung, W.-C.; Ong, T.-G.; Li, W.-S. *Journal of Medicinal Chemistry* **2011**, *54*, 5245.

(95)   Wang, P.-P.; Wang, Y.-J.; Lin, Q.-Y.; Shen, L.-L.; Zhao, Y.-L. *Chinese Journal of Structural Chemistry* **2012**, *31*, 1175.

(96)   Wang, Y.; Ai, J.; Liu, G.; Geng, M.; Zhang, A. *Organic & Biomolecular Chemistry* **2011**, *9*, 5930.

(97)   Yano, S.; Ohi, H.; Ashizaki, M.; Obata, M.; Mikata, Y.; Tanaka, R.; Nishioka, T.; Kinoshita, I.; Sugai, Y.; Okura, I.; Ogura, S.-i.; Czaplewska, J. A.; Gottschaldt, M.; Schubert, U. S.; Funabiki, T.; Morimoto, K.; Nakai, M. *Chemistry & Biodiversity* **2012**, *9*, 1903.

(98)   Zhang, J.; Li, L.; Ma, L.; Zhang, F.; Zhang, Z.; Wang, S. *European Journal of Medicinal Chemistry* **2011**, *46*, 5711.

(99)   Zhang, J.; Li, L.; Wang, L.; Zhang, F.; Li, X. *European Journal of Medicinal Chemistry* **2010**, *45*, 5337.

(100) Zhang, J.; Ma, L.; Lu, H.; Wang, Y.; Li, S.; Wang, S.; Zhou, G. *European Journal of Medicinal Chemistry* **2012**, *58*, 281.

(101) Zhang, J.; Ma, L.; Zhang, F.; Zhang, Z.; Li, L.; Wang, S. *Journal of Coordination Chemistry* **2012**, *65*, 239.

(102) Zhang, J.-C.; Li, L.-W.; Wang, L.-W.; Zhang, F.-F.; Qin, X.-Y.; Li, X.-L. *Wuji Huaxue Xuebao* **2010**, *26*, 1699.

(103) Abbehausen, C.; Sucena, S. F.; Lancellotti, M.; Heinrich, T. A.; Abrao, E. P.; Costa-Neto, C. M.; Formiga, A. L. B.; Corbi, P. P. *Journal of Molecular Structure* **2013**, *1035*, 421.

(104) Aslan, H. G.; Ozcan, S.; Karacan, N. *Inorganic Chemistry Communications* **2011**, *14*, 1550.

(105) Azam, M.; Warad, I.; Al-Resayes, S. I.; Alzaqri, N.; Khan, M. R.; Pallepogu, R.; Dwivedi, S.; Musarrat, J.; Shakir, M. *Journal of Molecular Structure* **2013**, *1047*, 48.

(106) Badea, M.; Iosub, E.; Chifiriuc, C. M.; Marutescu, L.; Iorgulescu, E. E.; Lazar, V.; Marinescu, D.; Bleotu, C.; Olar, R. *Journal of Thermal Analysis and Calorimetry* **2013**, *111*, 1753.

(107) Biswas, C.; Zhu, M.; Lu, L.; Kaity, S.; Das, M.; Samanta, A.; Naskar, J. P. *Polyhedron* **2013**, *56*, 211.

(108) Chary, M. R.; Padmaja, N.; Ravinder, M.; Srihari, S. *Oriental Journal of Chemistry* **2010**, *26*, 1159.

(109) Djordjevic, M. M.; Jeremic, D. A.; Rodic, M. V.; Simic, V. S.; Brceski, I. D.; Leovac, V. M. *Polyhedron* **2014**, *68*, 234.

(110) El-Sawi, E. A.; Hosny, M. A.; Mokbel, W. A.; Sayed, T. M. *Synthesis and Reactivity in Inorganic, Metal-Organic, and Nano-Metal Chemistry* **2010**, *40*, 934.

(111) El-Sawi, E. A.; Sayed, T. M. *Synthesis and Reactivity in Inorganic, Metal-Organic, and Nano-Metal Chemistry* **2013**, *43*, 722.

(112) El-Sonbati, A. Z.; Diab, M. A.; El-Bindary, A. A.; Abou-Dobara, M. I.; Seyam, H. A. *Spectrochimica Acta, Part A: Molecular and Biomolecular Spectroscopy* **2013**, *104*, 213.

(113) Elgazwy, A. S. S. H.; Ismail, N. S. M.; Atta-Allah, S. R.; Sarg, M. T.; Soliman, D. H. S.; Zaki, M. Y.; Elgamas, M. A. *Current Medicinal Chemistry* **2012**, *19*, 3967.

(114) Elhusseiny, A. F.; Hassan, H. H. A. M. *Spectrochimica Acta, Part A: Molecular and Biomolecular Spectroscopy* **2013**, *103*, 232.

(115) Guo, H.-f.; Pan, Y.; Ma, D.-y.; Yan, P. *Wuji Huaxue Xuebao* **2013**, *29*, 1447.

(116) Hegazy, W. H. *International Research Journal of Pure and Applied Chemistry* **2012**, *2*, 170.

(117) Ibrahim, K. M.; Zaky, R. R.; Gomaa, E. A.; Abd El-Hady, M. N. *Spectrochimica Acta, Part A: Molecular and Biomolecular Spectroscopy* **2013**, *107*, 133.

(118) Ilic, D. R.; Vujiv, J. M.; Radojevic, I. D.; Stefanovic, O. D.; Comic, L. R.; Bankovic, D. D.; Trifunovic, S. R. *Hemijska Industrija* **2012**, *66*, 349.

(119) Jagadeesh, M.; Rashmi, H. K.; Subba Rao, Y.; Sreenath Reddy, A.; Prathima, B.; Uma Maheswari Devi, P.; Reddy, A. V. *Spectrochimica Acta, Part A: Molecular and Biomolecular Spectroscopy* **2013**, *115*, 583.

(120) Juribasic, M.; Molcanov, K.; Kojic-Prodic, B.; Bellotto, L.; Kralj, M.; Zani, F.; Tusek-Bozic, L. *Journal of Inorganic Biochemistry* **2011**, *105*, 867.

(121) Lee, H. J.; Lee, S. H.; Kim, H. C.; Lee, Y.-E.; Park, S. *Journal of Organometallic Chemistry* **2012**, *717*, 164.

(122) Masih, I.; Fahmi, N. *Spectrochimica Acta, Part A: Molecular and Biomolecular Spectroscopy* **2011**, *79*, 940.

(123) Nichick, M. N.; Voitekhovich, S. V.; Lesnyak, V.; Matulis, V. E.; Zheldakova, R. A.; Lesnikovich, A. I.; Ivashkevich, O. A. *Journal of Physical Chemistry C* **2011**, *115*, 16928.

(124) Ozbek, N.; Alyar, S.; Alyar, H.; Sahin, E.; Karacan, N. *Spectrochimica Acta, Part A: Molecular and Biomolecular Spectroscopy* **2013**, *108*, 123.

(125) Park, S. Y.; Chung, J. W.; Priestley, R. D.; Kwak, S.-Y. *Cellulose (Dordrecht, Netherlands)* **2012**, *19*, 2141.

(126) Patel, M. N.; Dosi, P. A.; Bhatt, B. S. *Journal of Coordination Chemistry* **2012**, *65*, 3833.

(127) Patel, M. N.; Dosi, P. A.; Bhatt, B. S. *Spectrochimica Acta, Part A: Molecular and Biomolecular Spectroscopy* **2012**, *86*, 508.

(128) Petrovic, Z. D.; Comic, L.; Stefanovic, O.; Simijonovic, D.; Petrovic, V. P. *Journal of Molecular Liquids* **2012**, *170*, 61.

(129) Radic, G. P.; Glodjovic, V. V.; Ratkovic, Z. R.; Novakovic, S. B.; Garcia-Granda, S.; Roces, L.; Menendez-Taboada, L.; Radojevic, I. D.; Stefanovic, O. D.; Comic, L. R.; Trifunovic, S. R. *Journal of Molecular Structure* **2012**, *1029*, 180.

(130) Radic, G. P.; Glodovic, V. V.; Radojevic, I. D.; Stefanovic, O. D.; Comic, L. R.; Dinovic, V. M.; Trifunovic, S. R. *Inorganica Chimica Acta* **2012**, *391*, 44.

(131) Radic, G. P.; Glodovic, V. V.; Radojevic, I. D.; Stefanovic, O. D.; Comic, L. R.; Ratkovic, Z. R.; Valkonen, A.; Rissanen, K.; Trifunovic, S. R. *Polyhedron* **2012**, *31*, 69.

(132) Rosu, T.; Pahontu, E.; Pasculescu, S.; Georgescu, R.; Stanica, N.; Curaj, A.; Popescu, A.; Leabu, M. *European Journal of Medicinal Chemistry* **2010**, *45*, 1627.

(133) Samota, M. K.; Seth, G. *Heteroatom Chemistry* **2010**, *21*, 44.

(134) Seleem, H. S. *Chemistry Central Journal* **2011**, *5*, 35.

(135) Shaheen, F.; Badshah, A.; Gielen, M.; Croce, G.; Florke, U.; de Vos, D.; Ali, S. *Journal of Organometallic Chemistry* **2010**, *695*, 315.

(136) Sharma, K.; Singh, R.; Fahmi, N.; Singh, R. V. *Spectrochimica Acta, Part A: Molecular and Biomolecular Spectroscopy* **2010**, *75A*, 422.

(137) Sharma, K.; Singh, R. V.; Fahmi, N. *Spectrochimica Acta, Part A: Molecular and Biomolecular Spectroscopy* **2011**, *78A*, 80.

(138) Tamayo, L. V.; Burgos, A. E.; Brandao, P. F. B. *Phosphorus, Sulfur and Silicon and the Related Elements* **2014**, *189*, 52.

(139) Varbanov, H.; Bakalova, A.; Buyukliev, R.; Momekov, G.; Baykushev, R. *Transition Metal Chemistry (Dordrecht, Netherlands)* **2010**, *35*, 457.

(140)   Vasic, G. P.; Glodjovic, V. V.; Radojevic, I. D.; Stefanovic, O. D.; Comic, L. R.; Djinovic, V. M.; Trifunovic, S. R. *Inorganica Chimica Acta* **2010**, *363*, 3606.

(141)   Baidina, I. A.; Podberezskaya, N. V.; Borisov, S. V. *Zhurnal Strukturnoi Khimii* **1980**, *21*, 198.

(142)   Chernova, N. N.; Shakhova, L. P.; Kukushkin, Y. N. *Zhurnal Neorganicheskoi Khimii* **1976**, *21*, 3027.

(143)   Vicol, O. *Analele Stiintifice ale Universitatii Al. I. Cuza din Iasi, Sectiunea 1c: Chimie* **1973**, *19*, 27.

(144)   Spacu, P.; Ungureanu-Vicol, O. *Analele Universitatii Bucuresti, Seria Stiintele Naturii* **1966**, *15*, 109.

(145)   McAuliffe, C. A. *Journal of the Chemical Society [Section] A: Inorganic, Physical, Theoretical* **1967**, *1967*, 641.

(146)   Warren, R. C.; McConnell, J. F.; Stephenson, N. C. *Acta Crystallographica, Section B: Structural Crystallography and Crystal Chemistry* **1970**, *26*, 1402.

(147)   Livingstone, S. E.; Nolan, J. D. *Inorganic Chemistry* **1968**, *7*, 1447.

(148)   Shestakova, N. A.; Golubovskaya, E. V.; Mal'chikov, G. D.; Grankina, Z. A. *Koordinatsionnaya Khimiya* **1978**, *4*, 587.

(149)   Nakamoto, K.; Morimoto, Y.; Martell, A. E. *Journal of the American Chemical Society* **1961**, *83*, 4528.

(150)   Jarzab, T. C.; Hare, C. R.; Langs, D. A. *Crystal Structure Communications* **1973**, *2*, 395.

(151)   Vagg, R. S. *Acta Crystallogr B* **1979**, *35*, 341.

(152)   Sabat, M.; Jezowska, M.; Kozlowski, H. *Inorganica Chimica Acta* **1979**, *37*, L511.

(153)   Kozlowski, H.; Jezowska, M. *Chemical Physics Letters* **1977**, *47*, 452.

(154)   Kozlowski, H. *Inorganica Chimica Acta* **1978**, *31*, 135.

(155)   Aullon, G.; Alvarez, S. *Inorganic Chemistry* **1996**, *35*, 3137.

(156)   Jarzab, T. C.; Hare, C. R.; Langs, D. A. *Crystal Structure Communications* **1973**, *2*, 399.

(157)   Ito, T.; Marumo, F.; Saito, Y. *Acta Crystallographica, Section B: Structural Crystallography and Crystal Chemistry* **1971**, *27*, 1062.

(158)   Chernova, N. N.; Strukov, V. V.; Avetikyan, G. B.; Chernonozhkin, V. N. *Zhurnal Neorganicheskoi Khimii* **1980**, *25*, 1569.

(159)   Nakayama, Y.; Matsumoto, K.; Ooi, S.; Kuroya, H. *Journal of the Chemical Society, Chemical Communications* **1973**, 170.

(160)   Boudreau, P. A.; Hooper, R. J. *Journal of Inorganic and Nuclear Chemistry* **1977**, *39*, 1247.

(161)   Komorita, T.; Hidaka, J.; Shimura, Y. *Bull. Chem. Soc. Jap.* **1968**, *41*, 854.

(162)   Komorita, T.; Hidaka, J.; Shimura, Y. *Bull. Chem. Soc. Jap.* **1971**, *44*, 3353.

(163)   Shestakova, N. A.; Kuklina, U. F.; Mal'chikov, G. D. *Izvestiya Sibirskogo Otdeleniya Akademii Nauk SSSR, Seriya Khimicheskikh Nauk* **1977**, 102.

(164)   Baidina, I. A.; Podberezskaya, N. V.; Borisov, S. V.; Golubovskaya, E. V. *Zhurnal Strukturnoi Khimii* **1980**, *21*, 188.

(165)   Vicol, O.; Repede, S.; Lascar, V. *Buletinul Institutului Politehnic din Iasi, Sectia 2: Chimie si Inginerie Chimica* **1980**, *25*, 17.

(166)   Vicol, O.; Repede, S. *Buletinul Institutului Politehnic din Iasi, Sectia 2: Chimie si Inginerie Chimica* **1980**, *26*, 37.

(167)   Sullivan, E. A. *Can J Chem* **1979**, *57*, 62.

(168)   Yamauchi, O.; Odani, A. *Journal of the American Chemical Society* **1981**, *103*, 391.

(169)   Odani, A.; Yamauchi, O. *Bulletin of the Chemical Society of Japan* **1981**, *54*, 3773.

(170) Gao, E.; Liu, C.; Zhu, M.; Lin, H.; Wu, Q.; Liu, L. *Anti-Cancer Agents in Medicinal Chemistry* **2009**, *9*, 356.

(171) Charlson, A. J.; Banner, R. J.; Gale, R. P.; McArdle, N. T.; Trainor, K. E.; Watton, E. C. *Journal of Clinical Hematology and Oncology* **1977**, *7*, 293.

(172) Puthraya, K. H.; Srivastava, T. S.; Amonkar, A. J.; Adwankar, M. K.; Chitnis, M. P. *Journal of Inorganic Biochemistry* **1985**, *25*, 207.

(173) Puthraya, K. H.; Srivastava, T. S.; Amonkar, A. J.; Adwankar, M. K.; Chitnis, M. P. *Journal of Inorganic Biochemistry* **1986**, *26*, 45.

(174) Mital, R.; Srivastava, T. S.; Parekh, H. K.; Chitnis, M. P. *Journal of Inorganic Biochemistry* **1991**, *41*, 93.

(175) Lin, H.; Li, Z.; Dai, G.; Bi, Q.; Yu, R. *Science in China, Series B: Chemistry, Life Sciences, & Earth Sciences* **1993**, *36*, 1216.

(176) Paul, A. K.; Mansuri-Torshizi, H.; Srivastava, T. S.; Chavan, S. J.; Chitnis, M. P. *Journal of Inorganic Biochemistry* **1993**, *50*, 9.

(177) Matilla, A.; Tercero, J. M.; Dung, N. H.; Viossat, B.; Perez, J. M.; Alonso, C.; Martin-Ramos, J. D.; Niclos-Gutierrez, J. *Journal of Inorganic Biochemistry* **1994**, *55*, 235.

(178) Nijasure, A. M.; Joshi, V. N.; Sawant, A. D. *Journal of Inorganic Biochemistry* **1999**, *73*, 109.

(179) Offiong, O. E.; Nfor, E.; Ayi, A. A.; Martelli, S. *Transition Metal Chemistry (Dordrecht, Netherlands)* **2000**, *25*, 369.

(180) Gupta, M.; Sihag, S.; Varshney, A. K.; Varshney, S. *Journal of Chemistry* **2013**, 745101.

(181) Li, L.; Zhang, J.; Ma, L.; Zhang, Z.; Wang, S.; Li, S.; Zhou, G. *Journal of Coordination Chemistry* **2013**, *66*, 638.

(182) Al-Fregi, A. A.; Abood, H. A. A.; Al-Saimary, I. E. *Internet Journal of Microbiology* **2007**, *4*, No pp given.

(183) Do, C. H. *Hwahak Kyoyuk* **2010**, *37*, 12.

(184) Heck, R. F.; Nolley, J. P., Jr. *Journal of Organic Chemistry* **1972**, *37*, 2320.

(185) Miyaura, N.; Yamada, K.; Suzuki, A. *Tetrahedron Letters* **1979**, 3437.

(186) Sonogashira, K. *Journal of Organometallic Chemistry* **2002**, *653*, 46.

(187) Milstein, D.; Stille, J. K. *Journal of the American Chemical Society* **1978**, *100*, 3636.

(188) Hiyama, T. *Journal of Organometallic Chemistry* **2002**, *653*, 58.

(189) Surry, D. S.; Buchwald, S. L. *Chemical Science* **2011**, *2*, 27.

(190) Kikukawa, K.; Matsuda, T. *Chemistry Letters* **1977**, 159.

(191) Jin, L. Q.; Lei, A. W. *Science China: Chemistry* **2012**, *55*, 2027.

(192) Beccalli, E. M.; Broggini, G.; Martinelli, M.; Sottocornola, S. *Chemical Reviews (Washington, DC, United States)* **2007**, *107*, 5318.

(193) Obora, Y.; Ishii, Y. *Molecules* **2010**, *15*, 1487.

(194) Stahl, S. S. *Angewandte Chemie, International Edition* **2004**, *43*, 3400.

(195) Wu, W.; Jiang, H. *Accounts of Chemical Research* **2012**, *45*, 1736.

(196) Zeni, G.; Larock, R. C. *Chemical Reviews (Washington, DC, United States)* **2006**, *106*, 4644.

(197) Gligorich, K. M.; Cummings, S. A.; Sigman, M. S. *Journal of the American Chemical Society* **2007**, *129*, 14193.

(198) Adamo, C.; Amatore, C.; Ciofini, I.; Jutand, A.; Lakmini, H. *Journal of the American Chemical Society* **2006**, *128*, 6829.

(199) Canovese, L.; Visentin, F.; Chessa, G.; Santo, C.; Levi, C.; Uguagliati, P. *Inorganic Chemistry Communications* **2006**, *9*, 388.

(200)   Hull, K. L.; Lanni, E. L.; Sanford, M. S. *Journal of the American Chemical Society* **2006**, *128*, 14047.

(201)   Hull, K. L.; Sanford, M. S. *Abstracts of Papers, 239th ACS National Meeting, San Francisco, CA, United States, March 21-25, 2010* **2010**, ORGN.

(202)   Lu, Y.; Wang, D.-H.; Engle, K. M.; Yu, J.-Q. *Journal of the American Chemical Society* **2010**, *132*, 5916.

(203)   Muzart, J. *Chemistry - An Asian Journal* **2006**, *1*, 508.

(204)   Chen, Q.; Li, C. *Organometallics* **2007**, *26*, 223.

(205)   Herr, R. J.; Dowling, M. S.; Scampini, A. C.; Smith, T. M. *Abstracts, 35th Northeast Regional Meeting of the American Chemical Society, Burlington, VT, United States, June 29-July 2* **2008**, NERM.

(206)   Horiguchi, H.; Tsurugi, H.; Satoh, T.; Miura, M. *Advanced Synthesis & Catalysis* **2008**, *350*, 509.

(207)   Jin, L.; Zhao, Y.; Wang, H.; Lei, A. *Synthesis* **2008**, 649.

(208)   Johnson, T.; Lautens, M. *Organic Letters* **2013**, *15*, 4043.

(209)   Jordan-Hore, J. A.; Sanderson, J. N.; Lee, A.-L. *Organic Letters* **2012**, *14*, 2508.

(210)   Khabibulin, V. R.; Kulik, A. V.; Oshanina, I. V.; Bruk, L. G.; Temkin, O. N.; Nosova, V. M.; Ustynyuk, Y. A.; Bel'skii, V. K.; Stash, A. I.; Lysenko, K. A.; Antipin, M. Y. *Kinetics and Catalysis* **2007**, *48*, 228.

(211)   Lei, A.; Zhang, X. *Tetrahedron Letters* **2002**, *43*, 2525.

(212)   Liegault, B.; Lee, D.; Huestis, M. P.; Stuart, D. R.; Fagnou, K. *Journal of Organic Chemistry* **2008**, *73*, 5022.

(213)   Liu, C.; Jin, L.; Lei, A. *Synlett* **2010**, 2527.

(214)   Martinez, C.; Alvarez, R.; Aurrecoechea, J. M. *Organic Letters* **2009**, *11*, 1083.

(215)   Prateeptongkum, S.; Driller, K. M.; Jackstell, R.; Spannenberg, A.; Beller, M. *Chemistry--A European Journal* **2010**, *16*, 9606.

(216)   Van Aeken, S.; Verbeeck, S.; Deblander, J.; Maes, B. U. W.; Tehrani, K. A. *Tetrahedron* **2011**, *67*, 2269.

(217)   Venkatraman, S.; Huang, T.; Li, C.-J. *Advanced Synthesis & Catalysis* **2002**, *344*, 399.

(218)   Wakioka, M.; Mutoh, Y.; Takita, R.; Ozawa, F. *Bulletin of the Chemical Society of Japan* **2009**, *82*, 1292.

(219)   Yoo, K. S.; O'Neill, J.; Sakaguchi, S.; Giles, R.; Lee, J. H.; Jung, K. W. *Journal of Organic Chemistry* **2010**, *75*, 95.

(220)   Yoo, K. S.; Park, C. P.; Yoon, C. H.; Sakaguchi, S.; O'Neill, J.; Jung, K. W. *Organic Letters* **2007**, *9*, 3933.

(221)   Yoo, K. S.; Yoon, C. H.; Jung, K. W. *Journal of the American Chemical Society* **2006**, *128*, 16384.

(222)   Alvarez, R.; Martinez, C.; Madich, Y.; Denis, J. G.; Aurrecoechea, J. M.; de Lera, A. R. *Chemistry--A European Journal* **2010**, *16*, 12746.

(223)   Aouf, C.; Thiery, E.; Le Bras, J.; Muzart, J. *Organic Letters* **2009**, *11*, 4096.

(224)   Beccalli, E. M.; Borsini, E.; Broggini, G.; Rigamonti, M.; Sottocornola, S. *Synlett* **2008**, 1053.

(225)   Maehara, A.; Satoh, T.; Miura, M. *Tetrahedron* **2008**, *64*, 5982.

(226)   Thiery, E.; Harakat, D.; Le Bras, J.; Muzart, J. *Organometallics* **2008**, *27*, 3996.

(227)   Xi, P.; Yang, F.; Qin, S.; Zhao, D.; Lan, J.; Gao, G.; Hu, C.; You, J. *Journal of the American Chemical Society* **2010**, *132*, 1822.

(228)   Yamashita, M.; Hirano, K.; Satoh, T.; Miura, M. *Organic Letters* **2009**, *11*, 2337.

(229) Yang, S.-D.; Sun, C.-L.; Fang, Z.; Li, B.-J.; Li, Y.-Z.; Shi, Z.-J. *Angewandte Chemie, International Edition* **2008**, *47*, 1473.

(230) Bardhan, S.; Wacharasindhu, S.; Wan, Z.-K.; Mansour, T. S. *Organic Letters* **2009**, *11*, 2511.

(231) Belitsky, J. M. *Abstracts of Papers, 236th ACS National Meeting, Philadelphia, PA, United States, August 17-21, 2008* **2008**, ORGN.

(232) Belitsky, J. M. *Abstracts, Central Regional Meeting of the American Chemical Society, Cleveland, OH, United States, May 20-23* **2009**, CRM.

(233) Clawson, R. W.; Deavers, R. E.; Akhmedov, N. G.; Soederberg, B. C. G. *Tetrahedron* **2006**, *62*, 10829.

(234) Djakovitch, L.; Rouge, P. *Journal of Molecular Catalysis A: Chemical* **2007**, *273*, 230.

(235) Gong, X.; Song, G.; Zhang, H.; Li, X. *Organic Letters* **2011**, *13*, 1766.

(236) He, C.-Y.; Fan, S.; Zhang, X. *Journal of the American Chemical Society* **2010**, *132*, 12850.

(237) Wang, Z.; Li, K.; Zhao, D.; Lan, J.; You, J. *Angewandte Chemie, International Edition* **2011**, *50*, 5365.

(238) Henke, A.; Srogl, J. *Chemical Communications (Cambridge, United Kingdom)* **2011**, *47*, 4282.

(239) Kirchberg, S.; Tani, S.; Ueda, K.; Yamaguchi, J.; Studer, A.; Itami, K. *Angewandte Chemie, International Edition* **2011**, *50*, 2387.

(240) Amatore, C.; Jutand, A.; Le Duc, G. *Chemistry – A European Journal* **2011**, *17*, 2492.

(241) Lima, C. F. R. A. C.; Rodrigues, A. S. M. C.; Silva, V. L. M.; Silva, A. M. S.; Santos, L. M. N. B. F. *ChemCatChem* **2014**, *6*, 1291.

(242) Vasu, D.; Yorimitsu, H.; Osuka, A. *Synthesis* **2015**, *47*, 3286.

(243) Iranpoor, N.; Firouzabadi, H.; Tarassoli, A.; Fereidoonnezhad, M. *Tetrahedron* **2010**, *66*, 2415.

(244) Wang, P.; Zhang, J.; Cai, M. *Journal of Chemical Research* **2012**, *36*, 629.

(245) Suleiman, R.; Shakil Hussain, S. M.; Fettouhi, M.; El Ali, B. *Synthesis and Reactivity in Inorganic, Metal-Organic, and Nano-Metal Chemistry* **2012**, *42*, 850.

(246) Kantam, M. L.; Reddy, P. V.; Srinivas, P.; Bhargava, S. *Tetrahedron Letters* **2011**, *52*, 4490.

(247) Lindhardt, A. T.; Mantel, M. L. H.; Skrydstrup, T. *Angewandte Chemie, International Edition* **2008**, *47*, 2668.

(248) Lehmler, H.-J.; Brock, C. P.; Patrick, B.; Robertson, L. W. *PCBs, Recent Advances in Environmental Toxicology and Health Effects* **2001**, 57.

(249) Chen, J.-S.; Krogh-Jespersen, K.; Khinast, J. G. *Journal of Molecular Catalysis A: Chemical* **2008**, *285*, 14.

(250) Koza, D. J.; Carita, E. *Synthesis* **2002**, 2183.

(251) Xu, Z.; Mao, J.; Zhang, Y. *Catalysis Communications* **2007**, *9*, 97.

(252) Yamamoto, Y. *Synlett* **2007**, 1913.

(253) Miller, W. D.; Fray, A. H.; Quatroche, J. T.; Sturgill, C. D. *Organic Process Research & Development* **2007**, *11*, 359.

(254) Hsu, C.-M.; Li, C.-B.; Sun, C.-H. *Journal of the Chinese Chemical Society (Taipei, Taiwan)* **2009**, *56*, 873.

(255) Xu, X.; Xu, B.; Li, Y.; Hong, S. H. *Organometallics* **2010**, *29*, 6343.

(256) Yu, J.; Liu, J.; Shi, G.; Shao, C.; Zhang, Y. *Angewandte Chemie, International Edition* **2015**, *54*, 4079.

(257) Pryjomska-Ray, I.; Trzeciak, A. M.; Ziolkowski, J. J. *Journal of Molecular Catalysis A: Chemical* **2006**, *257*, 3.

Chapter 2. Bis-Glycinato Complexes of Palladium(II):   Synthesis,   Molecular Structure,   and   Hydrogen   Bonding Interactions

2.1   INTRODUCTION

This chapter discusses the palladium(II)-amino acid chelates where glycine, *N*-methylglycine, and *N,N*-dimethylglycine were used as the chelating ligands.   Subsequent chapters will discuss the chiral palladium(II) amino acid chelates, with an eye toward ultimately using those complexes for asymmetric catalysis.   This chapter details the syntheses, structural and spectroscopic characterization of palladium glycine complexes that clarify some earlier studies and add new information on structures, both solid state and in solution.   Also examined here are the series of *N*-methylated glycines and the effect of methyl substitution on structures and isomer formation.

Palladium(II) amino acid complexes are known although only a few of the possible amino acid complexes have been made and their properties have not been studied in great depth.[1] Prior to beginning a study of the catalytic and biological activity of transition metal amino acid complexes,[2] it became apparent that there was still much to be learned about the bis-glycine palladium(II) complexes and those findings are reported in this chapter.   The simplest amino

acid, glycine, affords some advantages in terms of analytical simplicity for a beginning of a broader, more detailed study of these complexes.

Pinkard reported the first syntheses of *cis* and *trans* palladium(II) glycine complexes.[1] Ley[3] and Grundberg[4] had earlier reported analogous platinum complexes. Assignment of *cis* and *trans* isomers was based on differing crystal habits and on differing reaction products with aqueous thiourea. Saraceno[5] and Lane[6] made detailed assignments of infrared bands for the *trans* and *cis* isomers, respectively. Further infrared spectral analysis was reported by Condrate,[7] and far-infrared peak assignments of these complexes were made by Walter.[8] The electronic spectra and photochemical behavior of palladium(II)-amino acid complexes were investigated by Balzani.[9] Balzani reported that *trans*-Pd(gly)$_2$ undergoes decomposition resulting from electron-transfer transitions when irradiated with ultraviolet radiation at 254 nm yet suffered no decomposition when irradiated at 313 nm, which corresponds to the d→d transition seen in the UV-vis spectrum. Zhang reported on the photoacoustic spectrum.[10] Thermal isomerization (ca. 100°C) of *trans*-Pd(gly)$_2$ to *cis*-Pd(gly)$_2$ was reported by Coe along with the first-order rate constant for the isomerization.[11] Farooq studied the formation of palladium(II)-glycine complexes by titrating the [H$^+$] liberated during the reaction of glycine and Na$_2$PdCl$_4$ and calculated their stability constants.[12] The X-ray crystal structures of the *cis* and *trans* palladium(II)-glycine complexes were reported by Baidina.[13,14] Nuclear magnetic resonance data on ^{15}N labeled glycinate complexes of palladium(II) were reported by Appleton.[15] Two resonances were observed at δ 55.7 and 47.4 ppm indicating a mixture of *cis* and *trans* isomers of Pd(^{15}N-gly)$_2$. The ^{13}C NMR spectral data also shows a slight upfield shift of the methylene carbon resonance as compared to the free ligand. ^{13}C NMR data reported by Krylova[16] is in excellent agreement with that reported by Appleton; ^{1}H NMR data is reported as well with two

distinct resonances reported for –NH$_2$ and –CH$_2$- moieties. Electrochemical properties of Pd(gly)$_2$ complexes have been reported by Chornenka[17] and Kublanovsky.[18]

2.2   EXPERIMENTAL DETAILS

All reagents used in the preparation of the following compounds were purchased from commercial suppliers and used as-received. Palladium(II) acetate was obtained from Pressure Chemical, Pittsburgh, PA. Palladium(II) chloride was purchased from Alfa Aesar, Ward Hill, MA. Glycine was purchased from Qiagen Sciences, Germantown, MD. *N,N*-dimethylglycine was purchased from Spectrum Chemical, Gardena, CA. *N*-methylglycine and reagent grade solvents (ether, acetone) were purchased from Sigma-Aldrich, St. Louis, MO. Deuterated solvents for NMR spectroscopy were obtained from Cambridge Isotope Laboratories, Tewksbury, MA. Commercially available isotopically labeled glycines were provided by an anonymous donor.

^{1}H NMR spectra were collected on a Varian MR-400 NMR spectrometer or a Bruker Avance III 600 MHz NMR spectrometer. ^{13}C and ^{15}N NMR spectra were collected on a Bruker Avance III 600 MHz NMR spectrometer. High Resolution Mass Spectra (HRMS) were collected on an Agilent 6220 Accurate Mass TOF MS with an ESI source. Ultraviolet-Visible (UV-vis) spectra were collected on a Hewlett-Packard 8453 spectrophotometer with quartz cuvettes. Solid-state Fourier Transform Infrared (FTIR) spectra were collected on a Midac M2000 FTIR spectrometer equipped with a DuraScope diamond ATR accessory. X-ray crystallographic data were collected at 100 K on an Oxford Diffraction Gemini diffractometer with an EOS CCD detector and Mo Kα radiation. Data collection and data reduction were

performed using Agilent's CrysAlisPro software.[19] Structure solution and refinement were performed with ShelXL[20], and Olex2 was used for graphical representation of the data.[21] Powder X-ray diffraction data were collected on a Rigaku MiniFlex 600 powder X-ray diffractometer. Chromatographic data were collected on either an Agilent 7890A GC with a 5979C MSD or on a Hewlett-Packard 5890 GC-FID. Columns employed were either an Agilent HP5-MS (30m x 0.25mm, 0.25μm) or a J&W Cyclosil-B (30m x 0.25mm, 0.25μm).

All molecular modeling calculations were performed using Gaussian 09[22] on the Virginia Tech Chemistry Department Cluster, "Cerebro", using the WebMO interface. Full geometry optimizations and single-point energy calculations of all structures in water were performed via density functional theory (DFT) with the Becke-3-parameter exchange functional[23] and the Lee–Yang–Parr correlation functional.[24,25] Because palladium is not covered in the cc-pVDZ basis set used, computations involving Pd employed Stuttgart/Dresden quasi-relativistic pseudopotentials.[26]

A total of eight distinct palladium(II)-glycine complexes were synthesized during this study. Their structures and corresponding compound numbers, as referenced in this chapter, are summarized in Figure 21 with syntheses described in the following sections.
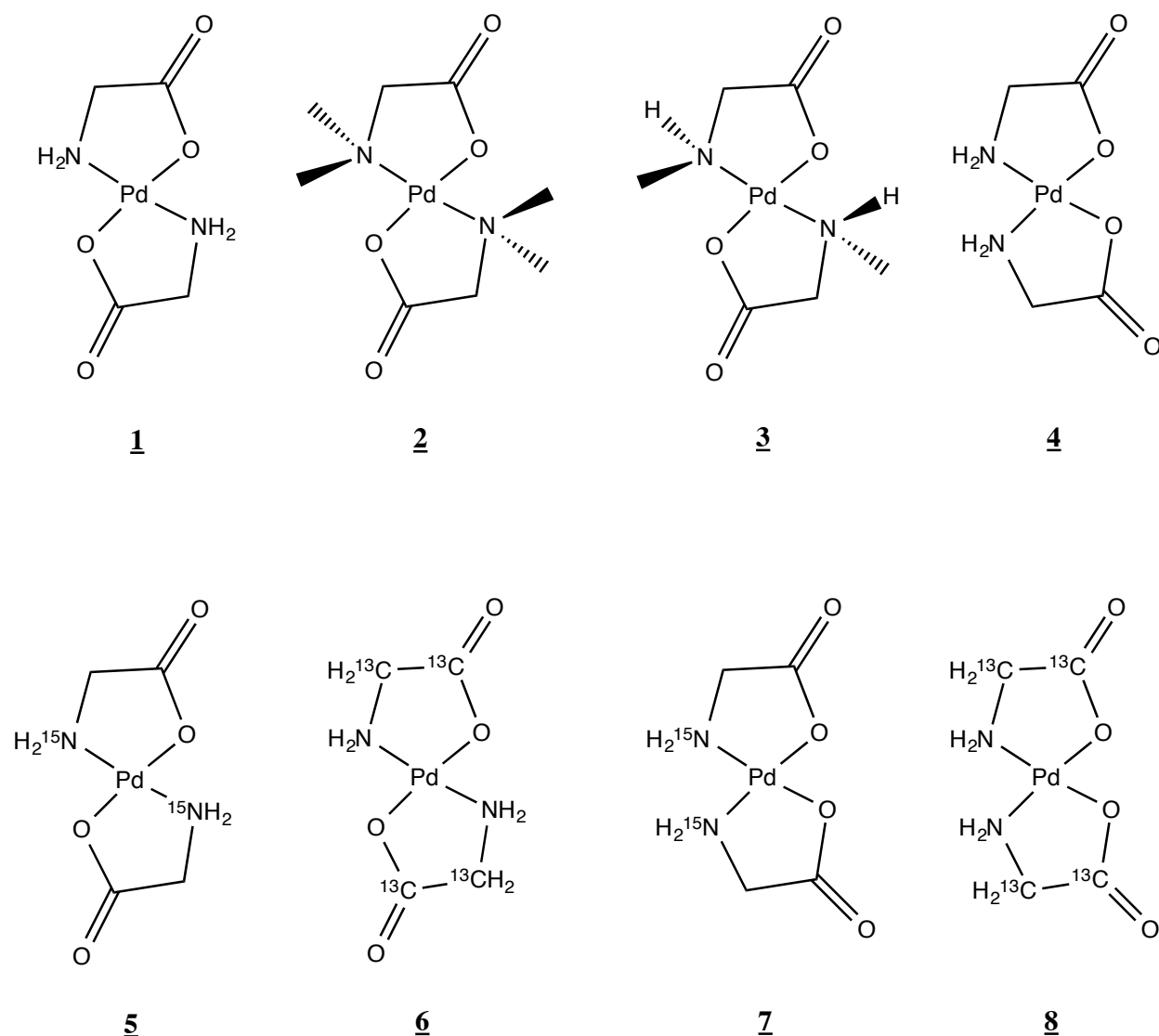
Figure 21. Structures and Corresponding Compound Numbers of Pd(II)-glycine Complexes

2.2.1   Synthesis of *trans*-bis(glycinato)palladium(II) (1, 5, 6)

A four dram vial was fitted with a magnetic stir bar and charged with 32.2 mg of palladium(II) acetate (0.1430 mmol) and 3.0 mL of 50/50 (v/v) acetone/water. The mixture was stirred until all solids had dissolved. To this solution was added 27.1 mg of glycine (0.3610 mmol), and the mixture was stirred overnight. The reaction solution turned from a clear red-orange to a clear pale-yellow supernatant with a pale-yellow precipitate. The supernatant was transferred via

pipette to a clean vial and allowed to evaporate to give clear yellow needles. The pale-yellow precipitate was washed with water and dried under vacuum. The combined yield of crystals and precipitate was 33.2 mg (0.1304 mmol, 91% yield). The same procedure was used to prepare the ^{15}N-enriched (**5**) and the doubly ^{13}C-enriched (**6**) variants, using ^{15}N and ^{13}C labeled glycine, respectively. *Trans*-Pd($C_2H_4NO_2$)$_2$ (**1, 5, 6**) were identified on the basis of the following data: ^{1}H NMR (400 MHz, 95/5 H_2O/D_2O) δ 3.55 (t, J = 6.4 Hz), 3.53 (t, J = 6.9 Hz) ppm. ^{13}C NMR (126 MHz, 95/5 H_2O/D_2O) δ 189.66 (d, J = 57.5 Hz), 188.04 (d, J = 57.3 Hz), 175.26 (d, J = 53.1 Hz), 50.39 (d, J = 57.3 Hz), 48.84 (d, J = 57.5 Hz), 44.49 (d, J = 53.3 Hz) ppm. ^{15}N NMR (61 MHz, 95/5 H_2O/D_2O, ref. to urea) δ -34.89, -26.52 ppm. HRMS/ESI+ (m/z): [M+H]+ calcd for Pd($C_2H_4NO_2$)$_2$, 254.9597; found, 254.9593. Anal. Calcd. for $C_4H_8N_2O_4Pd$: C, 18.80%; H, 3.55%; N, 11.01%. Found: C, 19.09%; H, 3.19%; N, 11.06%. FTIR (solid state): 3234, 3106, 1592 cm^{-1}. UV-VIS (H_2O): λ_{max}=194 nm, ε=26793 M^{-1}cm^{-1}; λ_{max}=323 nm, ε=244 M^{-1}cm^{-1}.

2.2.2 Synthesis of *trans*-bis(*N,N*-dimethylglycinato)palladium(II) (2)

A four dram vial was fitted with a magnetic stir bar and charged with 33.7 mg of palladium(II) acetate (0.1500 mmol) and 2.5 mL of 2/1 (v/v) acetone/water. The mixture was stirred until all solids had dissolved. To this mixture was added *N,N*-dimethylglycine (31.2 mg, 0.3000 mmol) and stirred overnight. The reaction solution changed from a clear red-orange to a clear pale-yellow supernatant with a pale yellow precipitate. The supernatant was transferred via pipette to a clean vial and allowed to evaporate to give clear yellow needles which were used for X-ray diffraction. The precipitate was washed with water and dried under vacuum. The combined yield of crystals and precipitate was 43.3 mg (0.1394 mmol, 93% yield). *Trans*-Pd($C_4H_8NO_2$)$_2$ (**2**) was identified on the basis of the following data: ^{1}H NMR (400 MHz, Deuterium Oxide) δ

3.41 (s, 2H), 2.46 (s, 6H) ppm. HRMS/ESI+ (m/z): [M+H]+ calcd for Pd(C$_4$H$_8$NO$_2$)$_2$, 311.0223; found, 311.0216. Anal. Calcd. for Pd(C$_4$H$_8$NO$_2$)$_2$: C, 30.93%; H, 5.19%; N, 9.02%. Found: C, 31.05%; H, 5.23%; N, 9.03%. FTIR (solid state): $\nu_{C=O}$ 1636 cm^{-1}. UV-VIS (H$_2$O): λ_{max}= 205 nm, ε= 22899 M^{-1}cm^{-1}; λ_{max}= 316 nm, ε= 285 M^{-1}cm^{-1}.

2.2.3   Synthesis of *trans*-bis(*N*-methylglycinato)palladium(II) (3)

A four dram vial was fitted with a magnetic stir bar and charged with 35.2 mg of palladium(II) acetate (0.1570 mmol) and 3.0 mL of 50/50 (v/v) acetone/water. The mixture was stirred until all solids had dissolved. To this mixture was added 31.3 mg of *N*-methylglycine (0.3510 mmol) and stirred overnight. The mixture changed from a clear red-orange solution to a clear pale-yellow supernatant with a pale yellow precipitate. The supernatant was transferred via pipette to a clean vial and allowed to evaporate to give clear yellow needles. The precipitate was washed with water and dried under vacuum. The combined yield of crystals and precipitate was 41.3 mg (0.1461 mmol, 93% yield). *Trans*-Pd(C$_3$H$_6$NO$_2$)$_2$ (**3**) was identified on the basis of the following data: ^{1}H NMR (600 MHz, D$_2$O) **1**:   δ 3.58 (d, J = 13.3 Hz, 1H), 3.55 (d, J = 13.3 Hz, 1H), 3.33 (d, J = 11.8 Hz, 1H), 3.31 (d, J = 11.8 Hz, 1H), 2.34 (d, J = 0.9 Hz, 6H) ppm;   **2**: δ 3.77 (d, J = 15.0 Hz, 1H), 3.20 (d, J = 8.8 Hz, 1H), 2.47 (s, 3H) ppm;   **3**: δ 3.80 (d, J = 14.8 Hz, 1H), 3.22 (d, J = 8.6 Hz, 1H), 2.52 (s, 3H) ppm. ^{13}C NMR (151 MHz, Deuterium Oxide) δ 184.38, 183.02, 182.75, 58.44, 58.19, 56.89, 41.28, 40.46, 39.55, 39.52 ppm. HRMS/ESI+ (m/z): [M+H]+ calcd for Pd(C$_3$H$_6$NO$_2$)$_2$, 282.9910; found, 282.9930. Anal. Calcd. for Pd(C$_3$H$_6$NO$_2$)$_2$: C, 25.50%; H, 4.28%; N, 9.91%. Found: C, 25.56%; H, 4.34%; N, 9.91%.FTIR (solid state): 3107, 1625 cm^{-1}. UV-VIS (H$_2$O): λ_{max}=202 nm, ε=37605 M^{-1}cm^{-1}; λ_{max}=321 nm, ε=373 M^{-1}cm^{-1}.

2.2.4   Synthesis of *cis*-bis(glycinato)palladium(II) (4, 7, 8)

A 10-mL Erlenmeyer flask was fitted with a magnetic stir bar, glycine (0.5573 g, 7.424 mmol) and water (3.0 mL). The mixture was stirred until solids had completely dissolved then heated in a 70 °C water bath. To this mixture was added palladium(II) chloride (0.3061 g, 1.726 mmol). Stirring was continued for 30 minutes. The reaction solution changed from a red-brown suspension to a clear, pale orange-red solution. The reaction was cooled in an ice water bath (0 °C) and then placed in a refrigerator at 4 °C overnight to give clear yellow needles with an orange-red supernatant. The supernatant was decanted and the crystals were washed with cold water (2 x 1 mL), cold ethanol (2 x 1 mL), and followed by diethyl ether (2 x 1 mL) and dried under vacuum to yield the product (0.3911 g, 1.5365 mmol, 89% yield). The same procedure was utilized to prepare the ^{15}N-enriched (**7**) and the doubly ^{13}C-enriched (**8**) variants, using ^{15}N and ^{13}C labeled glycine respectively. *Cis*-Pd(C$_2$H$_4$NO$_2$)$_2$ (**4, 7, 8**) was identified on the basis of the following data: ^{1}H NMR (400 MHz, 95/5 H$_2$O/D$_2$O) δ 3.55 (t, J = 6.4 Hz), 3.52 (t, J = 6.5 Hz) ppm. ^{13}C NMR (126 MHz, Deuterium Oxide) δ 189.65 (d, J = 57.5 Hz), 188.04 (d, J = 57.4 Hz), 174.62 (d, J = 55.2 Hz), 50.39 (d, J = 57.2 Hz), 48.85 (d, J = 57.9 Hz), 44.10 (d, J = 54.8 Hz). ^{15}N NMR (61 MHz, 95/5 H$_2$O/D$_2$O, ref. to urea) δ -34.85, -26.50 ppm. HRMS/ESI+ (m/z): [M+H]+ calcd for C$_4$H$_8$N$_2$O$_4$Pd, 254.9597; found, 254.9592. Anal. Calcd. for C$_4$H$_8$N$_2$O$_4$Pd: C, 18.80%; H, 3.55%; N, 11.01%. Found: C, 19.09%; H, 3.19%; N, 11.06%. FTIR (solid state): 3221, 3118, 1625 cm^{-1}. UV-VIS (H$_2$O): λ_{max}<190 nm, ε>21108 M^{-1}cm^{-1}; λ_{max}=324 nm, ε=182 M^{-1}cm^{-1}.

2.2.5   Attempted syntheses of *cis*-bis(*N*-methylglycinato)palladium(II) and *cis*-bis(*N,N*-dimethylglycinato)palladium(II)

Attempts to synthesize the *cis* isomers of the N-methylglycine and N,N-dimethylglycine complexes using the same procedures outlined above for the *cis*-bis(glycinato)palladium(II) complex (Compounds 4, 7, and 8) were unsuccessful. No reaction was noted in either case.

2.2.6   General Oxidative Coupling of Phenylboronic Acid and Methyl Tiglate

A 10 mL roundbottom flask was charged with 51.8 mg (0.4248 mmol) of phenylboronic acid, 153.1 μL of methyl tiglate (1.2745 mmol), 5.4 mg of *cis*-bis(glycinato)palladium(II) (0.0212 mmol), 3 mL of DMF, and a micro stir bar. The flask was purged with oxygen gas and an oxygen balloon fitted. The reaction was then stirred under O_2 for 48 hours to ensure complete consumption of the phenylboronic acid substrate. The reaction was diluted with 10 mL of ethyl acetate and washed twice with 10 mL of water. The organic layer was retained, dried over anhydrous $MgSO_4$, filtered and concentrated under vacuum. A portion of the residue was re-dissolved in chloroform and separated chromatographically by GC-MS or GC-FID. The remaining residue was chromatographed on silica gel (hexanes/ethyl acetate @ 40:1). The cross-coupled products were characterized by comparing their NMR and/or mass spectral data to that previously reported in the literature.

2.3   RESULTS AND DISCUSSION

In the following discussions, the *trans* bis amino acid complexes **1**, **2**, **3**, **5** and **6** were synthesized via the following general reaction scheme (Figure 22):
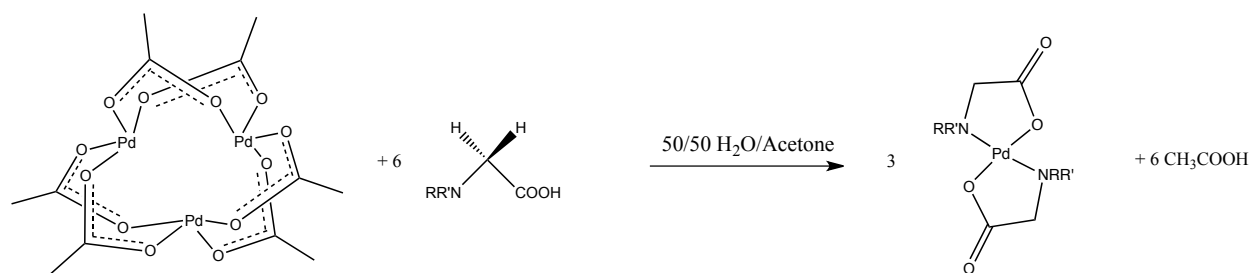
Figure 22. General reaction scheme for the synthesis of *trans*-palladium(II)-glycinate complexes.

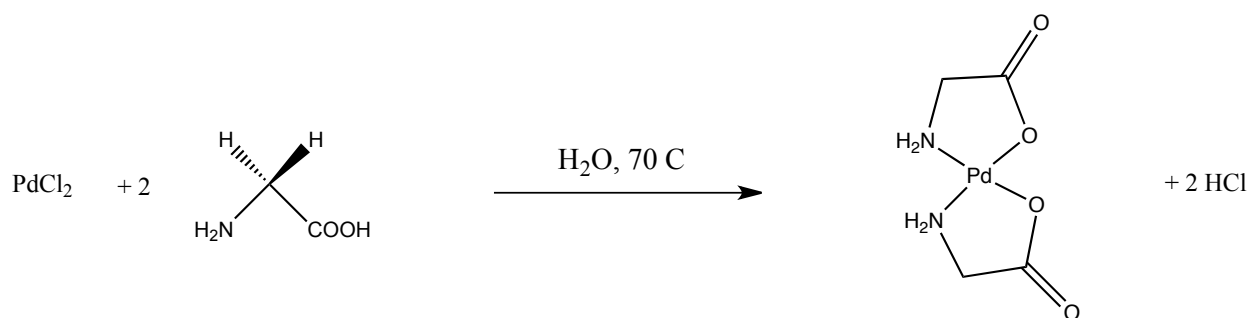The *cis* complexes **4, 7** and **8** were synthesized in a slightly different manner, as shown in Figure 23, below.

Figure 23. General reaction scheme for the synthesis of *cis*-palladium(II)-glycinate complexes.

2.3.1 *Trans*-bis(glycinato)palladium(II)

The simplest Pd(II)-amino acid complexes are those of the bis-glycinato chelates. Glycine, being achiral, is limited to the formation of only the *cis* or the *trans* isomers of the complex. Compounds **1, 5, and 6** were prepared as the *trans* isomer via the scheme shown in Figure 2 and confirmed by X-ray crystal structure analysis (Figure 24).
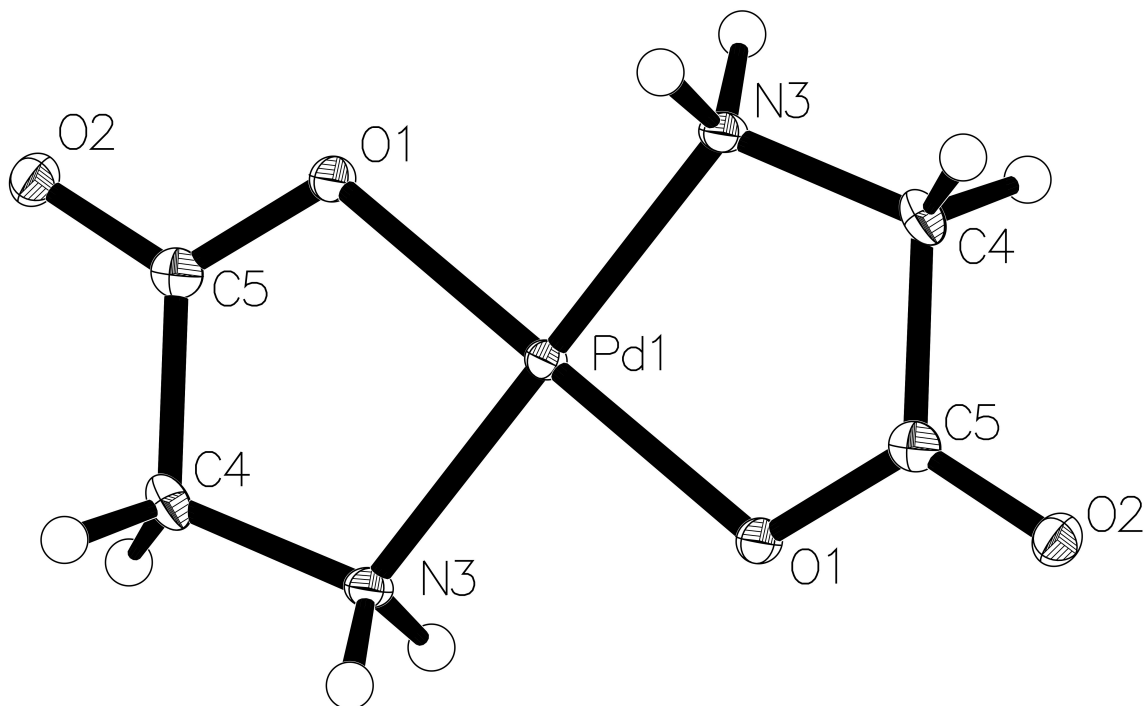
Figure 24. Thermal ellipsoid plot of the molecular structure of crystalline *trans*-Bis(glycinato)palladium(II), 1. Thermal ellipsoids are shown at the 50% probability level.

The complex crystallizes in the $P2_1/n$ space group. Pd-N and Pd-O bond lengths are 2.033 Å and 1.997 Å, respectively. N-Pd-O bond angles are 83.959 degrees for each chelate ring and 96.041 degrees between the chelate rings. All bond lengths and angles are within the ranges reported for similar d^8 metal chelates[27-32], and this newer 100 K data offers significant improvement in precision over that reported by Baidina at room temperature.[14] In addition, the current structure was refined in $P2_1/n$, as opposed to $P2_1/c$, in which the unit cell has the recommended smaller oblique value of β. Molecular modeling calculations place the *trans* isomer 0.56 kJ/mol lower in energy than the *cis* isomer.[22] Intermolecular hydrogen bonding is observed between the amine protons and the non-coordinated carboxyl oxygen atoms (Figure 25).
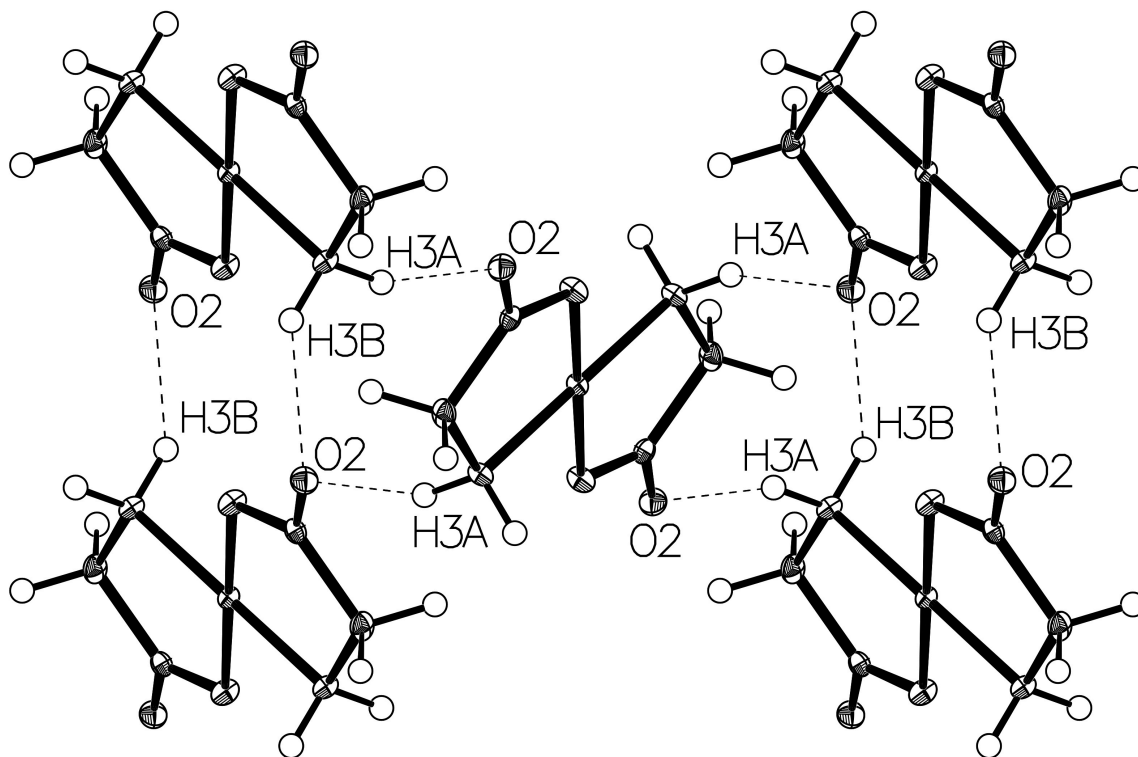
Figure 25. Crystal packing diagram of (1) as viewed along [100] showing the intermolecular hydrogen bonding motif.

The ^{1}H NMR spectrum in 95/5 H_2O/D_2O shows two inequivalent triplets for the methylene protons at δ 3.55 and 3.53 ppm, which are shifted upfield from the non-coordinated ligand at 3.57 ppm, indicating that these protons are slightly more shielded upon coordination. Interestingly both resonances collapse to singlets in D_2O, indicting that proton exchange does occur at the coordinated nitrogen atom. Krylova reported resonances for both –NH$_2$ (δ 4.85 and 4.51 ppm, singlets) and –CH$_2$- (3.09 ppm, multiplet) groups in a mixture of the *cis* and *trans* glycinate isomers in DMSO-*d6*.[16] The amine resonances disappeared on addition of D_2O, confirming what we observed with respect to amine proton exchange. They report that the methylene protons resolved into two singlets at δ 3.14 and 3.04 ppm on addition of D_2O and use this as evidence of the two isomers, providing a proposed pathway for *cis-trans* isomerization

through a DMSO-coordinated trigonal-bipyramidal intermediate. Our data show no evidence of *cis-trans* isomerization in H_2O or D_2O, which is expected given that free water is not likely to coordinate strongly to a chelated square planar palladium(II) center and displace a chelate. An intriguing possibility however, is the formation of aquo complexes upon solvation and this theory is examined in detail below. ^1H NMR spectra of the ^{15}N-enriched *trans* complex **5** were also obtained and showed the same triplets for the methylene protons. The amine protons were not observed, however two-bond J^{15}_{NCH} coupling of 0.9 Hz was observed for the *trans* glycine complex. ^{13}C NMR spectra of the doubly ^{13}C enriched complex show three peaks each for the carbonyl (189.7, 188.0, and 175.3 ppm) and methylene carbons (50.4, 48.9, and 44.5 ppm), and ^1H-^{15}N HSQC (Heteronuclear Single Quantum Coherence) NMR spectroscopy shows two resonances for the amine nitrogens at -34.89 and -26.52 ppm. The typical isotopic splitting pattern for palladium was observed in the HRMS spectrum with peaks at 252.960, 253.961, 256.962, and 258.962 amu.

2.3.2   Aquo Complex Formation

As mentioned above, there is an intriguing possibility of aquo complex formation that can occur with these bis-chelate complexes. The ^{13}C NMR data for the *trans*-bis(glycinate) complex clearly shows the presence of three ligand environments. Taken alongside the observation from powder X-ray diffraction that the bulk material does not undergo *cis-trans* isomerization in solution (see below, Section 2.3.9) we are left with the formation of aquo complexes as the most likely explanation for the observed spectroscopy. There is no evidence of free ligand in the NMR spectra, nor were any species other than a single crystal of the complex and D_2O solvent present for the NMR experiment. If *cis/trans* isomerization is not occurring and the ligands are

not de-coordinating from the metal, the only plausible explanation for different ligand environments is the formation of aquo complexes. This possibility is also critical to the potential catalytic activity of these complexes, as one end of the chelate must be able to de-coordinate in order to generate open *cis* reactive sites on the square planar metal center. The resulting geometries are depicted in Figure 26 (below) for the *trans*-bis(glycinate) complex. Although not shown, this scheme holds true for the *trans*-bis(*N,N*-dimethylglycinato) complex as well. Inversion at the nitrogen atom has no effect on the stereochemistry as the nitrogen atoms in these cases are symmetrically substituted. Asymmetric alkylation of the nitrogen atom, as seen for *N*-methylglycine, does affect the stereochemistry and will be discussed in turn.
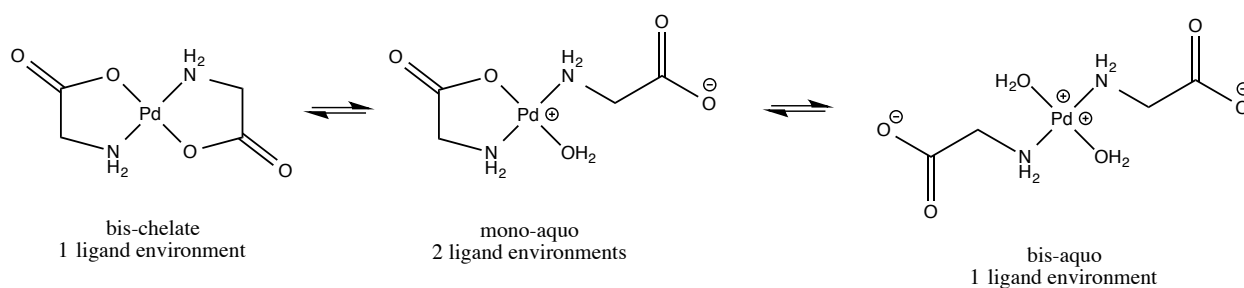

Figure 26. Aquo complex formation and ligand environments for symmetrically *N*-substituted amino acid complexes.

Starting with the bis-chelate, there is only one ligand environment for each carbon. The complex is C_2 symmetric, therefore the carbonyl carbons are related by symmetry as are the methylene carbons. In the ^{13}C NMR spectrum we would expect to see one resonance for each carbon type. The mono-aquo complex exhibits two ligand environments for each type of carbon. The chelated ligand will have one set of resonances, different from those of the bis-chelate, as the magnetic field environment has changed with decoordination of one of the ligands. The decoordinated ligand will also have a distinct set of resonances. We should therefore see two

sets of signals for each carbon type if the mono-aquo complex is present. Finally, in the case of the bis-aquo complex we return to a C_2 symmetric molecule and will observe one set of resonances for each type of carbon.

The bis-chelate and bis-aquo complexes are both C_2 symmetric and both will have one set of resonances for each type of carbon. In the case of *trans*-bis(glycinato)palladium(II) there are three ligand environments observed in the ^{13}C (doubly enriched) NMR spectrum (Figure 27, Figure 28).
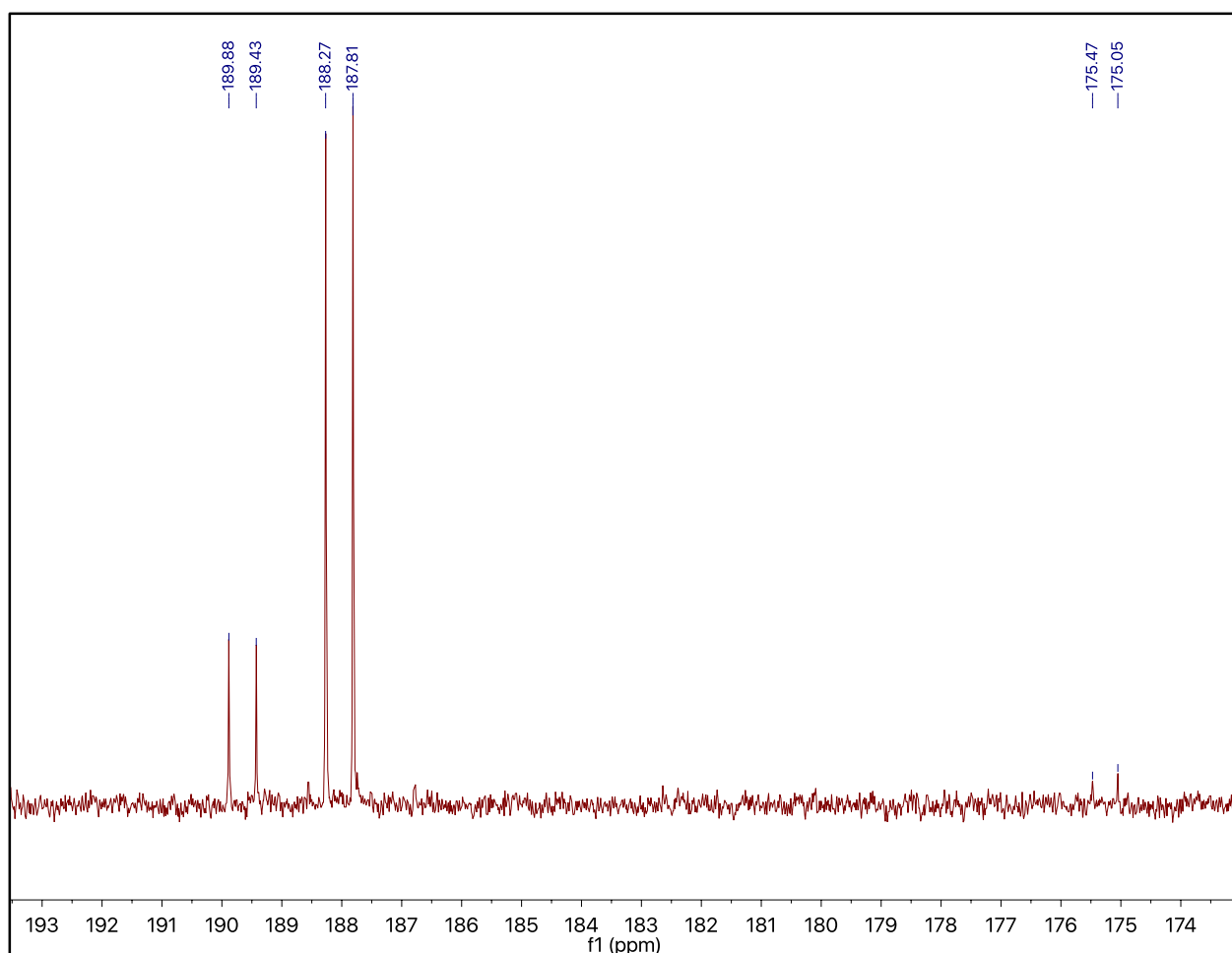

Figure 27. ^{13}**C (doubly enriched) NMR spectrum of *trans*-bis(glycinato)palladium(II) showing three ligand environments for the carbonyl carbon.**
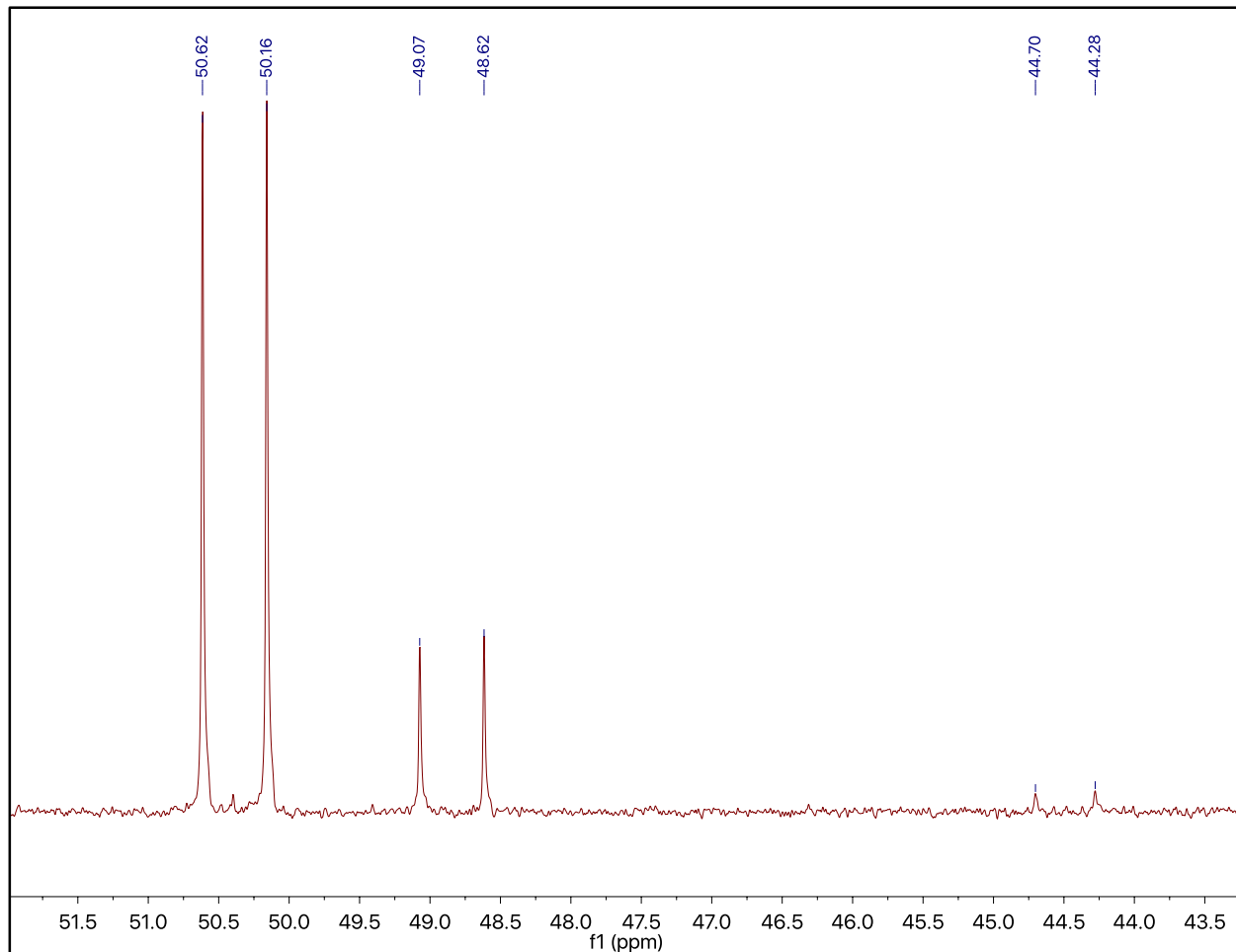
Figure 28. ¹³C (doubly enriched) NMR spectrum of *trans*-bis(glycinato)palladium(II) showing three ligand environments for the methylene carbon.

This necessitates that there is mono-aquo complex in solution along with either the bis-chelate or the bis-aquo. We turn to DFT calculations in order to predict which species is the more stable and most likely observed. DFT calculations performed on each of the aforementioned complexes yields the following order of stability in water:

Trans-Pd-(GLY)$_2$ isomer (Fig. 26)	ΔE from bis-chelate in water, kJ/mol
Bis-chelate	0
Mono-aquo	-4.0
Bis-aquo	-8.5

Table 2. DFT calculated energies of aquo complex species of trans-bis(glycinato)palladium(II) in water.

From this data it is apparent that the three ligand environments observed in the ^{13}C NMR spectrum arise from the presence in solution of the mono-aquo and bis-aquo complexes. Their DFT optimized geometries are shown below (Figure 29, Figure 30).
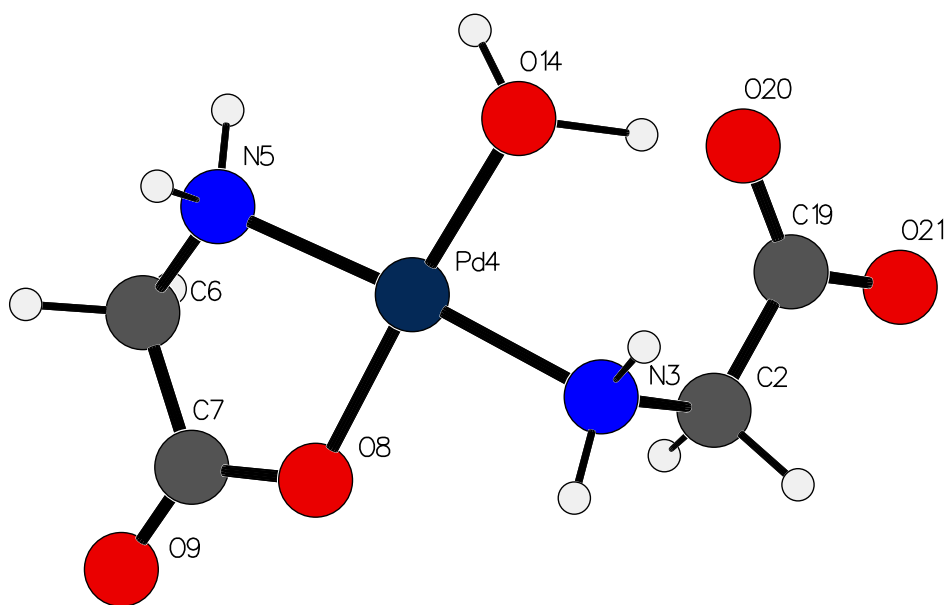

Figure 29. DFT calculated structure of trans-bis(glycinato)palladium(II) mono-aquo complex.
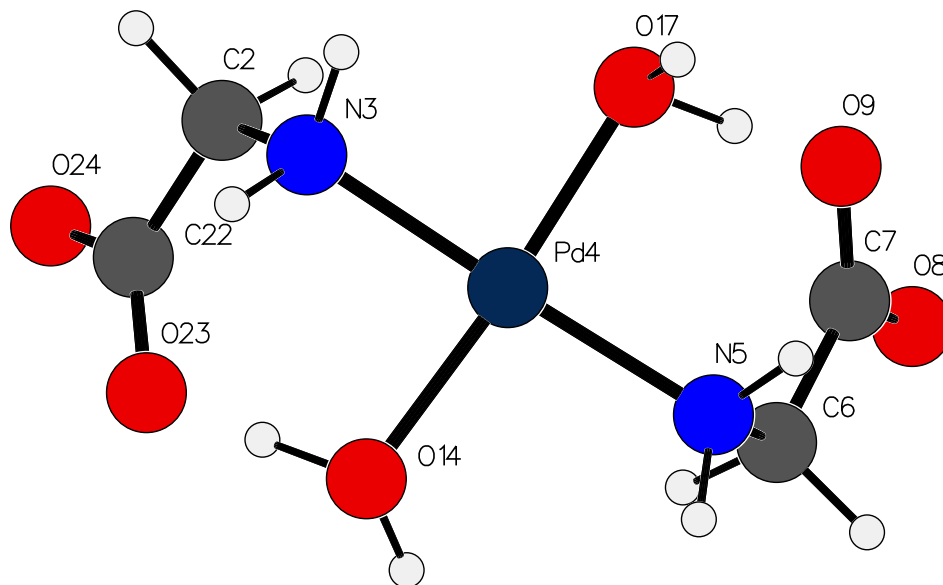
Figure 30. DFT calculated structure of trans-bis(glycinato)palladium(II) bis-aquo complex.

A lingering discrepancy with this analysis, that remains unexplained at this time, is the fact that the mono-aquo complex requires both two separate ligand environments and that the relative peak intensities of those signals be the same. In the case of *trans*-bis(glycinato)palladium(II) the three carbon signals for each type of carbon are all of differing intensities. This remains an unsolved issue and bears further study and clarification.

In the case of an asymmetrically substituted nitrogen atom, as is the case for *N*-methylglycine, we must take into account the diastereomeric differences that arise from inversion at the nitrogen atom.
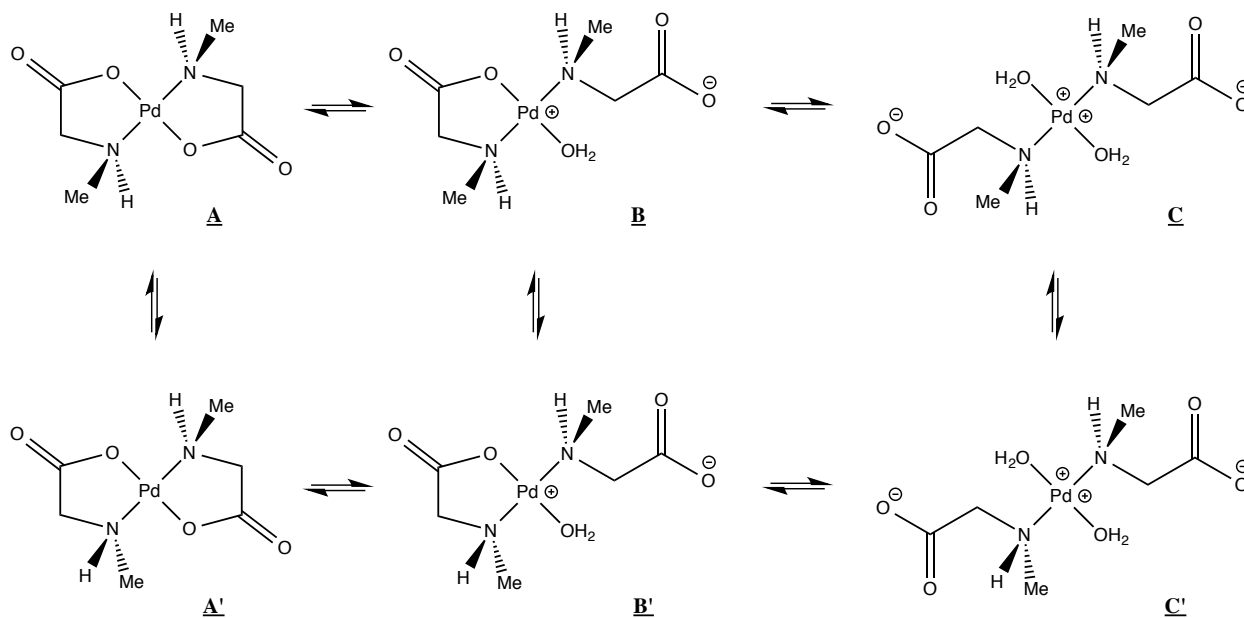
Figure 31. Aquo complex formation for asymmetrically *N*-substituted amino acid complexes.

Isomers **A** and **A'** are C_2 and C_i symmetric, respectively, and each have one ligand environment. The methylene protons in the ^1H NMR spectrum will be observed as a pair of doublets with a singlet for the *N*-methyl protons, and three carbon peaks in the ^{13}C NMR. The remaining isomers (**B**, **B'**, **C**, **C'**) pose a more complicated situation in that they all generate diastereomers. In each case there are two chiral nitrogen centers per molecule resulting in a possible four diastereomers for each aquo complex. This is somewhat simplified by the fact that the four diastereomers exist as two enantiomeric pairs. For the mono-aquo complex this will result in four pairs of doublets for the methylene protons and two singlets for the *N*-methyl protons. The ^{13}C NMR should then have a total of six carbon resonances. The bis-aquo complex re-establishes C_2/C_i symmetry and like the bis-chelate will show a pair of doublets for the methylene protons, a singlet for the *N*-methyl protons, and three peaks in the ^{13}C NMR spectrum.

2.3.3   *Trans*-bis(*N,N*-dimethylglycinato)palladium(II)

An analogous complex (Compound **2**) in which the amine protons were both replaced with methyl groups was synthesized in an effort to understand the effects of *N*-alkylation on the formation of Pd(II)-AA complexes. When *N,N*-dimethylglycine was used as the ligand, *trans*-bis(*N,N*-dimethylglycinato)palladium(II) is formed (Figure 32).
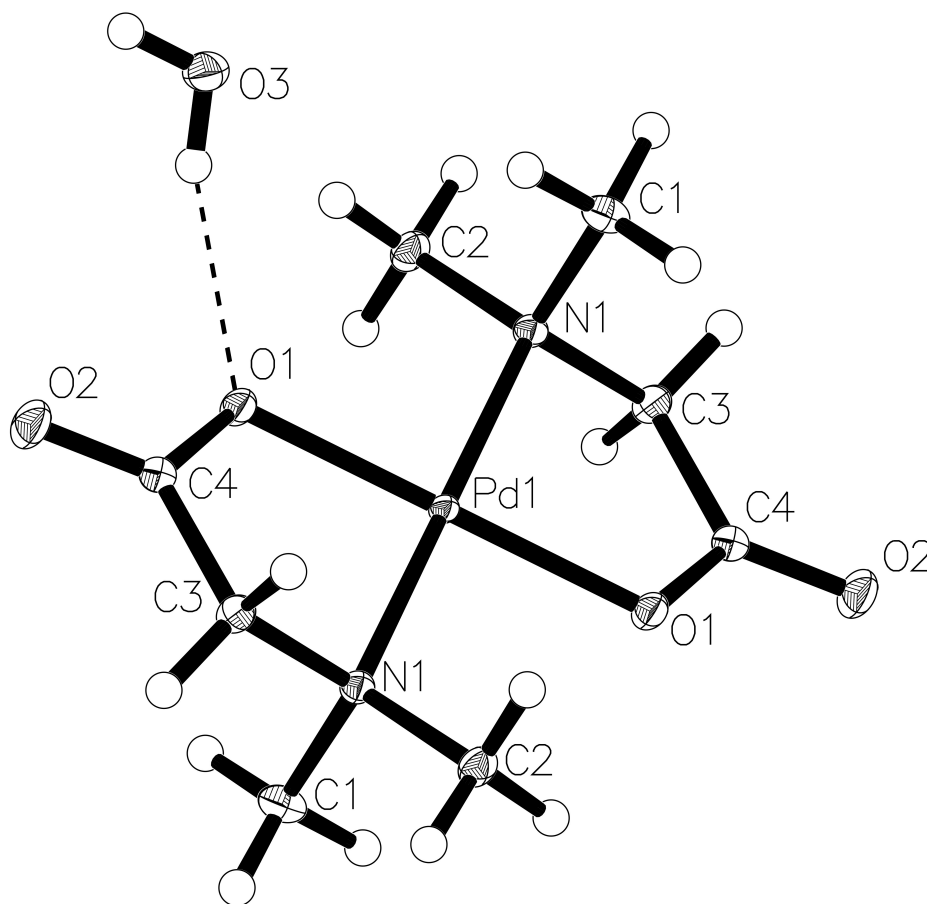

Figure 32. Thermal ellipsoid plot of the molecular structure of crystalline trans-bis(N,N-dimethylglycinato)palladium(II) hydrate, 2. Thermal ellipsoids are shown at the 50% probability level.

X-ray crystallographic analysis confirmed formation of the *trans* isomer, which would be expected based upon considerations of the steric bulk about the nitrogen atoms and that using

Pd(OAc)$_2$ usually yields the *trans* isomer. Placing the fully methylated amine nitrogens adjacent to one another results in such a degree of steric crowding that formation of the *cis* complex is not favorable. The *trans* complex, **2**, crystallizes in the P2$_1$/c space group. Pd-N and Pd-O bond lengths are 2.0481 Å and 2.0010 Å, respectively. N-Pd-O bond angles are 83.474 degrees in the chelate ring and N-Pd-O bond angles between the chelate rings are 96.531 degrees. All bond lengths and angles are within the ranges reported for similar d^8 metal chelates[27-32]. Molecular modeling calculations identify the *trans* isomer as the most stable isomer, the exact value depending upon the use of water solvent or no solvent in the calculations.[22] In the presence of water, the cis complex is less stable by 17.3 kJ/mol but in the absence of water, the difference increases greatly to 58.8 kJ/mol.

In the crystal lattice no intermolecular complex-to-complex hydrogen bonding is present; however, water is incorporated into the lattice and hydrogen bonding between water molecules in the crystal lattice and the carboxylate oxygen atom was observed (Figure 33).
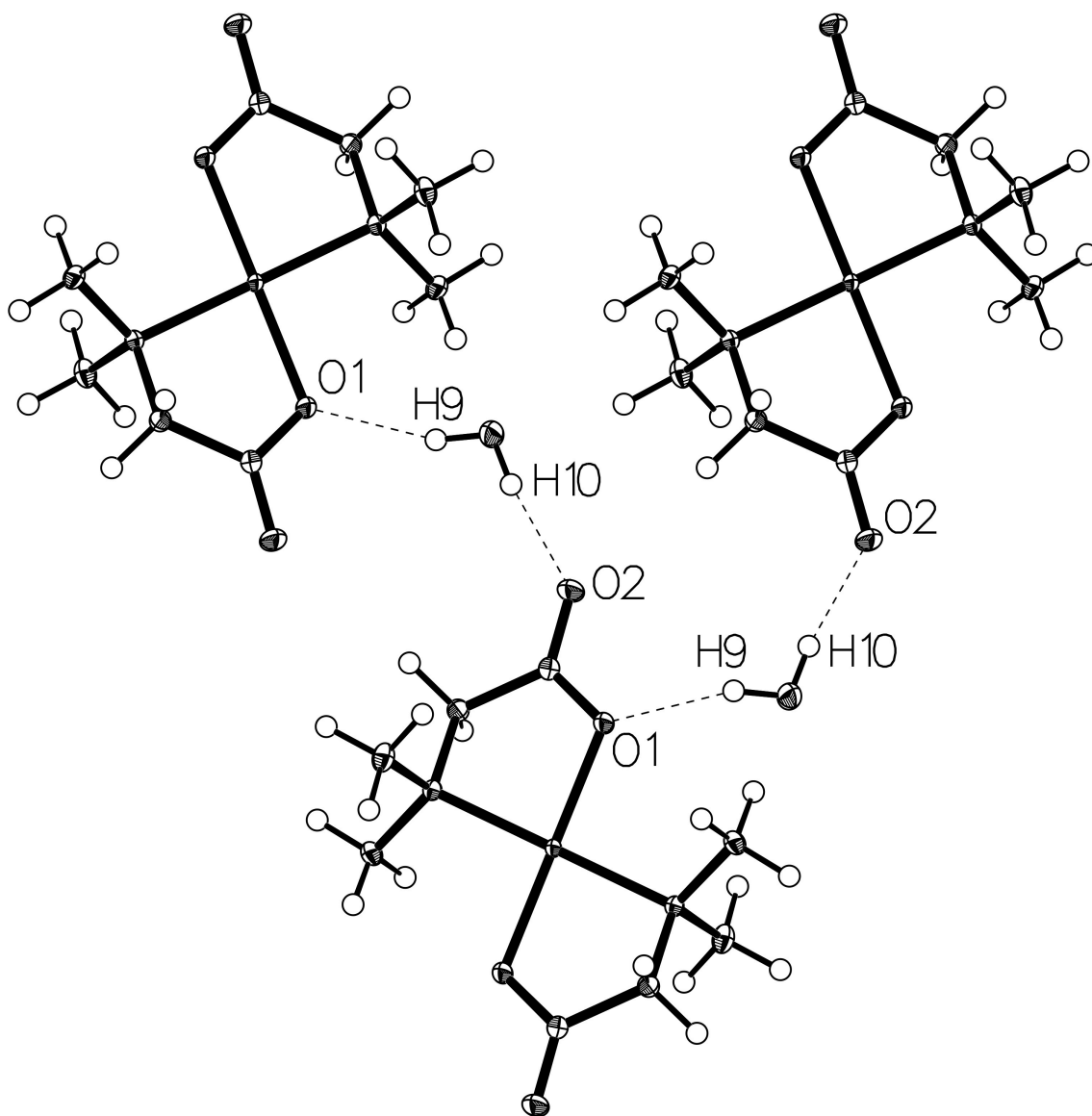
Figure 33. Crystal packing diagram of (2) as viewed along [101] showing the hydrogen bonding motif.

The ^{1}H NMR spectrum in D$_2$O shows a singlet for the methylene protons at δ 3.56 ppm, which is shifted upfield from the non-coordinated ligand at 3.71 ppm. The methyl groups resonate at δ 2.60 ppm versus 2.91 ppm in the free ligand indicating that these protons are more shielded on coordination to the metal center. Based on the proton NMR data, there is no evidence to suggest

that multiple aquo species exist in solution. DFT calculations place the bis-chelate 3 kJ/mol lower in energy than the bis-aquo, suggesting that the observed species is in fact the bis-chelate. Again, the typical isotopic splitting pattern for palladium is observed in the HRMS spectrum with peaks at 309.0217, 310.0231, 313.0219, and 315.0230 amu.

2.3.4 *Trans*-bis(*N*-methylglycinato)palladium(II)

In an effort to more fully understand the effects of N-methylation on hydrogen bonding, on molecular geometry and on crystal packing, *trans*-bis(*N*-methylglycinato)palladium(II) was synthesized (Compound **3**, Figure 34) using *N*-methylglycine as the ligand.
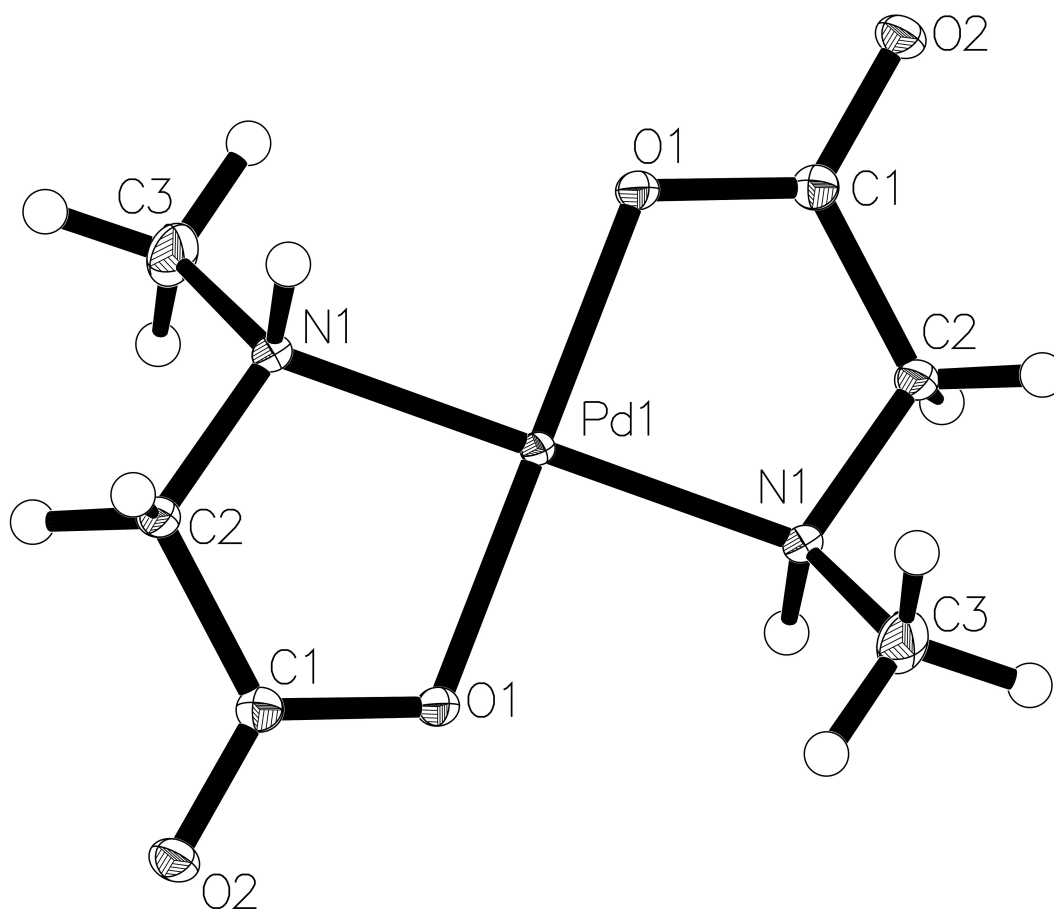
Figure 34. Thermal ellipsoid plot of the molecular structure of crystalline trans-bis(*N*-methylglycinato)palladium(II), 3. Thermal ellipsoids are shown at the 50% probability level.

N-methylglycine allows a degree of hydrogen bonding and steric control about the amine nitrogen atom in between that of glycine and *N,N*-dimethylglycine. There are seven different isomeric forms possible with this complex (Figure 35). The complexes can be *cis* or *trans*. The *cis* isomer can have three possible stereoisomers: the meso compound (**3a**) and the enantiomeric pair *cis*-(S,S) (**3b**) and *cis*-(R,R) (**3c**). The *trans* isomer has four possible stereoisomers: trans-(R,R) (**3d**), trans-(S,S) (**3e**), trans-(S,R) (**3f**), and trans-(R,S) (**3g**).
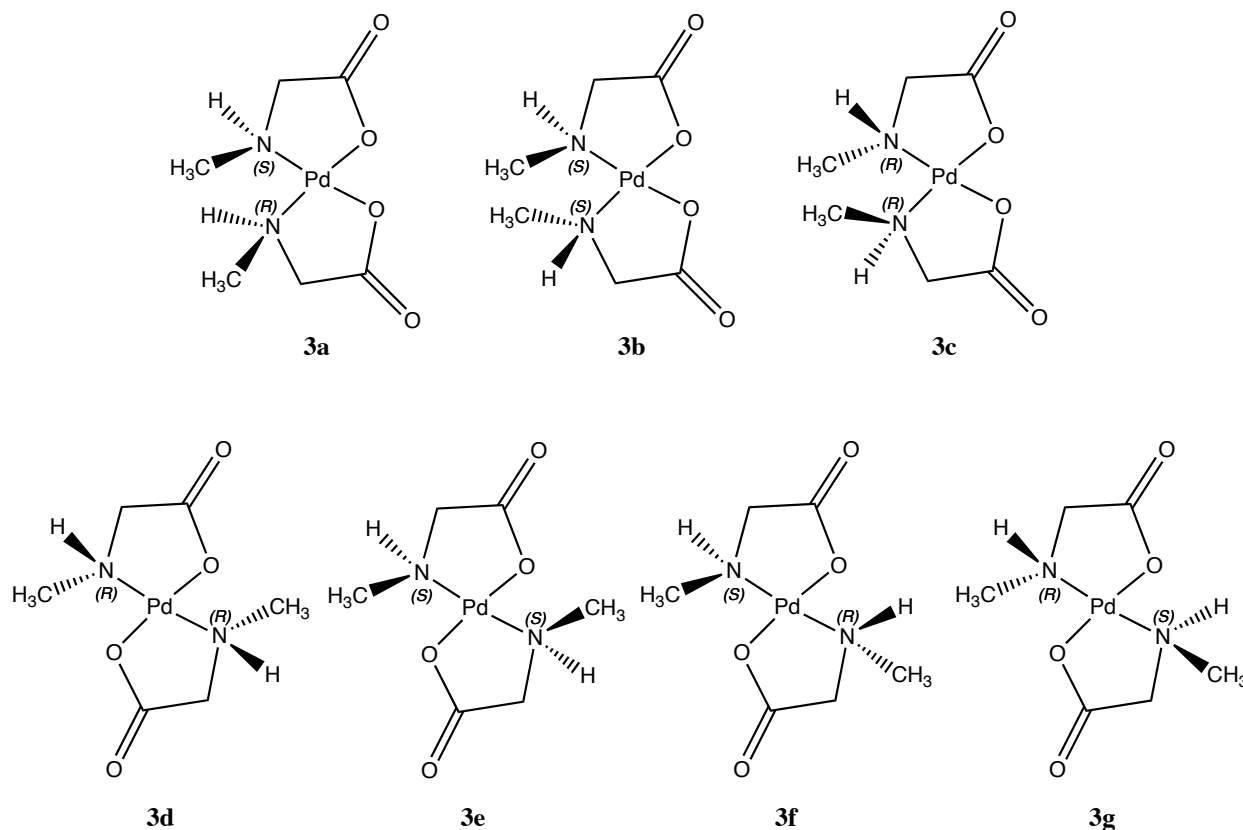
Figure 35. The seven possible isomers of bis(N-methylglycinato)palladium(II). Clockwise from upper left: cis-meso, cis-(S,S), cis-(R,R), trans-(R,S)= trans-(S,R), trans-(S,S), and trans-(R,R).

X-ray crystallography indicates that compound **3** crystallizes as the *trans*-(R,S) isomer, **3f**. The complex crystallizes in the P2$_1$/n space group with Pd-N and Pd-O bond lengths of 2.0341Å and 1.9921Å, respectively. N-Pd-O bond angles are 84.639 degrees in the chelate ring and N-Pd-O bond angles between the chelate rings are 95.361 degrees. All bond lengths and angles are within the ranges reported for similar d^8 metal chelates[27-32]. DFT calculations carried out on a water solution show that the *trans*-(R,S)/(S,R) isomers have the lowest calculated steric energy of all the isomers with the next lowest energy isomer set, the trans-(S,S)/(R/R) being +0.52 kJ/mol higher in energy; space filling models suggest that the *cis*-meso isomers may be unfavorable, however the calculated energy values are not unreasonable (Table 3).[22] The isomers

are ranked in the following order based on calculated molecular energy: *trans*-(R,S)/(S/R) < *trans*-(R,R)/(S,S) < *cis*-(R,R)/(S,S) < *cis*-meso.

Pd-(NMG)$_2$ isomer (Fig. 33)	ΔE from lowest energy isomer, kJ/mol in water	ΔE from lowest energy isomer, kJ/mol no solvent
3b, 3c	+13.7	+55.2
3a	+6.5	+49.9
3d, 3e	+0.52	+0.38
3f	0.0	0.0

Table 3. DFT energies for Pd(NMG)$_2$ isomers.

The amine proton forms an intermolecular hydrogen bond with the carboxylate oxygen of an adjacent molecule (Figure 36).
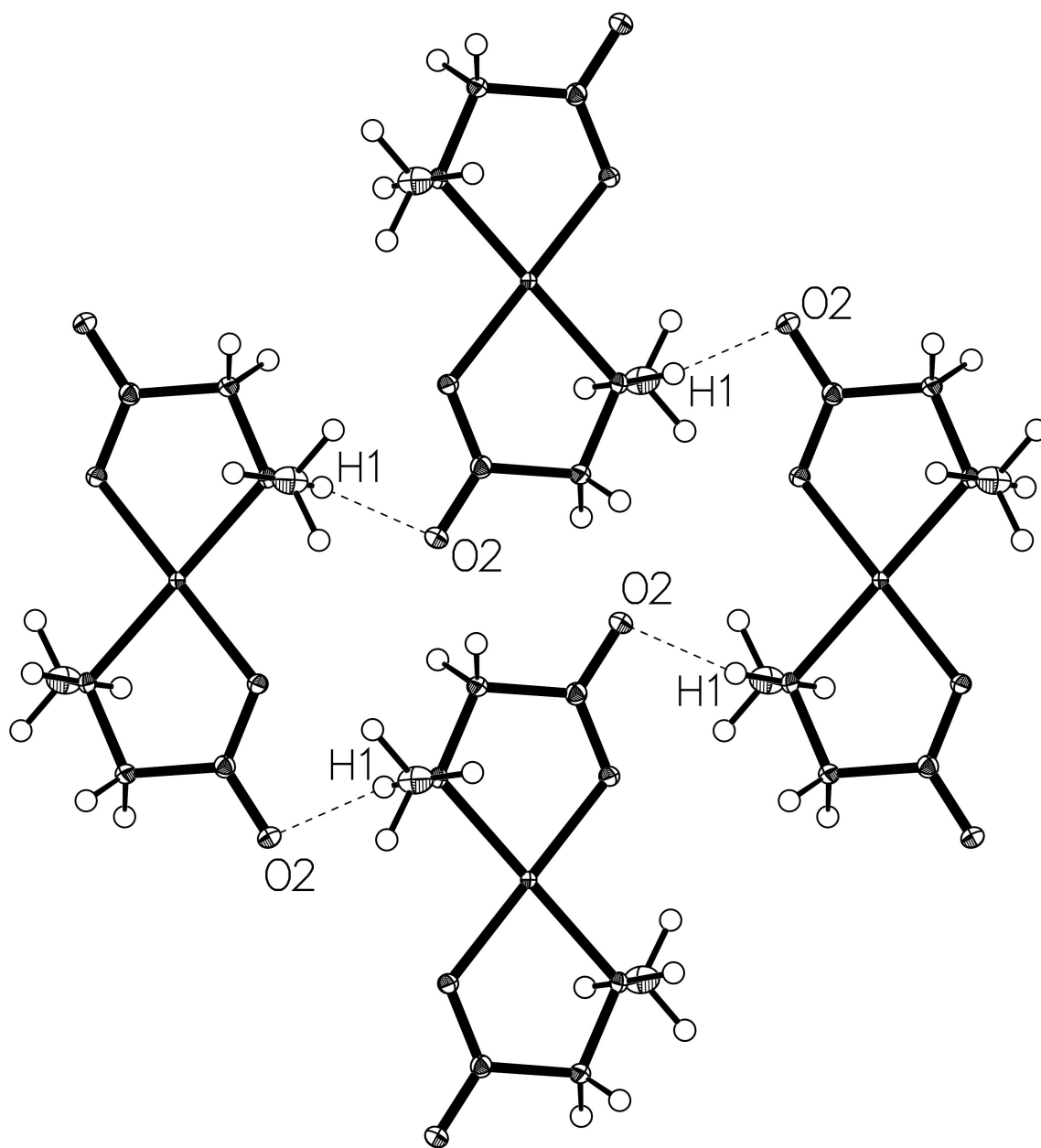
Figure 36. Crystal packing diagram of (3) as viewed along [100] showing the intermolecular hydrogen bonding motif.

The ^{1}H NMR spectrum of a single crystal of **3** in D_2O (Figure 37) shows a complex mixture of products. Three peaks at δ 2.34, 2.47 and 2.52 ppm correspond to the amine methyl groups and suggest that there are three diastereomers present in solution. The peak at 2.34 ppm appears as a

barely resolved doublet at 600 MHz, and at 400 MHz is a true singlet with a slightly broadened line width. The ratio of these peaks is approximately 4.67:1.21:1.00, which would correspond to a 67.9/17.6/14.5 percent isomeric distribution. The methylene protons in the chelate backbone give rise to a complicated set of resonances from 3.1-3.9 ppm.
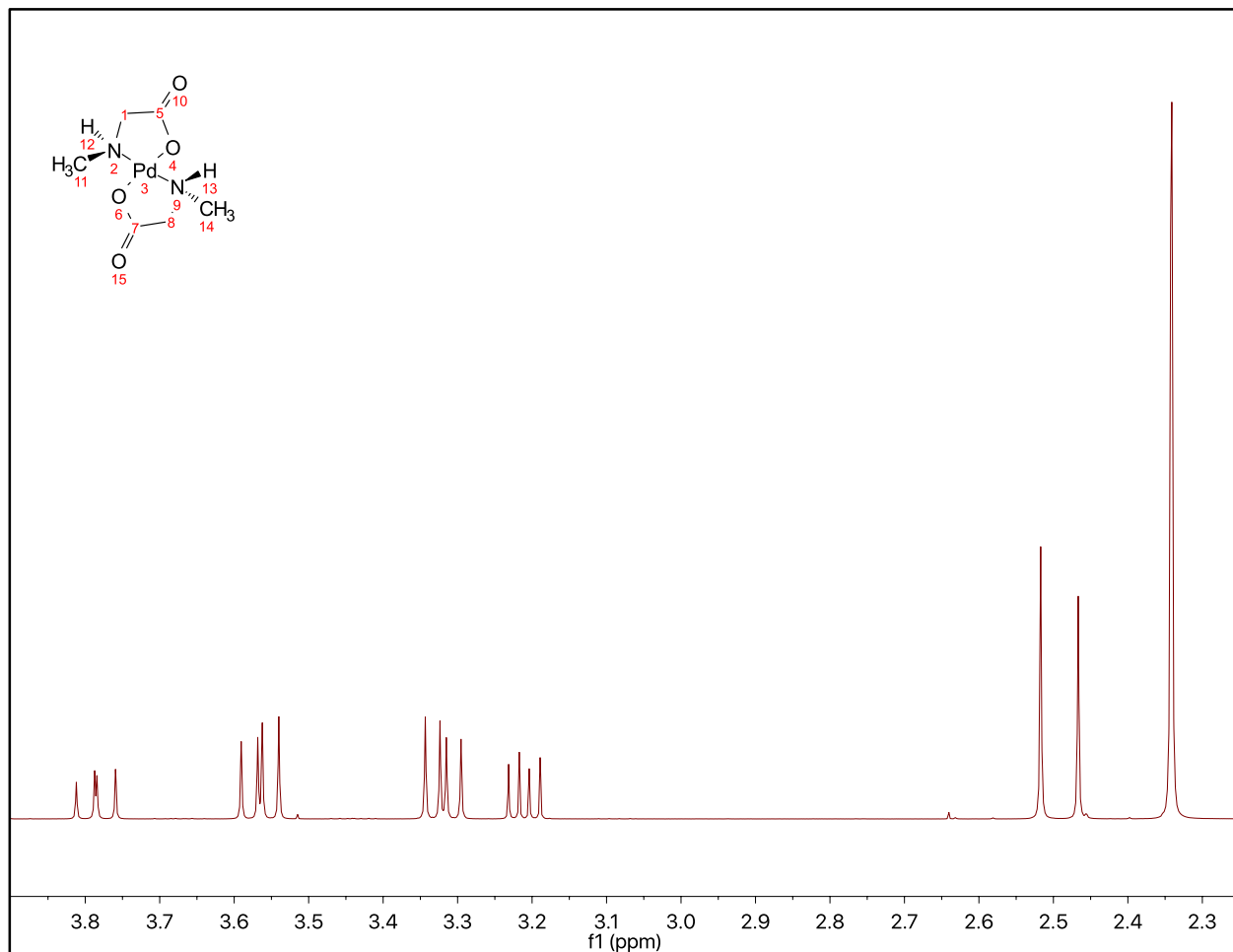

Figure 37. ^{1}H NMR spectrum of a single crystal of bis(N-methylglycinato)palladium(II) in D$_2$O.

In order to assign the methylene resonances a 1D NOESY (Nuclear Overhauser effect spectroscopy) experiment was performed. Irradiation of the methyl resonance at δ 2.34 shows a corresponding response in the peaks at δ 3.31, 3.33, 3.55 and 3.58 ppm, which correspond to

four pairs of doublets. Integration of these resonances yields peaks areas of 3:1:1. Irradiation at δ 2.47 ppm yields a methylene response at δ 3.20 and 3.77 ppm corresponding to a pair of doublets. Integration again shows a ratio of 3:1:1. Finally, irradiation at δ 2.52 ppm shows that the resonances at 3.22 and 3.80 correspond to another pair of doublets with area ratios of 3:1:1. A peak at 282.9930 amu in the HRMS corresponds to the [M+H]+ parent ion, and the typical isotopic splitting pattern for palladium is observed with peaks at 280.9977, 281.9975, 284.9935, 286.9947.

Per the prior discussion of aquo complex formation in asymmetrically *N*-substituted complexes, the proton and carbon NMR data allow us to postulate what species are present in solution. In the case of *trans*-bis(*N*-methylglycinato)palladium(II) we observe four *N*-methyl resonances and eight pairs of methylene doublets in the proton NMR spectrum. In the carbon NMR spectrum we observe four *N*-methyl signals, four methylene signals, and three carbonyl signals. We have previously shown that the mono-aquo complex should show four pairs of methylene doublets and two methyl singlets. The remaining four pairs of methylene doublets and two methyl singlets can be explained by slightly modifying the case for the bis-aquo complex. The bis-chelate is rigidly C_2 symmetric, however the bis-aquo complex allows for some relaxation of that rigidity. If the carboxylate end of each ligand is free it is conceivable that the bis-aquo complex adopts a configuration with C_1 symmetry. In this case we would expect to see four pairs of ^{1}H methylene doublets and two *N*-methyl carbon peaks. The fact that eight methylene ^{1}H signals are observed rather than six, and that four *N*-methyl carbon signals are seen rather than three is a strong indication that the solution species present are the mono- and bis-aquo. DFT calculations place the mono-aquo and bis-aquo complexes 3.0 and 5.4 kcal/mol lower in energy than the bis-chelate, respectively, further supporting the conclusion that

these are the species present in solution. Given the preceeding discussion, the "singlet" at 2.34 ppm and the four pairs of doublets at 3.31, 3.33, 3.55, and 3.58 ppm are assigned to the bis-aquo complex. The singlet at 2.47 and the doublets at 3.20 and 3.77 ppm are assigned to the de-coordinated NMG ligand of the mono-aquo complex. Finally, the singlet at 2.52 and the doublets at 3.22 and 3.80 ppm are assigned to the coordinated NMG ligand of the mono-aquo complex.

A further possibility that must be entertained is that all three species are present in solution. This premise requires the invocation of coincidental overlap of the carbonyl-carbon ^{13}C NMR signals. The interpretation of the proton NMR spectrum in this case changes so that the *N*-methyl singlets at 2.47 and 2.52, and their corresponding methylene doublets, are assigned to the rigidly C_2 symmetric bis-chelate and bis-aquo complexes. The *N*-methyl doublet at 2.34 ppm and its corresponding methylene doublets are then assigned to the mono-aquo complex. De-coordination of one carboxylate changes the ligand environment just enough to result in an observable shift in the proton resonances. The ^{13}C NMR spectrum shows four ligand environments for each of the methyl and methylene carbons, yet only three ligand environments for the carbonyl carbons. The bis-chelate clearly has only one ligand environment for the carbonyl carbon. The mono-aquo complex clearly has two distinct ligand environments. If the doubly de-coordinated carboxylates in the bis-aquo complex are indistinguishable by NMR from the de-coordinated carboxylate of the mono-aquo complex, then we would be left with only three ligand environments for the carbonyl carbons. This is what is observed in the ^{13}C NMR spectrum. The larger carbonyl carbon peak then is assigned to the de-coordinated carboxyl group of the mono- and bis-aquo complexes, with the smaller two carbonyl resonances assigned to the bis-chelate and coordinated carboxylate of the mono-aquo complex. The non-equivalent

integrated peak areas of the *N*-methyl protons does lend support to the argument that all three species are present in solution. If the *N*-methyl singlets at 2.47 and 2.52 were due to the mono-aquo complex they should be present in a 1:1 ratio, and they are not. However, there is little other hard evidence in the NMR data that tends to favor one argument over the other so we must therefore conclude that either case is equally valid and bears further investigstion.

2.3.5   *Cis*-bis(glycinato)palladium(II)

To complete the picture, the *cis* glycine complexes (Compounds **4, 7, 8**, Figure 40) were prepared following the procedures set forth by Chornenkba *et al.*[17] In this case palladium(II) chloride was used. Trans-effect theory predicts that a $PdCl_2$ precursor would be favored to yield the *cis* complex. If palladium has a higher affinity for nitrogen than oxygen, based on hard/soft acid-base theory, then the two chlorine ligands direct the incoming amine nitrogen atoms to positions *trans* to the chlorine atoms. This places the two nitrogen atoms *cis* to each other. Dissociation of the chloride ligand then opens up the adjacent coordination site, and formation of the chelate ring occurs with coordination of the carboxylate oxygen (Figure 38).
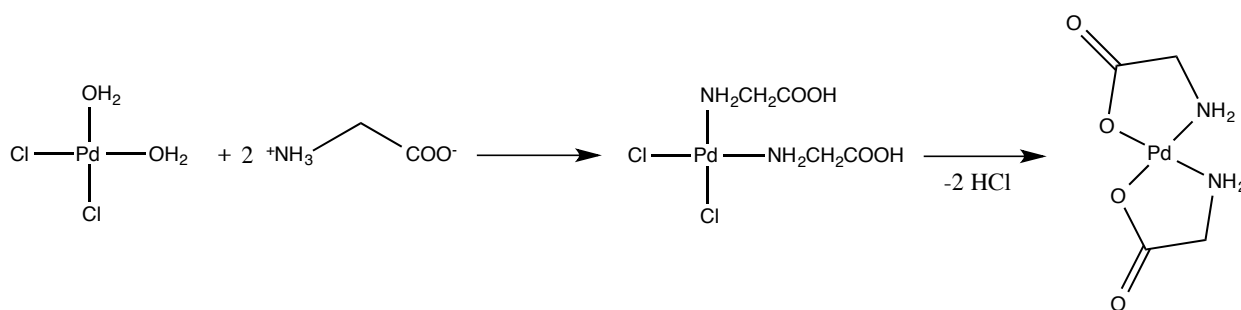

Figure 38. Proposed pathway for *cis* glycinate complex formation.

67

Indeed, molecular modeling calculations confirm that the *cis*-(*N*)-monodentate glycine dichloride complex is favored by approximately 4.92 kcal/mol over the *trans* isomer.[22] As discussed above for compound **1**, when utilizing palladium(II) acetate as the starting material we observe formation of the *trans* isomer. In this case coordination of the first amine nitrogen (N1) directs the second amine nitrogen to a position trans to N1. The carboxylate oxygen atoms coordinate to form the chelate ring resulting in the *trans* complex (Figure 39).
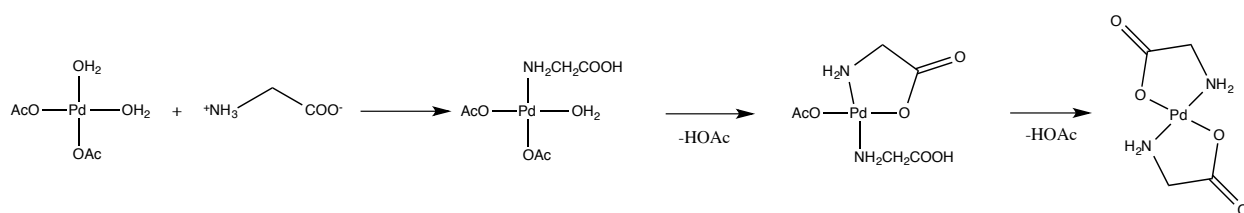

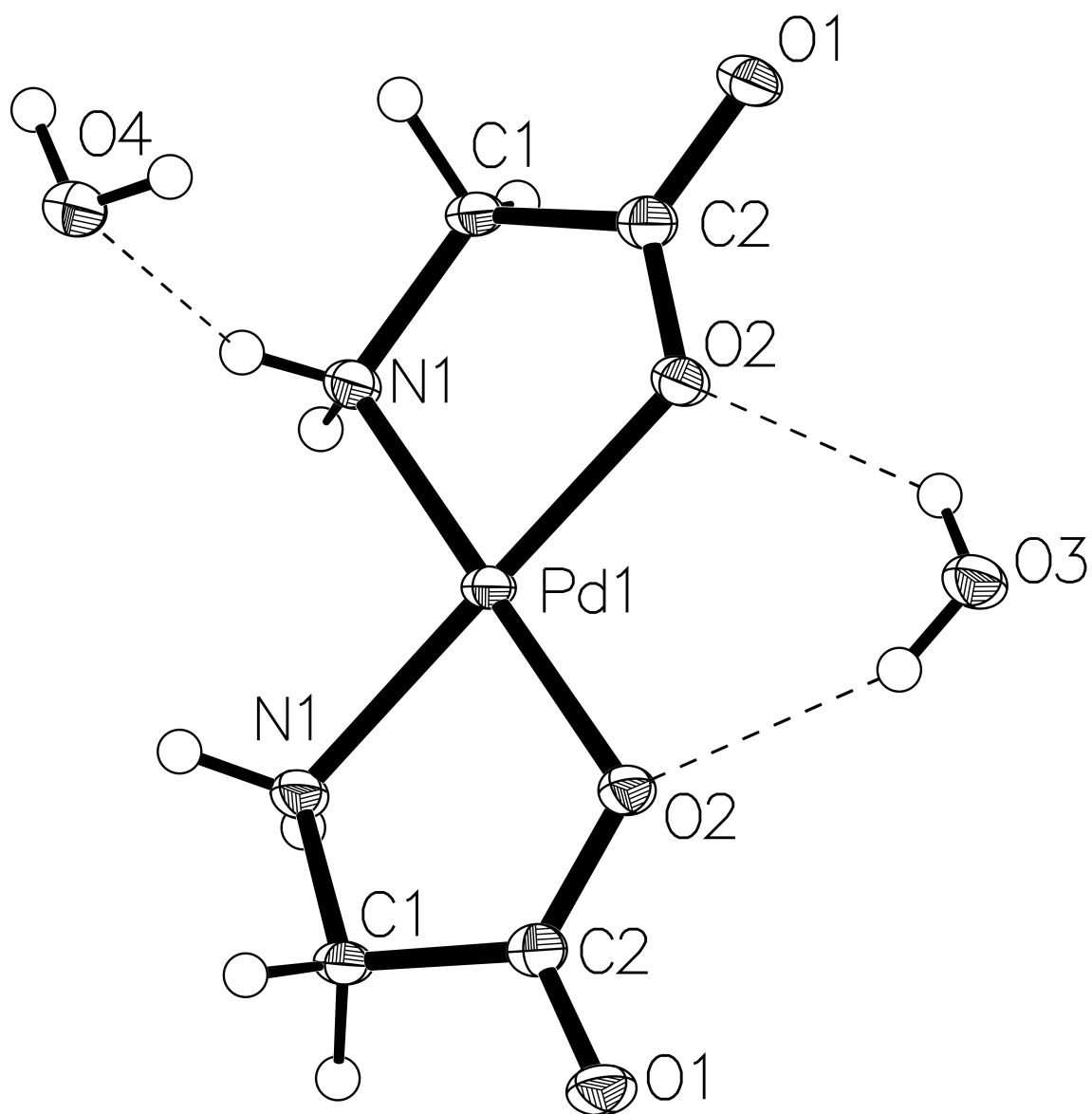**Figure 39. Proposed pathway for *trans* glycinate complex formation.**

Figure 40. Thermal ellipsoid plot of the molecular structure of crystalline cis-Bis(glycinato)palladium(II) trihydrate, 4. Thermal ellipsoids are shown at the 50% probability level.

X-ray crystallography confirms formation of the *cis* isomer from PdCl$_2$ starting material. The complex crystallizes in the C2/c space group. Pd-N and Pd-O bond lengths are 2.006Å and 2.017Å, respectively. N-Pd-O bond angles are 84.21 degrees in the chelate ring. The N-Pd-N

bond angles between the chelate rings are 96.156 degrees and the O-Pd-O bond angles between the chelate rings are 95.418 degrees. There are three water molecules in the lattice; two are hydrogen bonded between the amine protons and non-coordinated carboxylate oxygen atoms in adjacent molecules, and one is hydrogen bonded to the coordinated oxygen atoms of a single molecule (Figure 41). As before with the *trans* complex **1**, these newer 100 K data provide greater precision when compared with the room temperature data reported by Baidina.[13] One other key difference is that hydrogen atom positions are reported for the structure whereas Baidina did not report these.
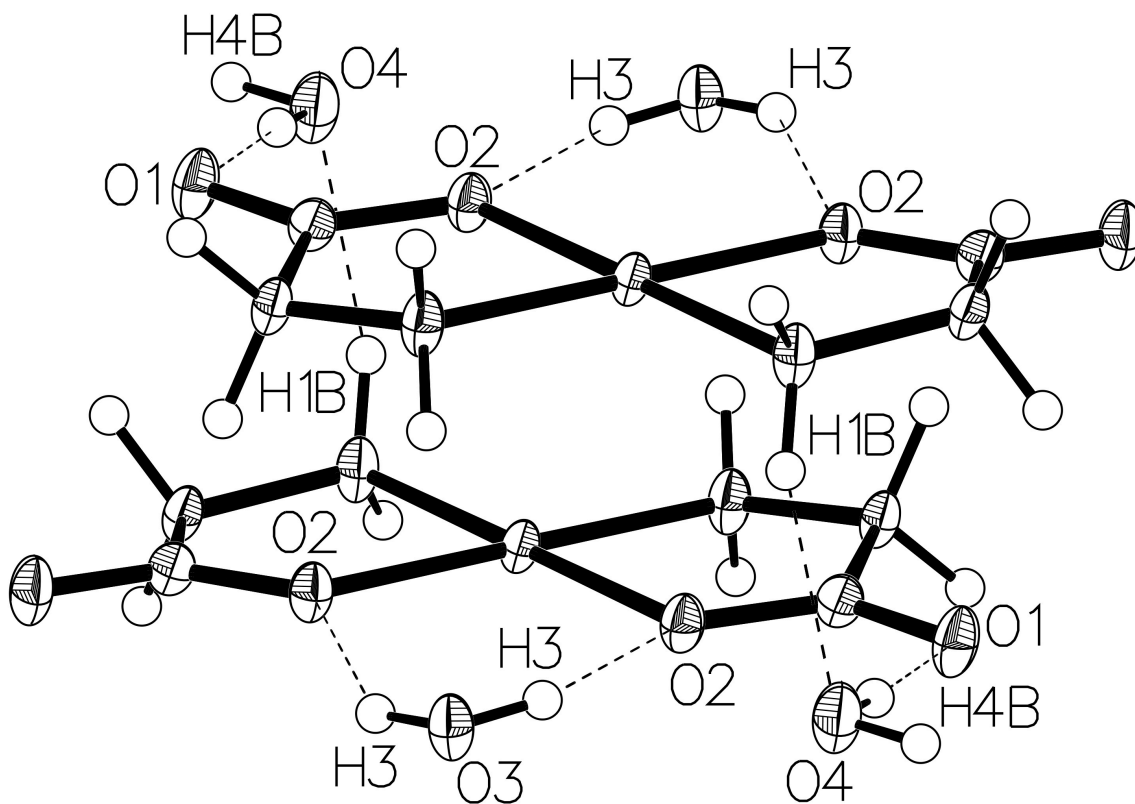

Figure 41. Crystal packing diagram of (4) as viewed along [0 2/3 -1/3] showing the intermolecular hydrogen bonding motif.

As in the case for the *trans* complex, the ^{1}H NMR spectrum in 95/5 H_2O/D_2O shows two triplets for the methylene protons at δ 3.55 and 3.52 ppm. Both resonances appear as singlets in D_2O. The ^{1}H NMR spectrum of the ^{15}N-enriched *cis* complex **7** was also obtained and showed the same triplets for the methylene protons. The amine protons were again not observed; two-bond J^{15}_{NCH} coupling of 0.7 Hz was observed for the *cis* glycine complex. The range of J^{15}_{NCH} couplings reported in the literature span from 0.6-1.4 Hz.[33] The difference observed of 0.2 Hz between *cis* and *trans* isomers may therefore lend itself as another tool for the determination of chelate geometry in solution. ^{13}C NMR spectra again show three peaks each for the carbonyl (189.65, 188.04, and 174.62 ppm) and methylene carbons (50.39, 48.85, and 44.10 ppm), and the ^{1}H-^{15}N HSQC NMR spectrum shows two resonances for the amine nitrogens at -34.85 and -26.50 ppm. Taken as a whole, the NMR data of the cis-bis(glycinate) complex once again strongly suggests the formation of an aquo complex in solution (Figure 42).
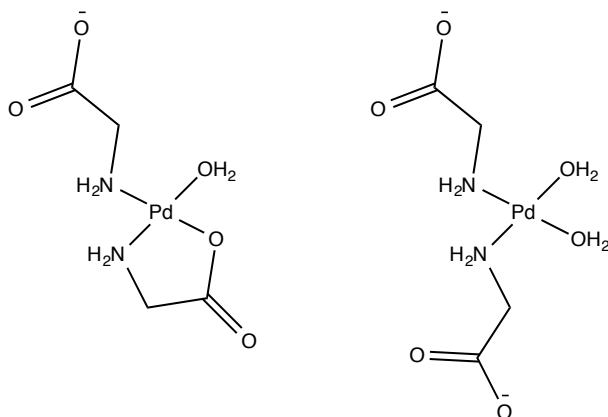

Figure 42. Proposed structures of the mono-aquo (left) and bis-aquo (right) cis-Pd(GLY)2 complexes.

As a further probe to rule out *cis/trans* isomerization in favor of aquo complex formation, a variable-temperature, NOE-suppressed ^{13}C NMR experiment was performed on the *cis-*

bis(glycinato) complex **8** in order to confirm that the three species present are aquo complexes

and not due to isomerization in solution. ^{13}C NMR data were collected at 25 °C, 50 °C, and 75

°C, and again at 25 °C. The integrated peak ratios are summarized in Table 4, below.

Temperature, °C	^{13}C C=O Peak Ratios
25	1.00:4.36:1.16
50	1.00:3.86:1.42
75	1.00:2.62:1.04
25	1.00:4.16:1.19

Table 4. ^{13}C VT-NMR C=O Peak Ratios

The data clearly show that isomerization is not occurring and that generation of the aquo

complex is favored at higher temperatures. It was previously shown that the *trans* isomer is

approximately 0.56 kcal/mol lower in energy than the *cis*. If *cis/trans* isomerization were

occurring at higher temperature, the major:minor peak ratio would not return to its initial value

on cooling from higher temperature. Molecular modeling calculations were performed in an

attempt to model the various aquo complexes; those data are summarized below in Table 5.

Complex	ΔE from bis-chelate
Bis-chelate	0
Mono-aquo	-4.2 kcal/mol
Bis-aquo	-7.0 kcal/mol

Table 5. Calculated Energy Values for cis-glycinate aquo species

The calculated energy differences show that dissociation of the carboxylate to generate the aquo complexes is plausible. When the carboxylate dissociates the carbonyl carbon moves further away from the metal center, effectively deshielding it more than a coordinated carbonyl carbon. This is borne out in the NMR data by a downfield shift in the carbonyl resonance for the major bis-aquo species. Similar shifts are observed for the amine nitrogen and methylene carbon resonances. As stated earlier, the ability of these complexes to form aquo complexes may hold significant importance to their catalytic activity.

2.3.6   Catalytic Activity of Glycinate Complexes

A simple oxidative coupling reaction[34] between phenylboronic acid and methyl tiglate (Figure 43, below) was carried out to determine the suitability of these complexes as catalysts.
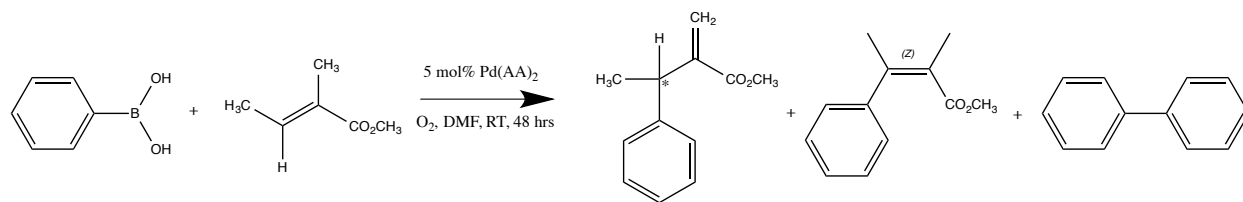
Figure 43. Model oxidative coupling reaction

Interestingly, the cis-bis(glycinato)palladium(II) isomer shows catalytic activity for the formation of the coupled products, whereas the trans-bis(glycinato)palladium(II) isomer does not. This is not surprising as two *cis* reactive sites are required for catalytic activity. At 48 hours reaction time complete consumption of the phenylboronic acid is observed in the presence of a 3-fold excess of methyl tiglate. The product ratios are 96:2:2 of the R/S product to the Z alkene to homocoupled biphenyl, respectively. Enantiomeric selectivity was not determined, since enantioselectivity is not expected due to the lack of a chiral center on the ligand. Catalytic asymmetric coupling is a key focus of our research group and later chapters will expand and expound upon these interesting results.

2.3.7 Structural Trends

Several observations can be made pertaining to the effects of *N*-alkylation on the ligand properties of glycines. From the crystallographic data, a lengthening of the Pd-N bonds is noted for the *trans* complexes as alkylation of the nitrogen atom progresses (Table 6).

Compound	Pd-N, Å	Pd-O, Å
1	2.033(3)	1.997(3)
2	2.048(1)	2.0009(9)
3	2.033(1)	1.991(1)
4	2.006(3)	2.017(3)

Table 6. Pd-N and Pd-O bond lengths for Compounds 1-4.

The addition of methyl groups onto the coordinated nitrogen atom results in sufficient steric bulk such that the nitrogen atoms are prevented from being drawn closer in to the metal center. The *cis*-Pd(GLY)$_2$ isomer has considerably shorter Pd-N bonds and longer Pd-O bonds than any of the *trans* complexes. In the case of the *trans* isomers, so long as there is at least one amine hydrogen atom remaining then no water molecules are incorporated into the crystal lattice. All of the *trans* isomers contain a 2_1 screw axis in the unit cell. A summary of selected single crystal X-ray diffraction data is shown in Table 7, below.

	1	**2**	**3**	**4**
Space Group	$P2_1/n$	$P2_1/n$	$P2_1/c$	$C2/c$
a, Å	5.6671	5.21929	5.87120	18.6605
b, Å	8.9795	10.14699	8.68080	8.0056
c, Å	6.9077	8.91248	12.7612	6.7424
α, deg	90	90	90	90
β, deg	105.158	104.336	94.8310	110.415
γ, deg	90	90	90	90
V, Å^3	339.287	457.308	648.086	943.973
Z	2	2	2	4

Table 7. Selected single crystal X-ray crystallographic data for Compounds 1-4

2.3.8 UV-vis and FTIR Spectroscopy

UV-vis spectrometric data shows two major electronic transitions for each complex. An ultraviolet absorption corresponding to a $\pi \rightarrow \pi^*$ transition from the carbonyl group of the amino acid ligand occurs at approximately 190-205 nm, with the λ_{max} shifting to higher wavelengths with increasing alkylation of the amine. Molar absorptivities (ε) for this transition are in the range of 21,000-38,000 $M^{-1}cm^{-1}$. A visible absorption corresponding to a $d \rightarrow d$ transition is observed at 316-324 nm, with the λ_{max} shifting to lower wavelengths with increasing amine alkylation. Molar absorptivities (ε) for this transition are in the range of 180-375 $M^{-1}cm^{-1}$. This

d→d transition can be assigned to a HOMO→LUMO transition from the d_z^2 to the $d_{x^2-y^2}$ orbitals based on molecular modeling calculations.

Fourier transform infrared spectra of these chelates show the expected absorption bands for carboxylate and amine stretching, and in the case of the *cis* and *trans* glycine isomers agree with previously published data. The *cis* isomer (Compound **4**) shows both symmetric and asymmetric stretching carbonyl bands at 1624 and 1576 cm^{-1}. The symmetric and asymmetric N-H stretches are evident at 3219 and 3118 cm^{-1}. Compound **1** shows a carbonyl stretch at 1612 cm^{-1} with a shoulder at 1592 cm^{-1}. Compound **3**'s carbonyl stretch is also centered at 1624 cm^{-1}, with a shoulder at 1587 cm^{-1}. Compound **2** displays a carbonyl stretch at 1636 cm^{-1} with a shoulder at 1607 cm^{-1}. Evident from this progression is the fact that, for the *trans* isomers, the carbonyl stretch is shifting to lower wavelengths as the Pd-O bond is shortened. The N-H stretches for Compound **1** absorb at 3234 and 3106 cm^{-1}; for Compound **3** at 3106 cm^{-1}; and for Compound **2** the N-H stretches are no longer observed.

2.3.9   Single Crystal vs. Powder XRD

The issue of how well a single crystal structure reflects the bulk constitution of a material is a perennial problem. For the *cis* and *trans* glycinate complexes, **1** and **4**, the calculated energy difference between them was small enough, approximately 0.13 kcal/mol, that it seemed plausible that isomerization in solution might occur and that single crystal structures do not necessarily represent the bulk. To address that issue powder X-ray diffraction spectra were collected on compounds **1**, **3**, and **4** and compared to the powder patterns calculated from the single-crystal X-ray diffraction data. If the bulk consisted of both cis and trans isomers, we would expect to see evidence of that mixture in the powder pattern. Comparison of the

calculated versus observed powder X-ray diffraction data shows extremely good correlation in

each case (Figure 44, Figure 45), indicating that the isolated product is in fact a single isomer.
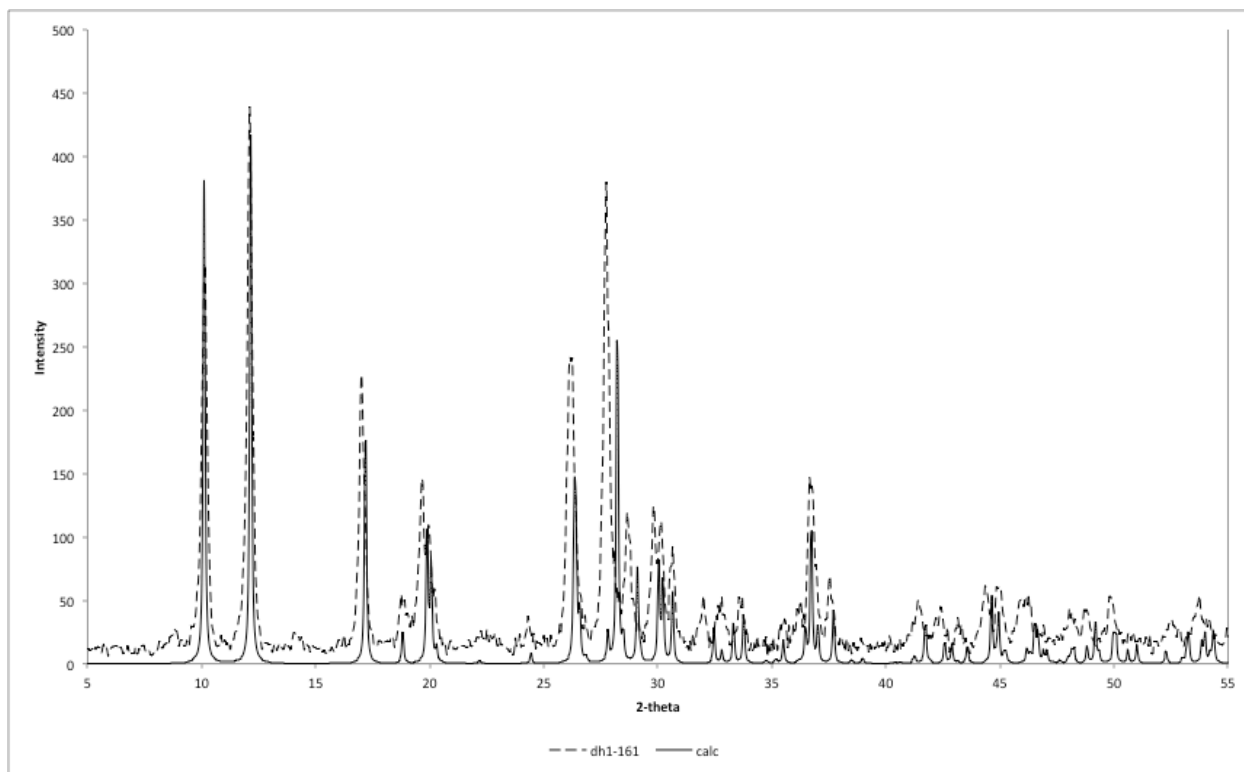
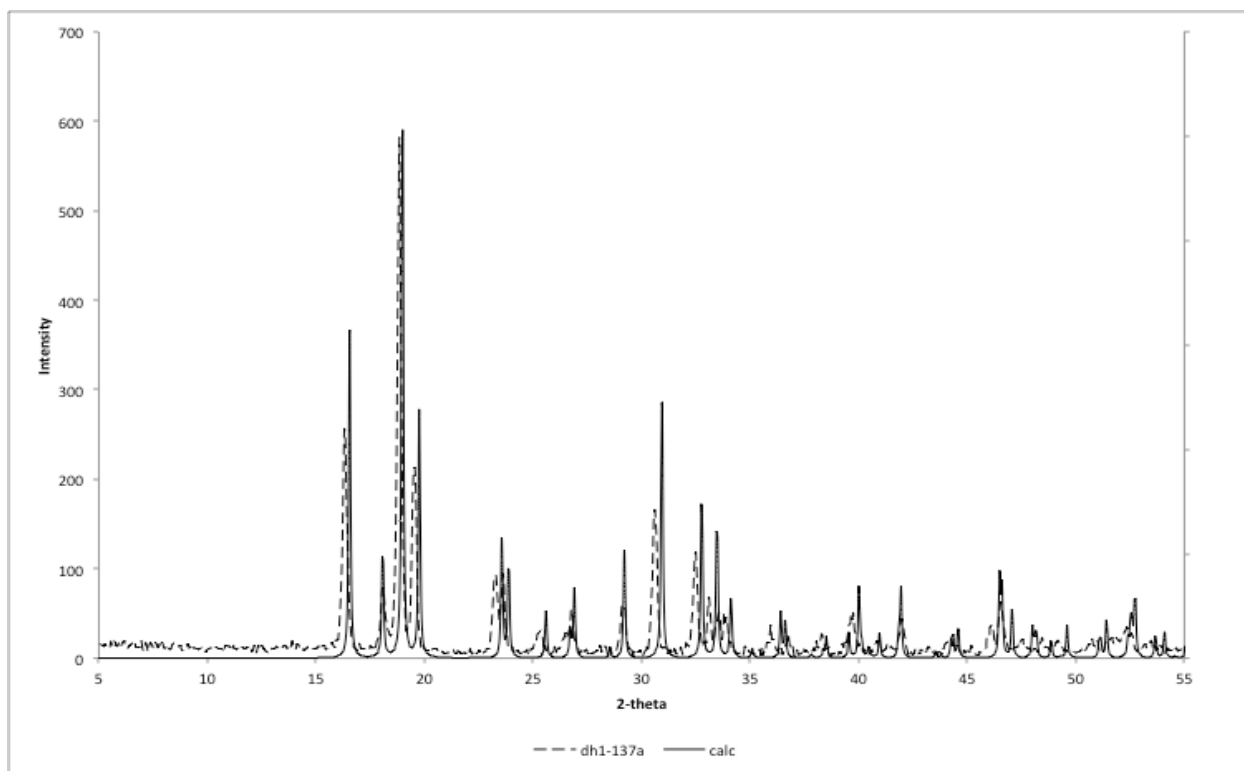**Figure 44. Calculated versus observed powder X-ray pattern for cis-Bis(glycinato)palladium(II) (4)**

Figure 45. Calculated versus observed powder X-ray pattern for trans-Bis(glycinato)palladium(II) (1)

For the *N*-methylglycinate complex **3** the range of calculated molecular energies is also small, and the NMR data does suggest that a mixture of products exists in solution. The calculated powder pattern (Figure 46) is again in extremely good agreement with the observed powder pattern. This seems to indicate that the crystalline product is a single isomer but that generation of aquo complexes in solution is possible.
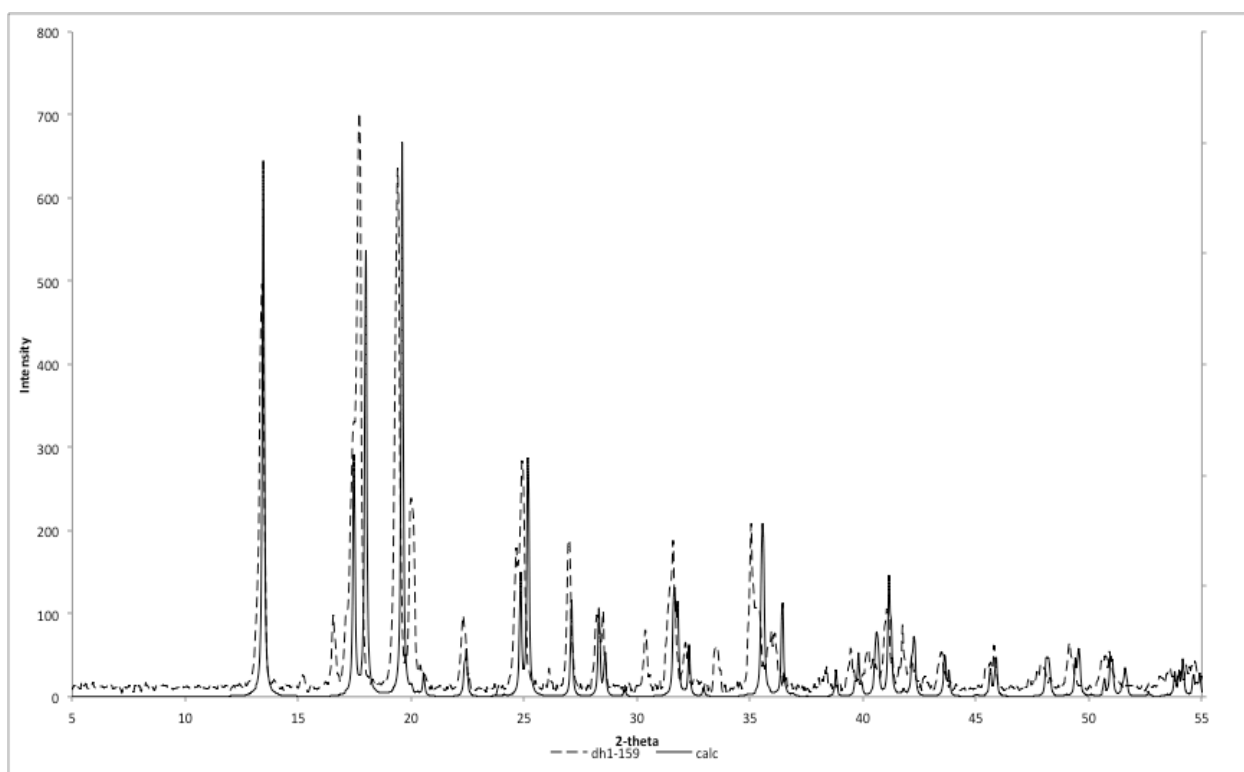
Figure 46. Calculated versus observed powder X-ray pattern for trans-Bis(N-methylglycinato)palladium(II) (3)

2.4   CONCLUSIONS

Alkylation of the coordinated nitrogen atom in palladium(II) bis-glycinates leads to the formation of only *trans* isomers. Attempts to prepare the *cis* isomers of the *N*-alkylated glycine complexes from $PdCl_2$, as was done for the non-*N*-alkylated glycine complexes, were unsuccessful. There is a lengthening of the Pd-N and shortening of the Pd-O bonds as alkylation proceeds from $n=0$ to $n=2$, where n is the number of methyl groups on the nitrogen. The electronic spectra show a shift of the UV absorption to longer wavelength with increasing alkylation, with a corresponding shift of the visible absorption to shorter wavelengths. Compelling evidence of the formation of a palladium-amino acid-aquo complex has been presented and catalytic activity confirmed for the *cis* complex. New X-ray crystal structures and NMR data on the *N*-methyl and *N,N*-dimethyl bis-glycinate complexes have been reported. Additionally, improved X-ray crystal structures and NMR data on the *cis* and *trans* bis-glycinate complexes of palladium(II) are reported, as well as confirmation of the previously reported infrared and electronic absorption spectra. Powder X-ray diffraction has been used to verify formation of a single isomer in the crystalline phase for the glycinate and *N*-methylglycinate complexes. Subsequent chapters will describe the synthesis, characterization, and catalytic and biological activity of palladium(II)-amino acid complexes possessed of chiral R-groups on the amino acid ligand. This chapter has appeared in press as "Bis-glycinato complexes of palladium(II): Synthesis, structural determination, and hydrogen bonding interactions," by Hobart, David B.; Berg, Michael A. G.; Merola, Joseph S.; Inorganica Chimica Acta (2014), 423, (Part_A), 21-30, doi:10.1016/j.ica.2014.07.024.

2.5 REFERENCES

(1) Pinkard, F. W.; Sharratt, E.; Wardlaw, W.; Cox, E. G. *Journal of the Chemical Society* **1934**, 1012.

(2) Karpin, G. W.; Merola, J. S.; Falkinham, J. O. *Antimicrobial Agents and Chemotherapy* **2013**, *57*, 3434.

(3) Ley, H.; Ficken, K. *Berichte der Deutschen Chemischen Gesellschaft* **1912**, *45*, 377.

(4) Grünberg, A. A.; Ptizyn, B. W. *Journal für Praktische Chemie* **1933**, *136*, 143.

(5) Saraceno, A. J.; Nakagawa, I.; Mizushima, S.; Curran, C.; Quagliano, J. V. *Journal of the American Chemical Society* **1958**, *80*, 5018.

(6) Lane, T. J.; Durkin, J. A.; Hooper, R. J. *Spectrochimica Acta* **1964**, *20*, 1013.

(7) Condrate, R. A.; Nakamoto, K. *Journal of Chemical Physics* **1965**, *42*, 2590.

(8) Walter, J. L.; Hooper, R. J. *Spectrochimica Acta, Part A: Molecular and Biomolecular Spectroscopy* **1969**, *25*, 647.

(9) Balzani, V.; Carassiti, V.; Moggi, L.; Scandola, F. *Inorganic Chemistry* **1965**, *4*, 1243.

(10) Zhang, Y.; Su, Q.; Zhao, G.; Li, J. *Spectroscopy Letters* **1992**, *25*, 521.

(11) Coe, J. S.; Lyons, J. R. *Journal of the Chemical Society [Section] A: Inorganic, Physical, Theoretical* **1971**, 829.

(12) Farooq, O.; Ahmad, N.; Malik, A. U. *Journal of Electroanalytical Chemistry and Interfacial Electrochemistry* **1973**, *48*, 475.

(13) Baidina, I. A.; Podberezskaya, N. V.; Bakakin, V. V.; Golubovskaya, E. V.; Shestakova, N. A.; Mal'chikov, G. D. *Zhurnal Strukturnoi Khimii* **1979**, *20*, 544.

(14) Baidina, I. A.; Podberezskaya, N. V.; Borisov, S. V.; Golubovskaya, E. V. *Zhurnal Strukturnoi Khimii* **1982**, *23*, 88.

(15) Appleton, T. G.; Bailey, A. J.; Bedgood, D. R., Jr.; Hall, J. R. *Inorganic Chemistry* **1994**, *33*, 217.

(16) Krylova, L. F.; Golovin, A. V. *Journal of Structural Chemistry (Translation of Zhurnal Strukturnoi Khimii)* **2000**, *41*, 243.

(17) Chornenka, N. V.; Nikitenko, V. N. *Ukrainskii Khimicheskii Zhurnal (Russian Edition)* **2006**, *72*, 48.

(18) Kublanovsky, V. S.; Nikitenko, V. N. *Electrochimica Acta* **2010**, *56*, 2110.

(19) Agilent; Agilent Technologies: Oxford, UK, 2012.

(20) Sheldrick George, M. *Acta crystallographica. Section A, Foundations of crystallography* **2008**, *64*, 112.

(21) Dolomanov, O. V.; Bourhis, L. J.; Gildea, R. J.; Howard, J. A. K.; Puschmann, H. *Journal of Applied Crystallography* **2009**, *42*, 339.

(22) Frisch, M. J. T., G. W.; Schlegel, H. B.; Scuseria, G. E.; Robb, M. A.; Cheeseman, J. R.; Scalmani, G.; Barone, V.; Mennucci, B.; Petersson, G. A.; Nakatsuji, H.; Caricato, M.; Li, X.; Hratchian, H. P.; Izmaylov, A. F.; Bloino, J.; Zheng, G.; Sonnenberg, J. L.; Hada, M.; Ehara, M.; Toyota, K.; Fukuda, R.; Hasegawa, J.; Ishida, M.; Nakajima, T.; Honda, Y.; Kitao, O.; Nakai, H.; Vreven, T.; Montgomery, Jr., J. A.; Peralta, J. E.; Ogliaro, F.; Bearpark, M.; Heyd, J. J.; Brothers, E.; Kudin, K. N.; Staroverov, V. N.; Kobayashi, R.; Normand, J.; Raghavachari, K.; Rendell, A.; Burant, J. C.; Iyengar, S. S.; Tomasi, J.; Cossi, M.; Rega, N.; Millam, J. M.; Klene, M.; Knox, J. E.; Cross, J. B.; Bakken, V.; Adamo, C.; Jaramillo, J.; Gomperts, R.; Stratmann, R. E.; Yazyev, O.; Austin, A. J.; Cammi, R.; Pomelli, C.; Ochterski, J. W.; Martin, R. L.; Morokuma, K.; Zakrzewski, V. G.; Voth, G. A.; Salvador, P.;

Dannenberg, J. J.; Dapprich, S.; Daniels, A. D.; Farkas, Ö.; Foresman, J. B.; Ortiz, J. V.; Cioslowski, J.; Fox, D. J.; Gaussian, Inc.: Wallingford, CT, 2009.

(23)   Becke, A. D. *Journal of Chemical Physics* **1993**, *98*, 5648.

(24)   Lee, C.; Yang, W.; Parr, R. G. *Physical Review B: Condensed Matter and Materials Physics* **1988**, *37*, 785.

(25)   Stephens, P. J.; Devlin, F. J.; Chabalowski, C. F.; Frisch, M. J. *Journal of Physical Chemistry* **1994**, *98*, 11623.

(26)   Andrae, D.; Haeussermann, U.; Dolg, M.; Stoll, H.; Preuss, H. *Theoretica Chimica Acta* **1990**, *77*, 123.

(27)   Komorita, T.; Hidaka, J.; Shimura, Y. *Bull. Chem. Soc. Jap.* **1971**, *44*, 3353.

(28)   Jarzab, T. C.; Hare, C. R.; Langs, D. A. *Crystal Structure Communications* **1973**, *2*, 399.

(29)   Jarzab, T. C.; Hare, C. R.; Langs, D. A. *Crystal Structure Communications* **1973**, *2*, 395.

(30)   Sabat, M.; Jezowska, M.; Kozlowski, H. *Inorganica Chimica Acta* **1979**, *37*, L511.

(31)   Vagg, R. S. *Acta Crystallogr B* **1979**, *35*, 341.

(32)   Chernova, N. N.; Strukov, V. V.; Avetikyan, G. B.; Chernonozhkin, V. N. *Zhurnal Neorganicheskoi Khimii* **1980**, *25*, 1569.

(33)   Binsch, G.; Lambert, J. B.; Roberts, B. W.; Roberts, J. D. *Journal of the American Chemical Society* **1964**, *86*, 5564.

(34)   Yoo, K. S.; Park, C. P.; Yoon, C. H.; Sakaguchi, S.; O'Neill, J.; Jung, K. W. *Organic Letters* **2007**, *9*, 3933.

Chapter 3: Synthesis, Structure, and Catalytic Reactivity of Pd(II) Complexes of Proline and Proline Homologs

3.1 INTRODUCTION

Oxidative coupling reactions are some of the most utilized reactions in modern synthetic chemistry, and transition metal catalyzed oxidations are well known.[1] Palladium(II) oxidative coupling catalysis is a growing field,[1-6] and some of the more recent developments are discussed in this section.

Reactions such as the Heck, Suzuki, and Sonogashira couplings are known to proceed via a Pd^0 species, with oxidative addition/reductive elimination yielding the desired products. Oxidative palladium(II) catalysis differs from these in that it utilizes molecular oxygen to regenerate the active catalyst in palladium(II) catalyzed coupling reactions. There are two proposed mechanisms for the catalytic cycle. In the first (Figure 47, Pathway A) reductive elimination of HX from complex **1** yields a Pd^0 species which is then oxidized by η^2-molecular oxygen. An initial protonation yields the Pd^{II} hydroperoxide species **4**, and a second protonation generates H_2O_2 and regenerates the catalyst. In the second proposed mechanism (Figure 47, Pathway B), molecular oxygen directly inserts into the palladium-hydride bond to generate the Pd^{II} hydroperoxide species **5**. Protonation again yields H_2O_2 and regenerates the catalyst. Note that between the two proposed pathways, species **4** and **5** are indistinguishable, the difference between the two pathways being whether molecular oxygen inserts directly into a Pd-H bond or

instead re-oxidizes the metal after a reductive elimination. Experimental evidence suggests that both pathways are possible and that the pathway observed for a catalytic system is dependent on catalyst structure and/or substrate conditions.[7-13]
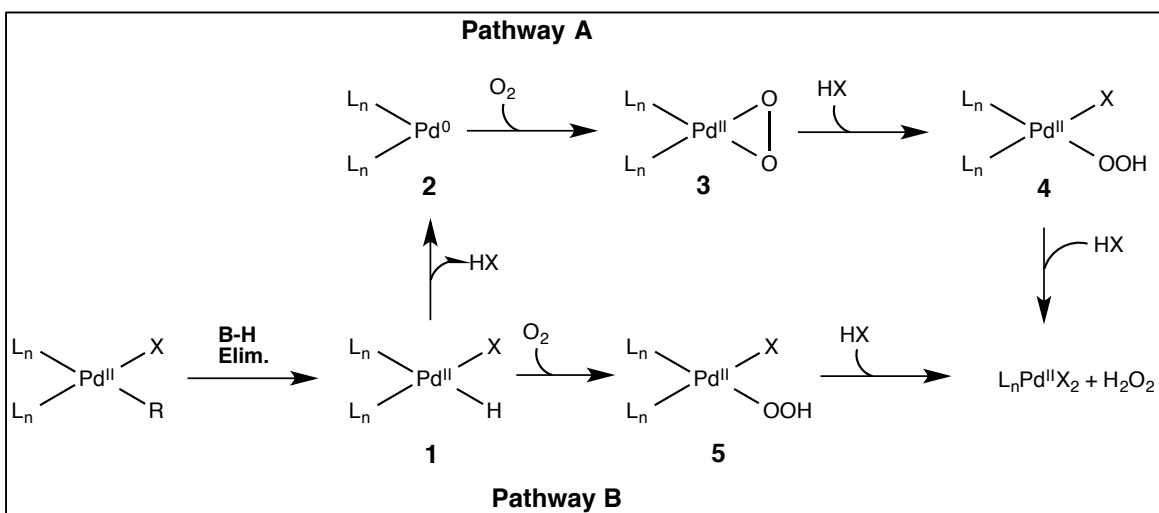

Figure 47. Proposed reaction pathways for Pd(II) oxidative catalysis.

There are many different types of coupling reactions noted to proceed via palladium(II) oxidative catalysis. There are hundreds of examples in the current literature of carbon-carbon,[2,5,14-32] carbon-oxygen,[33-40] carbon-nitrogen,[40-48] carbon-sulfur,[35,49,50] and carbon-phosphorous[51] couplings that are catalyzed by palladium(II) oxidative catalysis. These coupling reactions are used in the manufacture of many pharmaceuticals, natural products, fine chemicals, and polymers. In addition, palladium catalysts are known for their functional group tolerance, mild reaction conditions, and low sensitivity to air and water. Pairing these advantages with an abundant and easily accessible oxidant source shows the great utility and economic benefit that these systems can provide.

Two particularly interesting phenomena associated with our bis-chelated amino acid-palladium(II) catalyst systems are (1) the formation of symmetric biaryls and (2) the observation of reaction products that indicate that multiple phenylboronic acid additions to the olefin substrate are occurring. The formation of biaryl products from palladium catalyzed cross couplings is well known, and there are examples from the literature[22,43,52-56] that demonstrate that these biaryls can be formed as the desired reaction products or as undesired side products. Our palladium(II)-amino acid catalysts show a wide range in their ability to catalyze this coupling, with the degree of biaryl formation dependent on the nature of the R-group of the amino acid ligands.

Our catalyst systems also show the ability to catalyze multiple phenylboronic acid additions to an olefinic substrate. In this case the first coupling product undergoes a second PBA coupling to generate a second insertion product, and this second product can subsequently undergo a third PBA addition to yield a third product, a result previously unreported in the literature.

This chapter describes a study of palladium(II) complexes of proline, N-methylproline, 4-fluoroproline, 4-hydroxyproline, 2-benzylproline, azetidine-2-carboxylic acid, and pipecolinic acid. We have previously discussed the simpler glycine complexes, and these proline and proline homologs represent another unique subset of amino acid ligands where the R-group of the amino acid is a cyclic ring moiety. Subsequent chapters will discuss the beta-amino acid complexes and amino acids where the R-group is a linear substituent. This chapter presents our results on the syntheses, structural and spectroscopic characterization of palladium proline complexes, and their homologs, as well as the unique catalytic activity associated with these complexes.

3.2   EXPERIMENTAL DETAILS

All reagents used in the preparation of the following compounds were purchased from commercial suppliers and used as-received. Palladium(II) acetate was obtained from Pressure Chemical, Pittsburgh, PA.   Proline, N-methylproline, azetidine, and pipecolinic acid were purchased from Sigma-Aldrich, St. Louis, MO.   4-fluoroproline, 4-hydroxyproline, and 2-α-benzylproline were purchased from Chem-Impex International, Inc., Wood Dale, IL.   Reagent grade solvents (ether, acetone, ethyl acetate, DMF) were purchased from Sigma-Aldrich, St. Louis, MO.   Deuterated solvents for NMR spectroscopy were obtained from Cambridge Isotope Laboratories, Tewksbury, MA.

^{1}H and ^{13}C NMR spectra were collected on either a Varian MR-400 or a Bruker Avance III 600 MHz NMR spectrometer. High Resolution Mass Spectra (HRMS) were collected on an Agilent 6220 Accurate Mass TOF LC-MS. X-ray crystallographic data were collected at 100 K on an Oxford Diffraction Gemini diffractometer with an EOS CCD detector and Mo Kα radiation.   Data collection and data reduction were performed using Agilent's CrysAlisPro software.[57] Structure solution and refinement were performed with ShelXL,[58] and Olex2 was used for graphical representation of the data.[59]

All molecular modeling calculations were performed using Gaussian 09[60] on the Virginia Tech Chemistry Department Cluster, "Cerebro", using the WebMO interface. Full geometry optimizations and single-point energy calculations of all structures in water were performed via density functional theory (DFT) with the Becke-3-parameter exchange functional[61] and the Lee–Yang–Parr correlation functional.[62,63] Because palladium is not covered in the cc-pVDZ basis set

used, computations involving Pd employed Stuttgart/Dresden quasi-relativistic pseudopotentials.[64]

Synthesis of *cis*-bis(prolinato)palladium(II) (1)

A four dram vial was fitted with a magnetic stir bar and charged with 55.7 mg of palladium(II) acetate (0.2481 mmol) and 3.0 mL of 50/50 (v/v) acetone/water. The mixture was stirred until all solids had dissolved. To this was added 57.1 mg of L-proline (0.4960 mmol) and stirred overnight. The reaction solution turned from a clear red-orange to a clear pale-yellow supernatant with a pale-yellow precipitate. The supernatant was transferred via pipette to a clean vial and allowed to evaporate to give clear yellow needles. The pale-yellow precipitate was washed with water and dried under vacuum. The combined yield of crystals and precipitate was 79.3 mg of product (0.2369 mmol, 96% yield). *Cis*-Pd($C_5H_8NO_2$)$_2$ (**1**) was identified on the basis of the following data: ^{1}H NMR (400 MHz, D_2O) δ 4.08 – 3.63 (m, 1H), 3.37 – 2.73 (m, 2H), 2.28 – 1.52 (m, 4H). ^{13}C NMR (101 MHz, D_2O) δ 186.49, 64.89, 52.58, 29.31, 24.68. HRMS/ESI+ (m/z): [M+H]+ calcd for Pd($C_5H_8NO_2$)$_2$, 335.0218; found, 335.0224. Anal. Calcd. for Pd($C_5H_8NO_2$)$_2$: C, 35.89%; H, 4.82%; N, 8.37%. Found: C, 35.98%; H, 4.83%; N, 8.35%.

Synthesis of *trans*-bis(*N*-methyl-L-prolinato)palladium(II) (2)

A four dram vial was fitted with a magnetic stir bar and charged with 35.2 mg of palladium(II) acetate (0.1568 mmol) and 3.0 mL of 50/50 (v/v) acetone/water. The mixture was stirred until all solids had dissolved. To this mixture was added *N*-methyl-L-proline (42.7 mg, 0.3306 mmol) and stirred overnight. The reaction solution changed from a clear red-orange to a clear pale-yellow supernatant with a pale yellow precipitate. The supernatant was transferred via pipette to

a clean vial and allowed to evaporate to give clear yellow prisms which were used for X-ray diffraction. The precipitate was washed with water and dried under vacuum. The combined yield of crystals and precipitate was 53.6 mg of product (0.1477 mmol, 94% yield). *Trans*-Pd(C$_6$H$_{10}$NO$_2$)$_2$ (**2**) was identified on the basis of the following data: ^{1}H NMR (400 MHz, D$_2$O) δ 3.28 (dd, *J* = 10.4, 7.0 Hz, 1H), 3.12 (ddd, *J* = 10.9, 7.0, 2.8 Hz, 1H), 2.71 (s, 3H), 2.61 – 2.47 (m, 1H), 2.42 – 2.13 (m, 3H), 1.99 (dtt, *J* = 12.9, 6.7, 3.4 Hz, 1H). HRMS/ESI+ (m/z): [M+H]+ calcd for Pd(C$_6$H$_{10}$NO$_2$)$_2$, 363.0531; found, 363.0532. Anal. Calcd. for Pd(C$_6$H$_{10}$NO$_2$)$_2$·2H$_2$O: C, 36.15%; H, 6.07%; N, 7.03%. Found: C, 37.61%; H, 5.85%; N, 7.29%.

Synthesis of *cis*-bis(*trans*-4-hydroxyprolinato)palladium(II) (3)

A four dram vial was fitted with a magnetic stir bar and charged with 59.4 mg of palladium(II) acetate (0.2646 mmol) and 2.0 mL of 50/50 (v/v) acetone/water. The mixture was stirred until all solids had dissolved. To this mixture was added 77.1 mg of 4-hydroxy-L-proline (0.5880 mmol) and stirred overnight. The mixture changed from a clear red-orange solution to a clear pale-yellow supernatant with a pale yellow precipitate. The supernatant was transferred via pipette to a clean vial and allowed to evaporate to give clear yellow prisms. The precipitate was washed with water and dried under vacuum. The combined yield of crystals and precipitate was 94.3 mg of product (0.2572 mmol, 97% yield). *Cis*-Pd(C$_5$H$_8$NO$_3$)$_2$ (**3**) was identified on the basis of the following data: ^{1}H NMR (400 MHz, D$_2$O) δ 4.41 (s, 1H), 4.10 (t, *J* = 9.1 Hz, 1H), 3.35 – 3.28 (m, 1H), 3.27 – 3.15 (m, 2H), 3.10 (d, *J* = 12.7 Hz, 1H), 2.22 – 2.06 (m, 2H). HRMS/ESI+ (m/z): [M+H]+ calcd for Pd(C$_5$H$_8$NO$_3$)$_2$, 367.0116; found, 367.0130. Anal. Calcd. for Pd(C$_5$H$_8$NO$_3$)$_2$: C, 32.76%; H, 4.40%. Found: C, 32.88%; H, 4.42%.

Synthesis of *cis*-bis(*trans*-4-fluoroprolinato)palladium(II) (4)

A two dram vial was fitted with a magnetic stir bar and charged with 49.6 mg of palladium(II) acetate (0.2209 mmol) and 3.0 mL of acetone. The mixture was stirred until all solids had dissolved. To this mixture was added 64.6 mg of *trans*-4-fluoro-L-proline (0.4853 mmol) and stirred overnight. The mixture changed from a clear red-orange solution to a clear yellow supernatant with a pale yellow precipitate. The supernatant was transferred via pipette to a clean vial and allowed to evaporate to give clear yellow prisms. The precipitate was washed with acetone and dried under vacuum. The combined yield of crystals and precipitate was 78.1 mg of product (0.2107 mmol, 95% yield). *Cis*-Pd(C$_5$H$_7$FNO$_2$)$_2$ (**4**) was identified on the basis of the following data: ^{1}H NMR (400 MHz, Deuterium Oxide) δ 5.24 (dddt, J = 4.1, 3.3, 2.5, 0.8 Hz, 1H), 5.11 (tdd, J = 3.9, 2.9, 0.7 Hz, 1H), 4.13 (dd, J = 9.3, 8.8 Hz, 1H), 4.07 ‑ 3.98 (m, 1H), 3.47 ‑ 3.10 (m, 4H), 2.50 ‑ 2.34 (m, 2H), 2.25 ‑ 2.15 (m, 1H), 2.14 ‑ 2.05 (m, 1H). ^{13}C NMR (101 MHz, D$_2$O) δ 186.80 (s), 185.40 (s), 92.58 (d, $^1J_{CF}$ = 174 Hz), 92.46 (d, $^1J_{CF}$ = 174 Hz), 63.20 (s), 61.70 (s), 57.51 (d, $^2J_{CF}$ = 22 Hz), 56.19 (d, $^2J_{CF}$ = 22 Hz), 36.23 (d, $^2J_{CF}$ = 21 Hz), 35.94 (d, $^2J_{CF}$ = 22 Hz). ^{19}F NMR (471 MHz, D$_2$O) δ -179.33 (d, J = 140.9 Hz). HRMS/ESI+ (m/z): [M+H]+ calcd for Pd(C$_5$H$_7$FNO$_2$)$_2$, 371.0029; found, 371.0036. Anal. Calcd. for Pd(C$_5$H$_7$FNO$_2$)$_2$: C, 32.41%; H, 3.81%; N, 7.56%. Found: C, 32.99%; H, 3.92%; N, 7.53%.

Synthesis of *trans*-bis(2-benzylprolinato)palladium(II) (5)

A two dram vial was fitted with a magnetic stir bar and charged with 21.2 mg of palladium(II) acetate (0.0944 mmol) and 3.0 mL of 50/50 (v/v) acetone/water. The mixture was stirred until all solids had dissolved. To this mixture was added 50.2 mg of 2-benzylproline hydrochloride

(0.2077 mmol) and stirred overnight. The mixture changed from a clear red-orange solution to a clear yellow supernatant with an off white precipitate. The supernatant was transferred via pipette to a clean vial and allowed to evaporate to give clear yellow prisms. The precipitate was washed with cold water and dried under vacuum. The combined yield of crystals and precipitate was 44.7 mg of product (0.0868 mmol, 92% yield). *Trans*-Pd($C_{12}H_{14}NO_2$)$_2$ (**4**) was identified on the basis of the following data: ^{1}H NMR (400 MHz, D$_2$O) δ 7.32 – 7.15 (m, 5H), 3.42 (d, J = 14.6 Hz, 1H), 3.36 – 3.23 (m, 2H), 3.00 (d, J = 14.6 Hz, 1H), 2.48 – 2.37 (m, 1H), 2.09 – 1.96 (m, 2H), 1.87 (pd, J = 9.7, 8.8, 3.6 Hz, 1H). HRMS/ESI+ (m/z): [M+H]+ calcd for Pd($C_{12}H_{14}NO_2$)$_2$, 515.1157; found, 515.1175. Anal. Calcd. for Pd($C_{12}H_{14}NO_2$)$_2$: C, 55.98%; H, 5.48%; N, 5.44%. Found: C, 55.95%; H, 5.52%; N, 5.37%.

Synthesis of *trans*-bis(L-azetidine-2-carboxylato)palladium(II) (6)

A two dram vial was fitted with a magnetic stir bar and charged with 49.9 mg of palladium(II) acetate (0.2223 mmol) and 2.0 mL of 50/50 (v/v) acetone/water. The mixture was stirred until all solids had dissolved. To this mixture was added 51.2 mg of L-azetidine-2-carboxylic acid (0.5064 mmol) and stirred overnight. The mixture changed from a clear red-orange solution to a clear yellow supernatant with a pale yellow precipitate. The supernatant was transferred via pipette to a clean vial and allowed to evaporate to give clear yellow prisms. The precipitate was washed with cold water and dried under vacuum. The combined yield of crystals and precipitate was 66.7 mg of product (0.2175 mmol, 98% yield). *Trans*-Pd($C_4H_6NO_2$)$_2$ (**6**) was identified on the basis of the following data: ^{1}H NMR (400 MHz, Deuterium Oxide) δ 4.44 (dt, J = 8.8, 8.2 Hz, 2H), 3.69 (ddd, J = 15.7, 10.5, 8.0 Hz, 4H), 2.81 ‑ 2.56 (m, 4H). ^{13}C NMR (101 MHz, D$_2$O) δ 187.86, 186.59, 63.36, 61.42, 50.32, 48.79, 24.61, 24.58. HRMS/ESI+ (m/z): [M+H]+ calcd

for Pd(C$_4$H$_6$NO$_2$)$_2$, 515.1157; found, 515.1175. Anal. Calcd. for Pd(C$_4$H$_6$NO$_2$)$_2$: C, 55.98%; H, 5.48%; N, 5.44%. Found: C, 55.95%; H, 5.52%; N, 5.37%.

Synthesis of *cis*-bis(L-pipecolinato)palladium(II) (**7**)

A two dram vial was fitted with a magnetic stir bar and charged with 107.5 mg of palladium(II) acetate (0.4788 mmol) and 3.0 mL of 50/50 (v/v) acetone/water. The mixture was stirred until all solids had dissolved. To this mixture was added 126.6 mg of L-pipecolinic acid (0.9802 mmol) and stirred overnight. The mixture changed from a clear red-orange solution to a clear yellow supernatant with a pale yellow precipitate. The supernatant was transferred via pipette to a clean vial and allowed to evaporate to give clear yellow prisms. The precipitate was washed with cold water and dried under vacuum. The combined yield of crystals and precipitate was 152.4 mg of product (0.4202 mmol, 88% yield). *Cis*-Pd(C$_6$H$_{10}$NO$_2$)$_2$ (**7**) was identified on the basis of the following data: ^{1}H NMR (400 MHz, D$_2$O) δ 3.78 – 3.57 (m, 1H), 2.96 – 2.63 (m, 2H), 1.94 – 1.08 (m, 6H). HRMS/ESI+ (m/z): [M+H]+ calcd for Pd(C$_6$H$_{10}$NO$_2$)$_2$, 363.0531; found, 363.0543. Anal. Calcd. for Pd(C$_6$H$_{10}$NO$_2$)$_2$•4H$_2$O: C, 33.15%; H, 6.49%; N, 6.44%. Found: C, 33.30%; H, 6.50%; N, 6.45%.

Synthesis of *cis*-bis(D-prolinato)palladium(II) (**8**)

A two dram vial was fitted with a magnetic stir bar and charged with 50.2 mg of palladium(II) acetate (0.2236 mmol) and 2.0 mL of 50/50 (v/v) acetone/water. The mixture was stirred until all solids had dissolved. To this mixture was added 58.7 mg of D-proline (0.5099 mmol) and stirred overnight. The mixture changed from a clear red-orange solution to a clear yellow supernatant with a pale yellow precipitate. The supernatant was transferred via pipette to a clean

vial and allowed to evaporate to give clear yellow prisms. The precipitate was washed with cold water and dried under vacuum. The combined yield of crystals and precipitate was 71.1 mg of product (0.2124 mmol, 95% yield). Cis-Pd(C$_5$H$_8$NO$_2$)$_2$ (**8**) was identified on the basis of the following data: ^{1}H NMR (400 MHz, D$_2$O) δ 3.79 (dd, J = 9.1, 7.6 Hz, 1H), 3.10 – 2.96 (m, 2H), 2.17 – 2.06 (m, 1H), 1.99 – 1.78 (m, 2H), 1.67 – 1.54 (m, 1H). HRMS/ESI+ (m/z): [M+H]+ calcd for Pd(C$_5$H$_8$NO$_2$)$_2$, 335.0218; found, 335.0222. Anal. Calcd. for Pd(C$_5$H$_8$NO$_2$)$_2$: C, 35.89%; H, 4.82%; N, 8.37%. Found: C, 36.10%; H, 4.72%; N, 8.45%.

Synthesis of *cis*-bis(D-pipecolinato)palladium(II) (9)

A two dram vial was fitted with a magnetic stir bar and charged with 112.8 mg of palladium(II) acetate (0.5024 mmol) and 2.0 mL of 50/50 (v/v) acetone/water. The mixture was stirred until all solids had dissolved. To this mixture was added 132.2 mg of D-pipecolinic acid (1.0235 mmol) and stirred overnight. The mixture changed from a clear red-orange solution to a clear yellow supernatant with a pale yellow precipitate. The supernatant was transferred via pipette to a clean vial and allowed to evaporate to give clear yellow prisms. The precipitate was washed with cold water and dried under vacuum. The combined yield of crystals and precipitate was 151.9 mg of product (0.4188 mmol, 83% yield). Cis-Pd(C$_6$H$_{10}$NO$_2$)$_2$ (**9**) was identified on the basis of the following data: ^{1}H NMR (400 MHz, D$_2$O) δ 3.75 – 3.56 (m, 1H), 2.97 – 2.66 (m, 2H), 2.08 – 1.08 (m, 6H). HRMS/ESI+ (m/z): [M+H]+ calcd for Pd(C$_6$H$_{10}$NO$_2$)$_2$, 363.0531; found, 363.0520. Anal. Calcd. for Pd(C$_6$H$_{10}$NO$_2$)$_2$•4H$_2$O: C, 33.15%; H, 6.49%; N, 6.44%. Found: C, 35.09%; H, 6.02%; N, 6.85%.

3.3 CHARACTERIZATION AND HYDROGEN BONDING INTERACTIONS
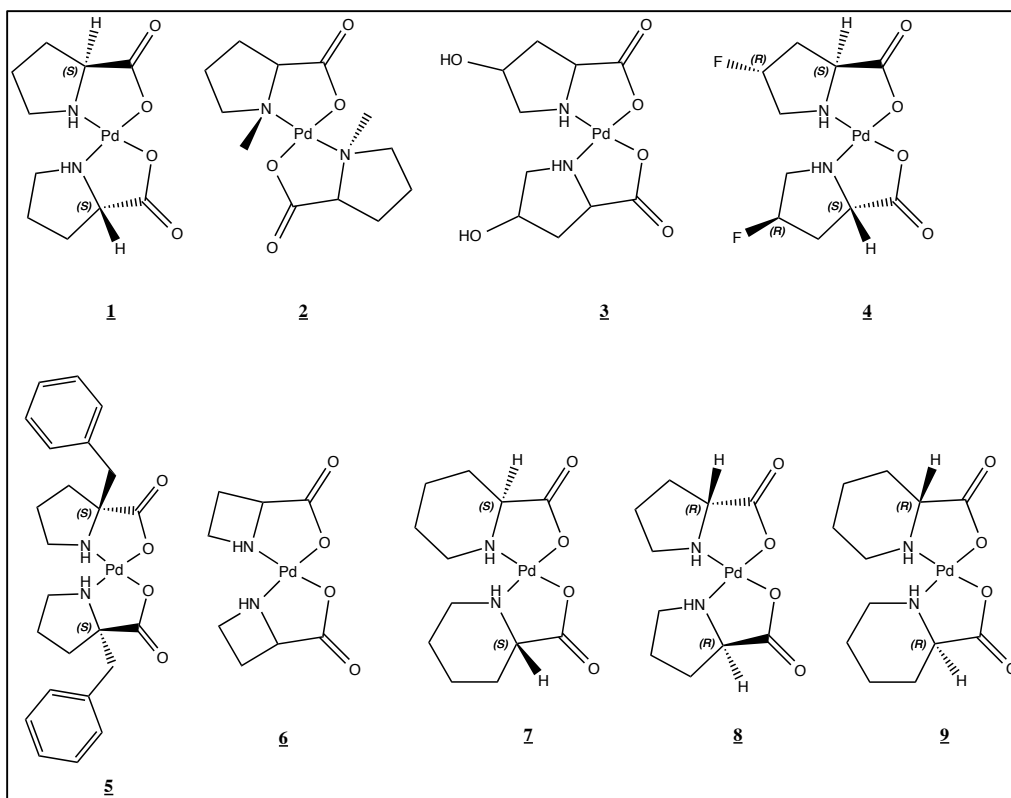
Figure 48. Compound structures and numbering scheme for proline and proline homolog complexes.

In the following discussions, compounds **1-9** (Figure 48, above) were synthesized via the following general reaction scheme (Figure 49):
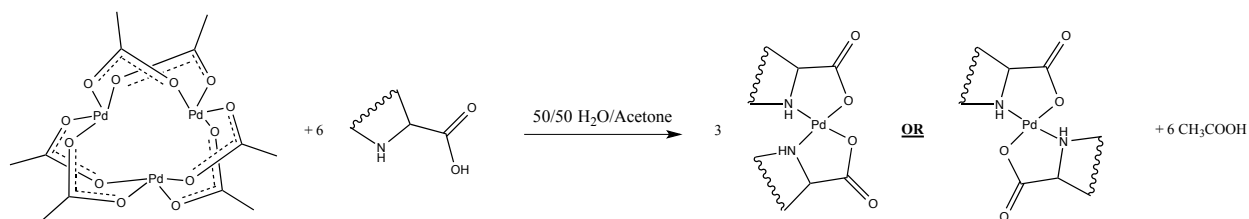
Figure 49. General reaction scheme for the synthesis of *cis* and *trans* palladium(II) proline/cyclic complexes.

The most common of the cyclic amino acids is L-proline and is one of the 20 naturally occurring α-amino acids. Compound **1** was prepared as the *cis* isomer via the scheme shown in Figure 2 and confirmed by X-ray crystal structure analysis (Figure 50).
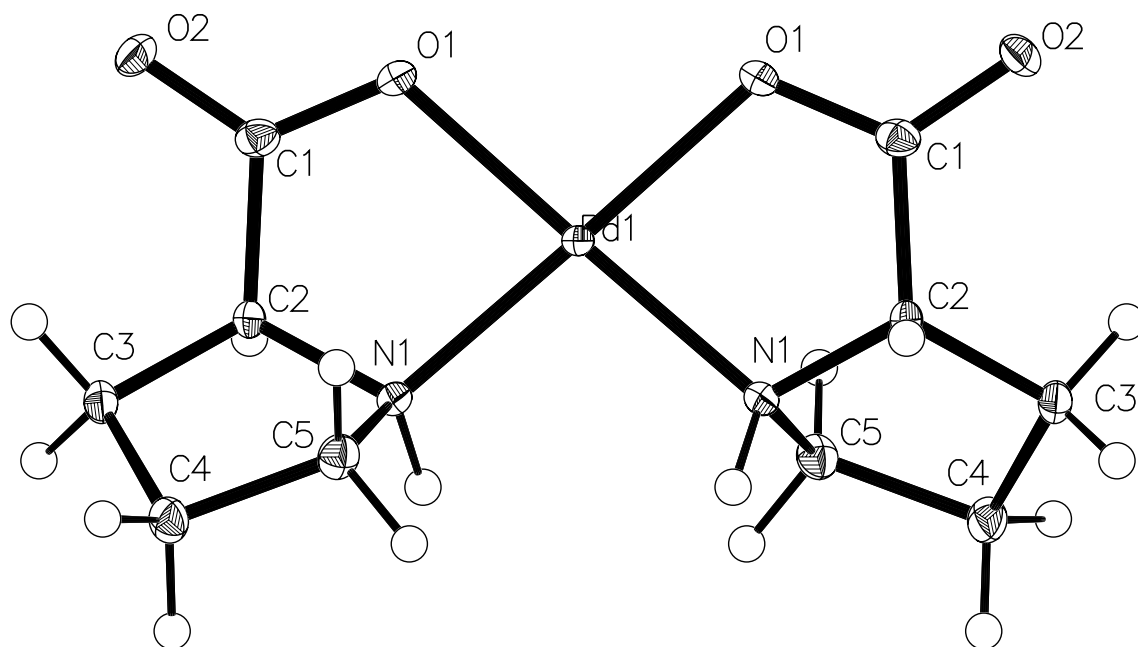
Figure 50. Thermal ellipsoid plot of the molecular structure of crystalline *cis*-bis(L-prolinato)palladium(II), 1. Thermal ellipsoids are shown at the 50% probability level.

The complex crystallizes in the $C222_1$ space group. Pd-N and Pd-O bond lengths are 2.0105Å and 2.0193Å respectively. N-Pd-O bond angles are 82.65 degrees for each chelate ring and

96.27 degrees between the chelate rings (O-Pd-O). All bond lengths and angles are within the ranges reported for similar d^8 metal chelates. Intermolecular hydrogen bonding is observed between the amine protons and the non-coordinated carboxyl oxygen atoms (Figure 51).
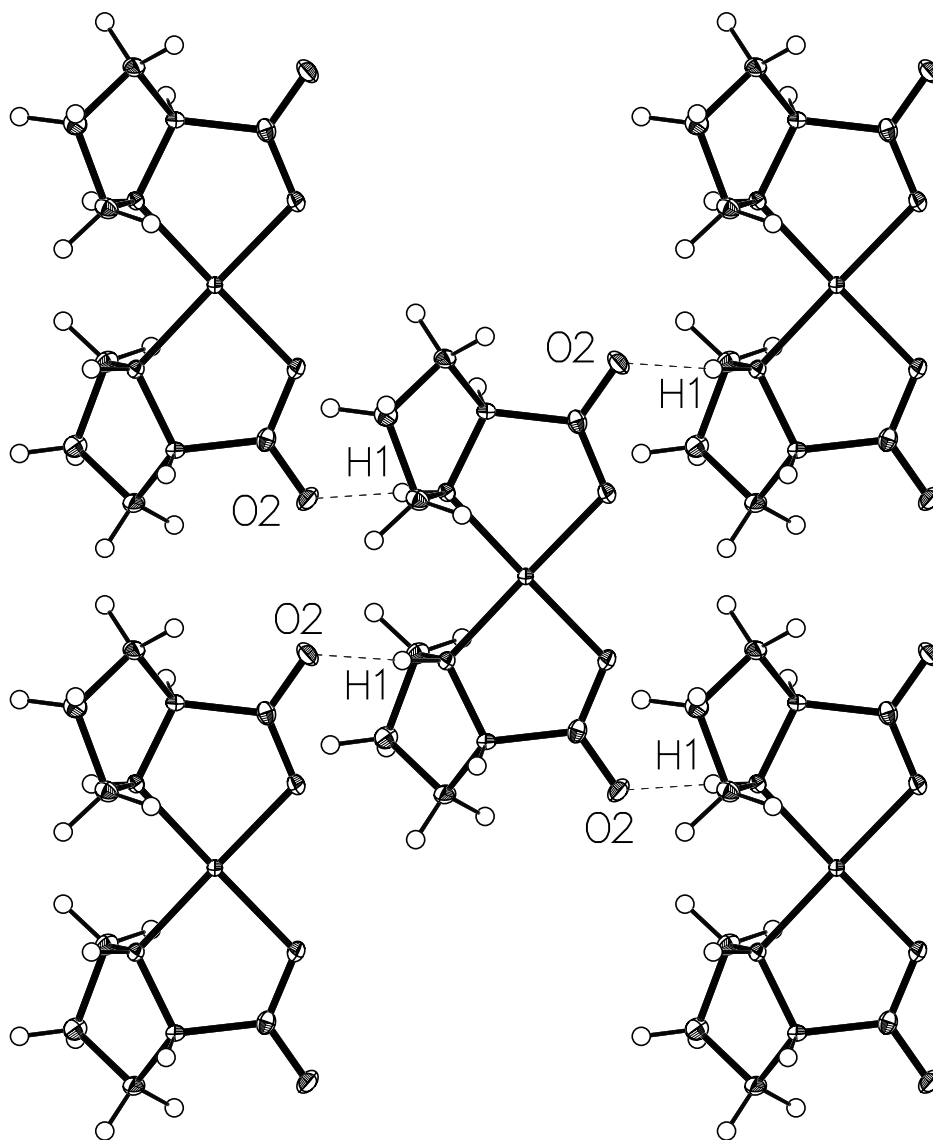
Figure 51. Crystal packing diagram viewed along [001] showing the intermolecular hydrogen bonding motif.

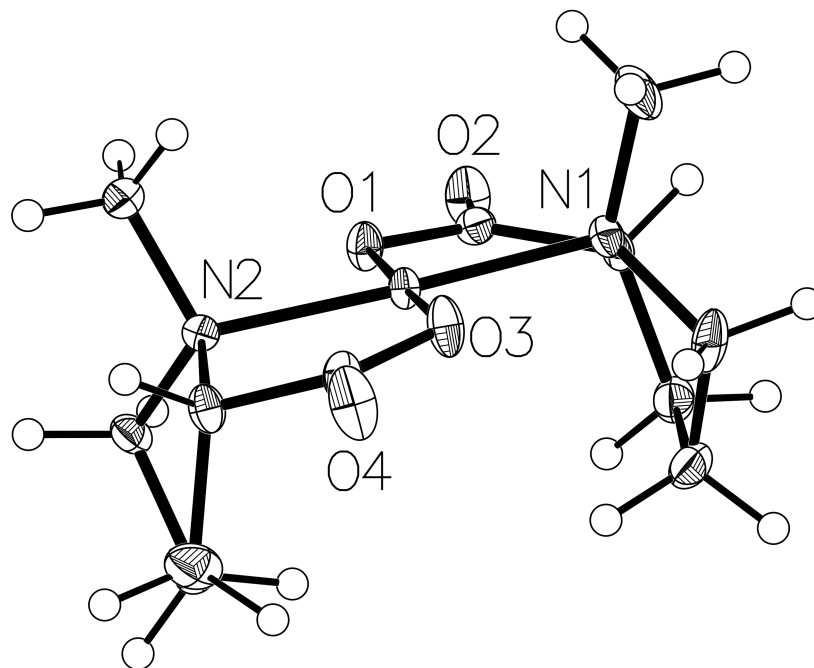The ^{1}H NMR spectrum in D$_2$O shows three multiplets at δ 4.08 – 3.63, 3.37 – 2.73, and 2.28 – 1.52, with integrated ratios of 1:2:4 respectively. As previously discussed for the palladium(II)-glycine complexes there is evidence of aquo-species formation in solution.[65] The ^{13}C NMR spectrum of *cis*-bis(prolinato)palladium(II) shows the expected five carbon resonances, suggesting one ligand environment in solution. This requires that either the bis-chelate or the bis-aquo species is the observed one. As we will discuss later, the proline complex is catalytically active which requires open *cis* sites on the metal. This alone suggests that the bis-aquo is the species present in solution, and is confirmed by DFT calculations which place the bis-aquo 9 kcal/mol lower in energy than the bis-chelate. The typical isotopic splitting pattern for palladium was observed in the HRMS spectrum with peaks at 333.0223, 334.0236, 335.0224, 337.0224, and 339.0236 amu (Figure 52).
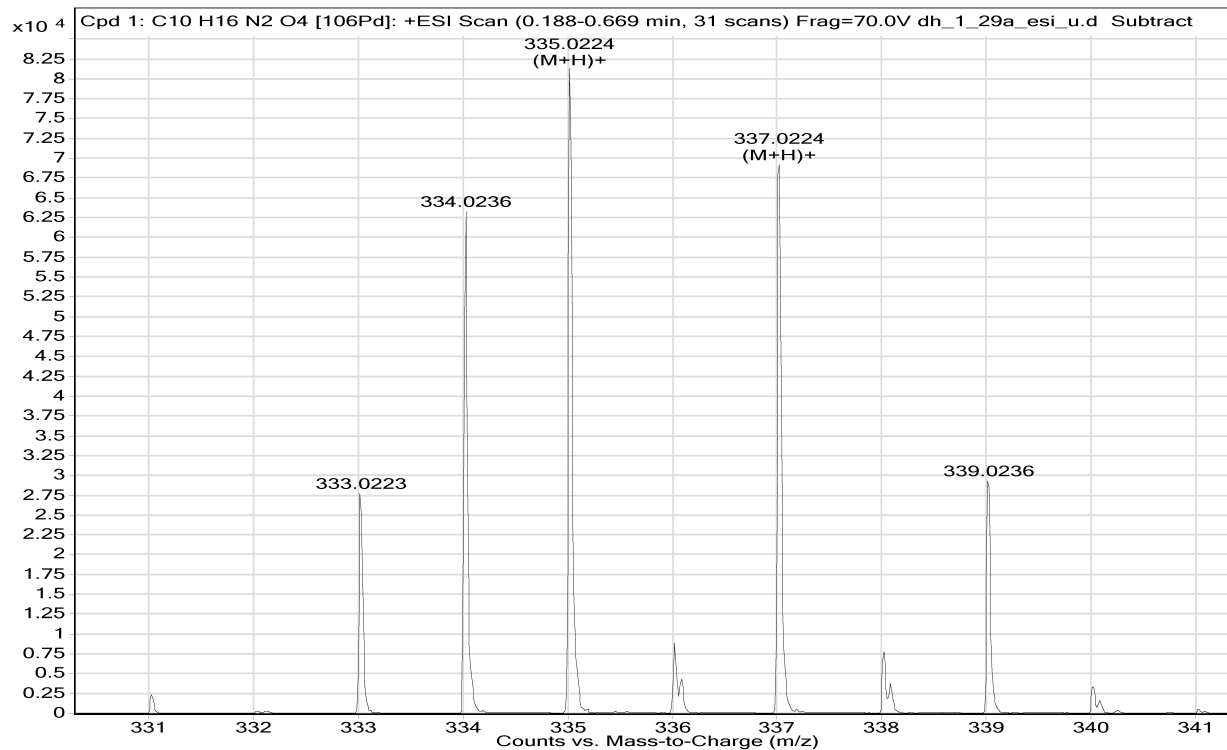
Figure 52. High-resolution time-of-flight mass spectrum of (<u>1</u>) showing the typical isotopic splitting pattern seen for

palladium compounds.

D-proline was used to prepare *cis*-bis(D-prolinato)palladium(II), Compound **8**. Characterization data for **8** was the same as that seen for **1**, with the stereochemistry of the chiral carbon reversed.

In *N*-methylproline the amine proton in proline is replaced with a methyl group. The resultant complex formed with this ligand is *trans*-bis(*N*-methylprolinato)palladium(II) (Figure 53), and this is confirmed by X-ray crystallographic analysis.
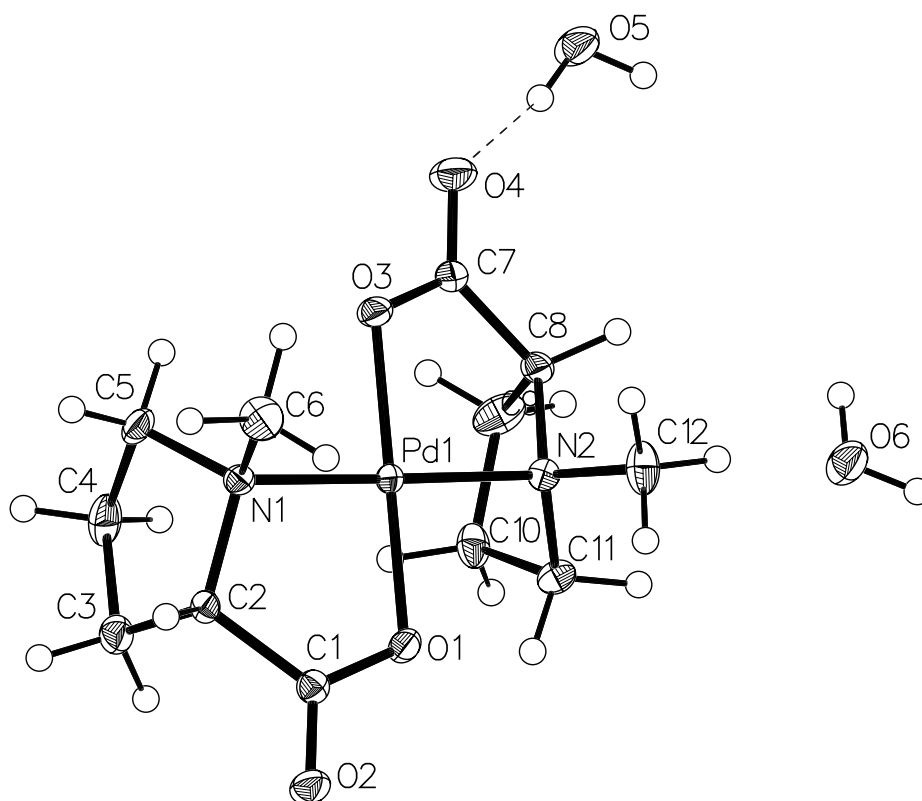
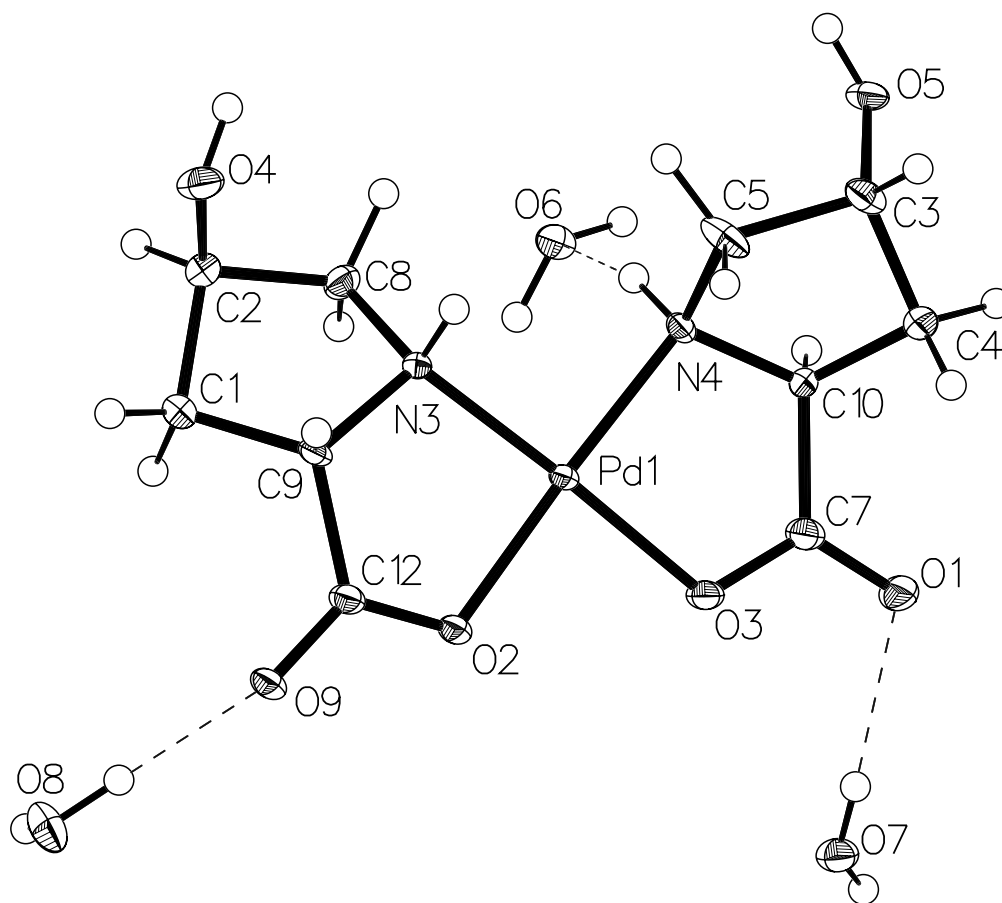**Figure 53. Thermal ellipsoid plot of the molecular structure of crystalline *trans*-bis(*N*-methylprolinato)palladium(II) dihydrate, <u>2</u>. Thermal ellipsoids are shown at the 50% probability level.**

As with the glycine complexes, replacement of the amine hydrogen atom with a methyl group results in a degree of steric crowding that disfavors formation of the *cis* isomer.[65] Similarly, all attempts to synthesize the *cis* isomer from PdCl$_2$ were unsuccessful. Complex **2** crystallizes in the P2$_1$2$_1$2$_1$ space group with Pd-N and Pd-O bond lengths of 2.051Å and 1.9900Å, respectively. N-Pd-O bond angles are 83.90 degrees in the chelate ring. N-Pd-O bond angles between the chelate rings are 95.42 degrees. All bond lengths and angles are within the ranges reported for similar d^8 metal chelates.[66-71] There is no intermolecular hydrogen bonding between complex molecules in the lattice, however there is hydrogen bonding between water molecules and complex molecules (Figure 54). Intermolecular hydrogen-bonded water molecules are observed

to bridge between the coordinated carboxylate oxygen atom of one complex molecule and the carbonyl oxygen of an adjacent complex molecule. It is also interesting to note that both of the pyrrolidine rings are turned down in the same direction such that they are oriented away from the chelate plane. This places the *N*-methyl groups on the opposite face of the chelate plane (Figure 55).
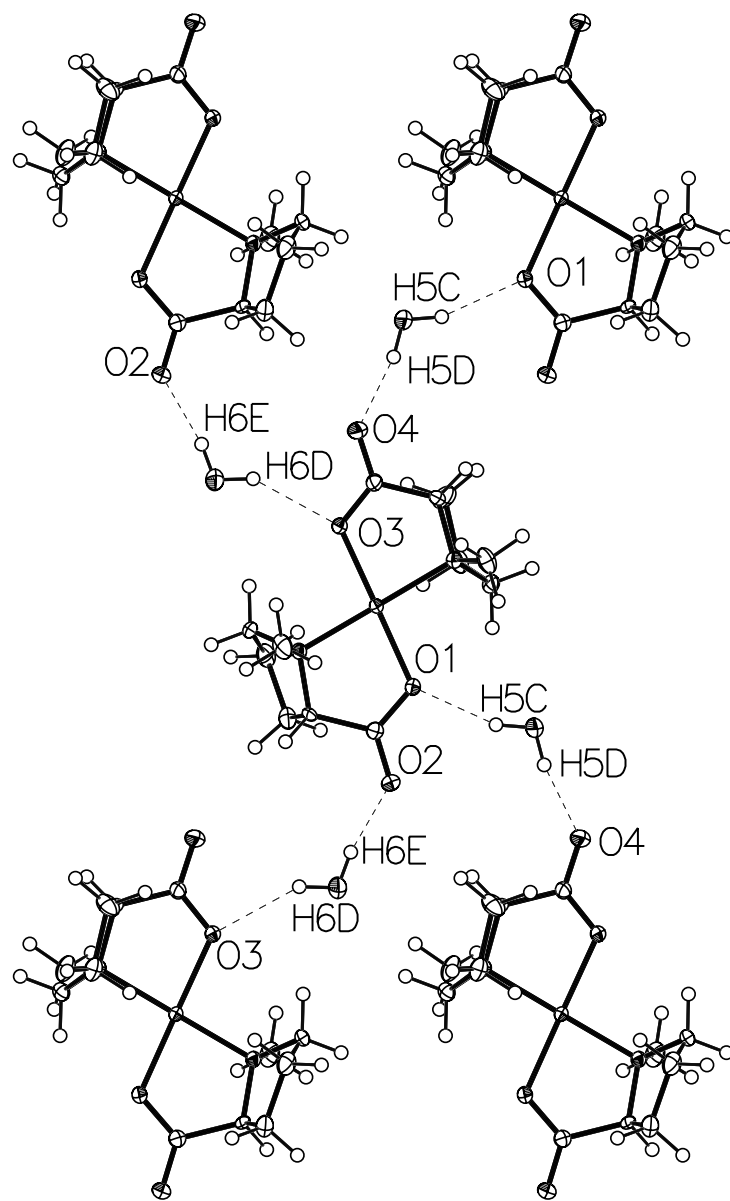
Figure 54. Crystal packing diagram of (**2**) as viewed along [010] showing the intermolecular hydrogen bonding motif.

Figure 55. ORTEP plot of (2) showing the orientation of the pyrrolidine rings and *N*-methyl groups in relation to the chelate plane. Only selected atoms are labeled for clarity.

The ^{1}H NMR spectrum in D_2O shows the expected singlet for the methyl protons at δ 2.71 ppm. The remaining proton resonances are present in the expected ratios, however the splitting patterns are complex. The typical isotopic splitting pattern for palladium is observed in the HRMS spectrum with peaks at 361.0526, 362.0542, 363.0532, 365.0531, and 367.0541 amu.

Hydroxyproline and fluoroproline are more electron-withdrawing than their unsubstituted analogues, and this influence was probed by synthesizing their respective complexes **3** and **4**. *Cis*-bis(*trans*-4-hydroxyprolinato)palladium(II) was synthesized (Compound **3**, Figure 56) using *trans*-4-hydroxyproline as the ligand.

Figure 56. **Thermal ellipsoid plot of the molecular structure of crystalline cis-bis(trans-4-hydroxyprolinato)palladium(II) trihydrate, (3). Thermal ellipsoids are shown at the 50% probability level.**

Complex **3** crystallizes in the P2$_1$ space group with 3 hydrogen bonded water molecules in the lattice. There is intermolecular hydrogen bonding between one of the 4-hydroxyl group hydrogen atoms and the carbonyl oxygen of an adjacent molecule. The hydroxyl oxygen atom is hydrogen bonded to a lattice water molecule that in turn hydrogen bonds to a coordinated carboxylate oxygen of the adjacent molecule. The other 4-hydroxyl group is hydrogen bonded to two lattice water molecules that also hydrogen bond to carbonyl oxygens on adjacent complex molecules in the lattice (Figure 57). The amine hydrogens are hydrogen bonded to lattice waters.
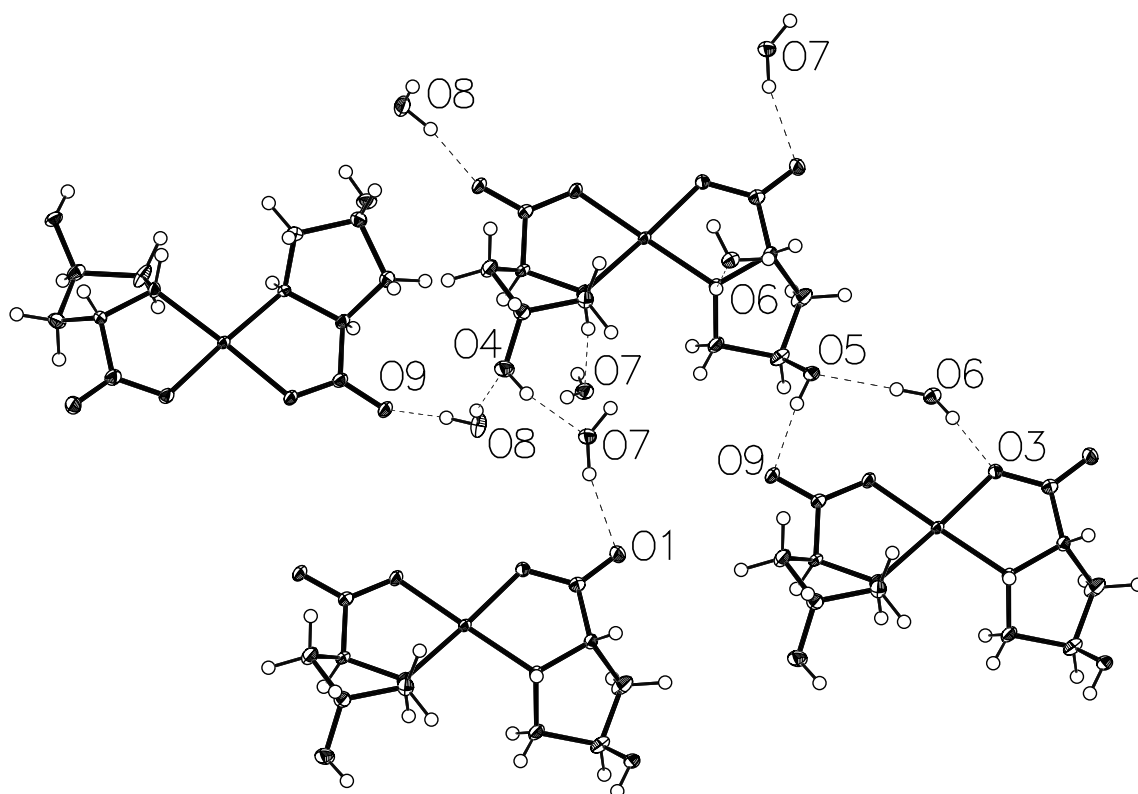
Figure 57. Extended hydrogen-bonding network of *cis*-bis(trans-4-hydroxyprolinato)palladium(II) (3).

Pd-N and Pd-O bond lengths are 2.0153Å and 2.0006Å, respectively. N-Pd-O bond angles are 83.92 degrees in the chelate ring with N-Pd-N bond angles between the chelate rings are 97.84 degrees. All bond lengths and angles are within the ranges reported for similar d^8 metal chelates. The ^{1}H NMR spectrum in D_2O shows a singlet at 4.41 ppm, indicating that the hydroxyl proton does not exchange, or exchanges very slowly. All other resonances are as expected. The typical palladium isotopic pattern is observed in the HRMS.

Cis-bis(*trans*-4-fluoroprolinato)palladium(II) (Figure 58) crystallizes in the C2 space group. There are no water molecules in the lattice, and the hydrogen bonding arrangement is quite different from that seen with the hydroxyproline complex. For the fluoroproline complex

there is hydrogen bonding from each amine hydrogen atom to a carbonyl oxygen atom on separate, adjacent complex molecules in the lattice (Figure 59). The fluorine atoms do not participate in a hydrogen bonding interaction.
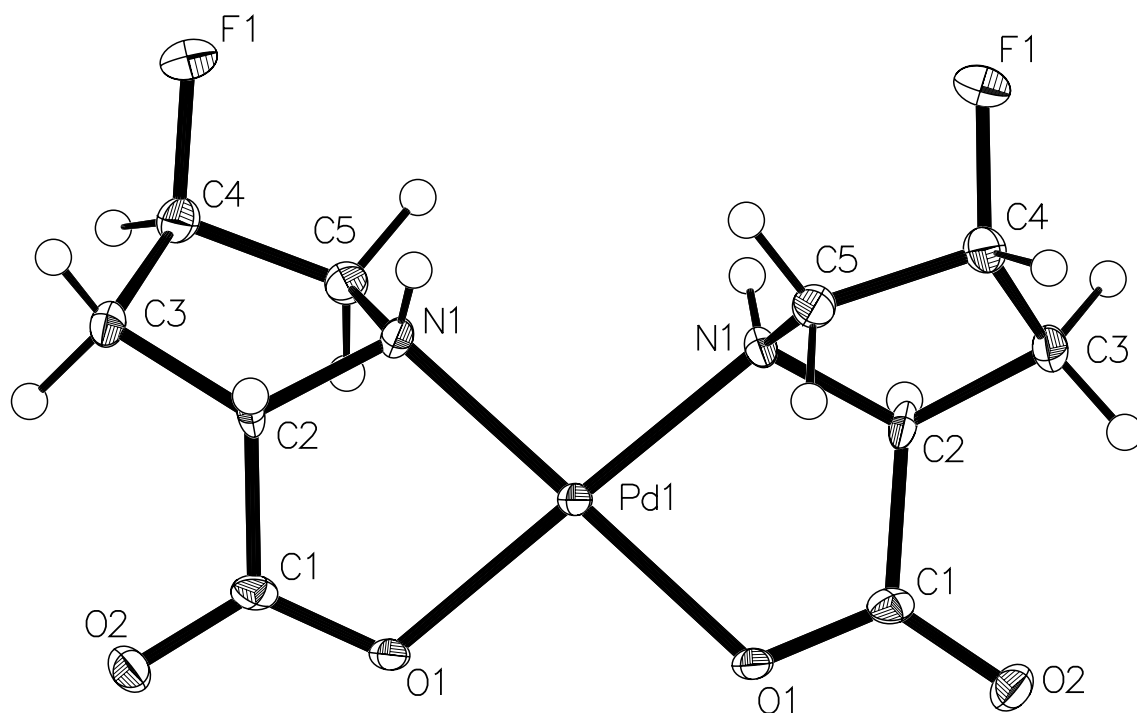
Figure 58. *Cis*-**bis(***trans***-4-fluoroprolinato)palladium(II), (4).**
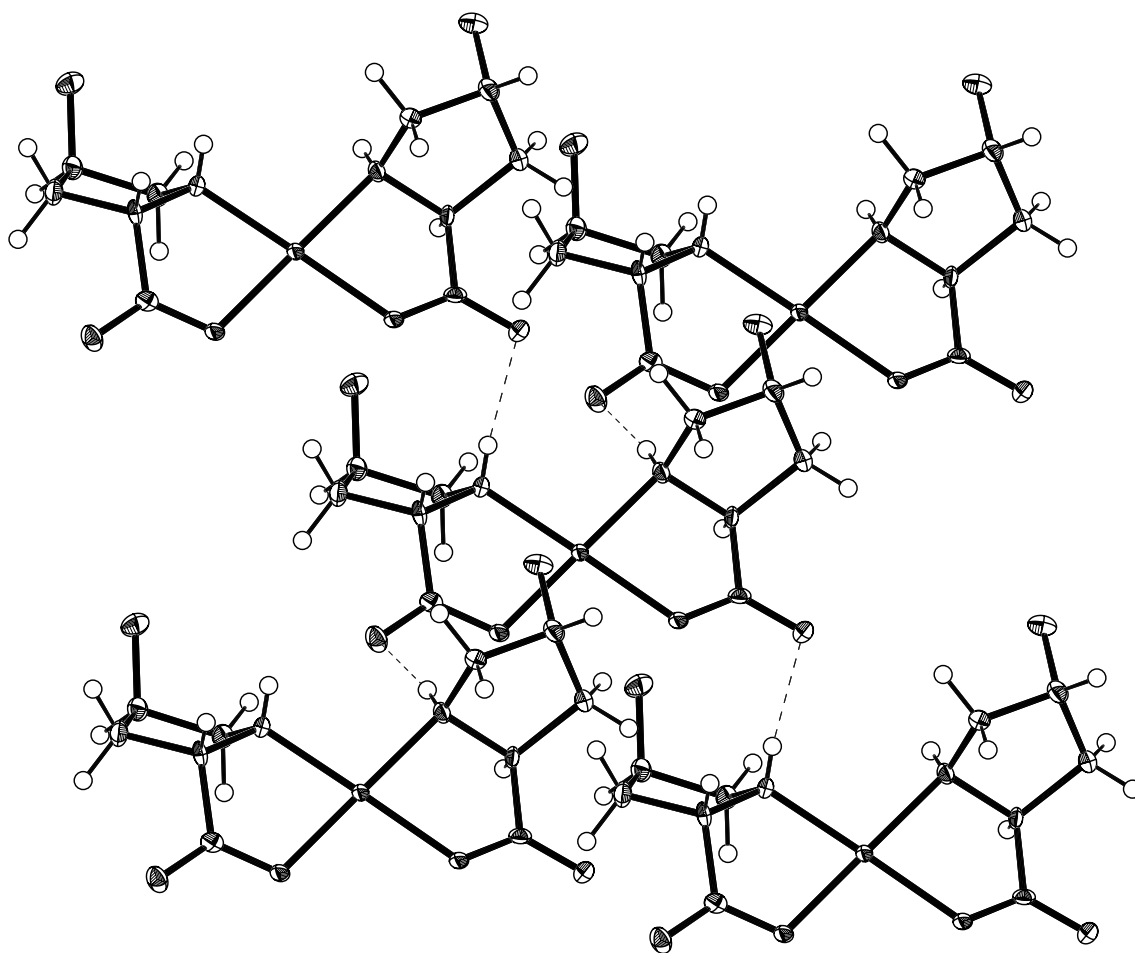
Figure 59. Crystal packing diagram of *cis*-bis(*trans*-4-fluoroprolinato)palladium(II) (<u>4</u>).

The Pd-N and Pd-O bond lengths in compound <u>4</u> are 2.006Å and 2.017Å respectively. The N-Pd-O bond angle in the chelate ring is 82.092 degrees, with the N-Pd-N bond angle between the chelate rings at 98.544 degrees. As with the previous complexes, these values are in good agreement with other square planar palladium *N,O* chelates.

The proton NMR spectrum of <u>4</u> shows a complicated set of multiplets due to ^{1}H-^{19}F coupling; however integration does show the expected ratios of protons (Figure 60). The

methine proton signals are fairly well resolved into two triplets, suggesting two different ligand environments.
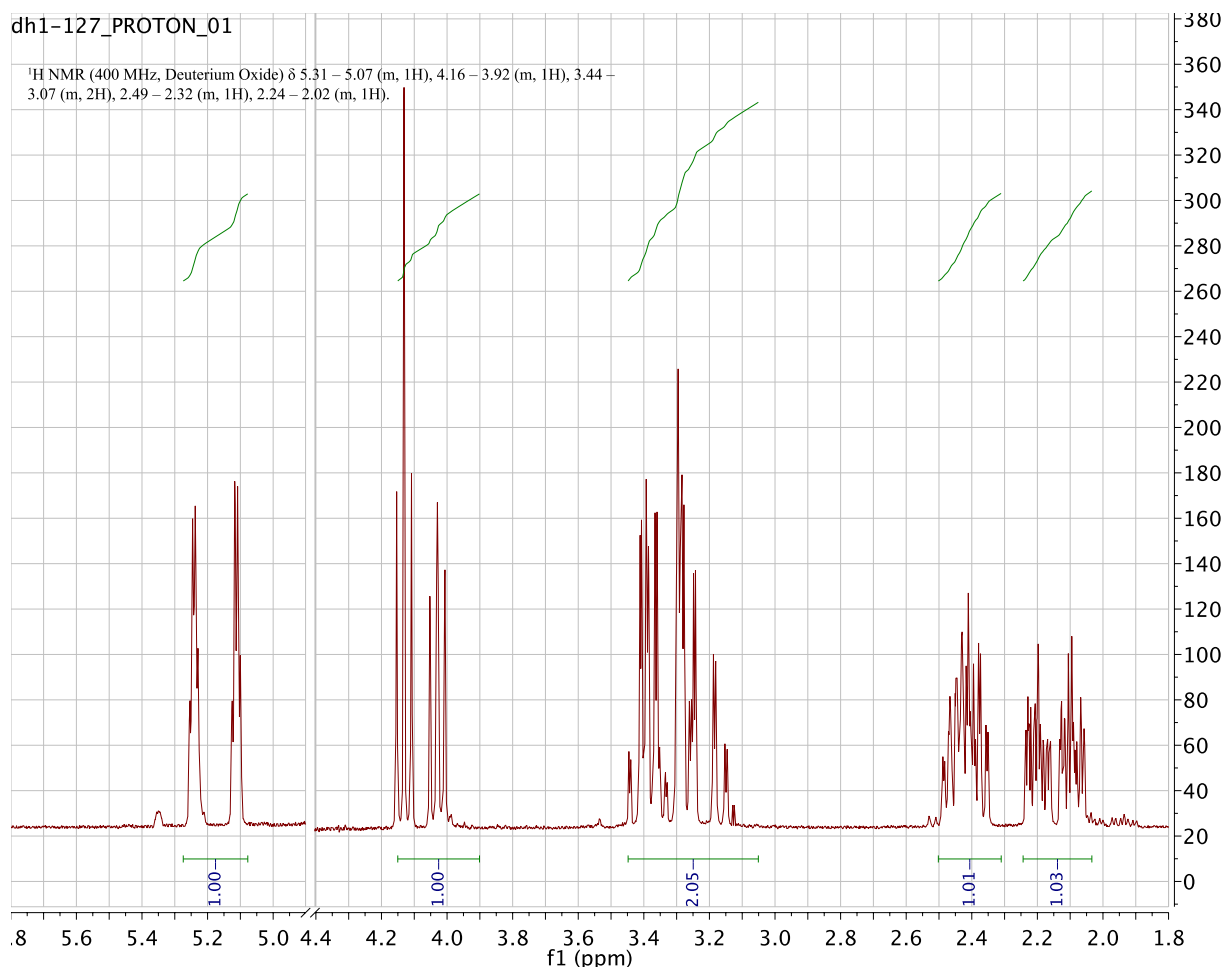
Figure 60. **^{1}H NMR spectrum of *cis*-bis(*trans*-4-fluoroprolinato)palladium(II) (4).**

The ^{13}C NMR (Figure 61) is somewhat easier to interpret, showing ten carbon resonances with ^{19}F coupling observed. This once again suggests two ligand environments. The ^{1}H-decoupled ^{19}F NMR spectrum (Figure 62) shows two singlets at -179.18 and 179.48 ppm, providing further evidence that there are two ligand environments present. A non-^{1}H-decoupled ^{19}F NMR spectrum was obtained. Careful integration of the slightly overlapped signals yields a

1:1 ratio for these peaks. The NMR data strongly suggests that there are two species present in solution. Turning to DFT calculations once again, the calculated stabilities of the fluoroproline complex are as follows: mono-aquo > bis-chelate > bis-aquo. This then suggests that the two species present are bis-chelate and bis-aquo, however it is far more plausible that the lower energy bis-aquo complex is the actual species in solution and that, like the *N*-methylglycine complex, it adopts C$_1$ symmetry in solution. HRMS shows the expected palladium isotopic pattern.
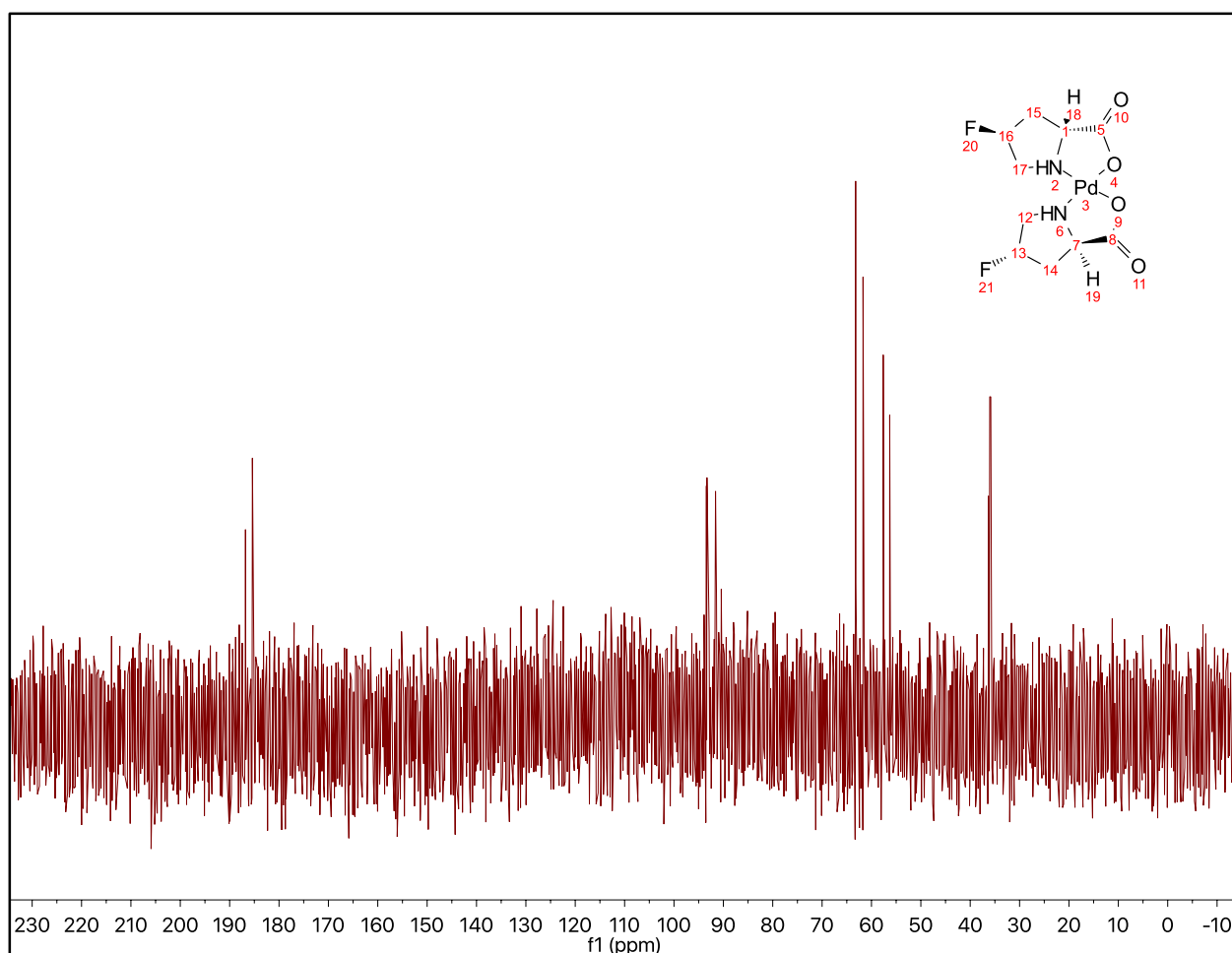
Figure 61. ^{13}C NMR spectrum of *cis*-bis(*trans*-4-fluoroprolinato)palladium(II) (<u>4</u>).
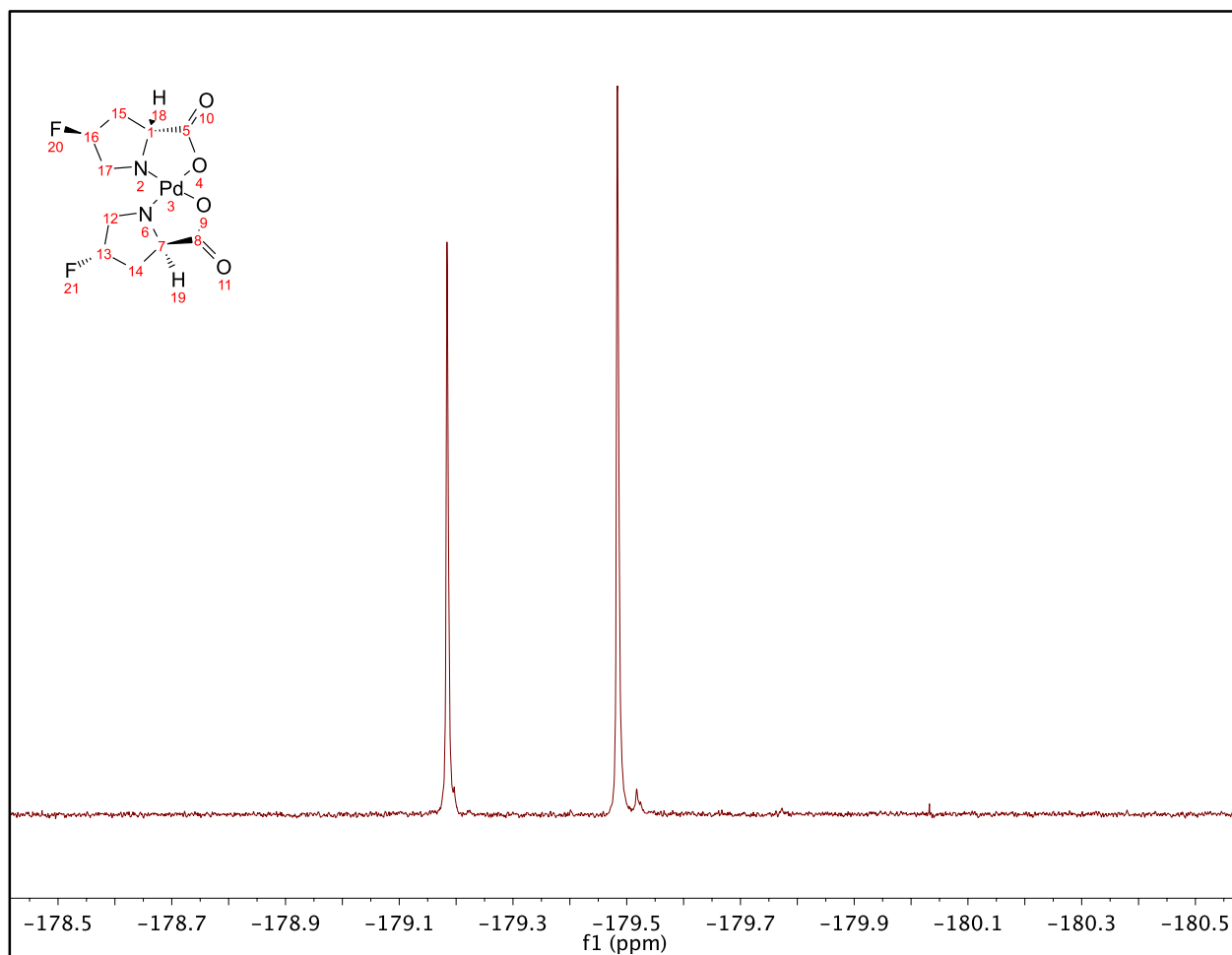
Figure 62. ¹⁹F NMR spectrum of *cis*-bis(*trans*-4-fluoroprolinato)palladium(II) (<u>4</u>).

2-Benzylproline adds additional steric and electronic density to the proline ligand. Compound **<u>5</u>**, *trans*-bis(2-benzylprolinato)palladium(II) (Figure 63), was prepared using 2-benzylproline hydrochloride as the ligand.
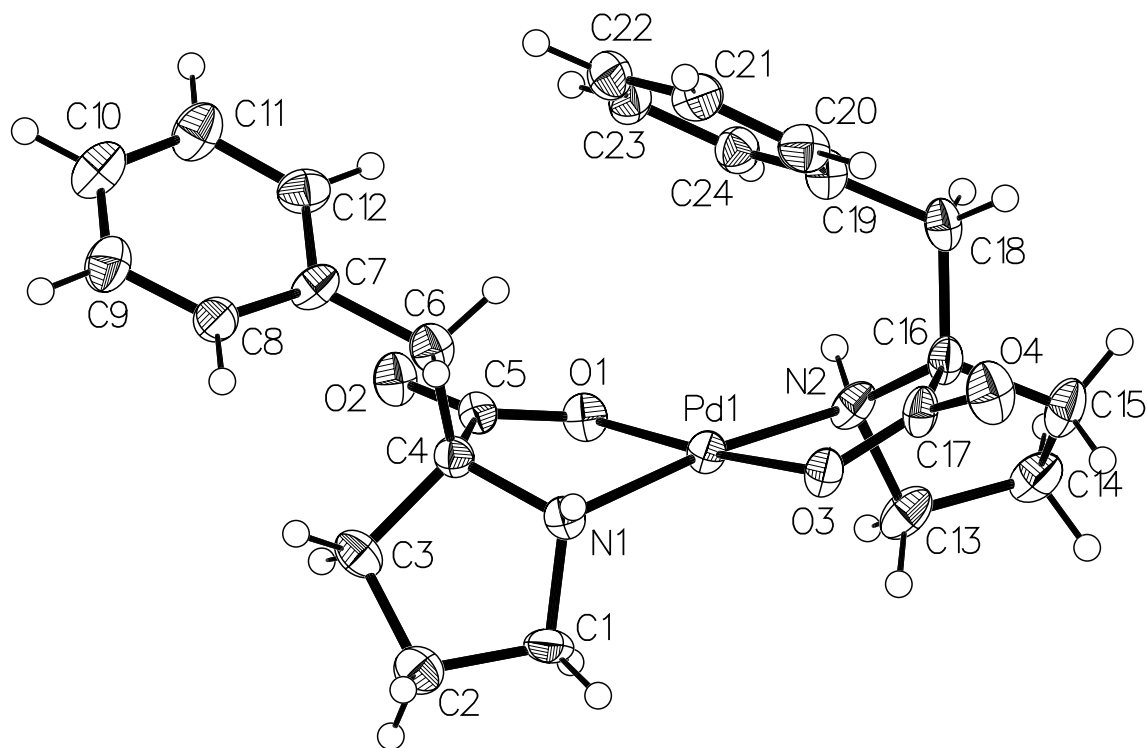
Figure 63. **Thermal ellipsoid plot of the molecular structure of crystalline *trans*-bis(2-benzylprolinato)palladium(II), 5. Thermal ellipsoids are shown at the 50% probability level.**

Crystallizing in the $P2_12_12_1$ space group, *trans*-bis(2-benzylprolinato)palladium(II) has Pd-N bond lengths of 2.024Å and 2.037Å. Pd-O bond lengths are 2.006Å and 2.004Å. The chelate rings are slightly twisted out of the square plane. The N-Pd-O angles between the chelate rings are 98.3 and 97.2 degrees. The N-Pd-O angles in the chelate rings are 82.6 degrees. The benzyl groups on the ligands are oriented up and away from the proline ring, with one of the benzyl groups laying over the square plane. This is the same arrangement reported by Sabat[70] for the palladium(II)-tyrosine complex, however in the case of **5** the second benzyl group does not lie over an adjacent metal center, but rather in the lattice space between complex molecules. This arrangement does suggest that there is a π-d interaction occurring between the metal and the

110

aromatic ring of the ligand. Two of the carbon atoms in the benzyl ring lie closer to the metal center than their calculated Van Der Waals radii. The Pd-C(19) contact distance is 3.452 Å and the Pd-C(24) contact distance is 3.472 Å. The calculated Van Der Waals radius[72] for a Pd-C bond is 3.91 Å, or approximately 0.45 Å more than what is observed in the crystal structure. This reduction in the Pd-C contact distances suggests an energetically favorable interaction between the π electron cloud of the benzyl ring and the empty $d_{x^2-y^2}$ orbital on the metal center. The other Pd-C contact distances within the benzyl ring are in the range of 4.009-4.565 Å. Hydrogen bonding is noted between the amine hydrogen atoms and the coordinated carboxylate oxygen atom of the adjacent molecule (Figure 64). There are no water molecules in the lattice, which is not surprising given the hydrophobicity of the benzyl groups.
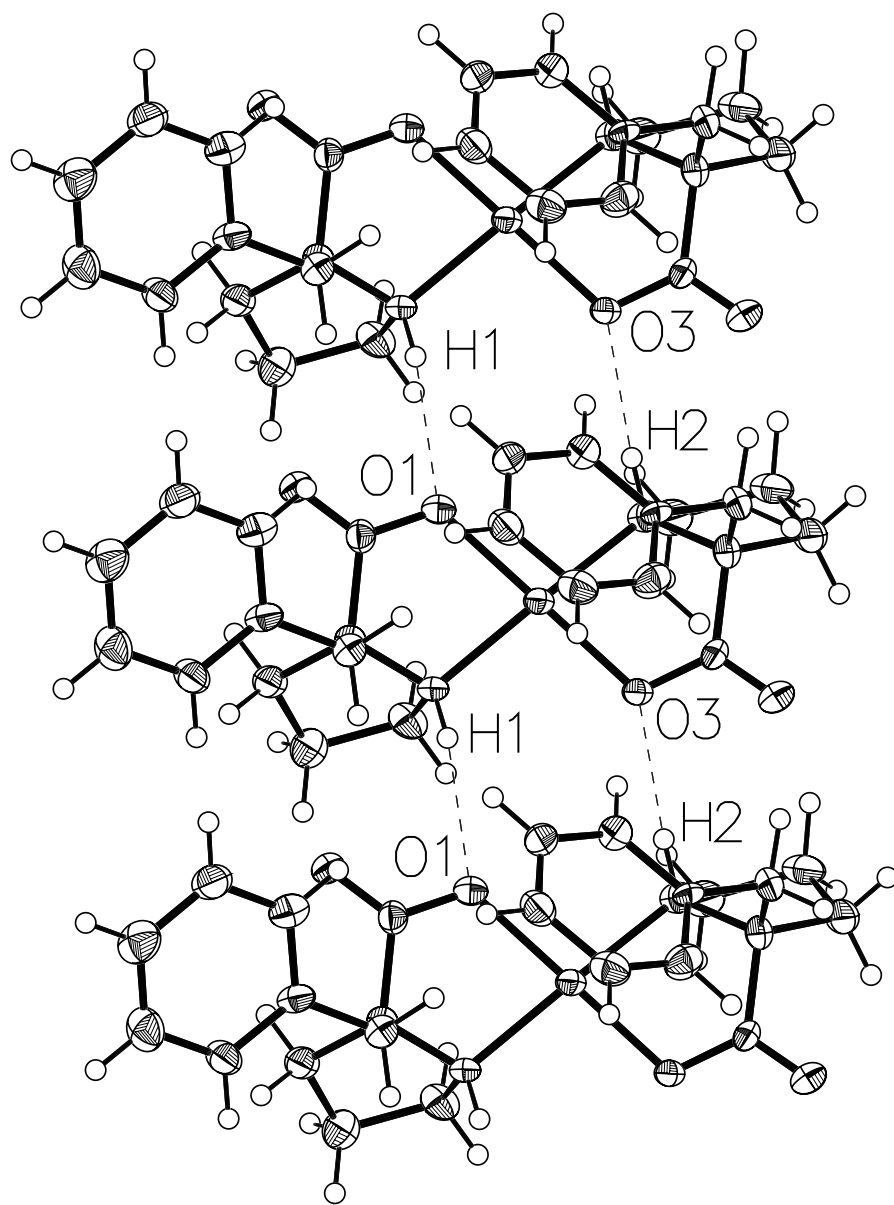
Figure 64. Crystal packing diagram of *trans*-bis(2-benzylprolinato)palladium(II), (5).

The ^{1}H NMR spectrum is somewhat complicated. The aromatic benzyl protons show a multiplet at 7.25 ppm with the benzyl methylene protons each resonating as a doublets at 3.42 and 3.00 ppm. The integrated ratio of the benzyl protons is the expected 5:2. The pyrrolidine ring protons

show multiplets at 3.29, 2.43, 2.02, and 1.87 ppm in a ratio of 2:1:2:1. The expected mass and isotopic splitting pattern is once again observed in the HRMS for complex **5** with the $[M+H]^+$ peak at 515.1175 amu.

The proline ring is a 5-membered moiety, and both four- and six-membered ring homologs are known. The 4-membered ring homolog, L-azetidine-2-carboxylic acid, was used to prepare *trans*-bis(L-azetidine-2-carboxylato)palladium(II) (Compound **6**, Figure 65).
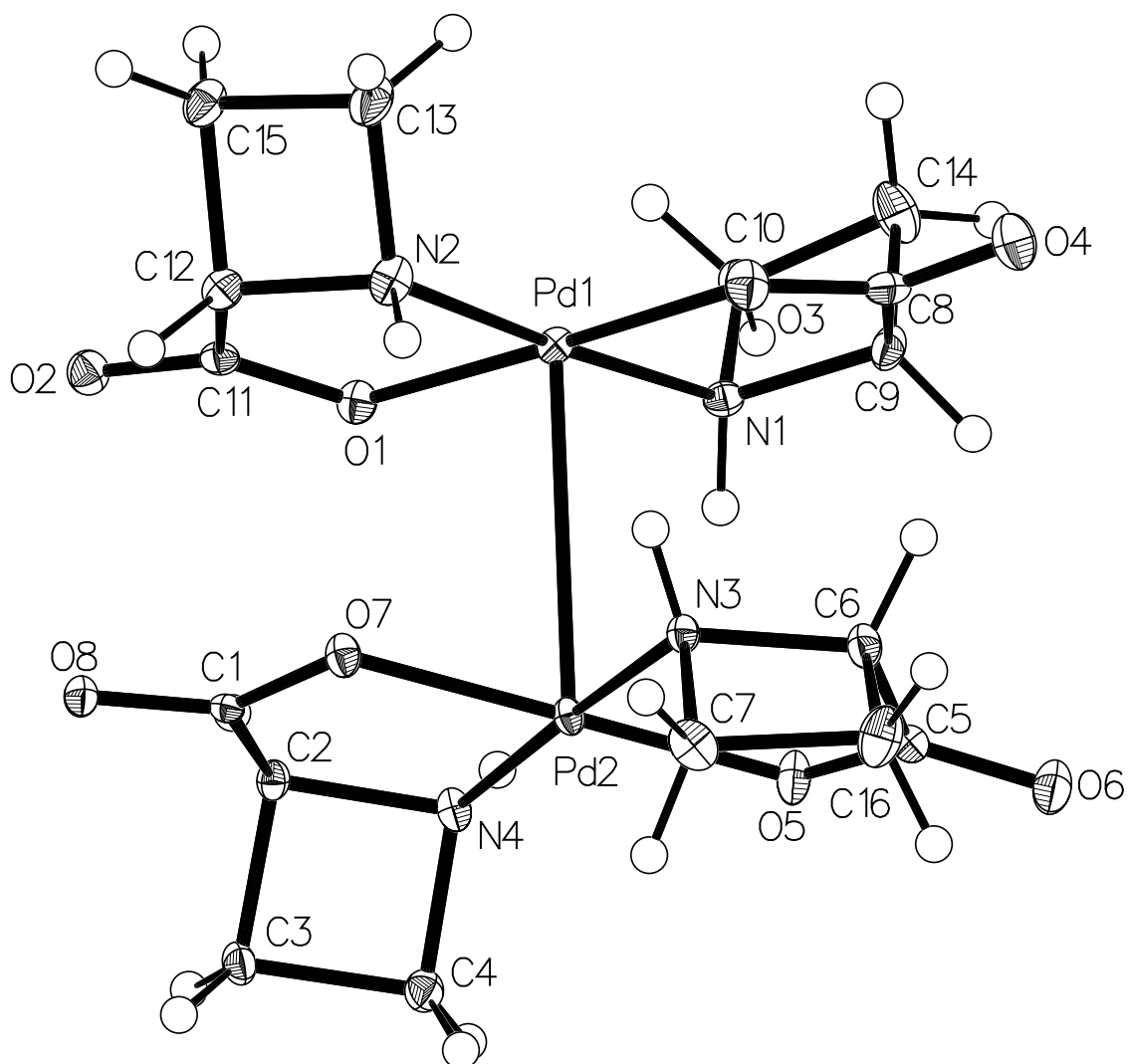
Figure 65. ORTEP plot of *trans*-bis(L-azetidine-2-carboxylato)palladium(II), (6). Thermal ellipsoids are shown at the 50% probability level.

The immediately obvious and unique aspect of this structure is that it crystallizes as an apparent dimer, with a Pd-Pd bond distance of 3.2479 angstroms at 100 K. At room temperature, however, the crystal structure was solved by Voureka[73] and reported as a monomer. To probe this difference, a variable temperature X-ray diffraction study was carried out on this complex and it was determined that a temperature induced phase change occurs between 200-220K.

Cryogenic differential scanning calorimetry was carried out on the complex and was able to confirm a thermal transition at 204K (Figure 66).
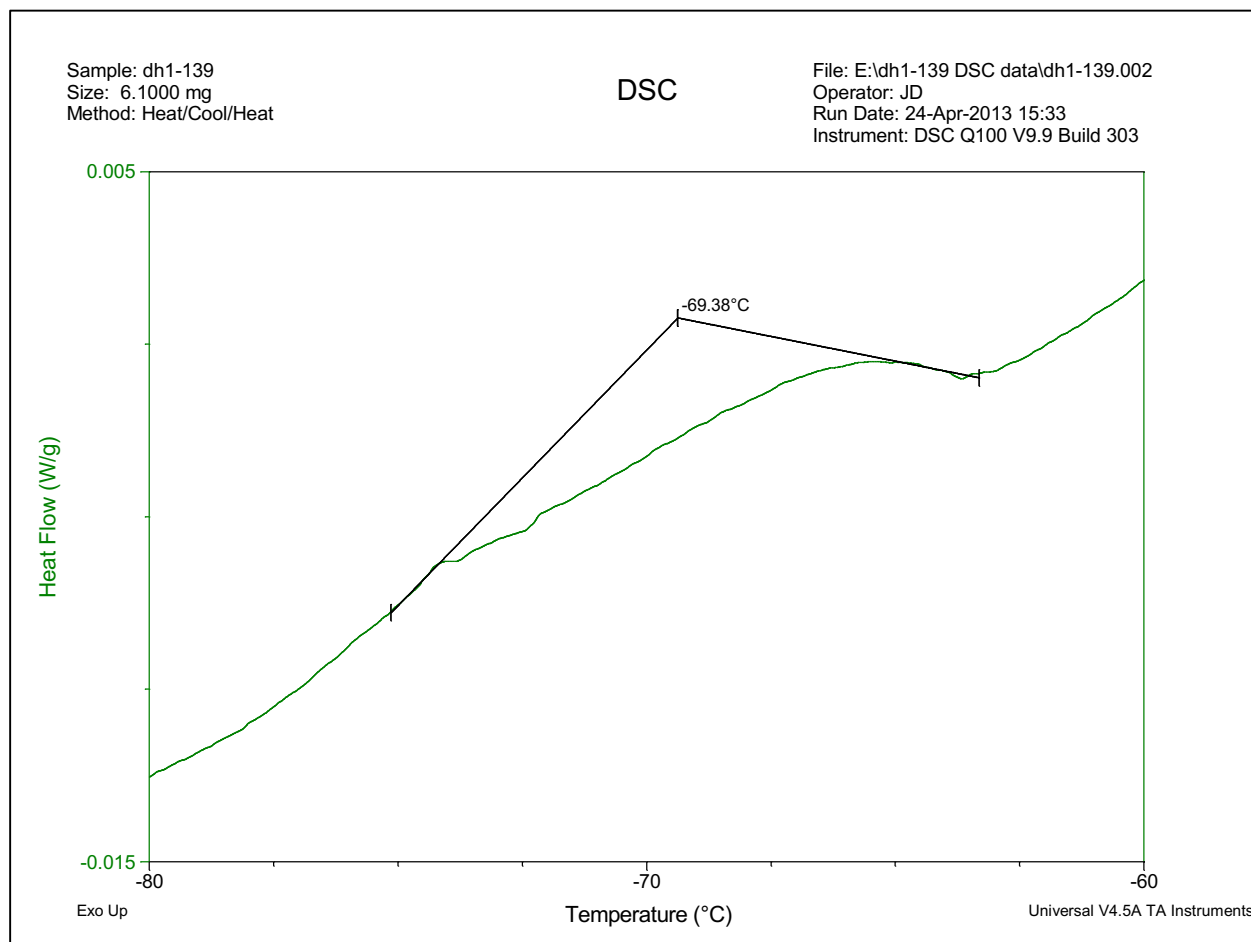
Figure 66. Cryo-DSC plot obtained on *trans*-bis(L-azetidine-2-carboxylato)palladium(II) showing a temperature induced phase change at 204 K.

This apparent phase change is in actuality a simple distortion of the lattice at low temperature. The high-temperature phase crystallizes in the space group $P6_4$ with $V \approx 1450$ Å^3. The low-temperature phase crystallizes in the space group $P6_5$ with $V \approx 2840$ Å^3. The doubling of the volume upon cooling is caused by the loss of the 2-fold symmetry in $P6_4$, which generates the space group $P6_5$ with a doubled c-axis. Figure 67 (below) shows an overlay plot of the two

halves of the dimer structure at 100 K, illustrating how the azetidine ring distortion breaks the $P6_4$ symmetry seen at higher temp.
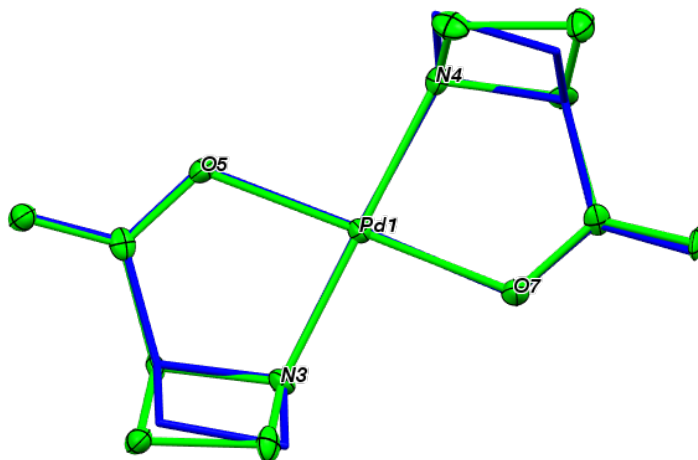
Figure 67. Overlay plot of the dimer halves of *trans*-bis(L-azetidine-2-carboxylato)palladium(II) (6) at 100 K illustrating the ring distortion that accounts for the apparent temperature-induced phase change below 204 K.

The ^{1}H NMR data shows the expected ratios of integrated resonances, and the ^{13}C NMR spectrum again shows evidence of aquo complex formation. As seen with the glycine complexes[65] discussed previously, the carbon NMR data for **6** shows two peaks for each carbon. The HRMS is as expected for a palladium complex.

The six-membered ring homolog, L-pipecolinic acid, was used to prepare *cis*-bis(L-pipecolinato)palladium(II) (Compound **7**, Figure 68). This complex crystallizes in the C2 space group. Pd-N and Pd-O bond lengths are approximately equivalent at 2.01-2.03Å, comparable to the other complexes discussed within. The piperidine ring adopts the classic "chair" formation seen in cyclohexyl ring systems.
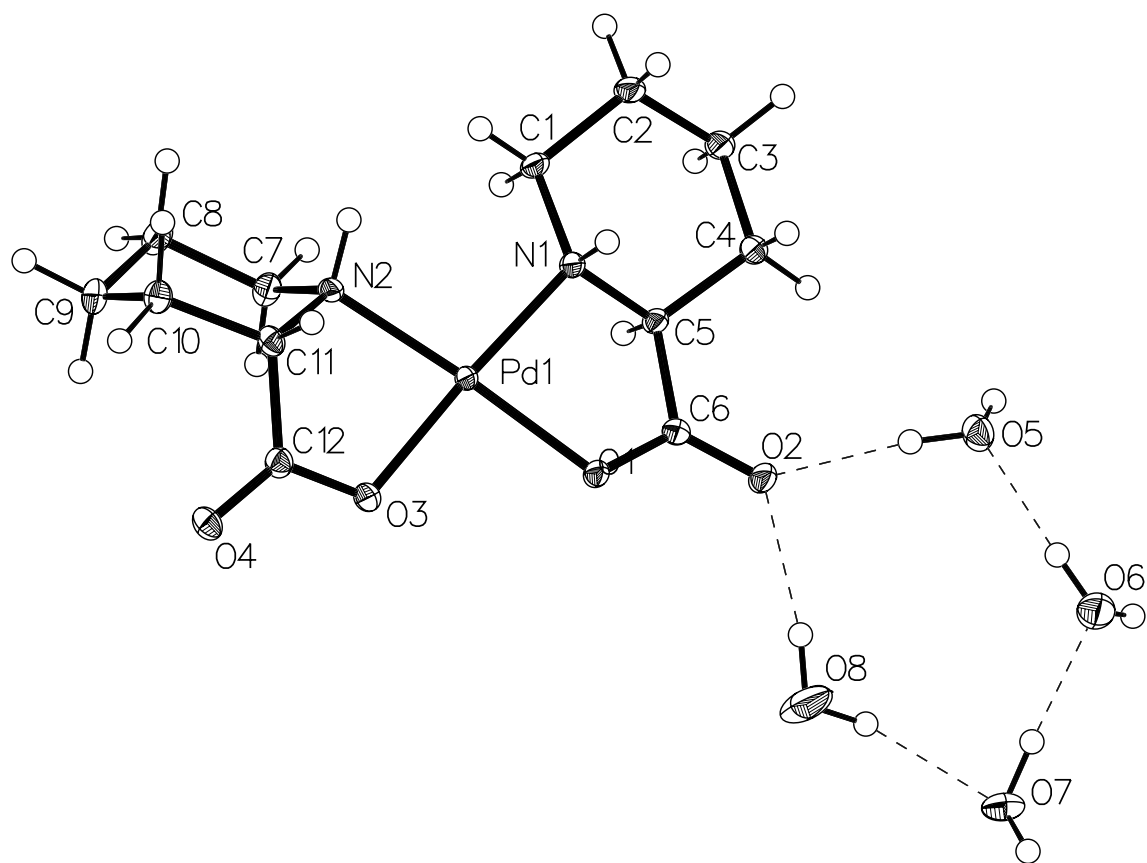
Figure 68. ORTEP plot of *cis*-bis(L-pipecolinato)palladium(II), (<u>7</u>). Thermal ellipsoids are shown at the 50% probability level.

There are four hydrogen bonded water molecules in the lattice that form a pentagonal ring structure with a carbonyl oxygen of the complex. One amine hydrogen atom is hydrogen bonded to the opposite carboxyl oxygen of the adjacent molecule in the lattice.   The other amine hydrogen is hydrogen bonded to one of the water molecules within the pentagonal water structure (Figure 69).
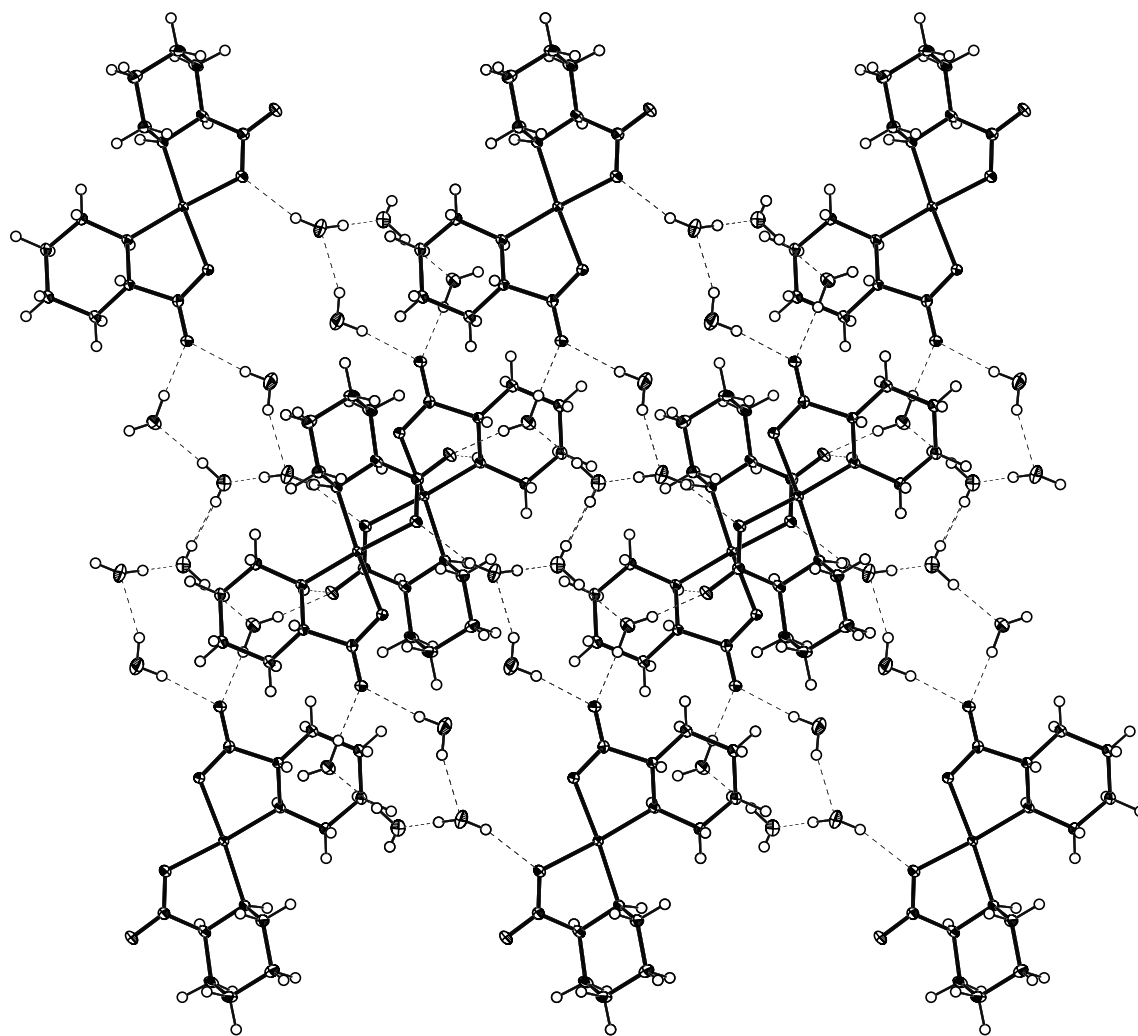
Figure 69. Packing diagram of *cis*-bis(L-pipecolinato)palladium(II) hydrate (7) as viewed along [010].

As with the proline complexes, D-pipecolinic acid was used to prepare cis-bis(D-pipicolinato)palladium(II), Compound **9**. Characterization data for **9** was the same as that seen for **7**, again with the stereochemistry of the chiral carbon inverted (Figure 70).
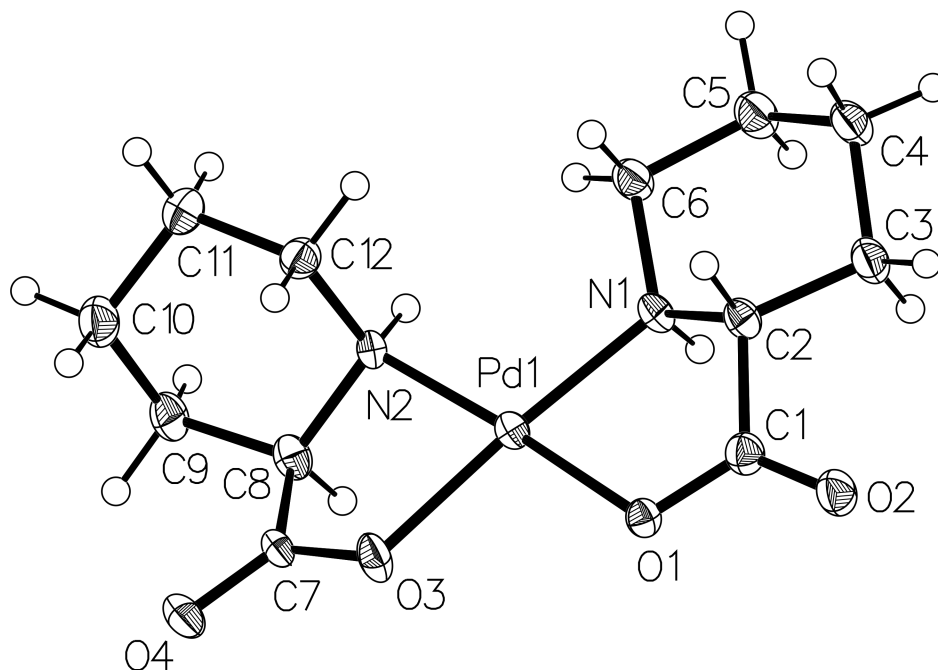
Figure 70. ORTEP plot of cis-bis(D-pipicolinato)palladium(II), (9). Lattice water molecules have been removed for clarity. Thermal ellipsoids are shown at the 50% probability level.

3.4 CATALYTIC ACTIVITY

Asymmetric carbon-carbon bond formation is one of the most useful transformations in synthetic chemistry.[74-80]

A palladium(II) catalyzed coupling reaction between phenylboronic acid and methyl tiglate was chosen as a model to evaluate the catalytic reactivity of these new palladium(II)-amino acid complexes (Figure 71).

119
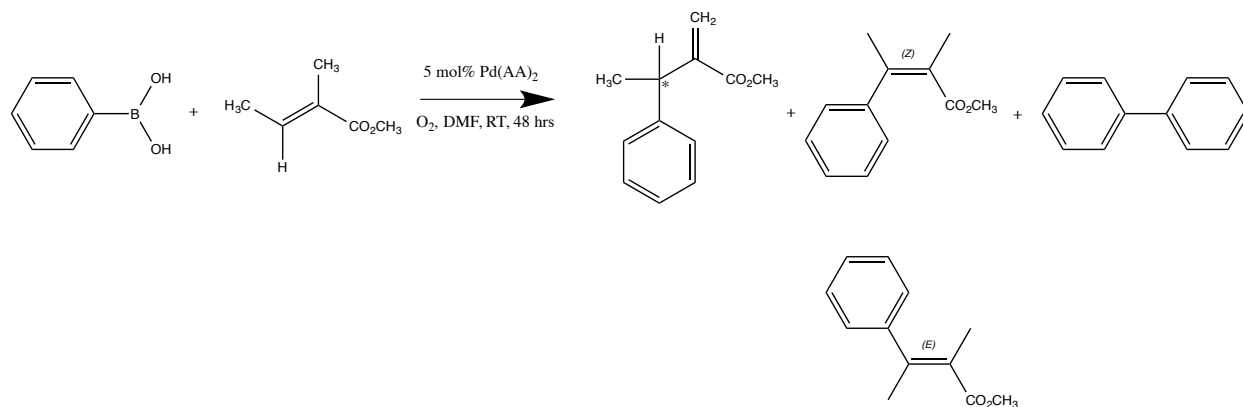
Figure 71. Bis(amino acid)Pd(II) catalyzed cross coupling of phenylboronic acid and methyl tiglate.

The couplings were carried out as previously described in the experimental section of Chapter 2. Substrate/catalyst ratios were maintained at 1:3:0.5 mmol for boronic acids, olefins, and catalysts, respectively. GC-MS was used to initially confirm the products and determine retention times on a chiral Cyclosil-B column. That column was then installed in a GC-FID and product ratios were determined directly from the peak areas on the chromatograms. As the products of interest are all positional isomers of each other and therefore have the same effective carbon number and calculated relative response factors, no further correction was applied to the chromatographic peak areas.

3.4.1   Oxidative Coupling of Phenylboronic Acids and Alkenes

The standard coupling reaction that was used to evaluate the catalytic potential for each of the catalyst complexes was the aforementioned oxidative coupling between phenylboronic acid and methyl tiglate.[30,31] All of the complexes described in this chapter, except the *N*-methylproline complex, were observed to catalyze this reaction and those data are summarized in Table 8 below. We have previously postulated that only the *cis* complexes are catalytically active, based on our observations with the glycine complexes described in Chapter 2. We see

120

here, however, that the azetidine complex catalyzes the reaction even though it exists as the *trans* isomer. This suggests that *N*-alkylation, and not *cis/trans* geometry, may be the limiting factor in the catalytic ability of these complexes. Conversely, we must also acknowledge the possibility of *cis/trans* isomerization occurring in solution, although direct evidence of this has not been observed.

Some general observations regarding product distributions and catalyst structure can be made. The presence of an electronegative group, -F or –OH, on the proline ring leads to a decrease in the formation of the E/Z products. The presence of purely alkyl functionality on the proline ring leads to an increase of the E/Z yield with corresponding loss of R/S product. The exception here is with the pipecolinic acid complex. This complex generates almost all R/S product, albeit with no selectivity, and very little E/Z or homocoupled product. These general observations not withstanding, there is still a great deal of variability in the product distributions that does not seem to follow any general trend. This suggests that the particular steric environment about the metal center during the catalytic cycle likely plays an important role in determining which products will form.
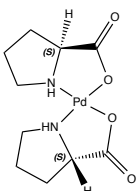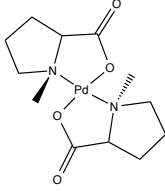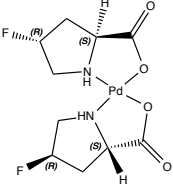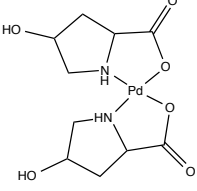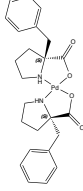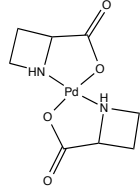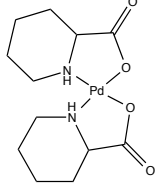
Complex	R/S yield, %	%ee	E/Z yield, %	Biaryl, %	Higher Couplings
	28	24	19	20	33
	NO REACTION OBSERVED				
	79	11	4	6	11
	76	14	6	5	13
	31	2	63	3	3
	54	11	14	3	29
	73	1	2	1	24

Table 8. Coupling reaction product distributions for catalysts <u>1</u>, <u>2</u>, <u>3</u>, <u>4</u>, <u>5</u>, <u>6</u>, <u>7</u>.

122

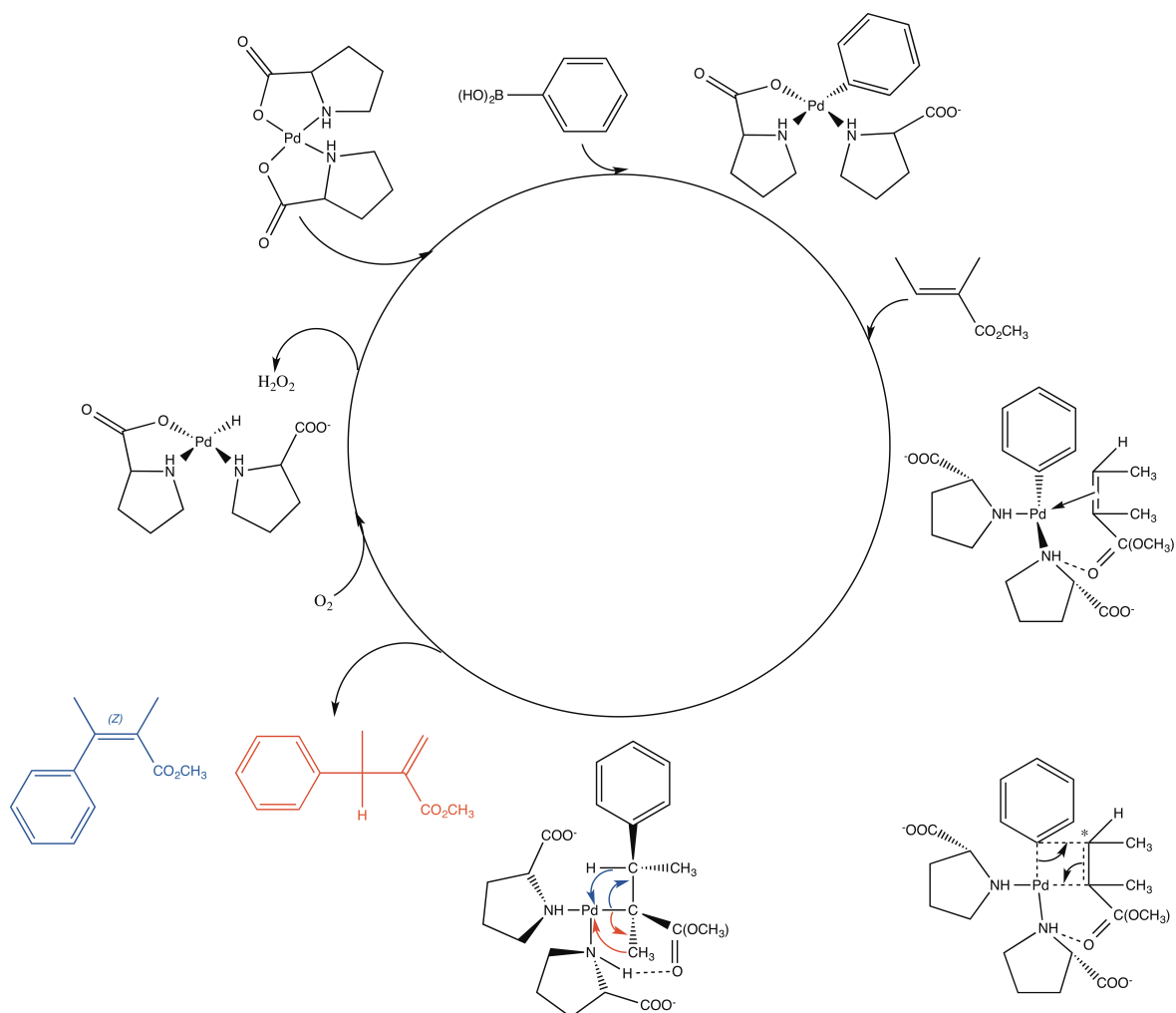### 3.4.1.1   Proposed Mechanism of Pd-AA$_2$ Oxidative Coupling

The following mechanism is proposed for the palladium(II)-amino acid complex catalyzed oxidative coupling of phenylboronic acids to olefins (Figure 72, below). Step 1 involves the transmetallation of phenylboronic acid onto the palladium center. This is accomplished by an associative mechanism whereby the carboxylate group of one of the ligands de-coordinates to maintain a 4-coordinate intermediate. The now-free carboxylate acts as a base towards the free boronic acid group, thus no addition of a base is required as is seen in a typical Suzuki coupling.

Figure 72. Proposed mechanism of the palladium(II)-amino acid complex catalyzed oxidative coupling of phenylboronic acids to olefins.

DFT calculations show that the transmetallated intermediate has a geometry such that the metal center is completely occluded with the exception of a lobe of an empty d-orbital that lies above the palladium atom (Figure 73).
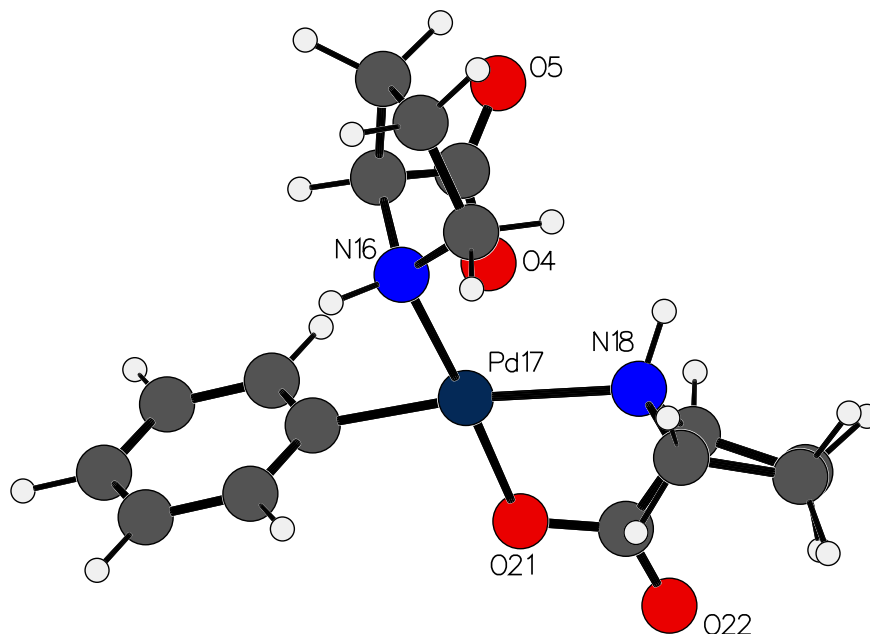
Figure 73. DFT-optimized geometry of the transmetallated intermediate. The non-occluded lobe of the d-orbital projects out of the page towards the reader.

The dissociated carboxylate of the ligand wraps under the metal and covers the other d-orbital lobe. The remaining empty d-orbital lobe is then free to coordinate a neutral olefin, maintaining charge neutrality. Insertion of the phenyl group into the olefin double bond, followed by β-hydride elimination, yields the observed products. There are two possible pathways for beta-hydride elimination. Hydride elimination from the methyl carbon yields the R/S product, while hydride elimination from the methine carbon yields the E/Z product. To regenerate the catalyst and begin the cycle again, molecular oxygen abstracts the hydride, generating a peroxide. Qualitative peroxide test strips do indicate the presence of minute quantities of peroxide in the 0-25 ppm range.

3.4.2   Biaryl Formation

Biaryl formation was noted to occur for every catalyst, however the degree of biaryl formation varied greatly. Biaryl formation results from the coupling of two phenyl boronic acid substrates. Steric considerations about the metal center must therefore allow for both of these groups to orient themselves *cis* to each other. The mechanism proposed above can be slightly modified to allow for this possibility. If we consider a second transmetallation step to occur rather than olefin coordination, the two phenyl groups are oriented *cis* to each other. Elimination of the biaryl yields a Pd^0 center which is then oxidized by molecular oxygen back to a Pd^{II} center.

3.4.3   Multiple Insertions

A unique aspect of this coupling/catalyst system is the ability for the products to undergo additional coupling cycles. The initial alkene products of the coupling reaction can in turn enter the catalytic cycle again and undergo an additional phenylboronic acid addition. This second product can also re-enter the cycle for a third phenylboronic acid addition. We have observed one, two, and three phenylboronic acid addition products for these catalyst systems; however a fourth addition product has not been observed for any catalyst. This is likely due to steric concerns whereby the third coupling product is simply too bulky to coordinate to the metal center. In the GC-MS of these coupling reactions, we observe three peaks of mass 190.2, six peaks of mass 266.3, and two peaks of mass 342.4; the fourth coupling product would have a mass of 418.5 if formed (Figure 74).
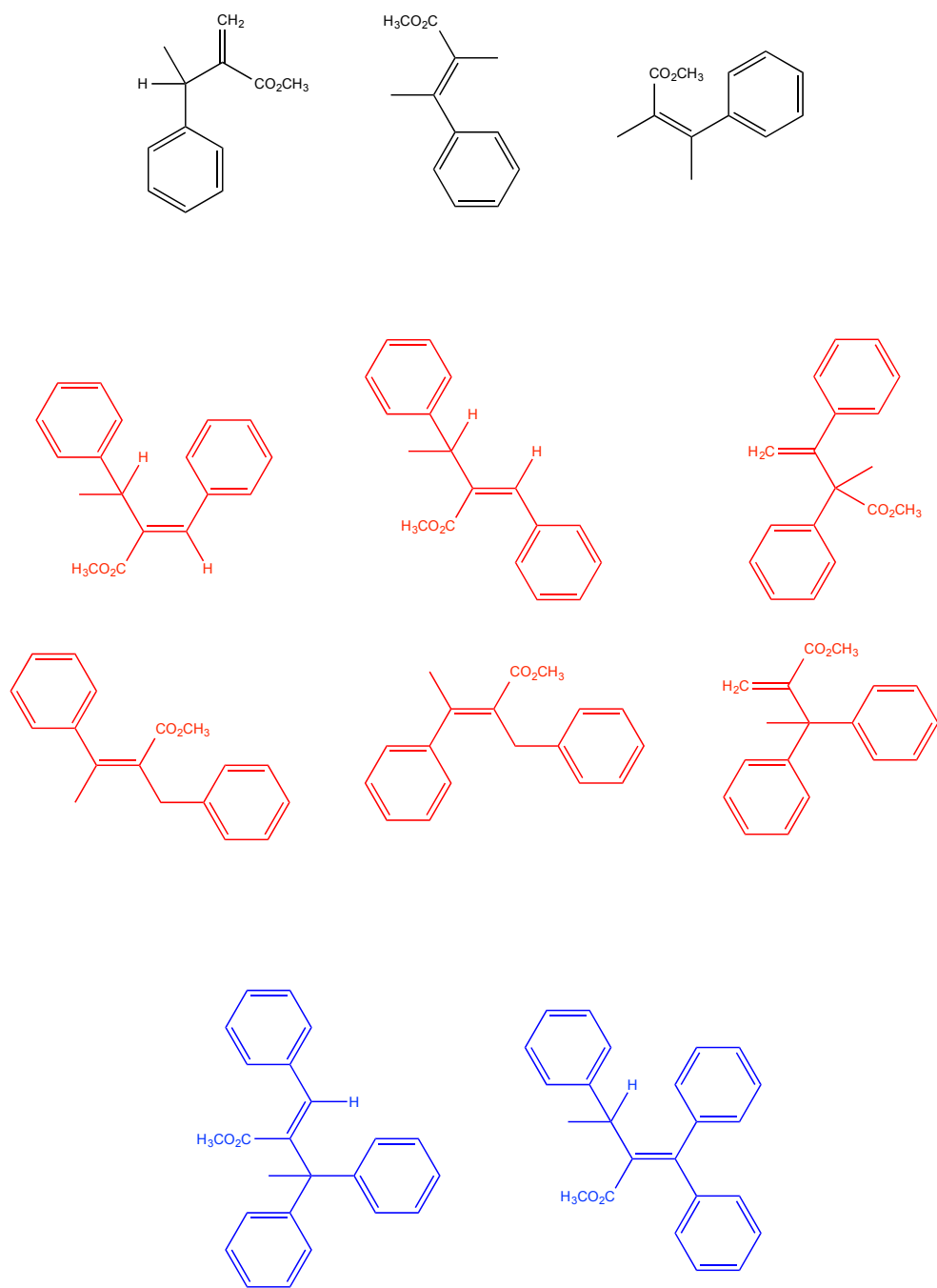
Figure 74. Postulated structures of multiple phenylboronic acid additions to the products of the bis(amino acid)Pd(II) catalyzed coupling of phenylboronic acid and methyl tiglate. First addition = black, second addition = red, third addition = blue.

3.4.4   Temperature Effects

Temperature has a significant effect on the enantioselectivity of the coupling reaction. The coupling reaction was run with the standard set of reaction conditions using the bis-proline complex as the catalyst at temperatures of 0, 25, and 65 degrees C. Enantioselectivities were noted to significantly increase with decreasing temperature as shown in Table 9, below.

Reaction Temperature, degrees C	%ee
65	~1
25	20
0	41

Table 9. Enantioselectivity versus Temperature for the bis(amino acid)palladium(II) catalyzed oxidative coupling of phenylboronic acid to methyl tiglate.

3.4.5   Solvent Effects

The standard coupling reaction was carried out in N,N-dimethylformamide, toluene, dichloromethane, and water solvents using the bis-proline complex as the catalyst. By far, DMF proved to be the superior solvent for this system. As a polar aprotic solvent, DMF has a hydrogen bond acceptor which greatly facilitates dissolution of the catalyst, which has unusually poor solubility in most common solvents. Subsequent trials were then made with DMSO and acetonitrile as the solvents, but neither of these solvents gave appreciable product formation. As strongly coordinating solvents, it is highly likely that solvent coordination to the complex blocks the active sites on the metal center required for reactivity. DMF, as a weakly coordinating solvent, does not suffer this effect. No reaction was noted for either the dichloromethane or

toluene systems. DCM is a very slightly polar aprotic solvent but lacks a hydrogen bond acceptor/donor, and toluene is a non-polar solvent. Neither of these solvents were observed to dissolve the catalyst, therefore the lack of any observed reactivity is not surprising. Water proved to be an interesting solvent choice. The catalyst is soluble in water, as is the phenylboronic acid substrate, and biphenyl formation was noted as the only reaction product. Methyl tiglate is extremely water-insoluble and the lack of PBA-MT cross coupling products can be attributed to the lack of alkene solubility in water. This suggests that water may indeed be a "green" solvent choice for these systems so long as appropriate water soluble substrates can be identified.

3.4.6   Pd(II)-Amino Acid complexes as polymerization catalysts

Given the observation that these catalysts facilitate multiple substrate additions, it was hoped that they might also serve as novel polymerization catalysts. A suitable monomer containing both alkene and phenylboronic acid moieties, 4-(trans-3-methoxy-3-oxo-1-propen-1-yl)benzene boronic acid, was identified (Figure 75) and obtained for study.
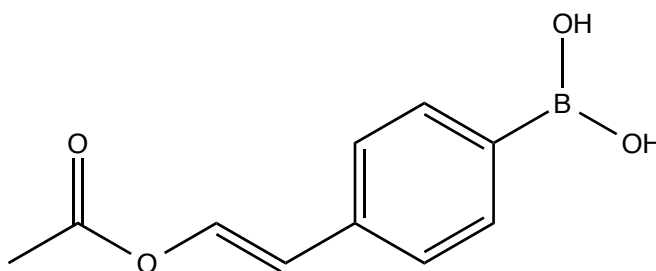

Figure 75. 4-(trans-3-methoxy-3-oxo-1-propen-1-yl)benzene boronic acid monomer

The polymerization reaction was run under identical conditions to the normal phenylboronic acid-methyl tiglate coupling using the *cis*-bis(L-pipecolinato)palladium(II) complex as the

catalyst. This complex was chosen due to the fact that it exhibited the least amount of homocoupling. While high molecular weight polymer was not isolated from the reaction, high-resolution time-of-flight mass spectrometric analysis of the reaction provides compelling evidence of oligomer formation. Mass spectral peaks (Figure 76) corresponding to oligomer masses where n=2, 3, 4, 5, and 6 were observed (n = number of monomeric repeat units) (Figure 77). The *cis*-bis(L-pipecolinato)palladium(II) catalyst once again showed no formation of homocoupled monomer.
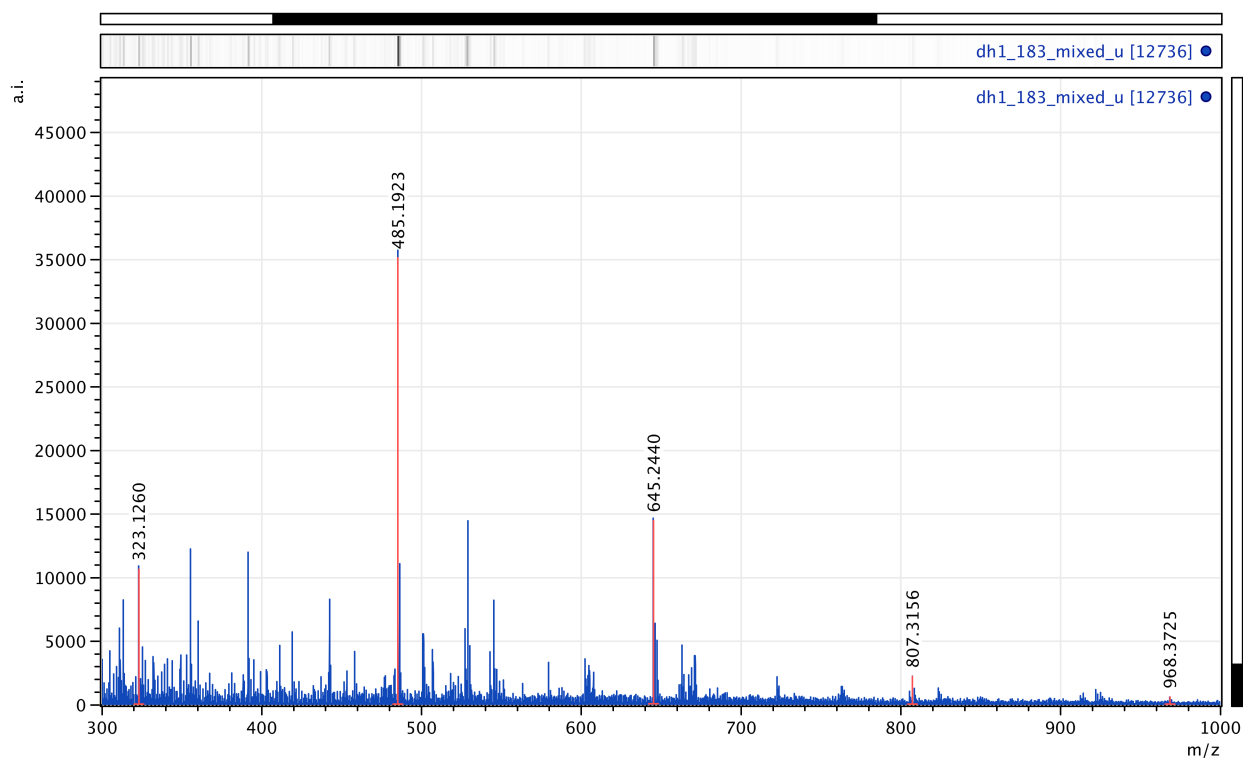
Figure 76. High-resolution time-of-flight mass spectrum of the polymerization reaction of 4-(trans-3-methoxy-3-oxo-1-propen-1-yl)benzene boronic acid catalyzed by *cis*-bis(L-pipecolinato)palladium(II).
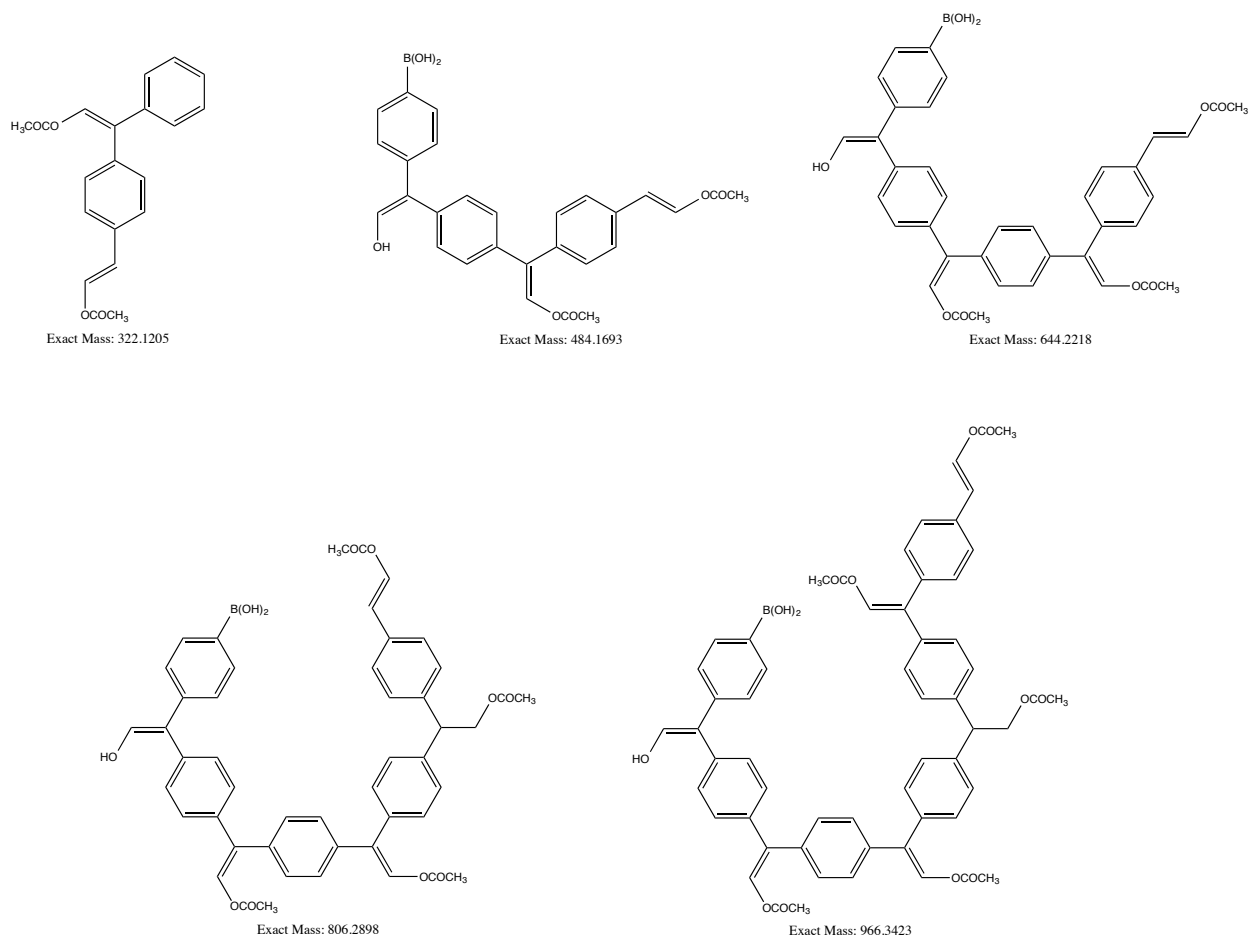
Exact Mass: 322.1205

Exact Mass: 484.1693

Exact Mass: 644.2218

Exact Mass: 806.2898

Exact Mass: 966.3423

Figure 77. Proposed oligomer structures corresponding to HR-TOF MS data. From top left, n=2, 3, 4, 5, and 6 where n = number of monomer units in the oligomer.

3.4.7   Other Coupling Substrates

There are many possible boronic acid/olefin combinations that could be studied with our palladium(II)-amino acid catalytic systems. In an effort to probe some of the other possibilities of these systems, several substituted phenyl boronic acids and olefins were also examined as substrates for the coupling reaction.

An electron-withdrawing group on the phenyl boronic acid was introduced in the form of 4-(trifluoromethyl)phenylboronic acid. The coupling reaction between this boronic acid and methyl tiglate was carried out as before with the bis(L-prolinato)palladium(II) catalyst. The

131

reaction proceeded smoothly with complete consumption of the phenylboronic acid substrate within the 48 hour reaction time. Product distributions were as follows: 71% R/S product with an enantiomeric excess of 11%, 24% homocoupled biaryl, 1% of the Z-alkene, and 4% of the secondary addition product (Figure 78).
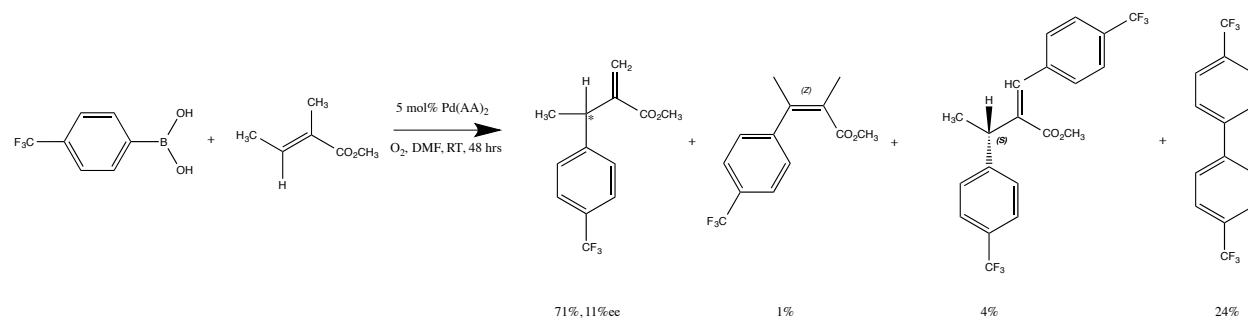

Figure 78. Reaction scheme and product distributions of the coupling reaction between 4-(trifluoromethyl)phenylboronic acid and methyl tiglate.

The same coupling reaction was also carried out with a phenylboronic acid with an electron donating group in the para position. In this case 4-methoxyphenylboronic acid was used (Figure 79).
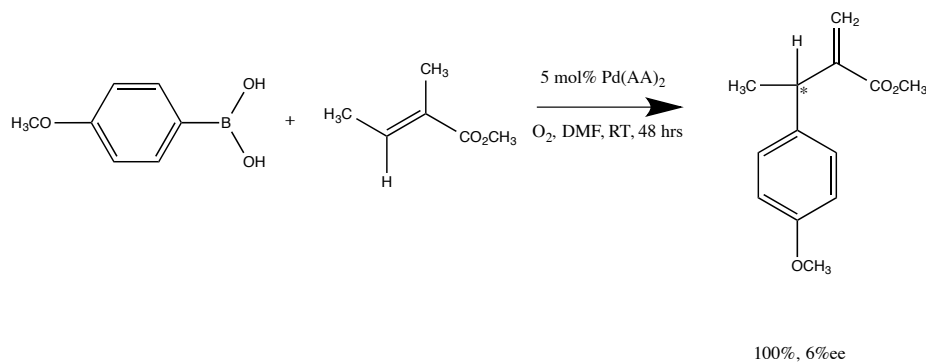

Figure 79. Reaction scheme and product distributions of the coupling reaction between 4-methoxyphenylboronic acid and methyl tiglate.

In this case, as before, complete consumption of the phenylboronic acid was observed. Interestingly, there was no evidence of homocoupling, alkene formation, or multiple phenylboronic acid additions noted for this reaction. The only product detected was the R/S product with an enantiomeric excess of 6%.

Methyl tiglate is considered to be an activated alkene, and it was hoped that our catalysts would also be useful for coupling non-activated alkenes. To this end *cis*-cyclooctene, 1,5-cyclooctadiene, and 1,5-hexadiene were evaluated with phenylboronic acid in the standard coupling reaction. To our delight, all three alkenes coupled with phenylboronic acid when the reaction was catalyzed by the *cis*-bis(L-prolinato)palladium(II) catalyst. The *cis*-cyclooctene coupling can generate four possible products (Figure 80), and four product peaks of the correct mass are observed in the GC-MS analysis of the reaction. The 1,5-cyclooctadiene coupling has two possible products (Figure 81), and here again we see two peaks of appropriate mass in the GC-MS trace. Finally, the 1,5-hexadiene coupling also has two possible products (Figure 82) and two peaks of correct mass are observed by GC-MS.
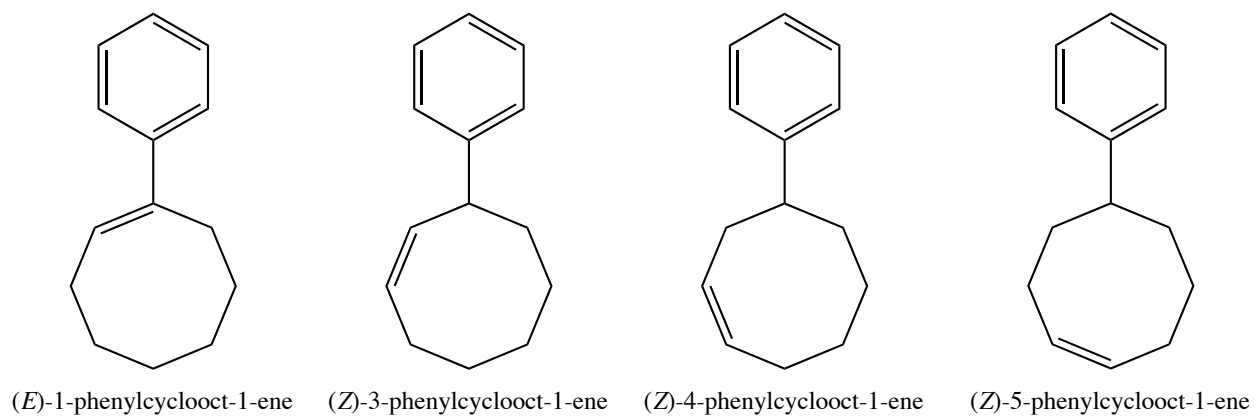
(*E*)-1-phenylcyclooct-1-ene   (*Z*)-3-phenylcyclooct-1-ene   (*Z*)-4-phenylcyclooct-1-ene   (*Z*)-5-phenylcyclooct-1-ene

Figure 80. Possible product structures for the coupling reaction between phenylboronic acid and *cis*-cyclooctene.

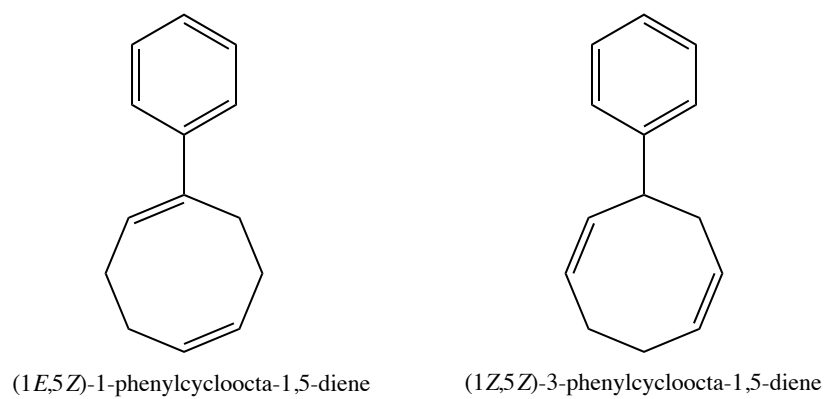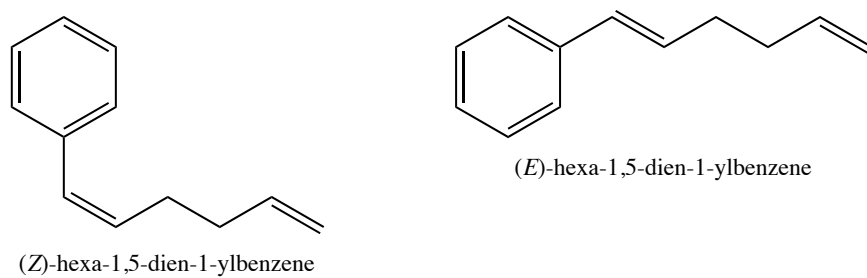(1*E*,5*Z*)-1-phenylcycloocta-1,5-diene   (1*Z*,5*Z*)-3-phenylcycloocta-1,5-diene

Figure 81. Possible product structures for the coupling reaction between phenylboronic acid and 1,5-cyclooctadiene.

(*E*)-hexa-1,5-dien-1-ylbenzene

(*Z*)-hexa-1,5-dien-1-ylbenzene

Figure 82. Possible product structures for the coupling reaction between phenylboronic acid and 1,5-hexadiene.

3.5 CONCLUSIONS

Nine palladium(II) bis-amino acid chelates with aliphatic ring structures for their R-group have been synthesized, characterized, and tested for catalytic activity for the oxidative coupling of phenylboronic acid with olefins. The amino acids employed include L-proline, D-proline, N-methylproline, azetidine, L-pipecolinic acid, D-pipecolinic acid, 2-α-benzylproline, 4-hydroxyproline, and 4-fluoroproline. The N-methylproline, 2-α-benzylproline, and azetidine complexes exist as the *trans* isomer, with all other complexes being *cis*. All of these complexes are square planar, C_2 symmetric molecules that exhibit varying degrees of intermolecular hydrogen bonding. All complexes are catalytically active with respect to the oxidative coupling of phenylboronic acids to olefins, with the exception of the N-methylproline complex. Enantioselectivities are modest with the best example, *cis*-bis(prolinato)palladium(II), yielding an enantiomeric excess of 24%. These complexes couple a wide variety of both electron-rich and electron-deficient phenylboronic acids and activated and non-activated olefins.

3.6 REFERENCES

(1)   Jin, L. Q.; Lei, A. W. *Science China: Chemistry* **2012**, *55*, 2027.
(2)   Beccalli, E. M.; Broggini, G.; Martinelli, M.; Sottocornola, S. *Chemical Reviews (Washington, DC, United States)* **2007**, *107*, 5318.
(3)   Obora, Y.; Ishii, Y. *Molecules* **2010**, *15*, 1487.
(4)   Stahl, S. S. *Angewandte Chemie, International Edition* **2004**, *43*, 3400.
(5)   Wu, W.; Jiang, H. *Accounts of Chemical Research* **2012**, *45*, 1736.
(6)   Zeni, G.; Larock, R. C. *Chemical Reviews (Washington, DC, United States)* **2006**, *106*, 4644.
(7)   Gligorich, K. M.; Cummings, S. A.; Sigman, M. S. *Journal of the American Chemical Society* **2007**, *129*, 14193.
(8)   Adamo, C.; Amatore, C.; Ciofini, I.; Jutand, A.; Lakmini, H. *Journal of the American Chemical Society* **2006**, *128*, 6829.

(9)   Canovese, L.; Visentin, F.; Chessa, G.; Santo, C.; Levi, C.; Uguagliati, P. *Inorganic Chemistry Communications* **2006**, *9*, 388.

(10)   Hull, K. L.; Lanni, E. L.; Sanford, M. S. *Journal of the American Chemical Society* **2006**, *128*, 14047.

(11)   Hull, K. L.; Sanford, M. S. *Abstracts of Papers, 239th ACS National Meeting, San Francisco, CA, United States, March 21-25, 2010* **2010**, ORGN.

(12)   Lu, Y.; Wang, D.-H.; Engle, K. M.; Yu, J.-Q. *Journal of the American Chemical Society* **2010**, *132*, 5916.

(13)   Muzart, J. *Chemistry - An Asian Journal* **2006**, *1*, 508.

(14)   Chen, Q.; Li, C. *Organometallics* **2007**, *26*, 223.

(15)   Heck, R. F.; Nolley, J. P., Jr. *Journal of Organic Chemistry* **1972**, *37*, 2320.

(16)   Herr, R. J.; Dowling, M. S.; Scampini, A. C.; Smith, T. M. *Abstracts, 35th Northeast Regional Meeting of the American Chemical Society, Burlington, VT, United States, June 29-July 2* **2008**, NERM.

(17)   Horiguchi, H.; Tsurugi, H.; Satoh, T.; Miura, M. *Advanced Synthesis & Catalysis* **2008**, *350*, 509.

(18)   Jin, L.; Zhao, Y.; Wang, H.; Lei, A. *Synthesis* **2008**, 649.

(19)   Johnson, T.; Lautens, M. *Organic Letters* **2013**, *15*, 4043.

(20)   Jordan-Hore, J. A.; Sanderson, J. N.; Lee, A.-L. *Organic Letters* **2012**, *14*, 2508.

(21)   Khabibulin, V. R.; Kulik, A. V.; Oshanina, I. V.; Bruk, L. G.; Temkin, O. N.; Nosova, V. M.; Ustynyuk, Y. A.; Bel'skii, V. K.; Stash, A. I.; Lysenko, K. A.; Antipin, M. Y. *Kinetics and Catalysis* **2007**, *48*, 228.

(22)   Lei, A.; Zhang, X. *Tetrahedron Letters* **2002**, *43*, 2525.

(23)   Liegault, B.; Lee, D.; Huestis, M. P.; Stuart, D. R.; Fagnou, K. *Journal of Organic Chemistry* **2008**, *73*, 5022.

(24)   Liu, C.; Jin, L.; Lei, A. *Synlett* **2010**, 2527.

(25)   Martinez, C.; Alvarez, R.; Aurrecoechea, J. M. *Organic Letters* **2009**, *11*, 1083.

(26)   Prateeptongkum, S.; Driller, K. M.; Jackstell, R.; Spannenberg, A.; Beller, M. *Chemistry--A European Journal* **2010**, *16*, 9606.

(27)   Van Aeken, S.; Verbeeck, S.; Deblander, J.; Maes, B. U. W.; Tehrani, K. A. *Tetrahedron* **2011**, *67*, 2269.

(28)   Venkatraman, S.; Huang, T.; Li, C.-J. *Advanced Synthesis & Catalysis* **2002**, *344*, 399.

(29)   Wakioka, M.; Mutoh, Y.; Takita, R.; Ozawa, F. *Bulletin of the Chemical Society of Japan* **2009**, *82*, 1292.

(30)   Yoo, K. S.; O'Neill, J.; Sakaguchi, S.; Giles, R.; Lee, J. H.; Jung, K. W. *Journal of Organic Chemistry* **2010**, *75*, 95.

(31)   Yoo, K. S.; Park, C. P.; Yoon, C. H.; Sakaguchi, S.; O'Neill, J.; Jung, K. W. *Organic Letters* **2007**, *9*, 3933.

(32)   Yoo, K. S.; Yoon, C. H.; Jung, K. W. *Journal of the American Chemical Society* **2006**, *128*, 16384.

(33)   Alvarez, R.; Martinez, C.; Madich, Y.; Denis, J. G.; Aurrecoechea, J. M.; de Lera, A. R. *Chemistry--A European Journal* **2010**, *16*, 12746.

(34)   Aouf, C.; Thiery, E.; Le Bras, J.; Muzart, J. *Organic Letters* **2009**, *11*, 4096.

(35)   Beccalli, E. M.; Borsini, E.; Broggini, G.; Rigamonti, M.; Sottocornola, S. *Synlett* **2008**, 1053.

(36)   Maehara, A.; Satoh, T.; Miura, M. *Tetrahedron* **2008**, *64*, 5982.

(37)   Thiery, E.; Harakat, D.; Le Bras, J.; Muzart, J. *Organometallics* **2008**, *27*, 3996.

(38) Xi, P.; Yang, F.; Qin, S.; Zhao, D.; Lan, J.; Gao, G.; Hu, C.; You, J. *Journal of the American Chemical Society* **2010**, *132*, 1822.

(39) Yamashita, M.; Hirano, K.; Satoh, T.; Miura, M. *Organic Letters* **2009**, *11*, 2337.

(40) Yang, S.-D.; Sun, C.-L.; Fang, Z.; Li, B.-J.; Li, Y.-Z.; Shi, Z.-J. *Angewandte Chemie, International Edition* **2008**, *47*, 1473.

(41) Bardhan, S.; Wacharasindhu, S.; Wan, Z.-K.; Mansour, T. S. *Organic Letters* **2009**, *11*, 2511.

(42) Belitsky, J. M. *Abstracts of Papers, 236th ACS National Meeting, Philadelphia, PA, United States, August 17-21, 2008* **2008**, ORGN.

(43) Belitsky, J. M. *Abstracts, Central Regional Meeting of the American Chemical Society, Cleveland, OH, United States, May 20-23* **2009**, CRM.

(44) Clawson, R. W.; Deavers, R. E.; Akhmedov, N. G.; Soederberg, B. C. G. *Tetrahedron* **2006**, *62*, 10829.

(45) Djakovitch, L.; Rouge, P. *Journal of Molecular Catalysis A: Chemical* **2007**, *273*, 230.

(46) Gong, X.; Song, G.; Zhang, H.; Li, X. *Organic Letters* **2011**, *13*, 1766.

(47) He, C.-Y.; Fan, S.; Zhang, X. *Journal of the American Chemical Society* **2010**, *132*, 12850.

(48) Wang, Z.; Li, K.; Zhao, D.; Lan, J.; You, J. *Angewandte Chemie, International Edition* **2011**, *50*, 5365.

(49) Henke, A.; Srogl, J. *Chemical Communications (Cambridge, United Kingdom)* **2011**, *47*, 4282.

(50) Kirchberg, S.; Tani, S.; Ueda, K.; Yamaguchi, J.; Studer, A.; Itami, K. *Angewandte Chemie, International Edition* **2011**, *50*, 2387.

(51) Schwan, A. L. *Chemical Society Reviews* **2004**, *33*, 218.

(52) Klaerner, C.; Greiner, A. *Macromolecular Rapid Communications* **1998**, *19*, 605.

(53) Wu, N.; Li, X.; Xu, X.; Wang, Y.; Xu, Y.; Chen, X. *Letters in Organic Chemistry* **2010**, *7*, 11.

(54) Xu, Z.; Mao, J.; Zhang, Y. *Catalysis Communications* **2007**, *9*, 97.

(55) Yamamoto, Y. *Synlett* **2007**, 1913.

(56) Zhou, L.; Xu, Q. X.; Jiang, H. F. *Chinese Chemical Letters* **2007**, *18*, 1043.

(57) Agilent; Agilent Technologies: Oxford, UK, 2012.

(58) Sheldrick George, M. *Acta crystallographica. Section A, Foundations of crystallography* **2008**, *64*, 112.

(59) Dolomanov, O. V.; Bourhis, L. J.; Gildea, R. J.; Howard, J. A. K.; Puschmann, H. *Journal of Applied Crystallography* **2009**, *42*, 339.

(60) Frisch, M. J. T., G. W.; Schlegel, H. B.; Scuseria, G. E.; Robb, M. A.; Cheeseman, J. R.; Scalmani, G.; Barone, V.; Mennucci, B.; Petersson, G. A.; Nakatsuji, H.; Caricato, M.; Li, X.; Hratchian, H. P.; Izmaylov, A. F.; Bloino, J.; Zheng, G.; Sonnenberg, J. L.; Hada, M.; Ehara, M.; Toyota, K.; Fukuda, R.; Hasegawa, J.; Ishida, M.; Nakajima, T.; Honda, Y.; Kitao, O.; Nakai, H.; Vreven, T.; Montgomery, Jr., J. A.; Peralta, J. E.; Ogliaro, F.; Bearpark, M.; Heyd, J. J.; Brothers, E.; Kudin, K. N.; Staroverov, V. N.; Kobayashi, R.; Normand, J.; Raghavachari, K.; Rendell, A.; Burant, J. C.; Iyengar, S. S.; Tomasi, J.; Cossi, M.; Rega, N.; Millam, J. M.; Klene, M.; Knox, J. E.; Cross, J. B.; Bakken, V.; Adamo, C.; Jaramillo, J.; Gomperts, R.; Stratmann, R. E.; Yazyev, O.; Austin, A. J.; Cammi, R.; Pomelli, C.; Ochterski, J. W.; Martin, R. L.; Morokuma, K.; Zakrzewski, V. G.; Voth, G. A.; Salvador, P.; Dannenberg, J. J.; Dapprich, S.; Daniels, A. D.; Farkas, Ö.; Foresman, J. B.; Ortiz, J. V.; Cioslowski, J.; Fox, D. J.; Gaussian, Inc.: Wallingford, CT, 2009.

(61) Becke, A. D. *Journal of Chemical Physics* **1993**, *98*, 5648.

(62) Lee, C.; Yang, W.; Parr, R. G. *Physical Review B: Condensed Matter and Materials Physics* **1988**, *37*, 785.

(63)   Stephens, P. J.; Devlin, F. J.; Chabalowski, C. F.; Frisch, M. J. *Journal of Physical Chemistry* **1994**, *98*, 11623.

(64)   Andrae, D.; Haeussermann, U.; Dolg, M.; Stoll, H.; Preuss, H. *Theoretica Chimica Acta* **1990**, *77*, 123.

(65)   Hobart, D. B.; Berg, M. A. G.; Merola, J. S. *Inorganica Chimica Acta* **2014**, *423*, 21.

(66)   Chernova, N. N.; Strukov, V. V.; Avetikyan, G. B.; Chernonozhkin, V. N. *Zhurnal Neorganicheskoi Khimii* **1980**, *25*, 1569.

(67)   Jarzab, T. C.; Hare, C. R.; Langs, D. A. *Crystal Structure Communications* **1973**, *2*, 399.

(68)   Jarzab, T. C.; Hare, C. R.; Langs, D. A. *Crystal Structure Communications* **1973**, *2*, 395.

(69)   Komorita, T.; Hidaka, J.; Shimura, Y. *Bull. Chem. Soc. Jap.* **1971**, *44*, 3353.

(70)   Sabat, M.; Jezowska, M.; Kozlowski, H. *Inorganica Chimica Acta* **1979**, *37*, L511.

(71)   Vagg, R. S. *Acta Crystallogr B* **1979**, *35*, 341.

(72)   Batsanov, S. S. *Inorganic Materials* **2001**, *37*, 871.

(73)   Voureka, E.; Tsangaris, J. M.; Terzis, A.; Raptopoulou, C. P. *Transition Metal Chemistry (London)* **1996**, *21*, 244.

(74)   Bhowmick, S.; Bhowmick, K. C. *Tetrahedron: Asymmetry* **2011**, *22*, 1945.

(75)   Hayashi, T. *Sentan Kagaku Shirizu* **2003**, *1*, 106.

(76)   Kawabata, T.; Fuji, K. *Kagaku to Seibutsu* **1993**, *31*, 817.

(77)   Reetz, M. T. *Pure and Applied Chemistry* **1988**, *60*, 1607.

(78)   Shibasaki, M. *Org. Synth. Organomet. (OSM4), Proc. Symp., 4th* **1993**, 11.

(79)   Shibasaki, M. *Advances in Metal-Organic Chemistry* **1996**, *5*, 119.

(80)   Tsubogo, T.; Ishiwata, T.; Kobayashi, S. *Angewandte Chemie, International Edition* **2013**, *52*, 6590.

Chapter 4:   Synthesis, Characterization, and Catalytic Activity of Bis-Chelates of Palladium(II) with Amino Acid Ligands

4.1   INTRODUCTION

The preceeding two chapters have dealt with the simplest amino acids, the glycines, and the cyclic amino acids, the prolines, respectively. In this chapter we will explore the synthesis, characterization, catalytic and biological activity of the palladium(II) complexes of the remaining naturally occurring amino acids. Containing aliphatic R-groups, these amino acids are perhaps less unique, but no less important than their previously discussed counterparts. As we move through a discussion of these complexes they are grouped according to the chemical nature of the R-group of the amino acid ligand into the following five catagories: aliphatic hydrophobic, aromatic hydrophobic, polar neutral, charged acidic, and charged basic.

Most of the palladium(II) complexes of the remaining naturally occurring alpha amino acids have been described to some extent in the literature dating back to the 1960s and 1970s. Many of these syntheses are from institutions in the former Soviet-bloc and eastern European countries, and their characterization data are fairly incomplete. A goal of our research from the outset has been to completely characterize these complexes to a degree not previously seen or reported in the literature. To this end we have obtained ^{1}H NMR data, MS data, elemental analyses, and ^{13}C NMR and X-ray crystal structures where possible. We have also evaluated these complexes as to their catalytic and biological activities.

Among the aliphatic hydrophobic amino acids, bis(alanino)palladium(II) was first reported by Sharma in 1964[1] and characterized solely by infrared spectroscopy. Farooq[2] prepared the complex in 1973, characterizing the product only by potentiometric titration. In 1976 Chernova[3] reported a synthesis characterized by elemental analysis and molar conductance measurements. Bis(isoleucinato)palladium(II) was prepapred by Patel in 1996 and characterized only by elemental microanalysis. The bis(leucinato) and bis(valinato) complexes were prepared by Farooq[2]. Once again, potentiometric titration was the only method of characterization reported. Jarzab[4] reported a room-temperature crystal structure of the bis(valinato) complex in 1973, however no hydrogen atom positions were included in the refinement, nor was any other characterization data presented in the paper.

The aromatic hydrophobic amino acid-containing palladium(II) complexes previously reported in the literature include the bis(phenylalaninato) and bis(tyrosinato). The crystal structure of bis(tyrosinato)palladium(II) was reported by Jarzab[5] with no other characterization data. As before, the structure was obtained at room temperature and with no hydrogen atom positions reported. Chernova[3], using the same methods mentioned above with the alanine complex, reported the bis(phenylalaninato) complex in 1976.

All of the complexes formed from polar neutral amino acid ligands were originally reported in the 1970s, however the trend of sparse characterization data continues. The palladium(II) bis-chelates of asparagine, methionine, and serine were reported by Farooq[2], who again used a potentiometric titration of ligand concentration to characterize the complexes. Vagg followed up with a room temperature crystal structure of the bis(serinato) complex in 1979. Hydrogen atom positions were not reported, nor were any other data were given. Kollmann[6] reported on the synthesis of gold(III), palladium(II) and platinum(II) complexes of threonine;

only melting point data were provided. Krylova[7] recently added to the data available for bis(threoninato)palladium(II) with ^{1}H and ^{13}C NMR data for both the *cis* and *trans* isomers, as well as room temperature crystal structures. Evidence of aquo complex formation was observed in their ^{13}C NMR spectra. Bis(glutaminato)palladium(II) and bis(cysteinato)palladium(II) were both reported in 1979 by Graham[8] and Pneumatikakis[9], respectively. Graham relied solely on elemental analysis for the characterization of bis(glutaminato)palladium(II) whereas Pneumatikakis relied on infrared spectra, elemental analysis and solution conductivity measurements to characterize the bis(cysteinato) complex. There is one other possible member of this group of complexes, the bis-chelate of cystine. Cystine is a derivative of cysteine, formed by the oxidation of cysteine to generate a disulfide bond (Figure 83). The complex has not been reported in the literature but may exhibit some interesting reactivity given its ability to crosslink multiple metal centers into clusters or nanoparticles.
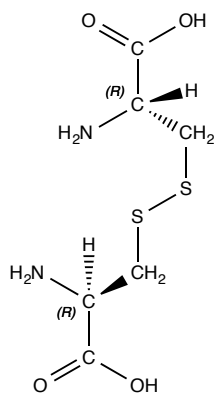
Figure 83. Molecular structure of L-cystine, (R,R)-3,3'-Dithiobis(2-aminopropionic acid).

Aspartic acid and glutamic acid comprise the group of amino acids with charged acidic R-groups. The bis-chelates of these amino acids were both reported by Spacu[10,11] in 1966 and 1962 respectively. Bis(glutamic acid)palladium(II) was characterized by elemental analysis and

on the basis of titration stoichiometry against ethylenediamine to form the $[Pd(en)_2]^{2+}$ cation and against thiourea to form the $[Pd(thio)_4]^{2+}$ cation. Bis(aspartic acid)palladium(II) was characterized in an identical manner.

The last of the groupings of amino acids, those with charged basic R-groups, is comprised of arginine, histidine, and lysine. Of these, only bis(histidinato)palladium(II) has been reported in the literature by Chernova. Elemental analysis and the carboxylate symmetric and asymmetric infrared stretching vibrations are reported to confirm the product.

4.2 AMINO ACIDS WITH ALIPHATIC HYDROPHOBIC R-GROUPS

The first class of amino acid ligands investigated were those that possess a hydrophobic, aliphatic R-group. Alanine, valine, isoleucine, *tert*-leucine, and leucine fall into this category. Containing only aliphatic R-groups, this grouping of amino acid ligands is solely capable of *N,O*-chelation (Figure 84). ^{1}H NMR data are consistent with a coordinated amino acid ligand, showing varying degrees of resonance shifting as compared to the free ligand. These complexes are extremely sparingly soluble in common solvents; as a result ^{13}C NMR spectra were unobtainable. In every case, high-resolution time-of-flight mass spectrometry verified formation of the complex.
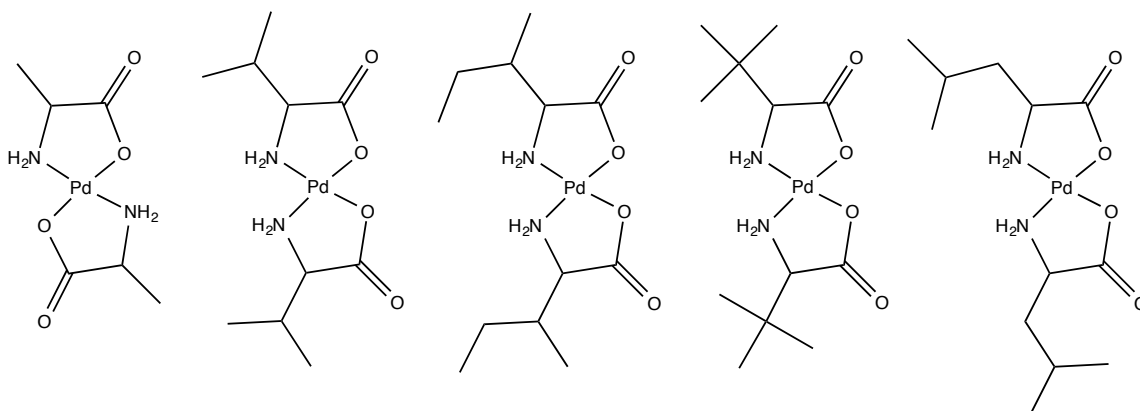
Figure 84. Pd(II) complexes of (*l* to *r*) alanine (**1**), L-valine (**2**), D-valine (**3**, not shown), isoleucine (**4**), *tert*-leucine (**5**), and leucine (**6**).

Crystals suitable for X-ray diffraction were obtained for the alanine, valine, and isoleucine complexes. The alanine complex adopts a *trans* geometry (Figure 85) much like the glycine complex when prepared from palladium(II) acetate.[12] This suggests that the nature of the R-group exerts some influence on the coordination geometry of the complex. If the R-group is a very weakly electron-donating species the complex forms the *trans* isomer. This is born out experimentally from the glycine and alanine complexes where the R-group is a hydrogen atom or methyl group, respectively. Once the R-group takes on more of an electron-donating nature the complex tends to form the *cis* isomer upon coordination. Valine, with an isopropyl R-group, has the next highest electron donating R-group and forms the *cis* isomer. All of the complexes that follow valine in order of increasing electron donating power of their R-group, for which we have X-ray crystal structures, adopt the *cis* geometry as well.
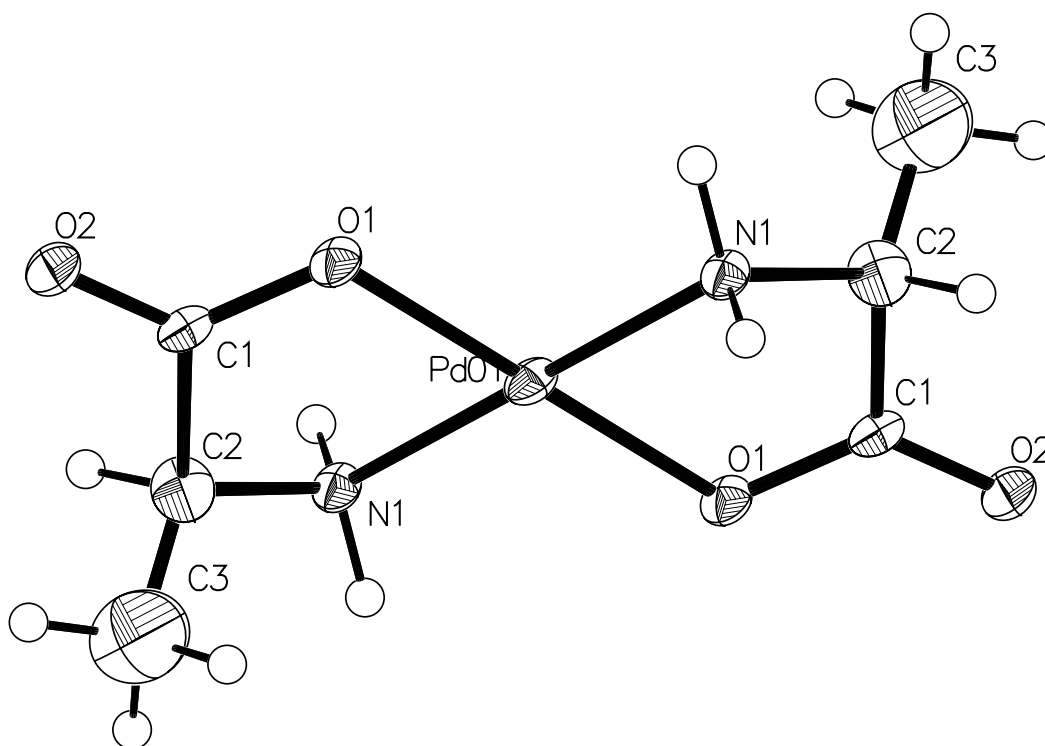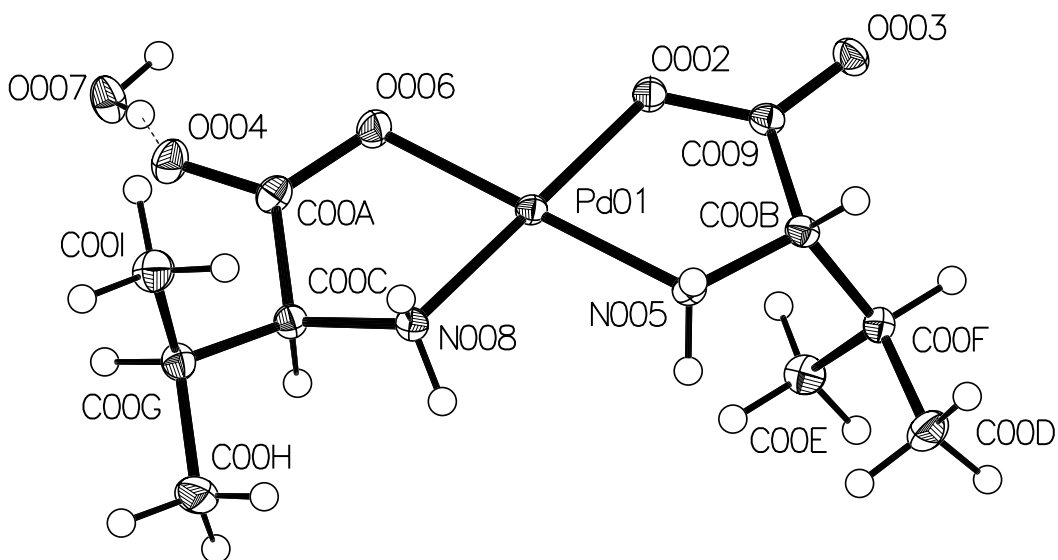
Figure 85. Thermal ellipsoid plot of *trans*-bis(alaninato)palladium(II) (1). Thermal ellipsoids are shown at the 50% probability level.

Trans-bis(alaninato)palladium(II) (**1**) crystallizes in the $P\bar{1}$ space group with no water molecules in the lattice. Pd-N and Pd-O bonds are 2.038 and 1.996 Angstroms, respectively. N-Pd-O bond angles within a chelate ring are 81.903 degrees, and the N-Pd-O bond angles between chelate rings are 98.097 degrees. These values compare favorably with other palladium(II) amino acid chelates previously reported.[4,5,12-16] Intermolecular hydrogen bonding is observed between an amine proton and a carbonyl oxygen on adjacent molecules in the lattice (Figure 86).
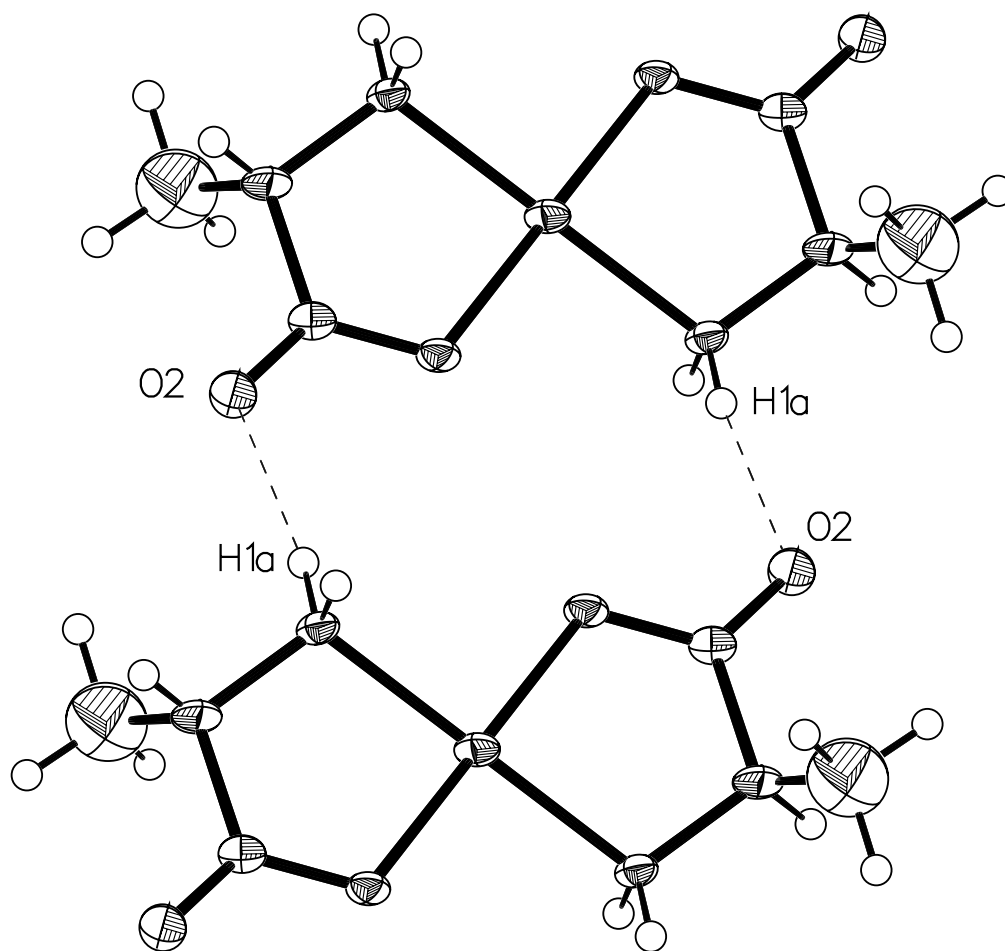
Figure 86. Intermolecular hydrogen bonding interactions observed in the crystal lattice of *trans*-bis(alaninato)palladium

(II) (1).

Cis-bis(L-valinato)palladium(II) (**2**) crystallizes in the $P2_12_12_1$ space group with one water molecule in the lattice (Figure 87). The Pd-N bonds are 2.0057 and 2.0103 Angstroms and the Pd-O bonds are 2.0052 and 2.0173 Angstroms. The O-Pd-O bond angle is 96.026 degrees and the N-Pd-N bond angle is 96.896 degrees. These values are comparable to values reported for other square planar palladium(II) chelates.[4,5,12-16]   Intermolecular hydrogen bonding is observed in the crystal lattice (Figure 88). An amine proton on each of the nitrogen atoms of one

complex molecule is hydrogen bonded to a carbonyl oxygen and a chelated carboxylate oxygen on the adjacent molecule. Both of these amine hydrogen atoms lie on the same side of the chelate plane. Additionally, the water molecule in the lattice is hydrogen bonded between two carbonyl oxygen atoms on adjacent complex molecules and also between the other two amine protons on yet a third complex molecule in the lattice.

Figure 87. Thermal ellipsoid plot of *cis*-bis(valinato)palladium(II) (2). Thermal ellipsoids are shown at the 50%
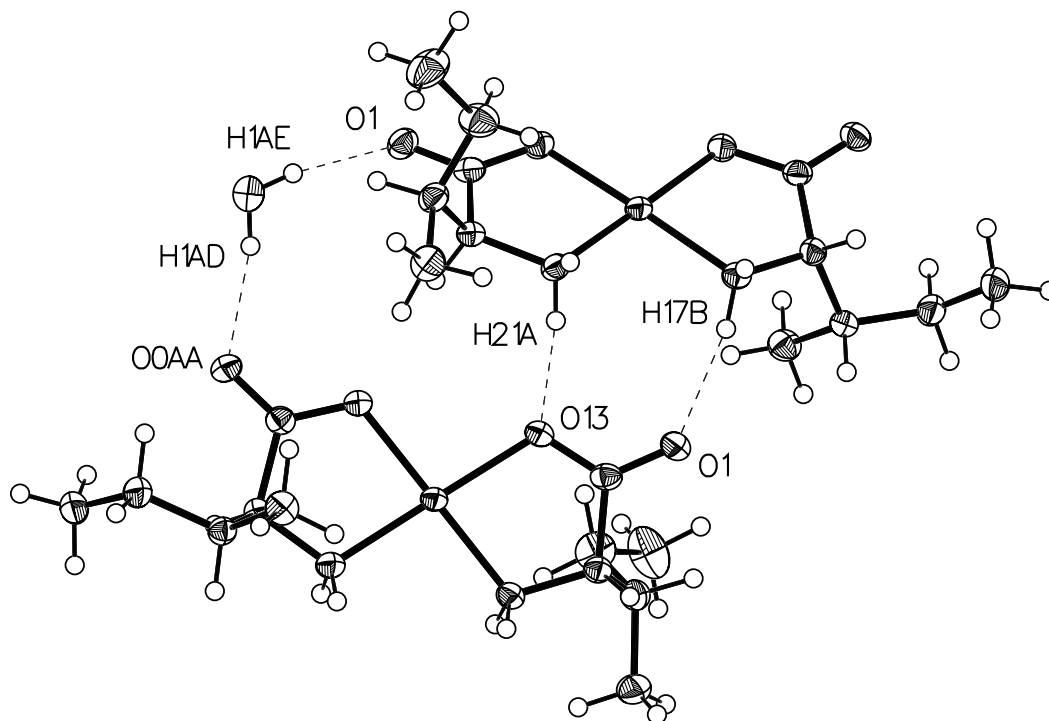
probability level.
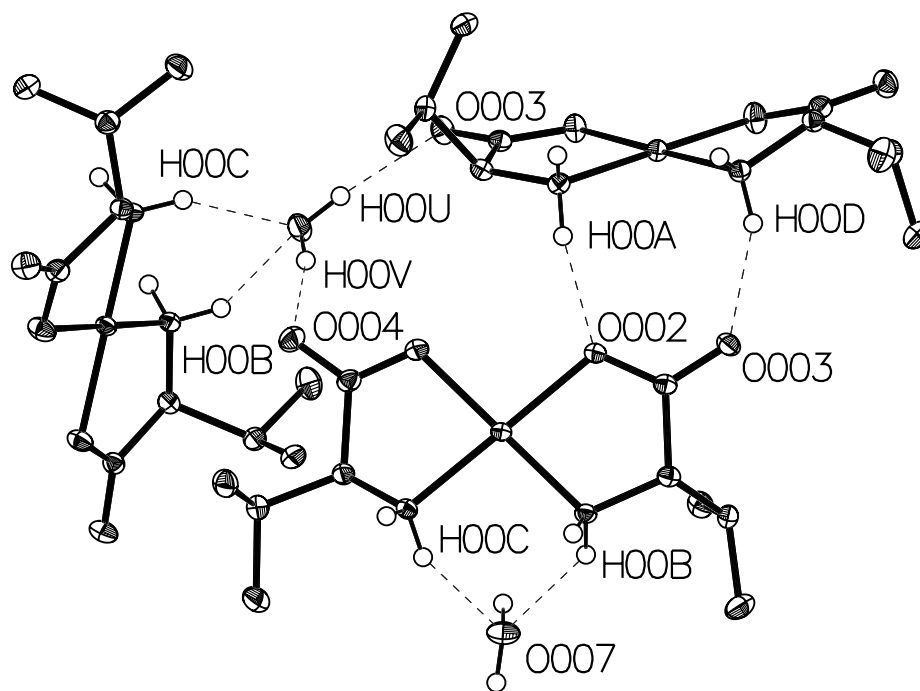
Figure 88. Intermolecular hydrogen bonding interactions observed in the crystal lattice of *cis*-bis(valinato)palladium (II) (2).

The last complex from this group for which a crystal structure was able to be determined was *cis*-bis(isoleucinato)palladium(II) (**4**) (Figure 89). Crystallizing in the $P2_12_12_1$ space group, it has Pd-N bond lengths of 2.009 and 2.005 Angstroms and Pd-O bond lengths of 2.015 and 1.996 Angstroms. As before, these values compare favorably with the literature.[4,5,12-16] There is one water molecule in the lattice. The R-groups are oriented such that one lies on either side of the chelate plane.
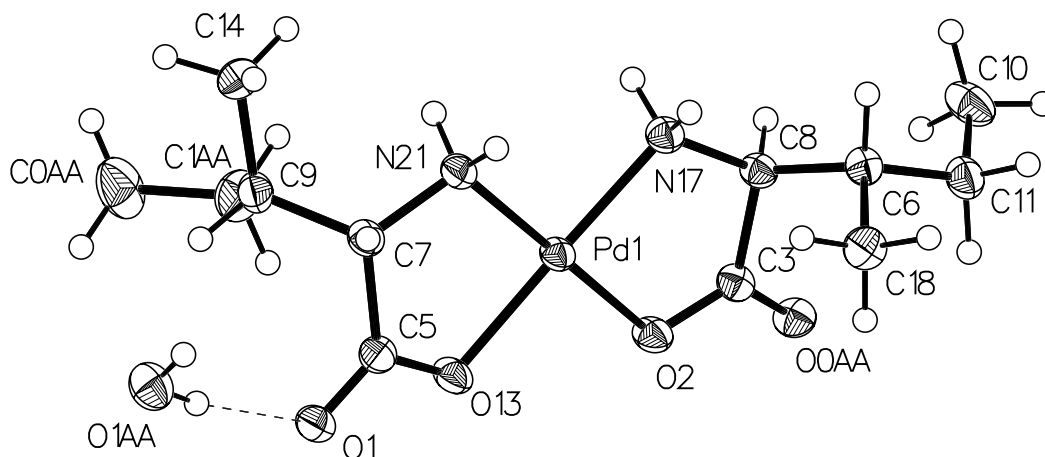
Figure 89. Thermal ellipsoid plot of *cis*-bis(isoleucinato)palladium(II) (**4**). Thermal ellipsoids are shown at the 50% probability level.

The extended lattice observed for this complex is similar to that seen for the valine complex and involves hydrogen bonding between amine protons on both nitrogens of one complex molecule to both oxygen atoms in one chelate ring on an adjacent molecule in the lattice (Figure 90). The water molecule in the lattice is hydrogen bonded between the two carbonyl oxygen atoms on adjacent complex molecules and in this case is not hydrogen bonded to the remaining amine hydrogen atoms.

Bis(*tert*-leucinato)palladium(II) (**5**) and bis(leucinato)palladium(II) (**6**) were also prepared, and although crystals were not able to be grown the HRMS and NMR data are consistent with formation of the bis-chelates.

Figure 90. Intermolecular hydrogen bonding interactions observed in the crystal lattice of *cis*-bis(isoleucinato)palladium

(II) (4).

A representative member of this group, *cis*-bis(isoleucinato)palladium(II) (**4**), was tested for catalytic activity and was shown to catalyze the oxidative coupling of phenylboronic acid and methyl tiglate (Figure 91). The R/S:Z product ratio was 1.1:1 and homocoupled phenylboronic acid accounted for 63% of the coupling yield. Enantioselectivity was low at 3% ee.
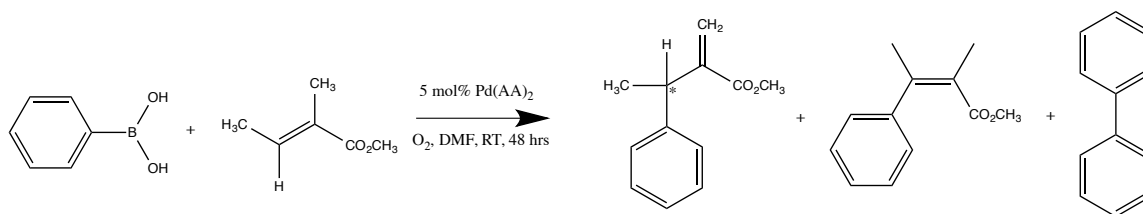
Figure 91. Oxidative coupling reaction between phenylboronic acid and methyl tiglate catalyzed by Pd(II)-AA complexes.

4.3 AMINO ACIDS WITH AROMATIC HYDROPHOBIC R-GROUPS

Tryptophan, phenylalanine, and tyrosine comprise the group of amino acids with aromatic R-groups; their proposed palladium bis-chelates are shown in Figure 92.
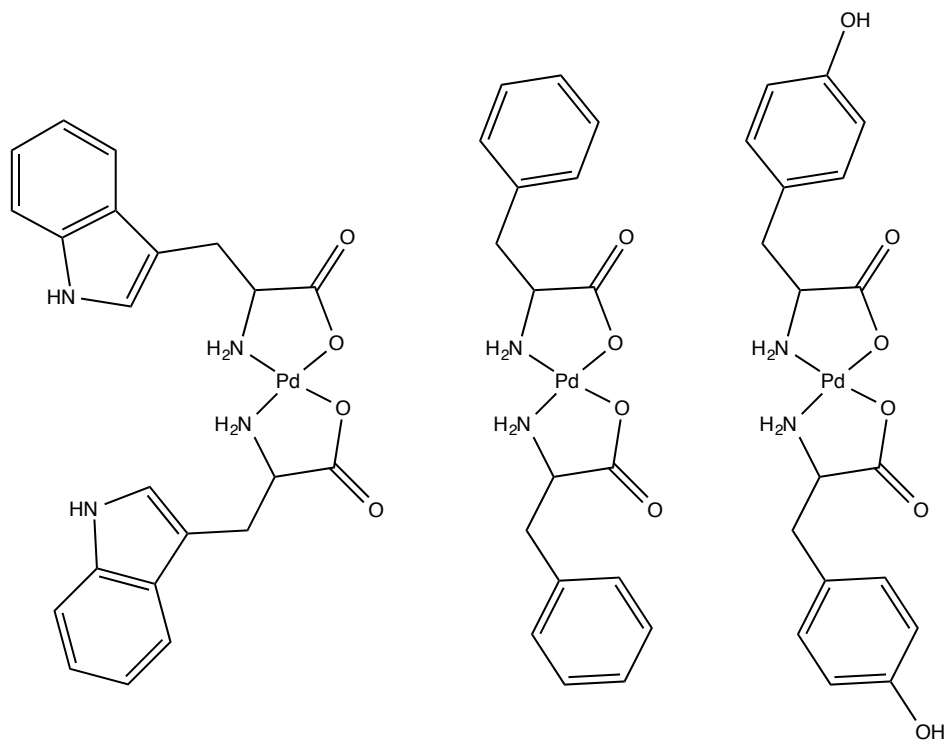
Figure 92. Pd(II) complexes of tryptophan (7), phenylalanine (8), and tyrosine (9).

Phenylalanine and tyrosine can only chelate in an *N,O* manner, as they lack another coordinating moiety on their R-groups. An argument could be made for *O,O* chelation with tyrosine, but that is extremely unlikely. *O,O* chelation would result in an 9-membered chelate ring which would be considerably less stable than the 5-membered chelate formed via *N,O* chelation. Additionally, the incorporation of a planar phenyl ring into the chelate ring is sterically very unfavorable. Tryptophan, on the other hand, does present an intriguing option for *N,N* chelation resulting in a 7-membered chelate ring. While not as stable as the 5-membered *N,O* chelate, it is nonetheless

possible as evidenced by Nakayama's preparation of the ornithine complex.[17] In this case we can turn to an interpretation of the infrared spectra of the chelated and free ligand to determine the coordination mode (Figure 93). The FTIR spectrum of the free ligand shows an asymmetric CO_2 stretch at 1573 cm^{-1} and a symmetric CO_2 stretch at 1406 cm^{-1}. This is expected when the carboxylate is in the zwitterionic state. When the carboxylate coordinates to the metal center its two-fold symmetry is lost resulting in different C-O and C=O stretches. This is exactly what is observed with bis(tryptophanato)palladium(II) (**7**). The FTIR spectrum of the complex shows that the asymmetric and symmetric stretching vibrations are absent and a new carbonyl stretch is present at 1647 cm^{-1}. In addition, the indole N-H stretch at 3407 cm^{-1} is unchanged between the free ligand and complex. Were tryptophan to coordinate through the indole nitrogen atom, a change in the indole N-H stretch would be observed. On the basis of this evidence we can say with some certainty that bis(tryptophanato)palladium(II) (**7**) is a 5-membered *N,O* chelate, however the *cis-trans* geometry of the ligands about the metal center remains undetermined. NMR and HRMS data for these compounds are as expected and unremarkable. They are summarized for each compound in Section 4.7.
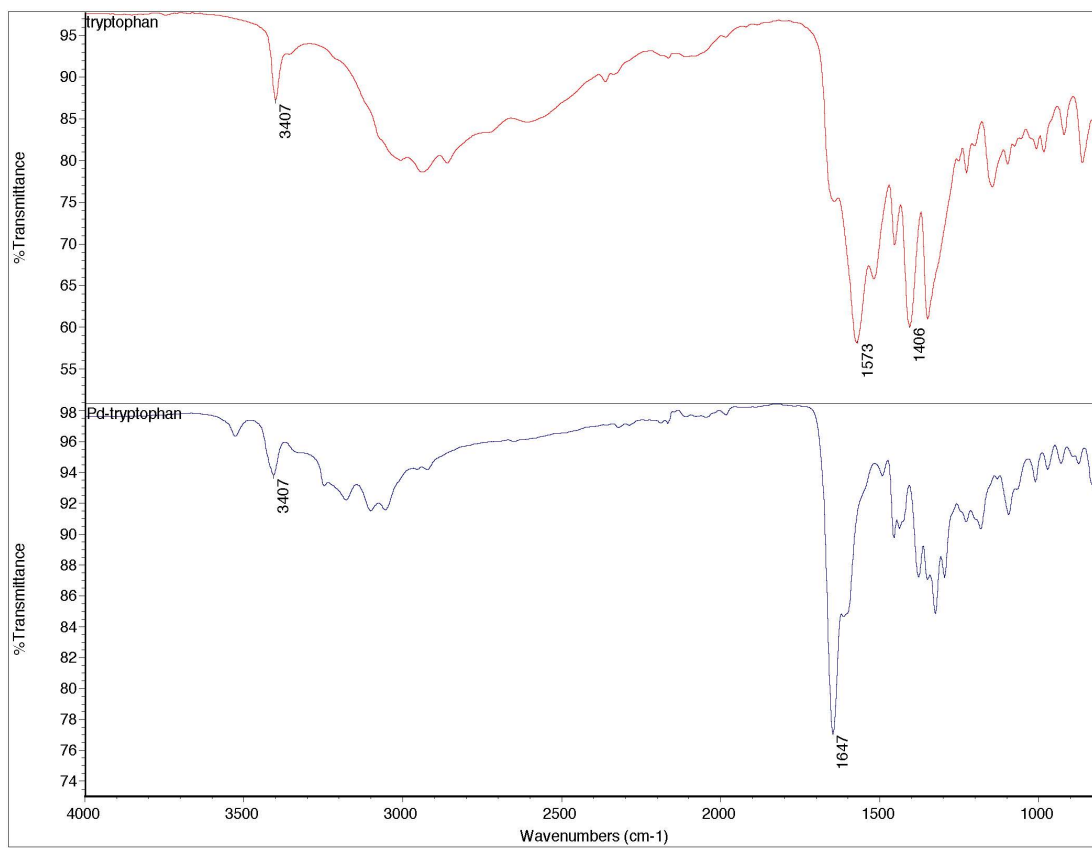
Figure 93. FTIR spectral comparison of tryptophan free ligand (top, in red) and the bis(tryptophanato)palladium(II) complex (7) (bottom, in blue).

Bis(phenylalininato)palladium(II) (**8**) was tested for catalytic activity against the aforementioned phenyl boronic acid-methyl tiglate oxidative coupling reaction. The R/S:Z product ratio was 3.5:1 and biphenyl accounted for 46% of the coupling yield. Enantioselectivity was again low at 2%ee.

4.4   AMINO ACIDS WITH POLAR NEUTRAL R-GROUPS

Neutral, polar side groups characterize the next grouping of Pd-AA catalysts (Figure 94).

These amino acids include asparagine, glutamine, cysteine, methionine, serine and threonine.
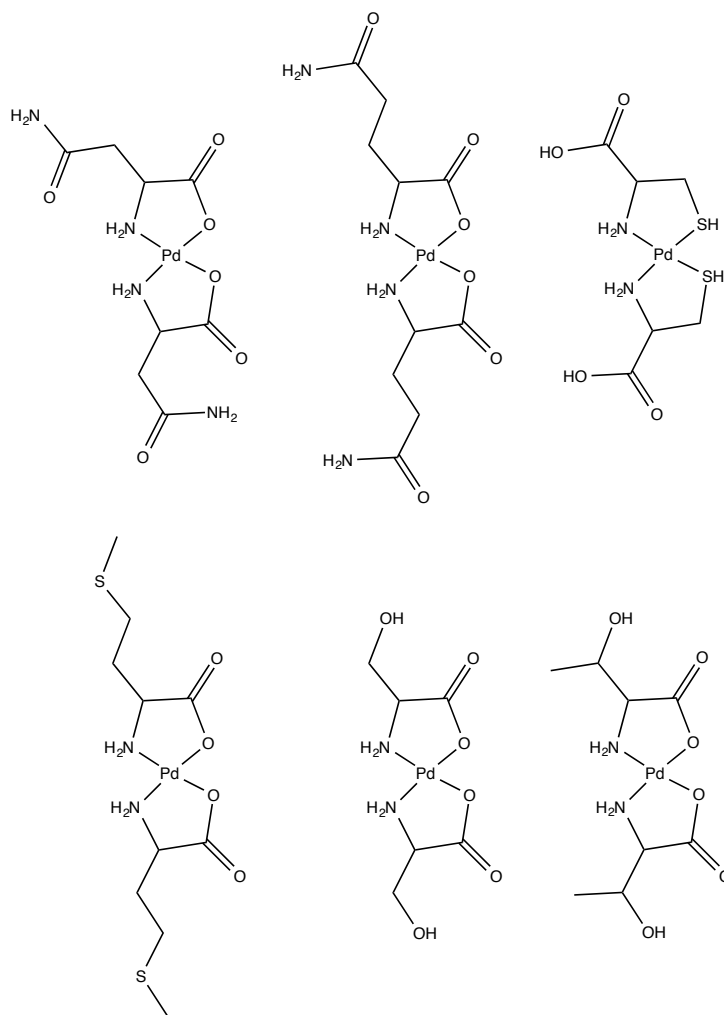
Figure 94. Pd(II) complexes of asparagine (<u>10</u>), glutamine (<u>11</u>), cysteine (<u>12</u>), methionine (<u>14</u>), serine (<u>15</u>) and threonine (<u>16</u>). The complex of cystine (<u>13</u>) is not shown.

Bis(asparaginato)palladium(II) (**<u>10</u>**) and bis(glutaminato)palladium(II) (**<u>11</u>**) both contain an amide group on the R-group terminus and differ only by one methylene unit in the side chain. HRMS confirms the formation of the bis-chelate in both instances, and the NMR data for each complex are as expected. As neither of these techniques speaks to the chelation geometry, we must again turn to the FTIR data to determine whether chelation is *N,N* or *N,O* in nature. Free

153

asparagine shows a symmetric CO_2 stretch at 1394 cm^{-1} and an asymmetric stretch at 1495 cm^{-1}. Both of these vibrations are missing in the spectrum of the complex with a new CO stretch appearing at 1688 cm^{-1}. Furthermore, the amide carbonyl stretching vibrations at 1601 and 1642 cm^{-1} remain unchanged in the spectrum of the complex. This is indicative of N,O chelation for bis(asparaginato)palladium(II) (**10**). This trend is seen as well for bis(glutaminato)palladium(II) (**11**) with symmetric and asymmetric CO_2 stretching vibrations at 1445 and 1572 cm^{-1}, respectively, disappearing from the spectrum of the chelate. A new CO stretch at 1636 cm^{-1} is observed in the spectrum of the complex. The amide CO stretching vibrations at 1327 and 1408 cm^{-1} remain unchanged in both the free ligand and the complex. Once again this is indicative of N,O chelation for bis(glutaminato)palladium(II) (**11**).

Serine and threonine both contain hydroxyl group functionality in their R-groups that lead to extended hydrogen bonded networks in the solid phase. *Cis*-bis(serinato)palladium(II) (**15**) (Figure 95) crystallizes in the $P2_12_12_1$ space group. Pd-N bond lengths are 2.0177 and 2.0124 Angstroms with a N-Pd-N bond angle of 100.28 degrees. Pd-O bond lengths are 2.0177 and 1.9989 Angstroms with an O-Pd-O bond angle of 94.22 degrees. These values are comparable to other square planar palladium(II) chelates reported in the literature.[4,5,12-16]
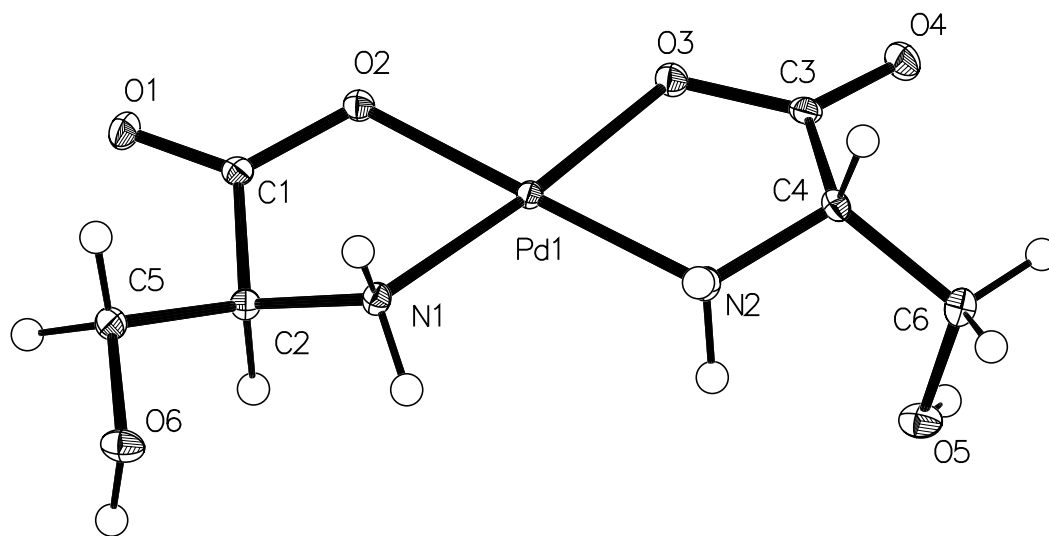
Figure 95. ORTEP plot of cis-bis(serinato)palladium(II) (15). Thermal ellipsoids are shown at the 50% probability level.

The extended lattice of **15** is extremely well ordered, with ten hydrogen bonding interactions present for each molecule. Each molecule in the lattice is hydrogen bonded to six other molecules within the lattice (Figure 96).
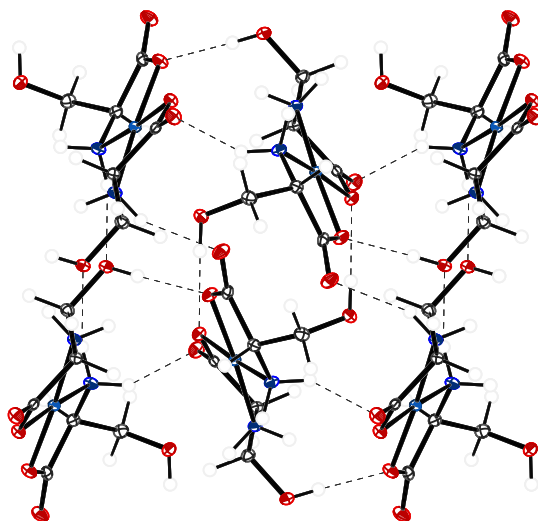
Figure 96. Hydrogen bonding interactions of *cis*-bis(serinato)palladium(II) (15) as viewed down [0 1 0]. Oxygen atoms = red, nitrogen atoms = blue, carbon atoms = grey, palladium atoms = silver. Thermal ellipsoids are shown at the 50% probability level.

Cis-bis(threoninato)palladium(II) (**16**) (Figure 97) differs from the serine complex by the replacement of one side-chain methylene hydrogen atom with a methyl group. This complex also crystallizes in the $P2_12_12_1$ space group with 2 complex molecules and 3 water molecules in the unit cell. Pd-N bond lengths are 2.015 and 2.014 Angstroms. Pd-O bond lengths are 2.014 and 2.031 Angstroms. Bond angles are 98.623 degrees for the N-Pd-N angles and 96.04 degrees for the O-Pd-O angles. Once again, these values are in line with other square planar palladium(II) chelates reported in the literature.[4,5,12-16] As seen with the serine complex, there is a very well ordered hydrogen bonding network present within the extended lattice for this complex (Figure 98). Each complex molecule in the lattice is involved in one intermolecular hydrogen bond from the side chain hydroxyl hydrogen atom to the coordinated carboxylate oxygen atom of another complex molecule. There are an additional 3 hydrogen bonds to water molecules in the lattice that bridge to three other distinct complex molecules in the lattice.
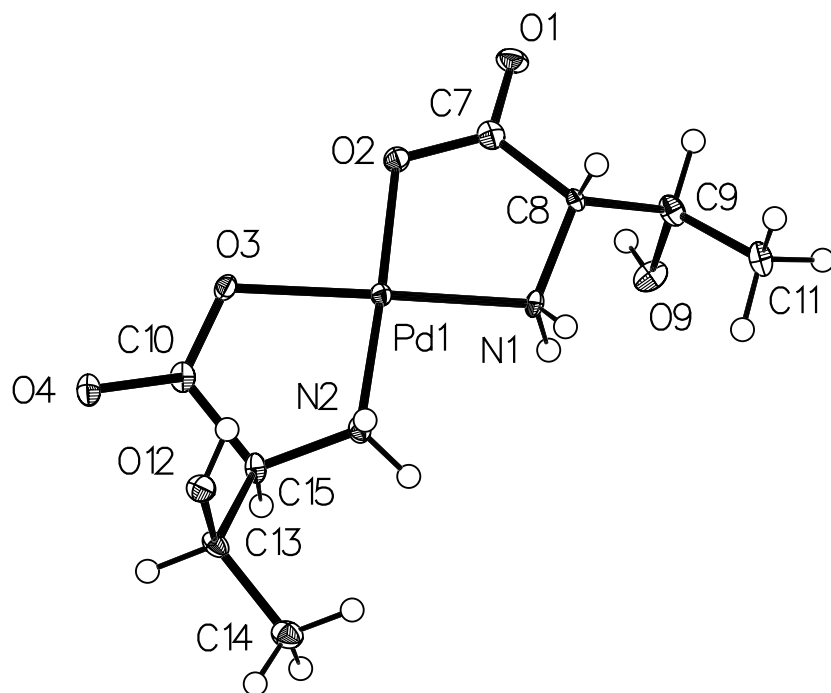
156

Figure 97. X-ray crystal structure of cis-bis(threoninato)palladium(II) (**16**). Thermal ellipsoids are shown at the 50% probability level.
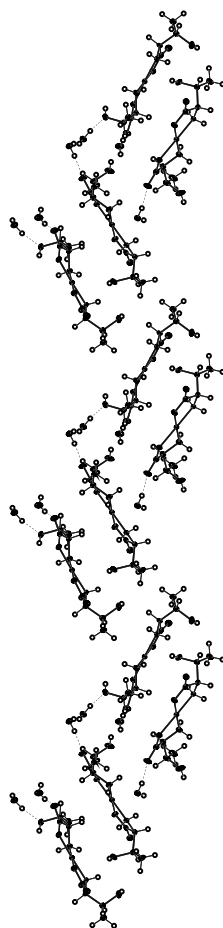
Figure 98. Hydrogen bonding interactions of cis-bis(threoninato)palladium(II) (<u>16</u>) as viewed along [$\frac{1}{8}$ 1 0].

Of the six amino acid ligands in this group, methionine and cysteine contain a sulfur atom in their molecular structure. A cysteine derivative, cystine, contains a disulfide group and will be discussed here as well. Sulfur containing ligands are an interesting choice for palladium(II) chemistry in that palladium has a noted affinity for sulfur over nitrogen and oxygen groups.[18] Incorporation of the sulfur moiety into an amino acid ligand structure provides one method of forming multi-dentate network structures. The first sulfur-containing amino acid complex of palladium(II) that was attempted to be synthesized was bis(methioninato)palladium(II) (<u>14</u>). It

158

was hoped that the thioether side chain would be less likely to coordinate than the thiol group present in cysteine. High–resolution time-of-flight mass spectrometry performed on a sample taken directly from the reaction mixture clearly showed the formation of the bis-chelate (Figure 99).
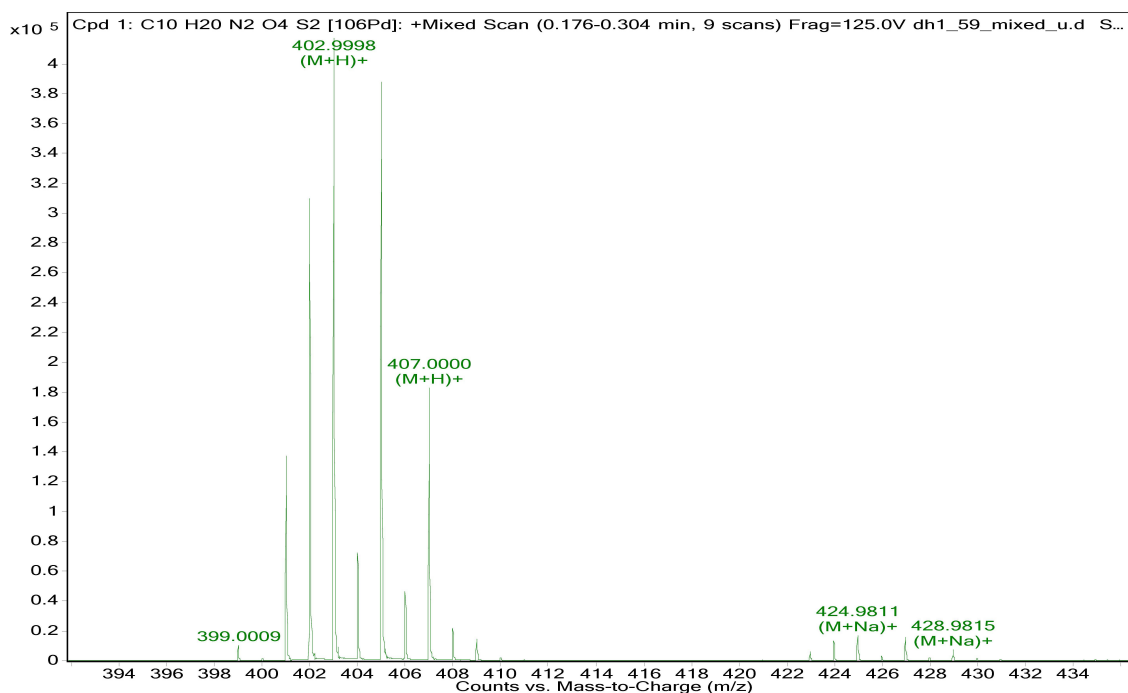
Figure 99. High-resolution TOF mass spectrum of bis(methioninato)palladium(II) (14).

Frustratingly, all subsequent attempts to isolate the bis-chelated product failed. NMR spectra were unable to be obtained, as were single crystals for X-ray diffraction. FTIR spectra were inconclusive and appeared to show a mixture of methionine ligand and palladium(II) acetate.

The reaction of cysteine with palladium(II) acetate to yield bis(cysteinato)palladium(II) (**12**) also failed to yield an isolatable product, however the HRMS data from the reaction mixture show a series of products whose masses correspond exactly to discreet ratios of ligand and metal. In these proposed structures (Figure 100) each palladium center is *N,O* chelated by the ligand,

with the thiol group and the non-coordinated carboxylate carbonyl oxygen coordinated to another palladium center.
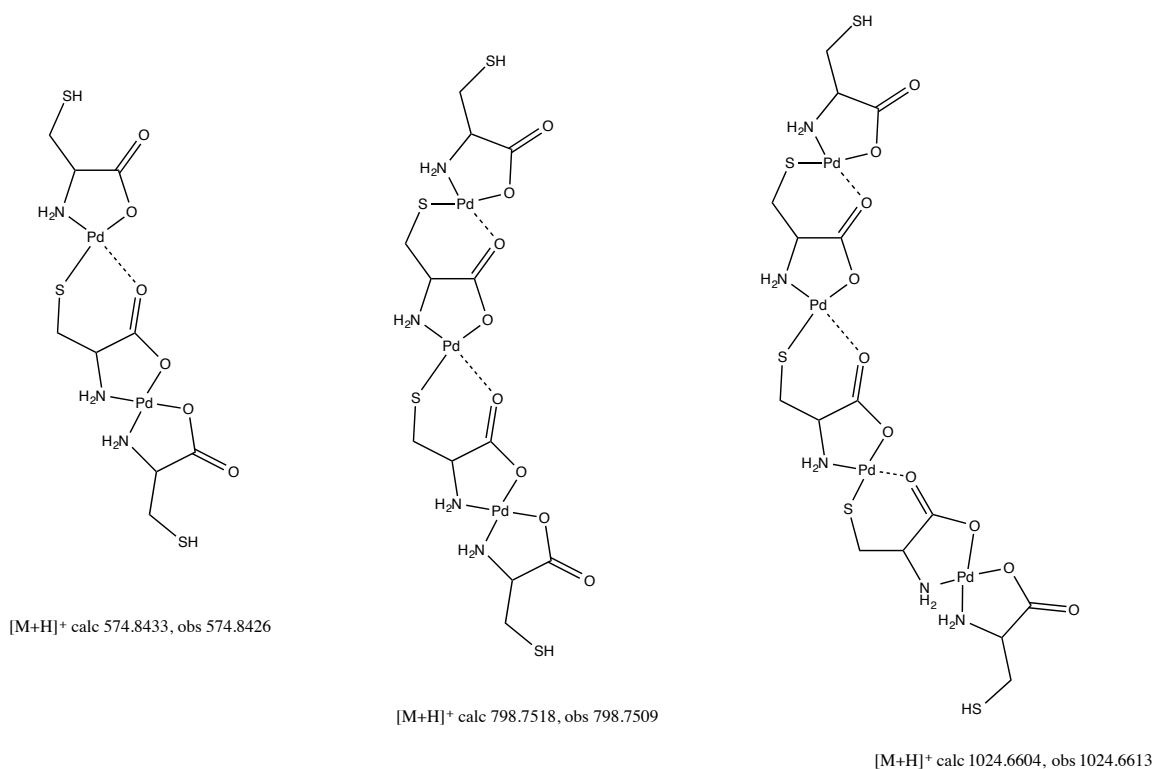

[M+H]+ calc 574.8433, obs 574.8426

[M+H]+ calc 798.7518, obs 798.7509

[M+H]+ calc 1024.6604, obs 1024.6613

Figure 100. Proposed molecular structures of cysteinato-linked palladium(II) network.

In this case di-, tri-, and tetra-nuclear palladium(II) complexes were detected. The synthesis of bis(cystinato)palladium(II) (**13**) was also attempted from cystine and palladium(II) acetate, and once again failed to yield an isolatable product. Palladium cluster aggregation is a noted phenomena with thioethers and disulfides[19,20] and likely accounts for the lack of product formation in the cases of methionine and cystine.

For this group of amino acid catalysts, *cis*-bis(serinato)palladium(II) (**15**) was chosen as the representative catalyst for study. The oxidative coupling of phenylboronic acid to methyl tiglate was again successful, with enantioselectivity of 3% ee. *Cis*-bis(serinato)palladium(II)

(**15**) showed the lowest level of homocoupling of any of the tested catalysts with biphenyl accounting for 27% of the product distribution.

4.5   AMINO ACIDS WITH CHARGED ACIDIC R-GROUPS

Aspartic acid and glutamic acid comprise the ligand set composed of acidic R-groups (Figure 101). Here again we see the possibility of multiple coordination modes. *N,O* chelation forms the more-stable 5-membered chelate ring, however *O,O* chelation is possible and would yield 6-membered and 7-membered chelate rings respectively.   Studies on donor atom preferences for palladium have clearly established that palladium prefers ligands containing sulfur over nitrogen, and nitrogen over oxygen (S>N>O).[18] On this reasoning alone we would expect the palladium complexes of aspartic and glutamic acids to adopt the 5-membered *N,O* chelate ring. Fortuitously, the crystal structure of *cis*-bis((η^2-*N,O*)-aspartate)palladium(II) (**17**) was obtained (Figure 102) and clearly shows that the chelation mode is *N,O*. It is not unreasonable to expect that glutamic acid would behave in the same manner.
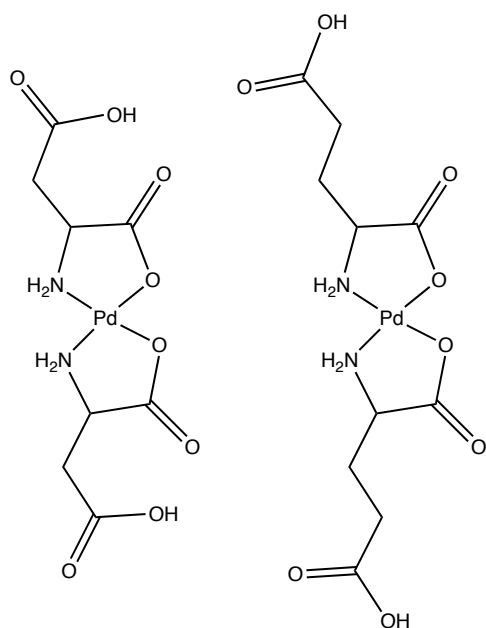
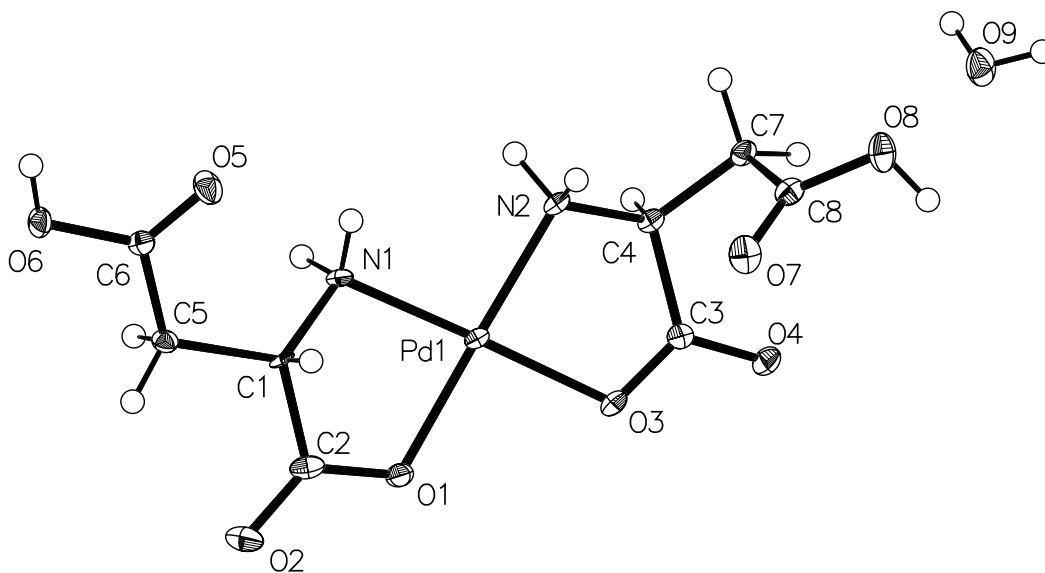**Figure 101. Pd(II) complexes of aspartic acid (17) and glutamic acid (18).**

Figure 102. ORTEP plot of the crystal structure of *cis*-bis((η²-*N,O*)-aspartate)palladium(II) (17).

Cis-bis((η²-*N,O*)-aspartate)palladium(II) (**17**) crystallizes in the *P*2₁ space group and exhibits an extensive hydrogen bonding network (Figure 103). Two amine protons that lie on

162

one side of the chelate plane are each hydrogen bonded to separate coordinated carboxyl oxygen atoms on an adjacent molecule. The two amine protons on the other side of the chelate plane are hydrogen bonded to the R-group aspartate carboxyl group of another adjacent molecule. Additionally there are three hydrogen bonded water molecules in the lattice that bridge the coordinated carbonyl oxygen atom on one molecule to the coordinated carbonyl oxygen atom on another molecule.
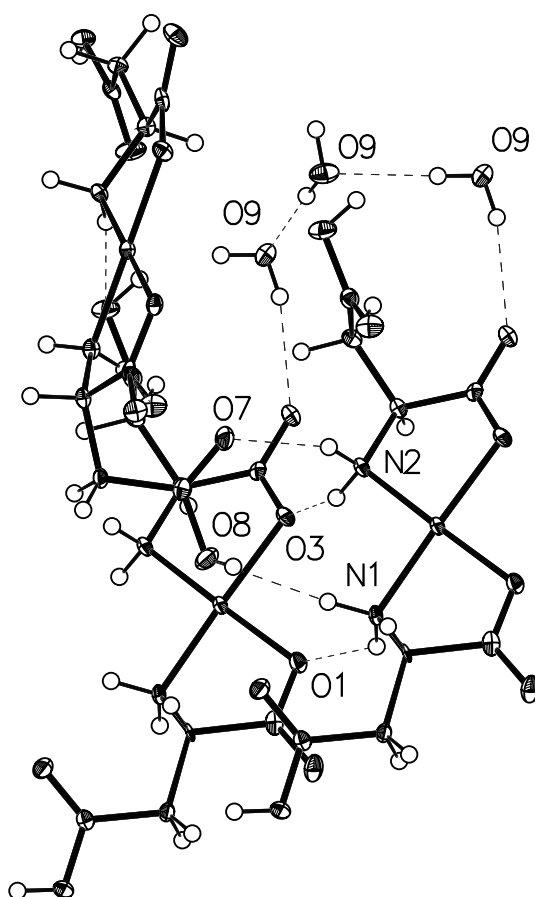
Figure 103. Hydrogen bonding interactions observed in the crystal lattice of *cis*-bis((η²-*N,O*)-aspartate)palladium(II) (17).

Cis-bis((η²-*N,O*)-aspartate)palladium(II) (**17**) was successfully employed as the catalyst in the oxidative coupling of phenylboronic acid to methyl tiglate. The R/S:Z product ratio was

1.2:1 and biphenyl accounted for 60% of the coupling yield. Low enantioselectivity was obtained, with ee's of 4%.

4.6 AMINO ACIDS WITH CHARGED BASIC R-GROUPS

Basic R-groups are present in the palladium(II) complexes of histidine, arginine, and lysine (Figure 104).
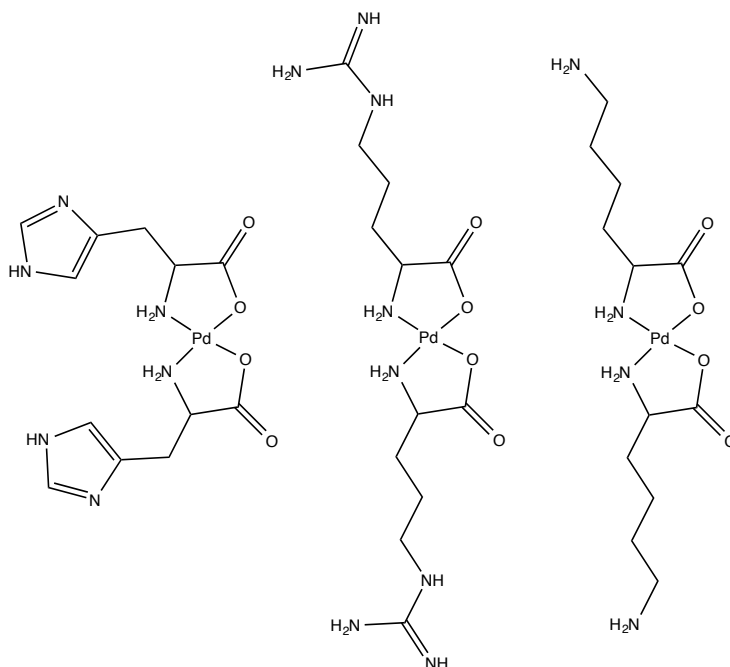

Figure 104. Pd(II) complexes of histidine (19), arginine (20), and lysine (21).

N,N chelation modes are possible for all of these complexes. For bis(lysinato)palladium(II) (**21**) *N,N* chelation would result in an unlikely 8-membered chelate ring. This leaves *N,O* chelation as the only possible and most favored coordination mode. Due to the complexity of the fingerprint region (1500-500 cm^{-1}) of the FTIR spectrum for this complex a definite assessment based on the carboxylate stretching vibrations cannot be made,

164

and attempts to grow crystals for X-ray diffraction were unsuccessful. The ^{1}H and ^{13}C NMR spectra are consistent with a coordinated lysine ligand, and HRMS confirms the formation of bis(lysinato)palladium(II) (**21**).

Bis(argininato)palladium(II) (**20**) contains a guanidine group on the terminus of the amino acid R-group that could form either a 7-membered or 9-membered chelate ring. The 9-membered ring is not likely to form, however as discussed above for tryptophan the possibility of a 7-membered ring cannot be dismissed out of hand. Fortunately the FTIR spectrum of the guanidine side chain of arginine is well-characterized[21] and there are several characteristic C-N stretches that indicate the presence of an un-coordinated guanidine group. Infrared absorptions at 920, 1180, 1614, and 1670 cm^{-1} have been assigned to various C-N stretching modes of the free guanidine group. These absorptions are present in both the free ligand and the complex (Figure 105) and support the premise that the arginine side chain is not involved in coordination to the metal. Proton NMR data are consistent with a coordinated arginine ligand and HRMS confirms formation of the bis-chelate.
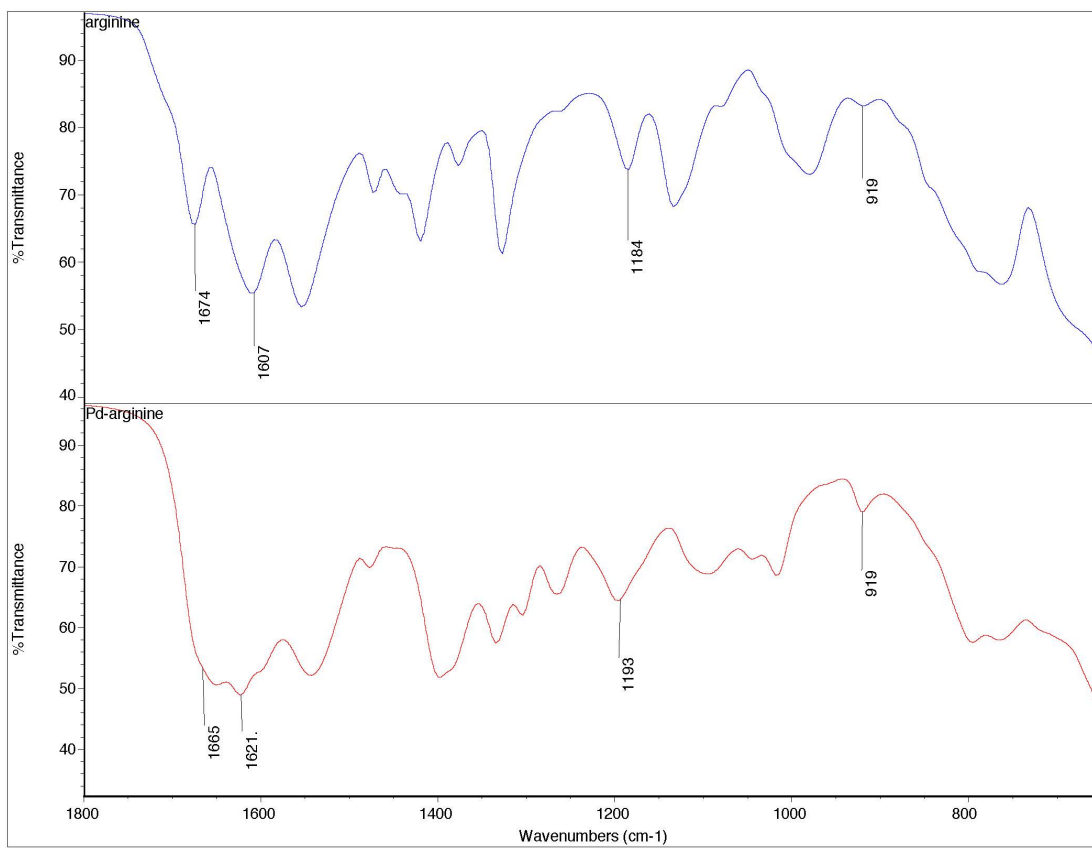
Figure 105. FTIR spectral comparison of the free arginine ligand (top, in blue) and bis(argininato)palladium(II) (20) (bottom, in red) showing the presence of characteristic guanidine C-N stretching vibrations in both molecules.

Histidine (Figure 106) provides an opportunity for *N,N* chelation with the formation of a 6-membered ring. The R-group terminus of the histidine molecule is an imidazole group.
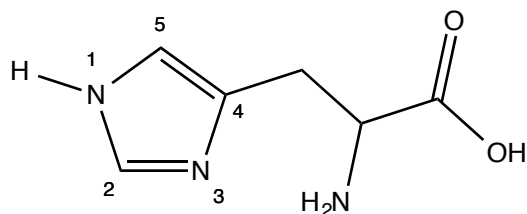

Figure 106. Molecular structure of histidine. The imidazole group is numbered for clarity.

166

Coordination through N-1 is unlikely as the lone pair of electrons on this nitrogen atom are involved in the aromatic π system of the imidazole ring. Coordination through N-3 is possible and would result in the formation of a 6-membered *N,N* chelate. Turning again to the FTIR spectrum of the free ligand versus the complex, the symmetric CO_2 stretch in the free ligand at 1449 cm^{-1} disappears and is not observed in the complex. The asymmetric CO_2 stretch at 1628 cm^{-1} in the free ligand is shifted to 1588 cm^{-1} in the complex (Figure 107). This is compelling evidence of the lack of free carboxylate functionality in the complex and strongly indicates the formation of the N,O chelate.
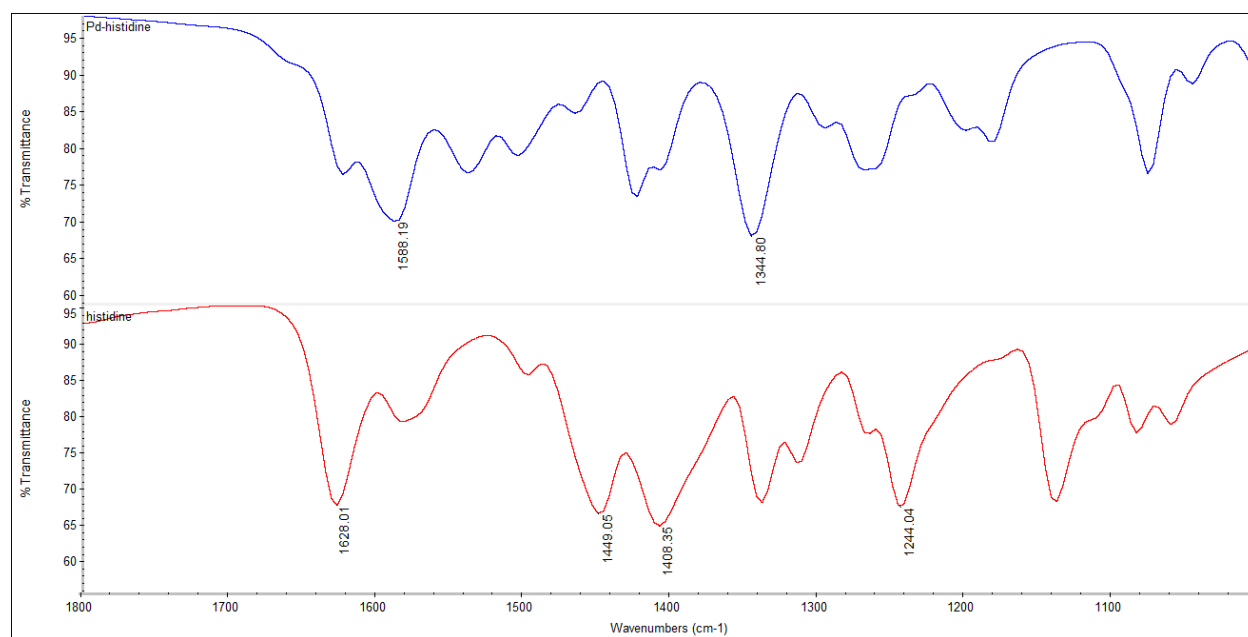
Figure 107. FTIR spectral comparison of histidine free ligand (red) and bis(histidinato)palladium(II) (blue).

HRMS confirms the formation of bis(histidinato)palladium(II) (**19**). Interestingly, the NMR data indicate the presence of two distinct complexes in D_2O solution. Each of the expected six carbon resonances in the ^{13}C NMR spectrum appears as a pair of resonances. Similarly, the ^1H NMR spectrum shows two sets of resonances for the methine and aromatic protons that each

integrate to a 1:1:1 ratio. The methylene protons show significant overlap and cannot be resolved, but they integrate to a total of 4 protons. It is very likely that we are seeing an aquo-complex formation in solution as we observed for the glycine complexes discussed in Chapter 1.[12]

Catalytic activity of this group of amino acid complexes was successfully tested with the bis(lysinato)palladium(II) (**21**) complex against the oxidative coupling of phenylboronic acid and methyl tiglate. The R/S:Z product ratio was 2.6:1 and biphenyl accounted for only 32% of the coupling yield. The trend of low enantioselectivity was continued, with ee's of 5% for this catalyst.

4.7   CONCLUSIONS

Twenty-one palladium(II) amino acid bis-chelates were synthesized, characterized, and assessed for catalytic activity against the oxidative coupling of phenylboronic acid and methyl tiglate. The amino acids employed came from five general classes based on the chemical nature of their R-groups: aliphatic hydrophobic, aromatic hydrophobic, polar neutral, charged acidic, and charged basic. Each complex coordinates via *N,O* chelation to the metal center. Six crystal structures were determined. Each class of amino acid complex shows catalytic activity as evidenced by a successful oxidative coupling of phenylboronic acid and methyl tiglate. Enantioselectivity was low across the range of catalysts tested with %ee's in the range of 2-5%.

4.8   EXPERIMENTALS

4.8.1 Synthesis of bis(alaninato)palladium(II) (1)

A four dram vial was charged with 0.0532 grams of palladium(II) acetate (2.37×10^{-4} mol) and 3.0 mL of 50/50 (v/v) acetone/water. The mixture was stirred until completely dissolved. To this was added 0.0464 grams of alanine (5.21×10^{-4} mol, 2.2 equivalents) and left to stir overnight. The reaction solution turned from a dark red-orange to a clear yellow with a pale yellow-white precipitate on overnight stirring. An odor of acetic acid was noted when the vial was opened. The supernatant was transferred via pipette to a clean vial and allowed to evaporate to give clear yellow needles. The pale-yellow precipitate was washed with cold water and dried under vacuum. The combined yield of crystals and precipitate was 63.3 mg of product (0.2240 mmol, 95% yield). $Pd(C_3H_6NO_2)_2$ was identified on the basis of the following data: ^{1}H NMR (400 MHz, Deuterium Oxide) δ 3.63 (q, J = 7.2 Hz, 1H), 1.33 (d, J = 7.3 Hz, 3H). HRMS/ESI+ (m/z): [M+H]+ calcd for $Pd(C_3H_6NO_2)_2$, 282.9905; found, 282.9916.

4.8.2 Synthesis of bis(L-valinato)palladium(II) (2)

A four dram vial was charged with 0.0256 grams of palladium(II) acetate (1.14×10^{-4} mol) and 2.5 mL of 2:1 (v/v) acetone:water. The mixture was stirred until completely dissolved. To this was added 0.0294 grams of L-valine (2.51×10^{-4} mol, 2.2 equivalents) and left to stir overnight. The reaction solution turned from a dark red-orange to a clear yellow with a pale yellow precipitate on overnight stirring. An odor of acetic acid was noted when the vial was opened. The supernatant was transferred via pipette to a clean vial and allowed to evaporate to give clear yellow plates. The pale-yellow precipitate was washed with cold water and dried under vacuum. The combined yield of crystals and precipitate was 36.6 mg of product (0.1081 mmol, 95% yield). $Pd(C_5H_{10}NO_2)_2$ was identified on the basis of the following data: ^{1}H NMR (400 MHz,

Deuterium Oxide) δ 3.47 (d, J = 4.4 Hz, 1H), 2.14 (pd, J = 7.0, 4.4 Hz, 1H), 0.91 (d, J = 7.0 Hz, 3H), 0.86 (d, J = 7.0 Hz, 3H). HRMS/ESI+ (m/z): [M+H]+ calcd for $Pd(C_5H_{10}NO_2)_2$, 339.0531; found, 339.0549.

4.8.3 Synthesis of bis(D-valinato)palladium(II) (3)

A four dram vial was charged with 0.0188 grams of palladium(II) acetate (8.37×10^{-5} mol) and 2.5 mL of 2:1 (v/v) acetone:water. The mixture was stirred until completely dissolved. To this was added 0.0216 grams of D-valine (1.84×10^{-4} mol, 2.2 equivalents) and left to stir overnight. The reaction solution turned from a dark red-orange to a clear yellow with a pale yellow precipitate on overnight stirring. An odor of acetic acid was noted when the vial was opened. The supernatant was transferred via pipette to a clean vial and allowed to evaporate however no crystals formed. The pale-yellow precipitate was washed with cold water and dried under vacuum to yield 27.1 mg of product (0.0800 mmol, 96% yield). $Pd(C_5H_{10}NO_2)_2$ was identified on the basis of the following data: ^{1}H NMR (400 MHz, Deuterium Oxide) δ 3.47 (d, J = 4.4 Hz, 1H), 2.14 (pd, J = 7.0, 4.4 Hz, 1H), 0.91 (d, J = 7.0 Hz, 3H), 0.86 (d, J = 7.0 Hz, 3H). HRMS/ESI+ (m/z): [M+H]+ calcd for $Pd(C_5H_{10}NO_2)_2$, 339.0531; found, 339.0557. Anal. Calcd. for $Pd(C_5H_{10}NO_2)_2 \cdot H_2O$: C, 33.67%; H, 6.22%; N, 7.85%. Found: C, 33.83%; H, 6.29%; N, 8.01%.

4.8.4 Synthesis of bis(isoleucinato)palladium(II) (4)

A four dram vial was charged with 0.1638 grams of palladium(II) acetate (7.30×10^{-4} mol) and 4.0 mL of 2:1 (v/v) acetone:water. The mixture was stirred until completely dissolved. To this was added 0.2105 grams of isoleucine (1.61×10^{-3} mol, 2.2 equivalents) and left to stir overnight.

Reaction solution turned from a dark red-orange to a pale, clear yellow with pale yellow precipitate on overnight stirring. An odor of acetic acid was noted when the vial was opened. The supernatant was transferred via pipette to a clean vial and allowed to evaporate to give clear yellow prisms which were used for X-ray diffraction. The remaining precipitate was washed with cold water and dried under vacuum. The yield of precipitate was 254.9 mg of product (0.6950 mmol, 95% yield). $Pd(C_6H_{12}NO_2)_2$ was identified on the basis of the following data: ^{1}H NMR (500 MHz, DMSO-d_6) δ 5.15 (dd, J = 10.5, 7.6 Hz, 1H), 4.72 (t, J = 8.9 Hz, 1H), 4.37 (dd, J = 10.6, 5.5 Hz, 1H), 3.84 (dd, J = 10.7, 5.2 Hz, 1H), 3.16 – 3.02 (m, 2H), 1.76 (m, 2H), 1.57 – 1.31 (m, 2H), 1.04 (d, J = 6.9 Hz, 4H), 0.89 (t, J = 7.4 Hz, 3H), 0.84 (t, J = 7.4 Hz, 3H). HRMS/ESI+ (m/z): [M+H]+ calcd for $Pd(C_6H_{12}NO_2)_2$, 367.0844; found, 367.0871.

4.8.5 Synthesis of bis(*tert*-leucinato)palladium(II) (5)

A four dram vial was charged with 0.0325 grams of palladium(II) acetate (1.45×10^{-4} mol) and 2.5 mL of 2:1 (v/v) acetone:water. The mixture was stirred until completely dissolved. To this was added 0.0418 grams of *tert*-leucine (3.18×10^{-4} mol, 2.2 equivalents) and left to stir overnight. The reaction solution turned from a dark red-orange to a clear yellow with a pale yellow precipitate on overnight stirring. An odor of acetic acid was noted when the vial was opened. The supernatant was transferred via pipette to a clean vial and allowed to evaporate however no crystals formed. The pale-yellow precipitate was washed with cold water and dried under vacuum to yield 50.6 mg of product (0.1378 mmol, 95% yield). $Pd(C_6H_{12}NO_2)_2$ was identified on the basis of the following data: ^{1}H NMR (400 MHz, Deuterium Oxide) δ 3.16 (s, 1H), 0.94 (s, 9H). HRMS/ESI+ (m/z): [M+H]+ calcd for $Pd(C_6H_{12}NO_2)_2$, 367.0844; found, 367.0877.

Anal. Calcd. for Pd(C$_6$H$_{12}$NO$_2$)$_2$: C, 39.30%; H, 6.60%; N, 7.64%. Found: C, 39.47%; H, 6.59%; N, 7.70%.

4.8.6   Synthesis of bis(leucinato)palladium(II) (6)

A four dram vial was charged with 0.0517 grams of palladium(II) acetate (2.30x10^{-4} mol) and 2.5 mL of 2:1 (v/v) acetone:water. The mixture was stirred until completely dissolved. To this was added 0.0665 grams of leucine (5.07x10^{-4} mol, 2.2 equivalents) and left to stir overnight. The reaction solution turned from a dark red-orange to a clear yellow with a pale yellow precipitate on overnight stirring. An odor of acetic acid was noted when the vial was opened. The supernatant was transferred via pipette to a clean vial and allowed to evaporate however no crystals formed. The pale-yellow precipitate was washed with cold water and dried under vacuum to yield 82.1 mg of product (0.2239 mmol, 97% yield).   Pd(C$_6$H$_{12}$NO$_2$)$_2$ was identified on the basis of the following data: ^{1}H NMR (400 MHz, Deuterium Oxide) δ 3.63 – 3.53 (m, 1H), 1.65 – 1.55 (m, 1H), 1.60 – 1.44 (m, 2H), 0.90 – 0.72 (m, 6H). ^{13}C NMR (101 MHz, D$_2$O) δ 175.70, 53.57, 39.94, 24.30, 22.16, 21.02.   HRMS/ESI+ (m/z):   [M+Na]+ calcd for Pd(C$_6$H$_{12}$NO$_2$)$_2$, 389.0663; found, 389.0692.

4.8.7   Synthesis of bis(tryptophanato)palladium(II) (7)

A four dram vial was charged with 0.0799 grams of palladium(II) acetate (3.56x10^{-4} mol) and 2.5 mL of 2:1 (v/v) acetone:water. The mixture was stirred until completely dissolved. To this was added 0.1599 grams of tryptophan (7.83x10^{-4} mol, 2.2 equivalents) and left to stir overnight. The reaction solution turned from a dark red-orange to clear with a white precipitate on overnight stirring. An odor of acetic acid was noted when the vial was opened. The supernatant was

transferred via pipette to a clean vial and allowed to evaporate however no crystals formed. The precipitate was washed with cold water and dried under vacuum to yield 178.2 mg of product (0.3475 mmol, 98% yield). $Pd(C_{11}H_{11}N_2O_2)_2$ was identified on the basis of the following data: ^{1}H NMR (400 MHz, DMSO-d6) δ 7.49 (d, J = 7.8 Hz, 1H), 7.30 (d, J = 7.8 Hz, 1H), 7.15 (d, J = 2.4 Hz, 1H), 7.03 (ddd, J = 8.1, 7.0, 1.2 Hz, 1H), 6.93 (ddd, J = 8.0, 7.0, 1.0 Hz, 1H), 4.60 (dd, J = 10.0, 6.5 Hz, 1H), 3.83 (dd, J = 9.6, 7.7 Hz, 1H), 3.47-3.33 (m, 1H). HRMS/ESI+ (m/z): [M+H]+ calcd for $Pd(C_{11}H_{11}N_2O_2)_2$, 513.0749; found, 513.0700. Anal. Calcd. for $Pd(C_{11}H_{11}N_2O_2)_2 \bullet H_2O$: C, 49.77%; H, 4.56%; N, 10.55%. Found: C, 49.00%; H, 4.51%; N, 10.41%.

4.8.8   Synthesis of bis(phenylalaninato)palladium(II) (8)

A four dram vial was charged with 0.1067 grams of palladium(II) acetate (4.75×10^{-4} mol) and 2.5 mL of 2:1 (v/v) acetone:water. The mixture was stirred until completely dissolved. To this was added 0.1727 grams of phenylalanine (1.05×10^{-3} mol, 2.2 equivalents) and left to stir overnight. The reaction solution turned from a dark red-orange to clear with a white precipitate on overnight stirring. An odor of acetic acid was noted when the vial was opened. The supernatant was transferred via pipette to a clean vial and allowed to evaporate however no crystals formed. The precipitate was washed with cold water and dried under vacuum to yield 190.1 mg of product (0.4373 mmol, 92% yield). $Pd(C_9H_{10}NO_2)_2$ was identified on the basis of the following data: ^{1}H NMR (400 MHz, Deuterium Oxide) δ 7.34 – 7.14 (m, 5H), 3.85 (dd, J = 8.0, 5.3 Hz, 1H), 3.15 (dd, J = 14.5, 5.2 Hz, 1H), 2.98 (dd, J = 14.5, 8.0 Hz, 1H). HRMS/ESI+ (m/z): [M+H]+ calcd for $Pd(C_9H_{10}NO_2)_2$, 435.0531; found, 435.0538.

4.8.9 Synthesis of bis(tyrosinato)palladium(II) (9)

A four dram vial was charged with 0.0511 grams of palladium(II) acetate (2.28×10^{-4} mol) and 2.5 mL of 2:1 (v/v) acetone:water. The mixture was stirred until completely dissolved. To this was added 0.0907 grams of tyrosine (5.01×10^{-4} mol, 2.2 equivalents) and left to stir overnight. The reaction solution turned from a dark red-orange to clear with a white precipitate on overnight stirring. An odor of acetic acid was noted when the vial was opened. The supernatant was transferred via pipette to a clean vial and allowed to evaporate however no crystals formed. The precipitate was washed with cold water and dried under vacuum to yield 92.1 mg of product (0.1973 mmol, 87% yield). $Pd(C_9H_{10}NO_3)_2$ was identified on the basis of the following data: ^1H NMR (400 MHz, Deuterium Oxide) δ 7.11 – 7.04 (m, 2H), 6.83 – 6.73 (m, 2H), 3.82 (dd, J = 7.8, 5.2 Hz, 1H), 3.09 (dd, J = 14.7, 5.2 Hz, 1H), 2.94 (dd, J = 14.7, 7.8 Hz, 1H). HRMS/ESI+ (m/z): [M+H]+ calcd for $Pd(C_9H_{10}NO_3)_2$, 467.0429; found, 467.0448.

4.8.10 Synthesis of bis(asparaginato)palladium(II) (10)

A four dram vial was charged with 0.0259 grams of palladium(II) acetate (1.15×10^{-4} mol) and 2.5 mL of 2:1 (v/v) acetone:water. The mixture was stirred until completely dissolved. To this was added 0.0335 grams of asparagine (2.54×10^{-4} mol, 2.2 equivalents) and left to stir overnight. The reaction solution turned from a dark red-orange to clear with an off-white precipitate on overnight stirring. An odor of acetic acid was noted when the vial was opened. The supernatant was transferred via pipette to a clean vial and allowed to evaporate however no crystals formed. The precipitate was washed with cold water and dried under vacuum to yield 39.7 mg of product (0.1077 mmol, 93% yield). $Pd(C_4H_7N_2O_3)_2$ was identified on the basis of the following data: ^1H NMR (400 MHz, Deuterium Oxide) δ 3.93 – 3.79 (m, 1H), 2.88 – 2.63 (m, 2H).

HRMS/ESI+ (m/z): [M+H]+ calcd for Pd(C$_4$H$_7$N$_2$O$_3$)$_2$, 369.0021; found, 369.0050. Anal. Calcd. for Pd(C$_4$H$_7$N$_2$O$_3$)$_2$: C, 26.06%; H, 3.83%; N, 15.20%. Found: C, 26.20%; H, 3.72%; N, 15.28%.

4.8.11 Synthesis of bis(glutaminato)palladium(II) (11)

A four dram vial was charged with 0.0218 grams of palladium(II) acetate (9.71x10^{-5} mol) and 2.5 mL of 2:1 (v/v) acetone:water. The mixture was stirred until completely dissolved. To this was added 0.0312 grams of glutamine (2.14x10^{-4} mol, 2.2 equivalents) and left to stir overnight. The reaction solution turned from a dark red-orange to clear with an off-white precipitate on overnight stirring. An odor of acetic acid was noted when the vial was opened. The supernatant was transferred via pipette to a clean vial and allowed to evaporate however no crystals formed. The precipitate was washed with cold water and dried under vacuum to yield 34.7 mg of product (0.0877 mmol, 90% yield). Pd(C$_5$H$_9$N$_2$O$_3$)$_2$ was identified on the basis of the following data: ^{1}H NMR (500 MHz, Deuterium Oxide) δ 3.50 (dt, J = 14.5, 6.5 Hz, 1H), 2.47 (dt, J = 15.3, 8.3, 7.6 Hz, 1H), 2.38 (ddd, J = 15.5, 8.8, 6.4 Hz, 1H), 2.10 (dq, J = 14.6, 7.1, 6.7 Hz, 1H), 1.94 (dq, J = 15.0, 7.4 Hz, 1H). HRMS/ESI+ (m/z): [M+Na]+ calcd for Pd(C$_5$H$_9$N$_2$O$_3$)$_2$, 419.0153; found, 419.0193. Anal. Calcd. for Pd(C$_5$H$_9$N$_2$O$_3$)$_2$: C, 30.28%; H, 4.57%; N, 14.12%. Found: C, 30.55%; H, 4.55%; N, 14.27%.

4.8.12 Synthesis of bis(cysteinato)palladium(II) (12)

A four dram vial was charged with 0.0466 grams of palladium(II) acetate (2.08x10^{-4} mol) and 2.5 mL of 2:1 (v/v) acetone:water. The mixture was stirred until completely dissolved. To this was added 0.0553 grams of cysteine (4.57x10^{-4} mol, 2.2 equivalents) and left to stir overnight.

Reaction solution turned from a dark red-orange to a yellow-red suspension. An odor of acetic acid was noted when the vial was opened. HRMS/ESI+ of the supernatant shows masses of 573.8426, 798.7509, and 1024.6613 amu. No further characterization was possible.

4.8.13 Synthesis of bis(cystinato)palladium(II) (13)

A four dram vial was charged with 0.0349 grams of palladium(II) acetate (1.55×10^{-4} mol) and 3.0 mL of 2:1 (v/v) acetone:water. The mixture was stirred until completely dissolved. To this was added 0.0822 grams of cystine (3.42×10^{-4} mol, 2.2 equivalents) and left to stir overnight. Reaction solution turned from a dark red-orange to a rust-red suspension. An odor of acetic acid was noted when the vial was opened. HRMS/ESI+ of the supernatant was inconclusive for Pd(II) species. No further characterization was possible.

4.8.14 Synthesis of bis(methioninato)palladium(II) (14)

A four dram vial was charged with 0.0203 grams of palladium(II) acetate (9.04×10^{-5} mol) and 2.5 mL of 2:1 (v/v) acetone:water. The mixture was stirred until completely dissolved. To this was added 0.0297 grams of methionine (1.99×10^{-4} mol, 2.2 equivalents) and left to stir overnight. Reaction solution turned from a dark red-orange to a very pale yellow with a rust-red precipitate. An odor of acetic acid was noted when the vial was opened. HRMS/ESI+ (m/z): [M+H]+ calcd for $Pd(C_5H_{10}NO_2S)_2$, 402.9972; found, 402.9998. No further characterization was possible.

4.8.15 Synthesis of bis(serinato)palladium(II) (15)

A four dram vial was charged with 0.1063 grams of palladium(II) acetate (4.73×10^{-4} mol) and 3.0 mL of 50/50 (v/v) acetone:water. The mixture was stirred until completely dissolved. To this

was added 0.1095 grams of serine (1.04×10^{-3} mol, 2.2 equivalents) and left to stir overnight. Reaction solution turned from a dark red-orange to a clear yellow with yellow precipitate on overnight stirring. An odor of acetic acid was noted when the vial was opened. The supernatant was transferred via pipette to a clean vial and allowed to evaporate to give clear yellow prisms which were used for X-ray diffraction. The remaining precipitate was washed with cold water and dried under vacuum. The combined yield of crystals and precipitate was 144.9 mg of product (0.4606 mmol, 97% yield). $Pd(C_3H_6NO_3)_2$ was identified on the basis of the following data: ^{1}H NMR (400 MHz, Deuterium Oxide) δ 3.77 (d, J = 5.3 Hz, 1H), 3.74 (d, J = 5.3 Hz, 1H), 3.65 (d, J = 3.7 Hz, 1H), 3.62 (d, J = 3.7 Hz, 1H), 3.57 (t, J = 4.9 Hz, 1H), 3.53 (t, J = 4.1 Hz, 1H). HRMS/ESI+ (m/z): [M+H]+ calcd for $Pd(C_3H_6NO_3)_2$, 314.9803; found, 314.9818.

4.8.16 Synthesis of bis(threoninato)palladium(II) (16)

A four dram vial was charged with 0.0236 grams of palladium(II) acetate (1.05×10^{-4} mol) and 3.0 mL of 50/50 (v/v) acetone:water. The mixture was stirred until completely dissolved. To this was added 0.0275 grams of threonine (2.31×10^{-3} mol, 2.2 equivalents) and left to stir overnight. Reaction solution turned from a dark red-orange to a clear yellow with yellow precipitate on overnight stirring. An odor of acetic acid was noted when the vial was opened. The supernatant was transferred via pipette to a clean vial and allowed to evaporate to give clear yellow prisms which were used for X-ray diffraction. The remaining precipitate was washed with cold water and dried under vacuum. The combined yield of crystals and precipitate was 35.0 mg of product (0.1021 mmol, 97% yield). $Pd(C_4H_8NO_3)_2$ was identified on the basis of the following data: ^{1}H NMR (400 MHz, Deuterium Oxide) δ 4.11 – 4.03 (m, 1H), 3.41 (dd, J = 4.9, 1.9 Hz, 1H), 1.14

(dd, J = 6.6, 1.9 Hz, 3H). HRMS/ESI+ (m/z): [M+H]+ calcd for Pd(C$_4$H$_8$NO$_3$)$_2$, 343.0116; found, 343.0152.

4.8.17 Synthesis of bis(aspartic acid)palladium(II) (17)

A four dram vial was charged with 0.1233 grams of palladium(II) acetate (5.49x10^{-4} mol) and 3.0 mL of 50/50 (v/v) acetone:water. The mixture was stirred until completely dissolved. To this was added 0.1608 grams of aspartic acid (1.21x10^{-3} mol, 2.2 equivalents) and left to stir overnight. Reaction solution turned from a dark red-orange to a clear yellow with yellow precipitate on overnight stirring. An odor of acetic acid was noted when the vial was opened. The supernatant was transferred via pipette to a clean vial and allowed to evaporate to give clear yellow prisms which were used for X-ray diffraction. The remaining precipitate was washed with cold water and dried under vacuum. The combined yield of crystals and precipitate was 192.4 mg of product (0.5191 mmol, 95% yield). Pd(C$_4$H$_6$NO$_4$)$_2$ was identified on the basis of the following data: ^{1}H NMR (400 MHz, Deuterium Oxide) δ 3.94 (dd, J = 7.0, 4.6 Hz, 1H), 2.93 – 2.80 (m, 2H). HRMS/ESI+ (m/z): [M+H]+ calcd for Pd(C$_4$H$_6$NO$_4$)$_2$, 370.9701; found, 370.9739.

4.8.18 Synthesis of bis(glutamic acid)palladium(II) (18)

A four dram vial was charged with 0.0194 grams of palladium(II) acetate (8.64x10^{-5} mol) and 2.0 mL of 2:1 (v/v) acetone:water. The mixture was stirred until completely dissolved. To this was added 0.0280 grams of glutamic acid (1.90x10^{-4} mol, 2.2 equivalents) and left to stir overnight. The reaction solution turned from a dark red-orange to pale yellow with an off-white precipitate on overnight stirring. An odor of acetic acid was noted when the vial was opened. The

supernatant was transferred via pipette to a clean vial and allowed to evaporate however no crystals formed. The precipitate was washed with cold water and dried under vacuum to yield 32.1 mg of product (0.0805 mmol, 93% yield). $Pd(C_5H_8NO_4)_2$ was identified on the basis of the following data: ^1H NMR (400 MHz, DMF-d7) δ 3.47 (s, 1H), 2.96 – 2.88 (m, 2H), 2.79 – 2.70 (m, 2H). HRMS/ESI+ (m/z): [M+H]+ calcd for $Pd(C_5H_8NO_4)_2$, 399.0014; found, 399.0044. Anal. Calcd. for $Pd(C_5H_8NO_4)_2$: C, 30.13%; H, 4.05%; N, 7.03%. Found: C, 30.29%; H, 4.01%; N, 7.12%.

4.8.19 Synthesis of bis(histidinato)palladium(II) (19)

A four dram vial was charged with 0.0188 grams of palladium(II) acetate (8.37×10^{-5} mol) and 2.0 mL of 2:1 (v/v) acetone:water. The mixture was stirred until completely dissolved. To this was added 0.0286 grams of histidine (1.84×10^{-4} mol, 2.2 equivalents) and left to stir overnight. The reaction solution turned from a dark red-orange to pale yellow with an off-white precipitate on overnight stirring. An odor of acetic acid was noted when the vial was opened. The supernatant was transferred via pipette to a clean vial and allowed to evaporate however no crystals formed. The precipitate was washed with cold water and dried under vacuum to yield 32.9 mg of product (0.0793 mmol, 95% yield). $Pd(C_6H_8N_3O_2)_2$ was identified on the basis of the following data: ^1H NMR (500 MHz, Deuterium Oxide) δ 7.77 (d, J = 1.4 Hz, 1H), 7.47 (d, J = 1.3 Hz, 1H), 6.99 (s, 1H), 6.97 (d, J = 1.3 Hz, 1H), 3.45 (t, J = 4.5 Hz, 1H), 3.38 (dd, J = 5.6, 3.7 Hz, 1H), 3.22 – 3.00 (m, 4H). ^{13}C NMR (126 MHz, Deuterium Oxide) δ 175.88, 175.73, 136.81, 135.80, 132.77, 132.72, 114.58, 114.28, 52.33, 52.23, 30.41, 30.30. HRMS/ESI+ (m/z): [M+H]+ calcd for $Pd(C_6H_8N_3O_2)_2$, 415.0341; found, 415.0327. Anal. Calcd. for $Pd(C_6H_8N_3O_2)_2$: C, 33.31%; H, 4.19%; N, 19.42%. Found: C, 33.19%; H, 4.25%; N, 19.21%.

4.8.20 Synthesis of bis(argininato)palladium(II) (20)

A four dram vial was charged with 0.0323 grams of palladium(II) acetate (1.44×10^{-4} mol) and 3.0 mL of acetone. The mixture was stirred until completely dissolved. To this was added 0.0599 grams of arginine (3.44×10^{-4} mol, 2.39 equivalents) and left to stir overnight. The reaction solution turned from a dark red-orange to a clear yellow on overnight stirring. An odor of acetic acid was noted when the vial was opened. The solvent was allowed to evaporate naturally. After all solvent had evaporated, an opaque yellow varnish was observed that was washed with 3x2mL of ice-cold deionized water. Upon drying overnight on a high-vacuum line 59.3 mg (0.1310 mmol, 91% yield) of a clear yellow varnish was obtained. $Pd(C_6H_{13}N_4O_2)_2$ was identified on the basis of the following data: ^{1}H NMR (400 MHz, Deuterium Oxide) δ 3.30 – 2.79 (m, 3H), 1.69 – 1.21 (m, 4H). HRMS/ESI+ (m/z): [M+2H]+2 calcd for $Pd(C_6H_{13}N_4O_2)_2$, 227.0629; found, 227.0646.

4.8.21 Synthesis of bis(lysinato)palladium(II) (21)

A four dram vial was charged with 0.1393 grams of palladium(II) acetate (6.20×10^{-4} mol) and 3.0 mL of 50/50 (v/v) acetone:water. The mixture was stirred until completely dissolved. To this was added 0.1996 grams of lysine (1.37×10^{-3} mol, 2.2 equivalents) and left to stir overnight. Reaction solution turned from a dark red-orange to a clear yellow with a pale yellow precipitate on overnight stirring. An odor of acetic acid was noted when the vial was opened. The supernatant was transferred via pipette to a clean vial and allowed to evaporate however no crystals formed. The precipitate was washed with cold water and dried under vacuum to yield 228.4 mg of product (0.5756 mmol, 93% yield). $Pd(C_6H_{13}N_4O_2)_2$ was identified on the basis of

the following data: ^{1}H NMR (400 MHz, Deuterium Oxide) δ 3.24 (td, J = 7.4, 4.5 Hz, 1H),

2.32 (dtd, J = 4.4, 2.2, 1.0 Hz, 2H), 2.20 (d, J = 1.0 Hz, 2H), 1.31 (d, J = 1.1 Hz, 2H), 1.29 (d, J

= 1.1 Hz, 2H). ^{13}C NMR (101 MHz, D$_2$O) δ 177.77, 109.99, 66.24, 26.64, 22.23, 22.04.

HRMS/ESI+ (m/z): [M+H]+ calcd for Pd(C$_6$H$_{13}$N$_4$O$_2$)$_2$, 397.1062; found, 397.1068.

4.9 REFERENCES

(1)   Sharma, V. S.; Mathur, H. B.; Biswas, A. B. *Indian Journal of Chemistry* **1964**, *2*, 257.
(2)   Farooq, O.; Ahmad, N.; Malik, A. U. *Journal of Electroanalytical Chemistry and Interfacial Electrochemistry* **1973**, *48*, 475.
(3)   Chernova, N. N.; Shakhova, L. P.; Kukushkin, Y. N. *Zhurnal Neorganicheskoi Khimii* **1976**, *21*, 3027.
(4)   Jarzab, T. C.; Hare, C. R.; Langs, D. A. *Crystal Structure Communications* **1973**, *2*, 395.
(5)   Jarzab, T. C.; Hare, C. R.; Langs, D. A. *Crystal Structure Communications* **1973**, *2*, 399.
(6)   Kollmann, J.; Schroeter, C.; Hoyer, E. *Journal fuer Praktische Chemie (Leipzig)* **1975**, *317*, 515.
(7)   Krylova, L. F.; Kovtunova, L. M.; Romanenko, G. V.; Sheludyakova, L. A.; Kurat'eva, N. V. *Russian Journal of Inorganic Chemistry* **2011**, *56*, 52.
(8)   Graham, R. D.; Williams, D. R. *Journal of Inorganic and Nuclear Chemistry* **1979**, *41*, 1245.
(9)   Pneumatikakis, G.; Hadjiliadis, N. *Journal of Inorganic and Nuclear Chemistry* **1979**, *41*, 429.
(10)   Spacu, P.; Ungureanu-Vicol, O. *Analele Universitatii Bucuresti, Seria Stiintele Naturii* **1966**, *15*, 109.
(11)   Spacu, P.; Scherzer, I. *Zeitschrift fuer Anorganische und Allgemeine Chemie* **1962**, *319*, 101.
(12)   Hobart, D. B.; Berg, M. A. G.; Merola, J. S. *Inorganica Chimica Acta* **2014**, *423*, 21.
(13)   Chernova, N. N.; Strukov, V. V.; Avetikyan, G. B.; Chernonozhkin, V. N. *Zhurnal Neorganicheskoi Khimii* **1980**, *25*, 1569.
(14)   Komorita, T.; Hidaka, J.; Shimura, Y. *Bull. Chem. Soc. Jap.* **1971**, *44*, 3353.
(15)   Sabat, M.; Jezowska, M.; Kozlowski, H. *Inorganica Chimica Acta* **1979**, *37*, L511.
(16)   Vagg, R. S. *Acta Crystallogr B* **1979**, *35*, 341.
(17)   Nakayama, Y.; Matsumoto, K.; Ooi, S.; Kuroya, H. *Journal of the Chemical Society, Chemical Communications* **1973**, 170.
(18)   Appleton, T. G. *Coordin Chem Rev* **1997**, *166*, 313.
(19)   Adachi, K.; Watarai, H. *Journal of Materials Chemistry* **2005**, *15*, 4701.
(20)   Konno, T.; Sasaki, C.; Okamoto, K.-i. *Chemistry Letters* **1996**, *25*, 977.
(21)   Braiman, M. S.; Briercheck, D. M.; Kriger, K. M. *The Journal of Physical Chemistry B* **1999**, *103*, 4744.

Chapter 5. Conclusions

5.1 CONCLUSIONS

This body of work represents the first systematic study of the bis-amino acid complexes of palladium(II). The synthesis, structural characterization, and catalytic activity and hydrogen bonding behavior of several new complexes of palladium(II) with amino acid ligands has been successfully undertaken. In most cases, high quality NMR, mass spectral, and microanalytical data have been added to the existing, yet incomplete, literature on these compounds. Additionally, several new X-ray crystal structures of these complexes have been determined that were heretofore not in the crystallographic literature. Several interesting trends have been identified based on the structural factors, catalytic activity, and hydrogen bonding interactions observed in these complexes.

5.1.1   Structural Conclusions

Palladium(II) amino acid chelates form *cis* and *trans* isomers depending on the starting palladium compound used. Alkylation of the coordinated nitrogen atom in palladium(II) bis-chelates leads to the formation of only *trans* isomers. Thus, complexes made with *N*-methylglycine, *N,N*-dimethylglycine, and *N*-methylproline all formed the *trans* isomer. Attempts to prepare the *cis* isomers of the *N*-alkylated glycine complexes from PdCl$_2$, as was done for the non-*N*-alkylated glycine complexes, were unsuccessful.

Compelling evidence of the formation of palladium(II) amino acid aquo complexes has been presented. Carbon-13 NMR spectroscopy is a powerful tool for elucidating the number of ligand environments and has been used to show that multiple aquo species are present in solution.

Improved X-ray crystal structures and NMR data on the *cis* and *trans* bis-glycinate complexes of palladium(II) are reported, as well as confirmation of the previously reported infrared and electronic absorption spectra. Powder X-ray diffraction has been used to verify formation of a single isomer in the crystalline phase for the glycinate and *N*-methylglycinate complexes.

5.1.2   Conclusions on Catalytic Activity

All of the *cis* complexes reported herein were determined to be catalytically active with respect to the oxidative coupling of phenylboronic acids to olefins. *Trans* complexes, with the exception of *trans*-bis(azetidine-2-carboxylato)palladium(II) are not catalytically active. Enantioselectivities were modest with the best example, *cis*-bis(prolinato)palladium(II), yielding an enantiomeric excess of 24%. One unique feature of these catalyst systems are the generation of coupled products not reported for other similar palladium(II) catalyzed systems. Selectivity for these additional products was low, and the concomitant formation of homocoupled products leads to the conclusion that these catalysts lack the chiral ridigity required to achieve high product selectivity and enantioselectivity. This is likely a consequence of aquo-complex formation, whereby the chiral ligand is partially de-coordinated and as such cannot direct the incoming substrates in a highly selective fashion. A second unique feature to these systems was the observation that the coupled products themselves can undergo further oxidative couplings.

The same lack of chiral rigidity responsible for poor selectivity/enantioselectivity has the benefit of not sterically restricting the coupled products from themselves participating in the reaction. This is almost certainly a steric control argument and bears further investigation. Nonetheless, this work represents a sound scientific starting point for the further study and optimization of such systems.

Some trends in product distribution are evident from the data reported here. The best catalyst, *cis*-bis(prolinato)palladium(II) was used to oxidatively couple methyl tiglate with phenylboronic acid, 4-(trifluoromethyl)phenylboronic acid, and 4-(methoxy)phenylboronic acid. A definite steric trend was observed with these substrates, whereby the larger group in the para position correlates with a higher percentage of the R/S product formation. In this series the para group size increases from –H to –CF$_3$ to –OCH$_3$. Conversely, the enantioselectivity decreases with increasing steric size of the para position group, as does the formation of the Z-alkene and homocoupled product (Table 10).

Product	PBA	PBA-CF$_3$	PBA-OCH$_3$
R/S, %	42	71	100
%ee	24	11	6
Z-alkene, %	28	1	0
Biphenyl, %	30	24	0

Table 10. Substrate steric trends in the product distributions of the cis-bis(prolinato)palladium(II) catalyzed coupling of methyl tiglate with various substituted phenylboronic acids.

Within the series of catalysts with fused ring R-groups, no definite trends were observed in terms of product formation when the substrates were held constant. Steric bulk, substituent electronegativity, and ring strain all were considered and have no obvious effect on product distribution ratios. R/S product yields vary from 28-79% with enantioselectivities of 1-24%. Z-

185

alkene and biaryl formation are similarly non-specific. Temperature did have a correlatable trend with respect to enantioselectivity, with lower reaction temperatures resulting in increased enantioselectivity.

The non-cyclic palladium(II) amino acid catalysts showed the same non-specificity in terms of product distribution ratios. The isoleucine, phenylalanine, serine, lysine and aspartic acid complexes were tested for catalytic oxidative coupling. R/S yields ranged from 22-58%. Enantioselectivities were uniformly low at 2-5%. Z-alkene yields were consistently in the 12-19% range. Comparing the fused ring systems to the acyclic systems, it is apparent that enantioselectivities are, on average, higher for the fused ring systems.

Finally, it was clearly demonstrated that both activated and non-activated olefins are capable of being coupled by the best of the catalysts employed, *cis*-bis(prolinato)palladium(II).

5.1.3 Conclusions on Hydrogen Bonding Interactions

The hydrogen bonding motifs observed in these palladium(II) amino acid complexes are extensive, various, and in some cases fascinating. These complexes adopt varied *cis/trans* geometries, with different degrees of internal symmetry. There are some trends that can be discerned from an analysis of the extended lattices. The fully *N*-alkylated complexes seen for ligands like *N,N*-dimethylglycine and *N*-methylproline incorporate water molecules into the lattice in each instance. Lacking amine protons, these complexes cannot form hydrogen bonded networks as they contain no hydrogen bond donor. The lattice water molecules act as bridging hydrogen bond donors between complex molecules in the lattice.

All of the other complexes for which crystal structures were able to be obtained have at least one amine proton that acts as an intermolecular hydrogen bond donor. Water molecules are

also incorporated into some of these lattices, and again act as bridging hydrogen bond donors. The incorporation of water into the lattice in these cases appears to be solely a function of minimizing packing forces as the crystals form. There appears to be no discernable pattern that governs water incorporation into the lattice. *Cis/trans* geometry has no correlation to lattice water incorporation. There is a qualitative observation that complexes with asymmetric steric bulk tend to incorporate water more than those that do not. The *cis* and *trans* bis(glycinato) complexes offer an example of this phenomena.
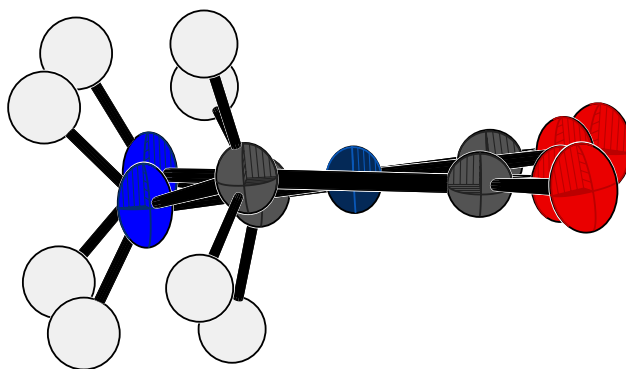
Figure 108. *Cis*-bis(glycinato)palladium(II) viewed edge-on to the chelate plane.
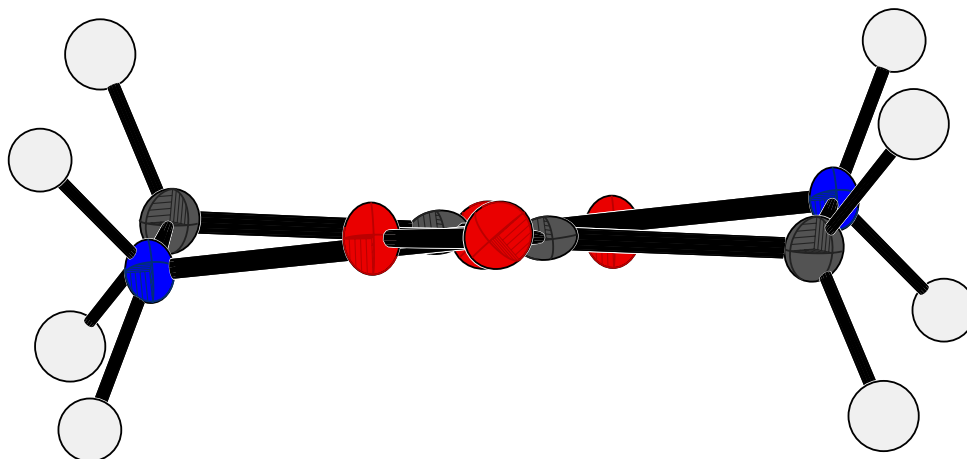
Figure 109. *Trans*-bis(glycinato)palladium(II) viewed edge-on to the chelate plane.

Note the asymmetric steric bulk in the *cis* complex (Figure 108) versus the more balanced case for the *trans* isomer (Figure 109). The *cis* complex incorporates water in the lattice whereas the *trans* does not. This is a pattern that is seen frequently with these complexes.

A final trend that is observed in these complexes is a lengthening of the Pd-N bonds as the amine nitrogen is alkylated. The greater electron donating power of the methyl group versus a hydrogen atom is postulated to be responsible for this trend. There is a simultaneous shortening of the Pd-O bonds as the more electronegative oxygen atoms draw this extra electron density onto itself.

Appendix A

Data for Selected Compounds

Compound 1

trans-bis(glycinato)palladium(II)
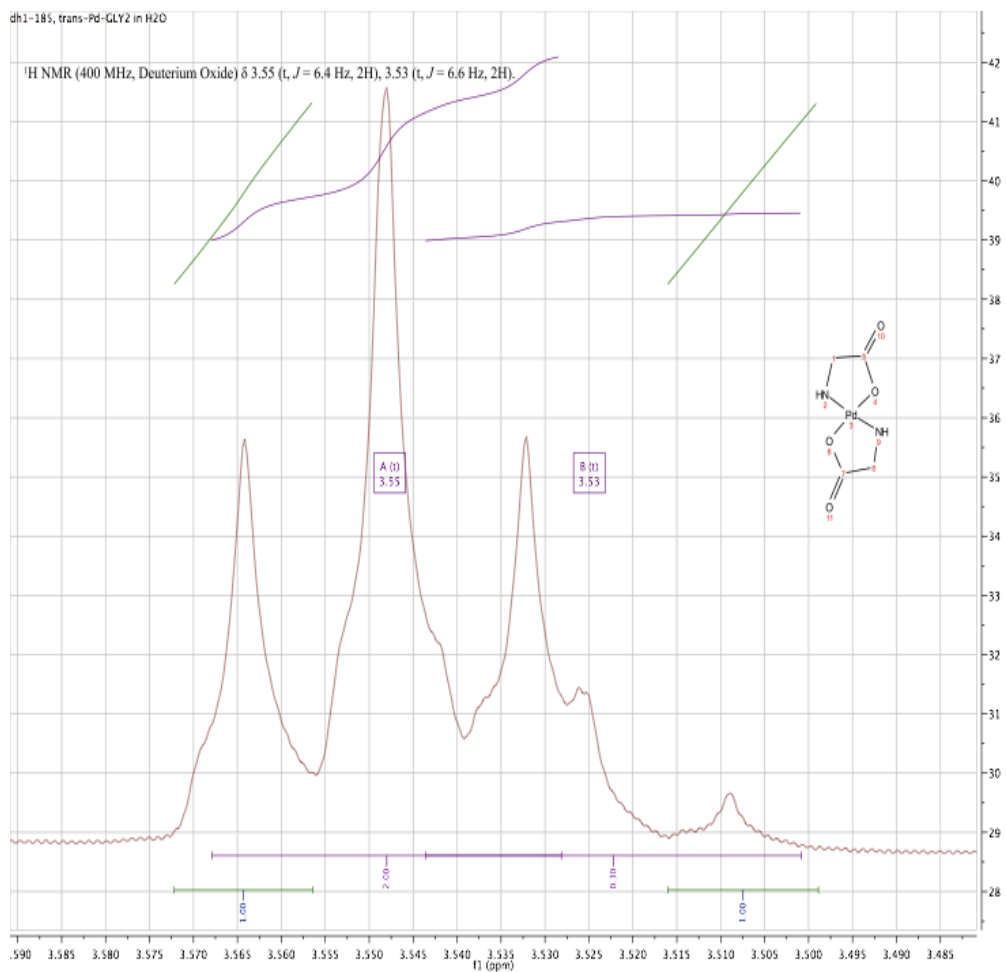
^{1}H NMR spectrum of trans-bis(glycinato)palladium(II)

^{13}C NMR spectrum of trans-bis(glycinato)palladium(II)

NS-DH-15N-Gly2-trans-020614/5
HSQCETF3GPSI

^{15}N NMR (61 MHz, H$_2$O+D2O) δ -34.89, -26.52

^{1}H NMR (600 MHz, H$_2$O+D2O) δ 3.48, 3.43.
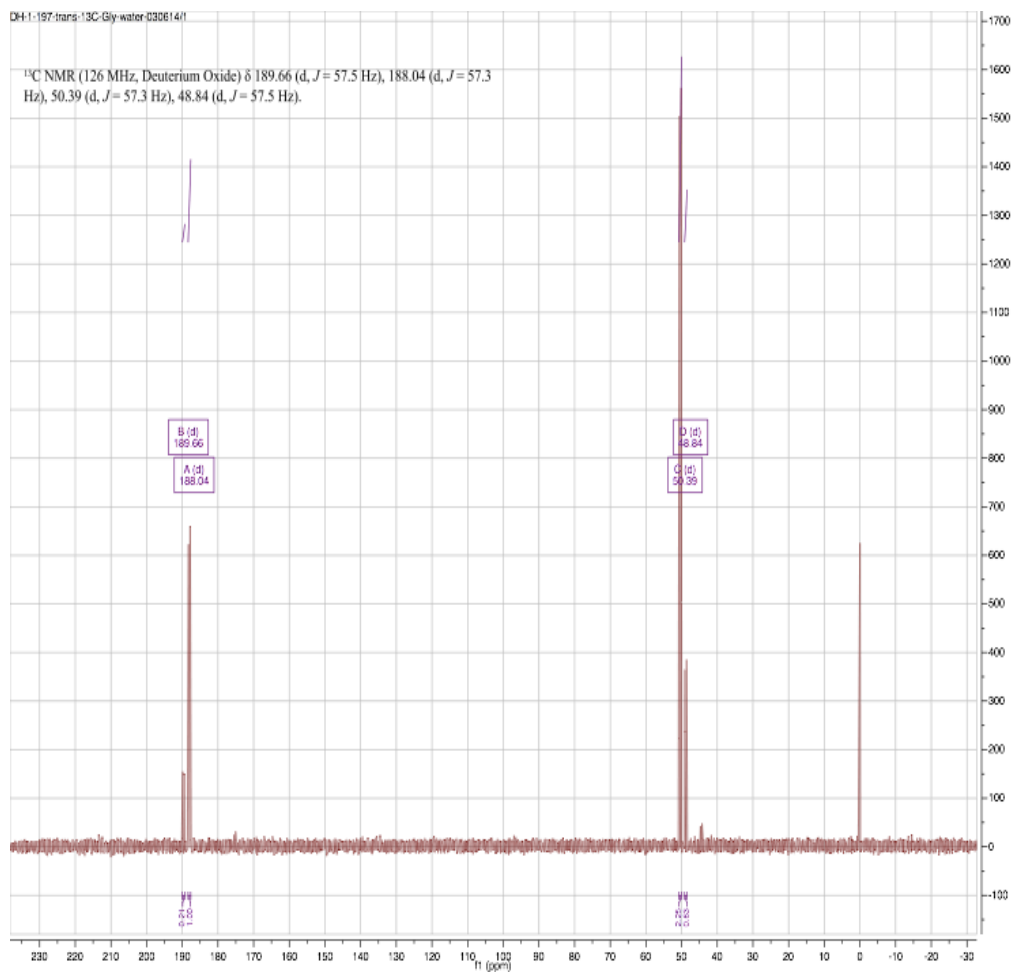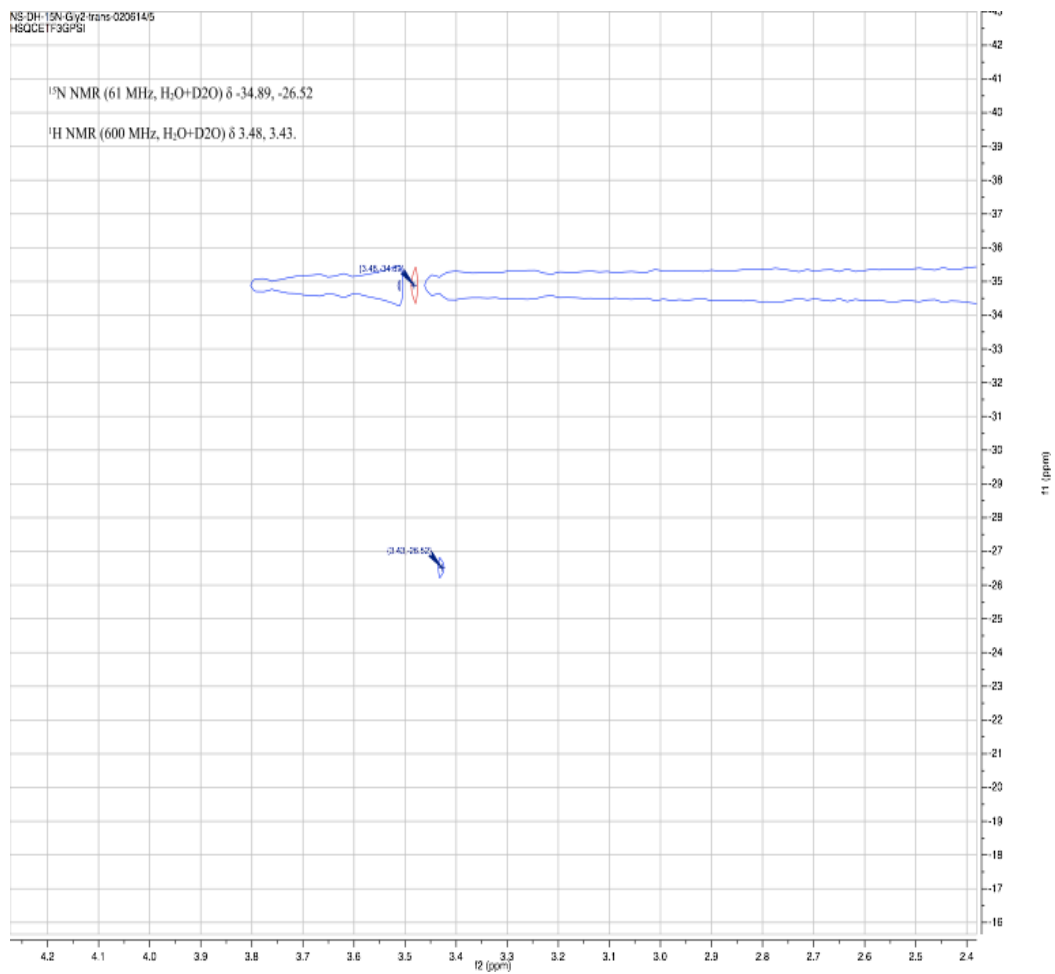
^{1}H-^{15}N HSQC NMR spectrum of trans-bis(glycinato)palladium(II)

Sample Name	dh1_101	Position	P1-A3	Instrument Name	Instrument 1	User Name	
Inj Vol	-1	InjPosition		SampleType	Sample	IRM Calibration Status	Success
Data Filename	dh1_101_esi_u.d	ACQ Method	MMI_esi_union.m	Comment	441382	Acquired Time	7/17/2013 5:19:57 PM

HRMS of trans-bis(glycinato)palladium(II)

Atlantic Microlab, Inc.

Sample No. dh1-137a

6180 Atlantic Blvd. Suite M
Norcross, GA 30071
www.atlanticmicrolab.com

Professor/Supervisor: Merola
PO# / CC# P2343956

Company/School Virginia Tech
Dept. Chemistry
Address Hahn Hall North
City, State, Zip Blacksburg, VA 24061
Name Dave Hobart   Date 01/08/2013
Phone (540) 231-4713

Element	Theory	Found		
C	18.87	21.02	20.90	
H	3.17	3.57	3.60	
N	11.01	11.83	11.73	
		NO CHARGE FOR DUPLICATES		

Single ☒   Duplicate ☐

Elements Present: C, H, N, O, Pd

Analyze for: C, H, N

Hygroscopic ☒   Explosive ☐
M.P. _____ B.P. _____

To be dried: Yes ☒ No ☐
Temp. RT   Vac. best   Time 1 hr

Rush Service ☐ Rush service guarantees analyses will be completed and results available by 5 PM EST on the day the sample is received by 11 AM.

Include Email Address or FAX # Below

dhobart@vt.edu

Date Received JAN 0 9 2013   Date Completed JAN 1 0 2013

Remarks: trans-bis-glycinato Pd(II)

Microanalysis of trans-bis(glycinato)palladium(II)
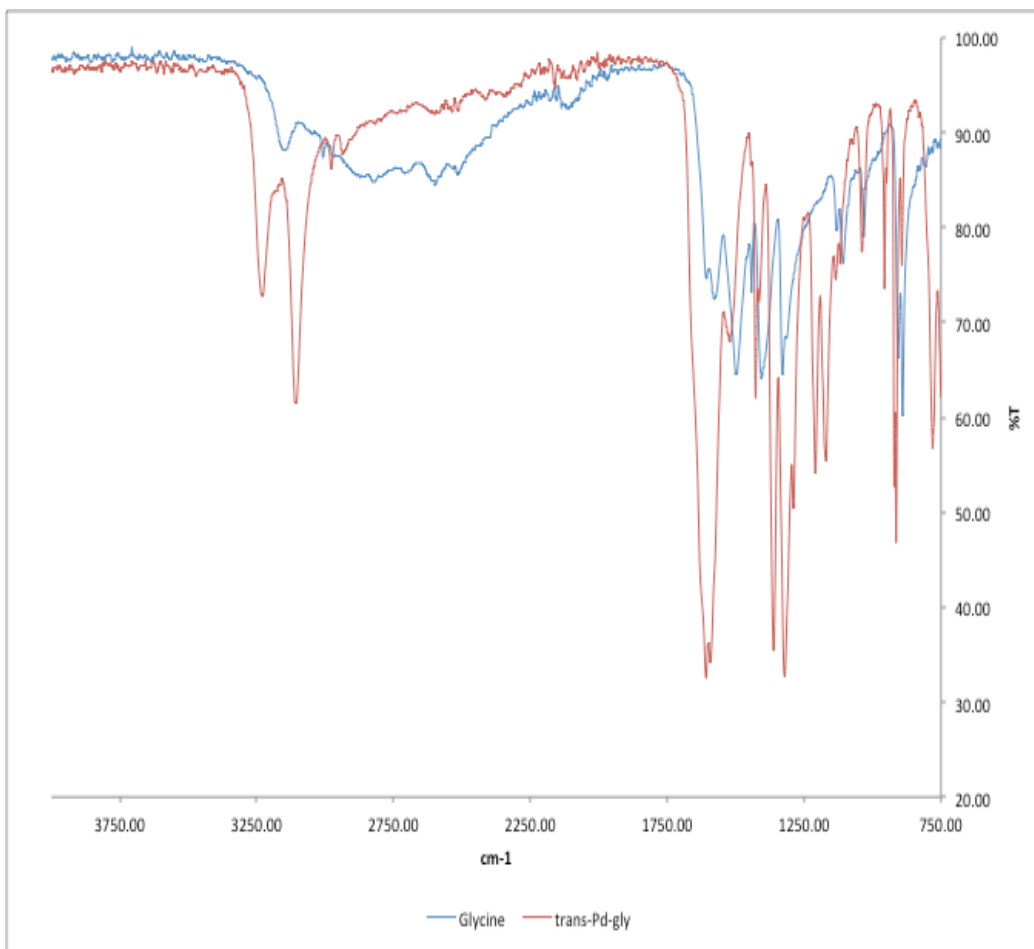
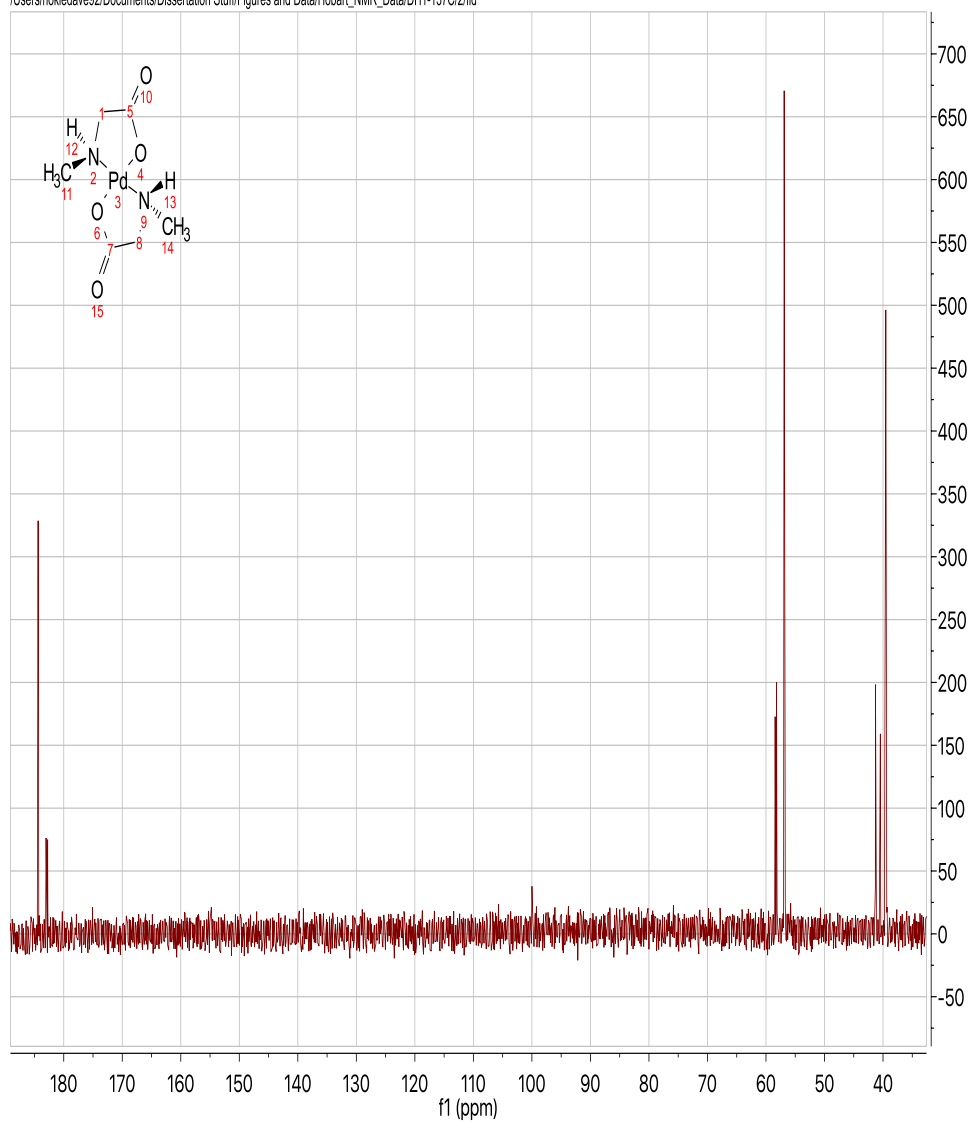FTIR overlay of trans-bis(glycinato)palladium(II) and glycine
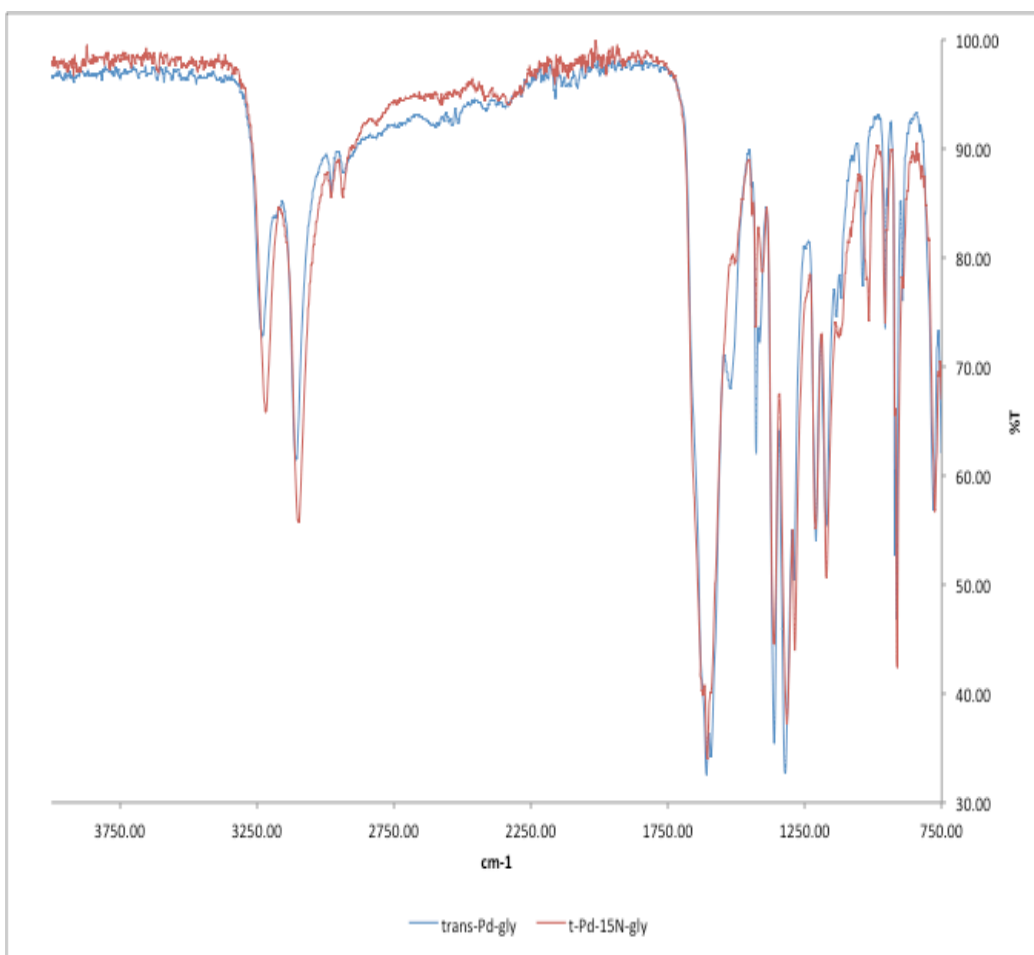
FTIR overlay of trans-bis(glycinato)palladium(II) and
trans-bis(^{15}N-glycinato)palladium(II)

Compound 2

trans-bis(N,N-dimethylglycinato)palladium(II)

¹H NMR spectrum of trans-bis(N,N-dimethylglycinato)palladium(II)

HRMS of trans-bis(N,N-dimethylglycinato)palladium(II)

Atlantic Microlab, Inc.

Sample No. dh1-137c

6180 Atlantic Blvd. Suite M
Norcross, GA 30071
www.atlanticmicrolab.com

Professor/Supervisor: Merola

PO# / CC# P2343956

Company/School Virginia Tech

Dept. Chemistry

Address Hahn Hall North

City, State, Zip Blacksburg, VA 24061

Name Dave Hobart   Date 01/08/2013

Phone (540) 231-4713

Element	Theory	Found	
C	30.93	31.05	
H	5.19	5.23	
N	9.02	9.03	

Single ☒   Duplicate ☐

Elements Present: C, H, N, O, Pd

Analyze for: C, H, N

Hygroscopic ☒   Explosive ☐
M.P. _____ B.P. _____

To be dried: Yes ☒ No ☐
Temp. RT   Vac. best   Time 1 hr

Rush Service ☐   Rush service guarantees analyses will be completed and results available by 5 PM EST on the day the sample is received by 11 AM.

Include Email Address or FAX # Below

dhobart@vt.edu

Date Received JAN 0 9 2013   Date Completed JAN 1 0 2013
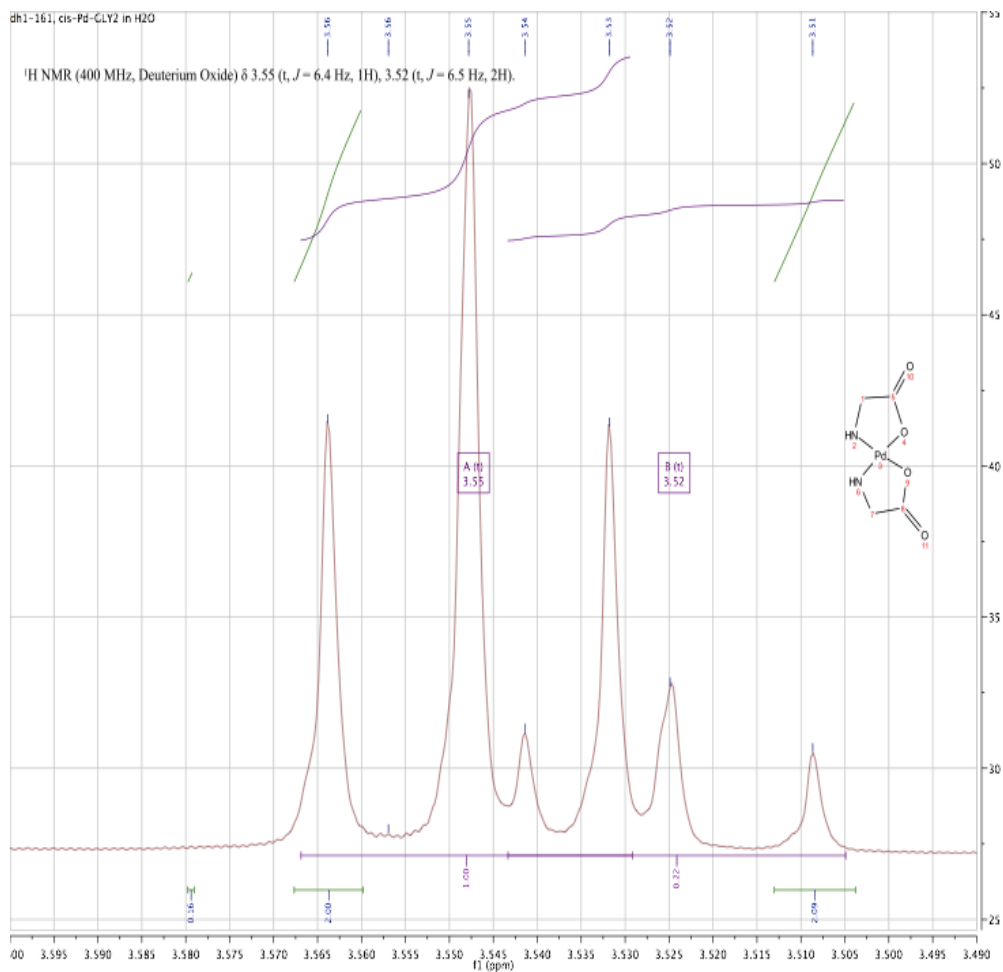
Remarks: trans-bis-N,N-dimethylglycinato Pd(II)

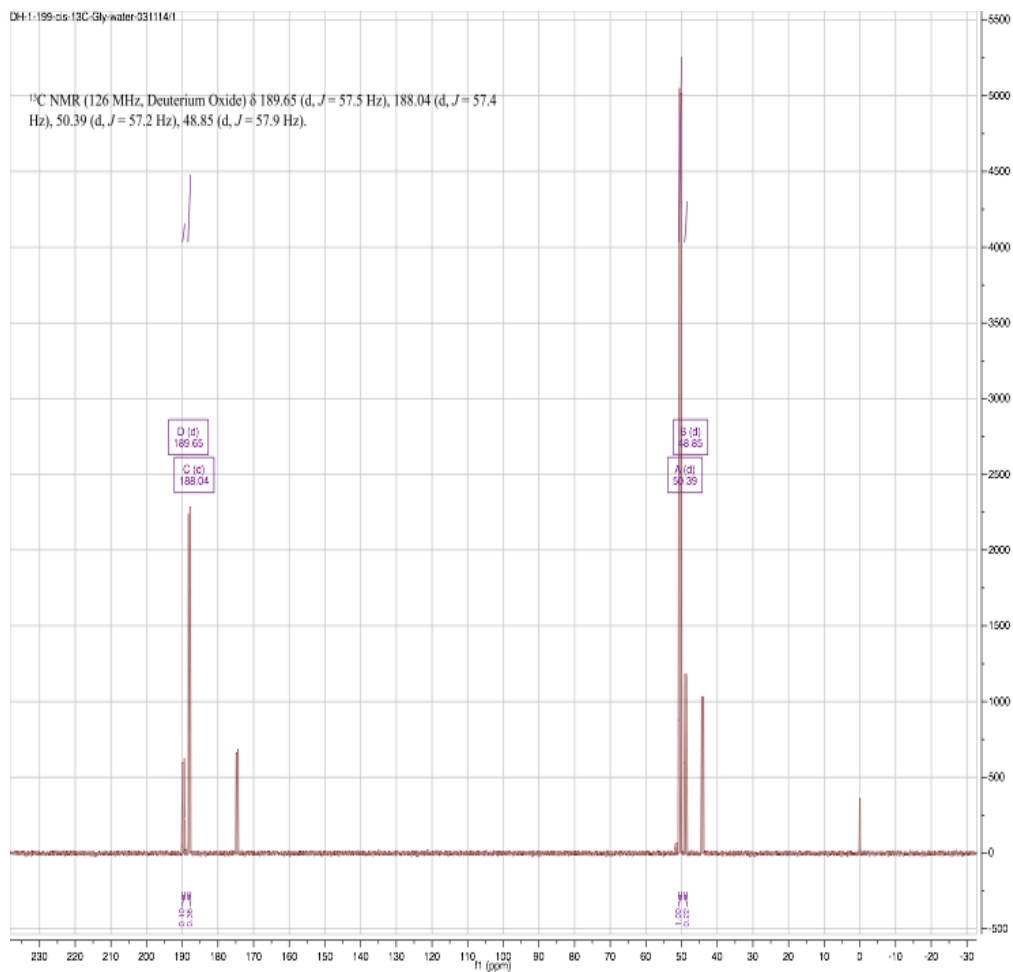Microanalysis of trans-bis(N,N-dimethylglycinato)palladium(II)
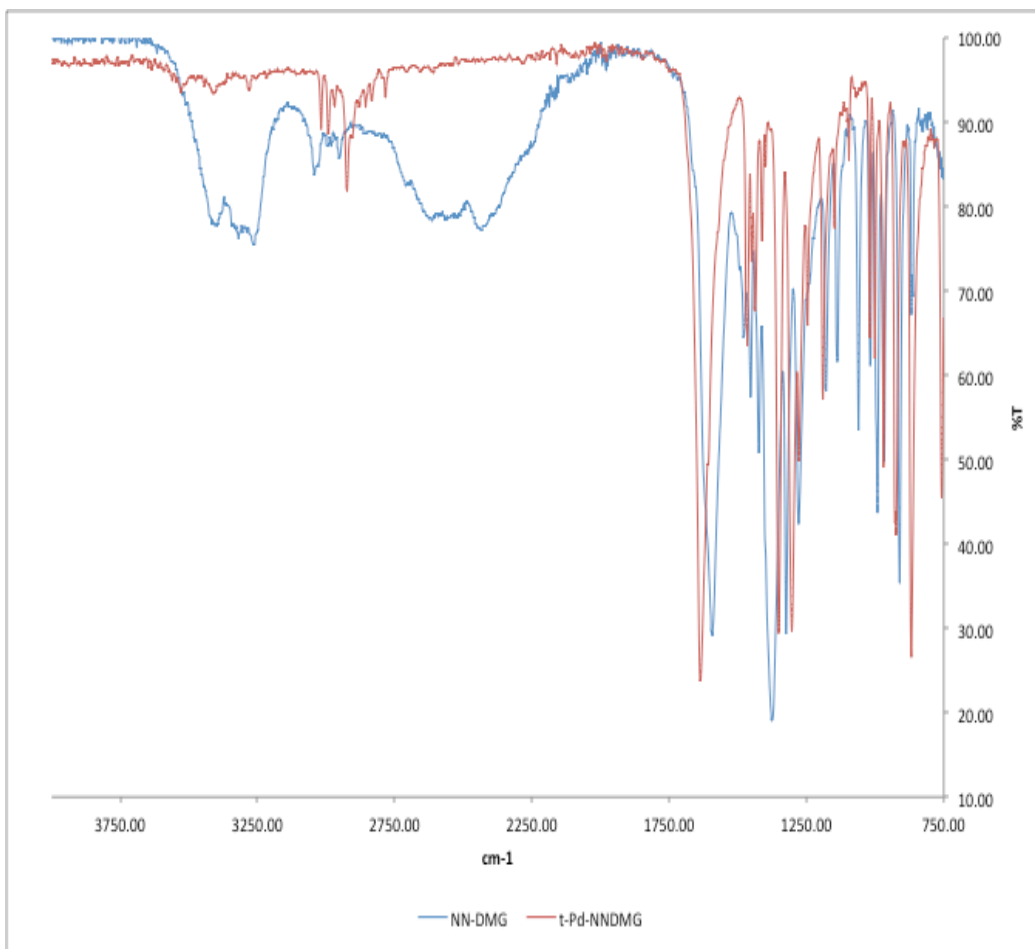
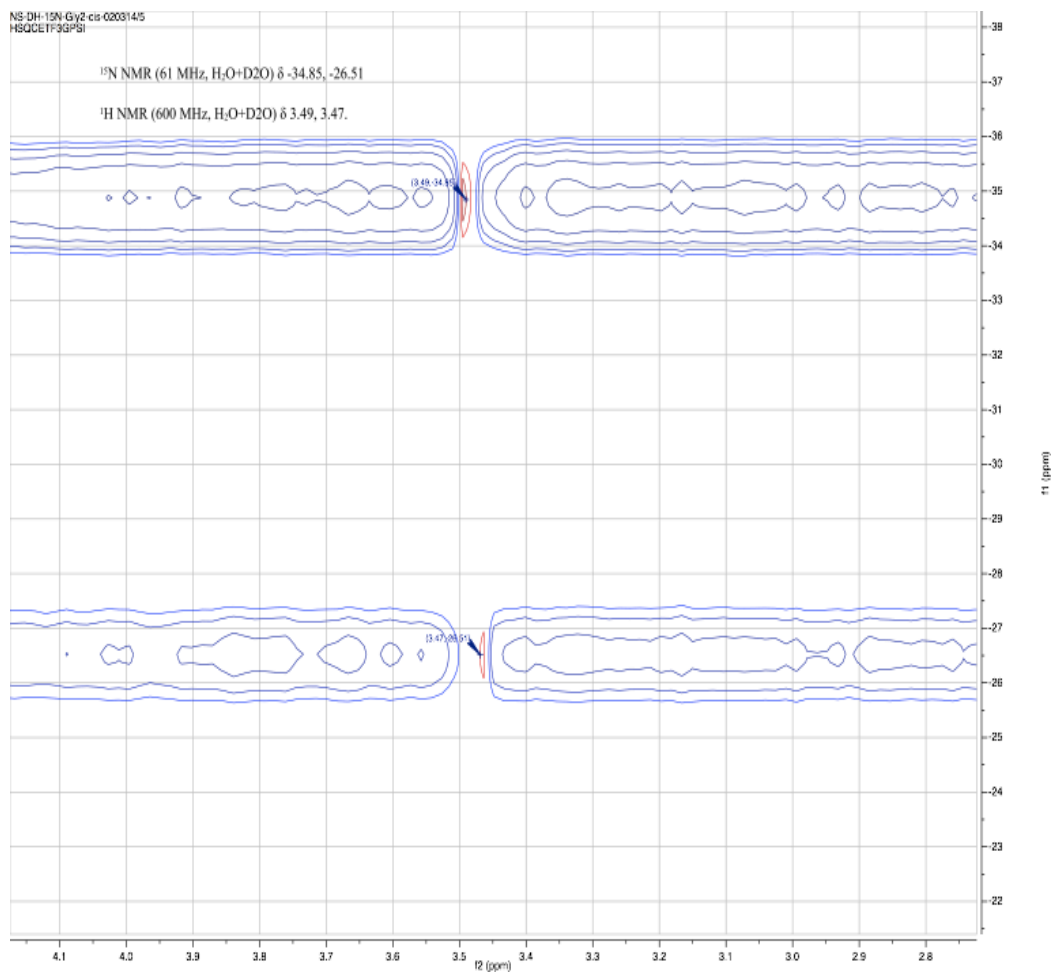FTIR overlay of trans-bis(N,N-dimethylglycinato)palladium(II) and glycine

Compound 3

trans-bis(N-methylglycinato)palladium(II)
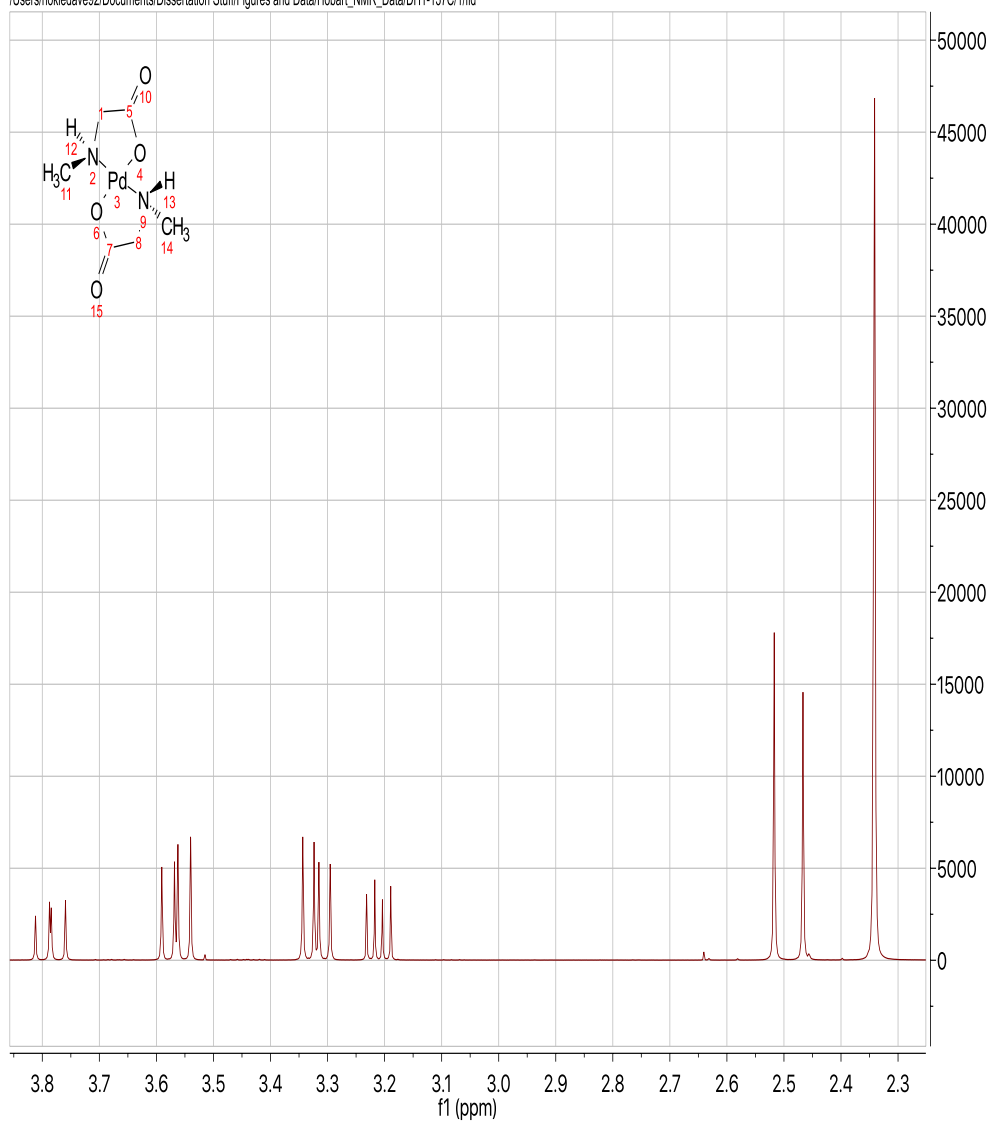
^{1}H NMR spectrum of trans-bis(N-methylglycinato)palladium(II)

^{13}C NMR spectrum of trans-bis(N-methylglycinato)palladium(II)
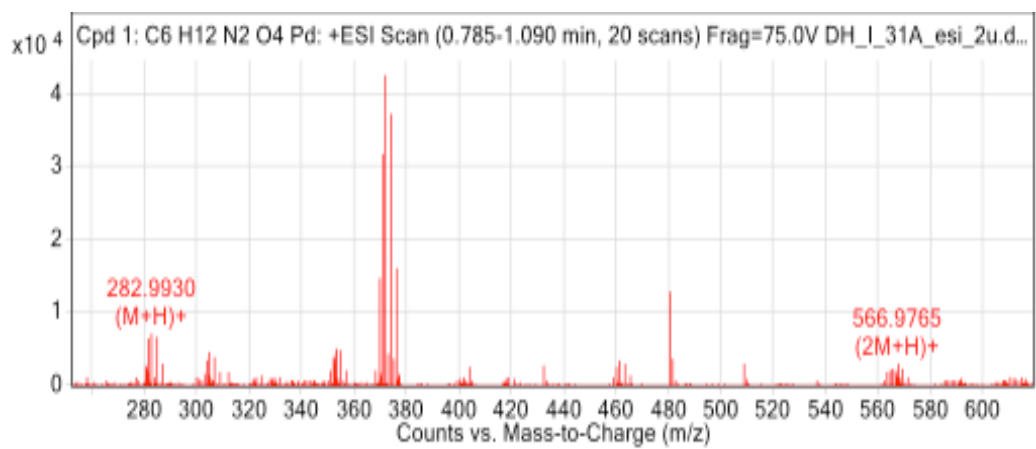
HRMS of trans-bis(N-methylglycinato)palladium(II)

Atlantic Microlab, Inc.

Sample No. dh1-137b

6180 Atlantic Blvd. Suite M
Norcross, GA 30071
www.atlanticmicrolab.com

Company/School Virginia Tech
Dept. Chemistry
Address Hahn Hall North
City, State, Zip Blacksburg, VA 24061

Professor/Supervisor: Merola
PO# / CC# P2343956

Name Dave Hobart   Date 01/08/2013
Phone (540) 231-4713

Element	Theory	Found	
C	25.50	25.56	
H	4.28	4.34	
N	9.91	9.91	

Single ☒   Duplicate ☐

Elements Present: C, H, N, O, Pd

Analyze for: C, H, N

Hygroscopic ☒   Explosive ☐
M.P. _____   B.P. _____

To be dried: Yes ☒ No ☐
Temp. RT   Vac. best Time 1 hr

Rush Service ☐   Rush service guarantees analyses will be completed and results available by 5 PM EST on the day the sample is received by 11 AM.

Include Email Address or FAX # Below

dhobart@vt.edu

Date Received ~~JAN 0 9 2013~~   Date Completed JAN 10 2013

Remarks: trans-bis-N-methylglycinato Pd(II)

Microanalysis of trans-bis(N-methylglycinato)palladium(II)
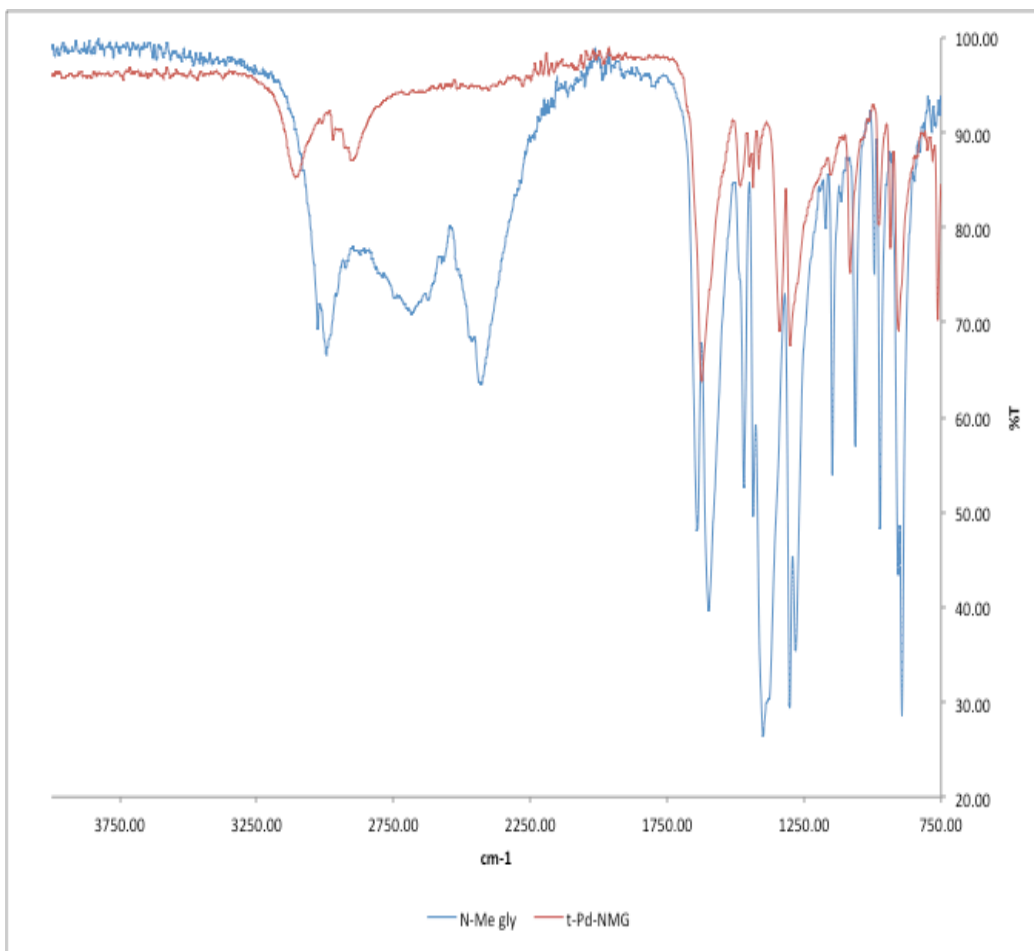
FTIR overlay of trans-bis(N-methylglycinato)palladium(II) and N-methylglycine

Compound 4

cis-bis(glycinato)palladium(II)

dh1-161, cis-Pd-GLY2 in H2O

^{1}H NMR (400 MHz, Deuterium Oxide) δ 3.55 (t, J = 6.4 Hz, 1H), 3.52 (t, J = 6.5 Hz, 2H).

^{1}H NMR spectrum of cis-bis(glycinato)palladium(II)

DH-1-199-cis-13C-Gly-water-031114/1

¹³C NMR (126 MHz, Deuterium Oxide) δ 189.65 (d, *J* = 57.5 Hz), 188.04 (d, *J* = 57.4 Hz), 50.39 (d, *J* = 57.2 Hz), 48.85 (d, *J* = 57.9 Hz).

¹³C NMR spectrum of cis-bis(glycinato)palladium(II)

^{15}N NMR (61 MHz, H$_2$O+D2O) δ -34.85, -26.51

^{1}H NMR (600 MHz, H$_2$O+D2O) δ 3.49, 3.47.

^{1}H-^{15}N HSQC NMR spectrum of cis-bis(glycinato)palladium(II)

Cpd 1: C4 H8 [15N]2 O4 [106Pd]: +ESI Scan (0.0866-0.2791 min, 13 scans) Frag=125.0V dh1_165_esi_u.d Subt...

HRMS of cis-bis(glycinato)palladium(II)

Atlantic Microlab, Inc.

Sample No. dh1-161

6180 Atlantic Blvd. Suite M
Norcross, GA 30071
www.atlanticmicrolab.com

Professor/Supervisor: Merola

PO# / CC# P2343956

Company/School Virginia Tech

Dept. Chemistry

Address Hahn Hall North

City, State, Zip Blacksburg, VA 24061

Name Dave Hobart   Date 01/08/2013

Phone (540) 231-4713

Element	Theory	Found	
C	18.87	19.09	
H	3.17	3.19	
N	11.01	11.06	

Single ☒   Duplicate ☐

Elements Present: C, H, N, O, Pd

Analyze for: C, H, N

Hygroscopic ☒   Explosive ☐
M.P. _____ B.P. _____

To be dried: Yes ☒ No ☐
Temp. RT ___ Vac. best __ Time 1 hr

Rush Service ☐ Rush service guarantees analyses will be completed and results available by 5 PM EST on the day the sample is received by 11 AM.

Include Email Address or FAX # Below

dhobart@vt.edu

Date Received JAN 0 9 2013

Date Completed JAN 1 0 2013

Remarks: cis-bis-glycinato Pd(II)

Microanalysis of cis-bis(glycinato)palladium(II)
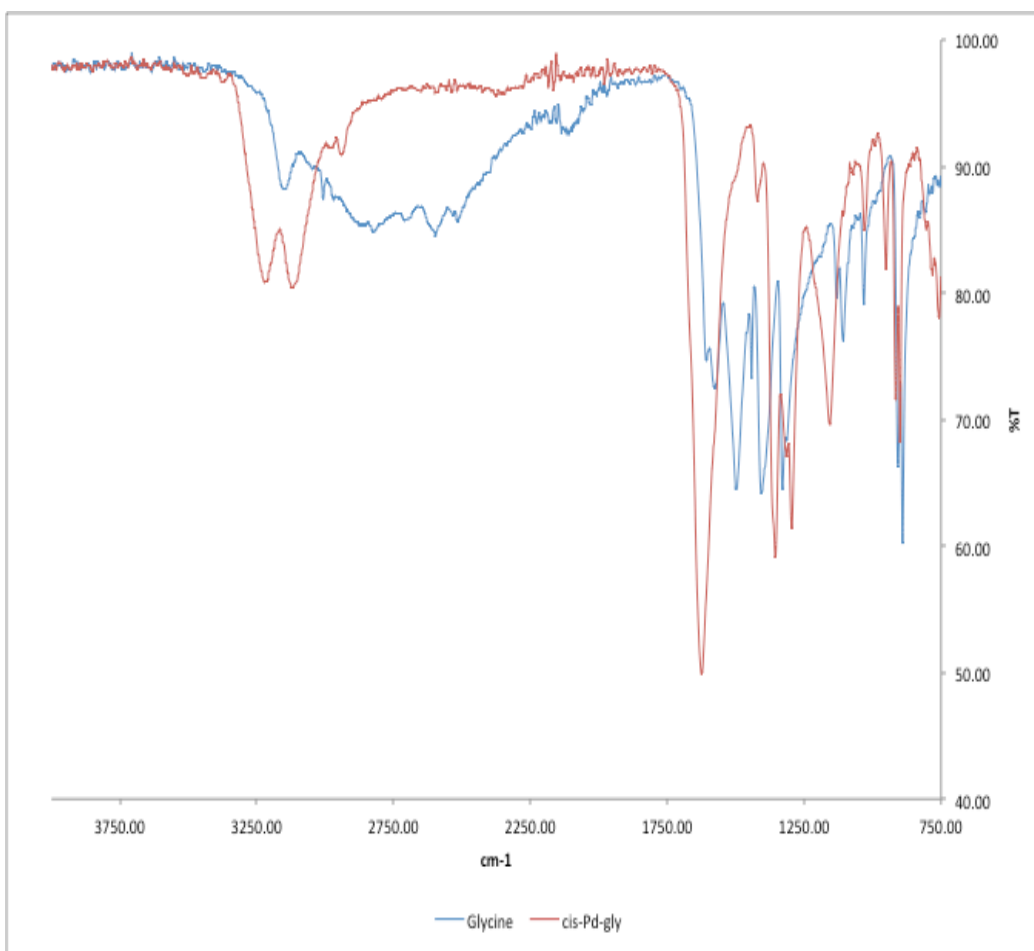
FTIR overlay of cis-bis(glycinato)palladium(II) and glycine

FTIR overlay of cis-bis(glycinato)palladium(II) and
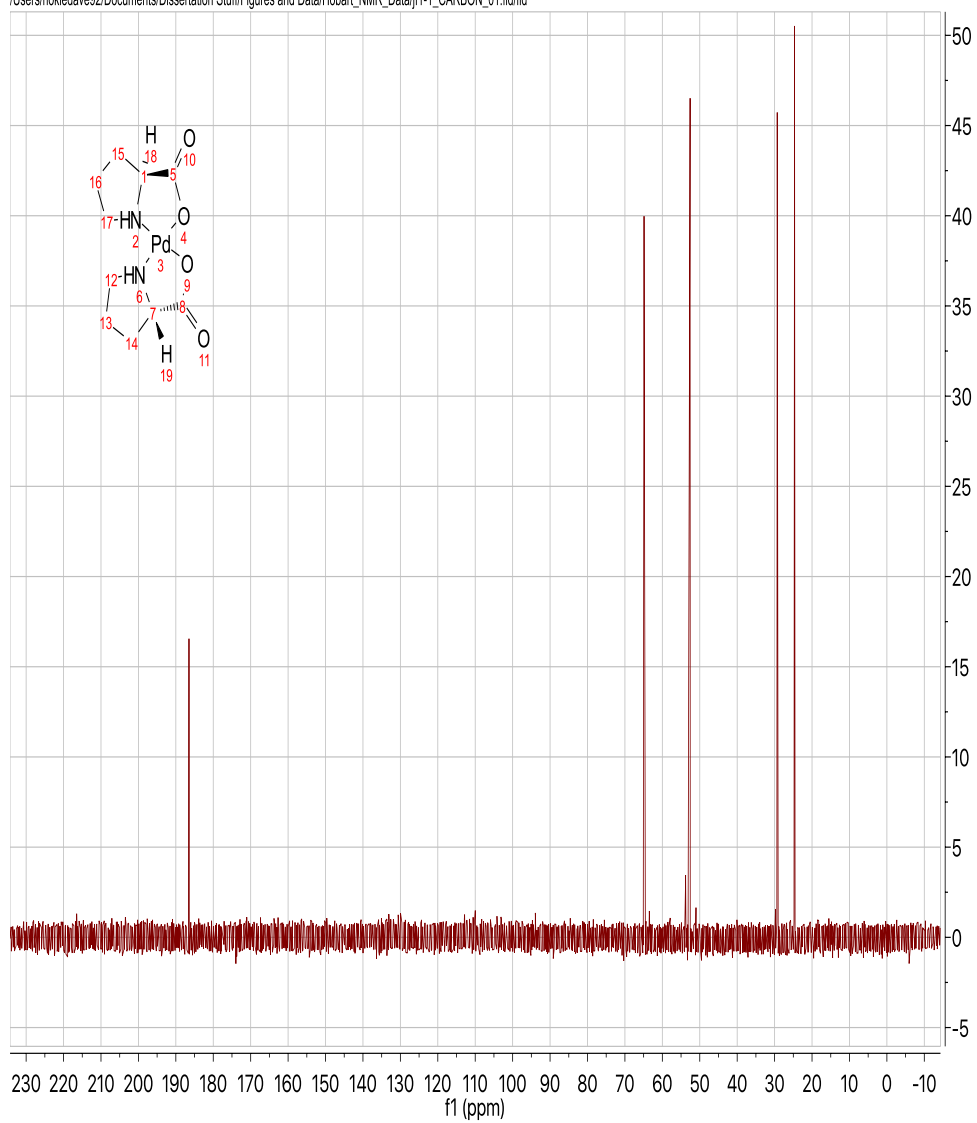cis-bis(^{15}N-glycinato)palladium(II)
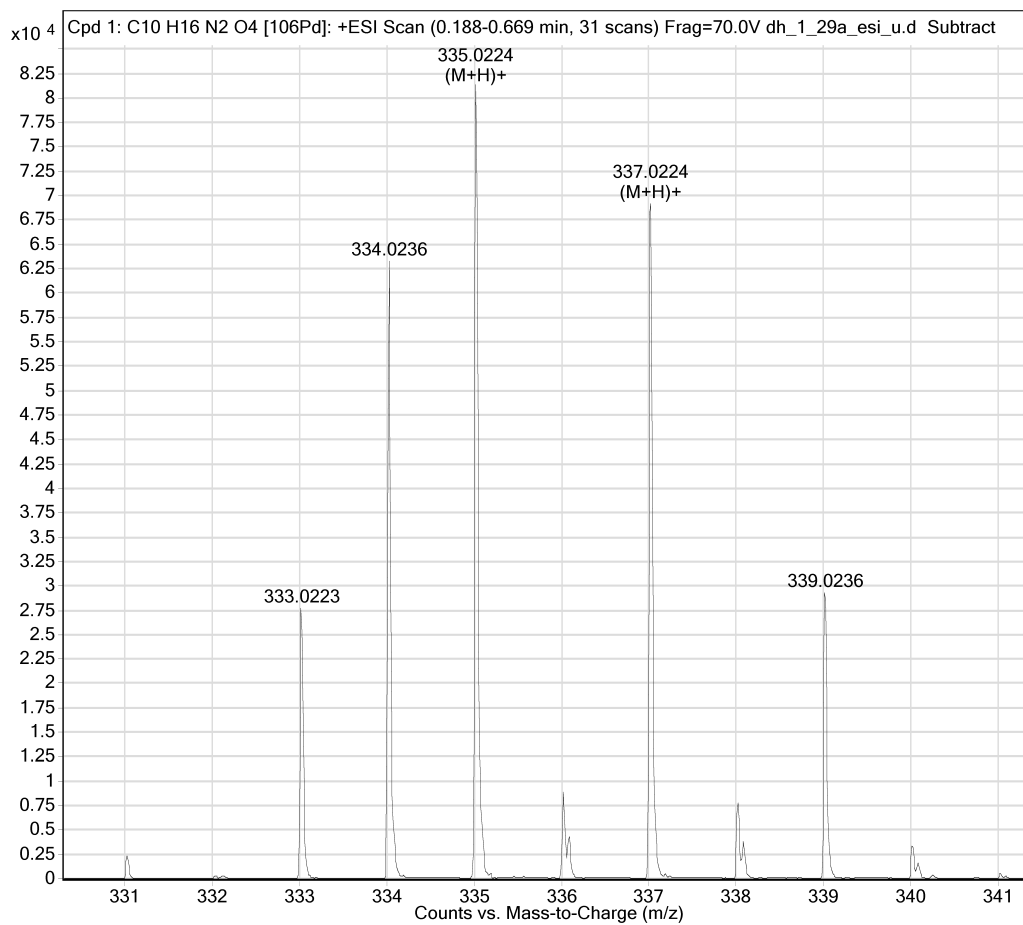
Compound 5

cis-bis(prolinato)palladium(II)

^{1}H NMR spectrum of cis-bis(prolinato)palladium(II)

^{13}C NMR spectrum of cis-bis(prolinato)palladium(II)

Cpd 1: C10 H16 N2 O4 [106Pd]: +ESI Scan (0.188-0.669 min, 31 scans) Frag=70.0V dh_1_29a_esi_u.d Subtract

x10 4

8.25
8
7.75
7.5
7.25
7
6.75
6.5
6.25
6
5.75
5.5
5.25
5
4.75
4.5
4.25
4
3.75
3.5
3.25
3
2.75
2.5
2.25
2
1.75
1.5
1.25
1
0.75
0.5
0.25
0

335.0224
(M+H)+

337.0224
(M+H)+

334.0236

339.0236

333.0223

331   332   333   334   335   336   337   338   339   340   341
Counts vs. Mass-to-Charge (m/z)

HRMS of cis-bis(prolinato)palladium(II)

Atlantic Microlab, Inc.

Sample No. mc1-01

6180 Atlantic Blvd. Suite M
Norcross, GA 30071
www.atlanticmicrolab.com

Professor/Supervisor: Merola
PO# / CC# P2343956

Company/School Virginia Tech
Dept. Chemistry
Address Hahn Hall North
City, State, Zip Blacksburg, VA 24061
Name Dave Hobart   Date 01/08/2013
Phone (540) 231-4713

Element	Theory	Found		
C	35.89	35.98		
H	4.82	4.83		
N	8.37	8.35		

Single ☒   Duplicate ☐

Elements Present: C, H, N, O, Pd

Analyze for: C, H, N

Hygroscopic ☒   Explosive ☐
M.P. _____ B.P. _____

To be dried: Yes ☒ No ☐
Temp. RT   Vac. best   Time 1 hr

Rush Service ☐ Rush service guarantees analyses will be completed and results available by 5 PM EST on the day the sample is received by 11 AM.

Include Email Address or FAX # Below

dhobart@vt.edu

Date Received   JAN 09 2013   Date Completed   JAN 10 2013

Remarks: bis-proline Pd(II)

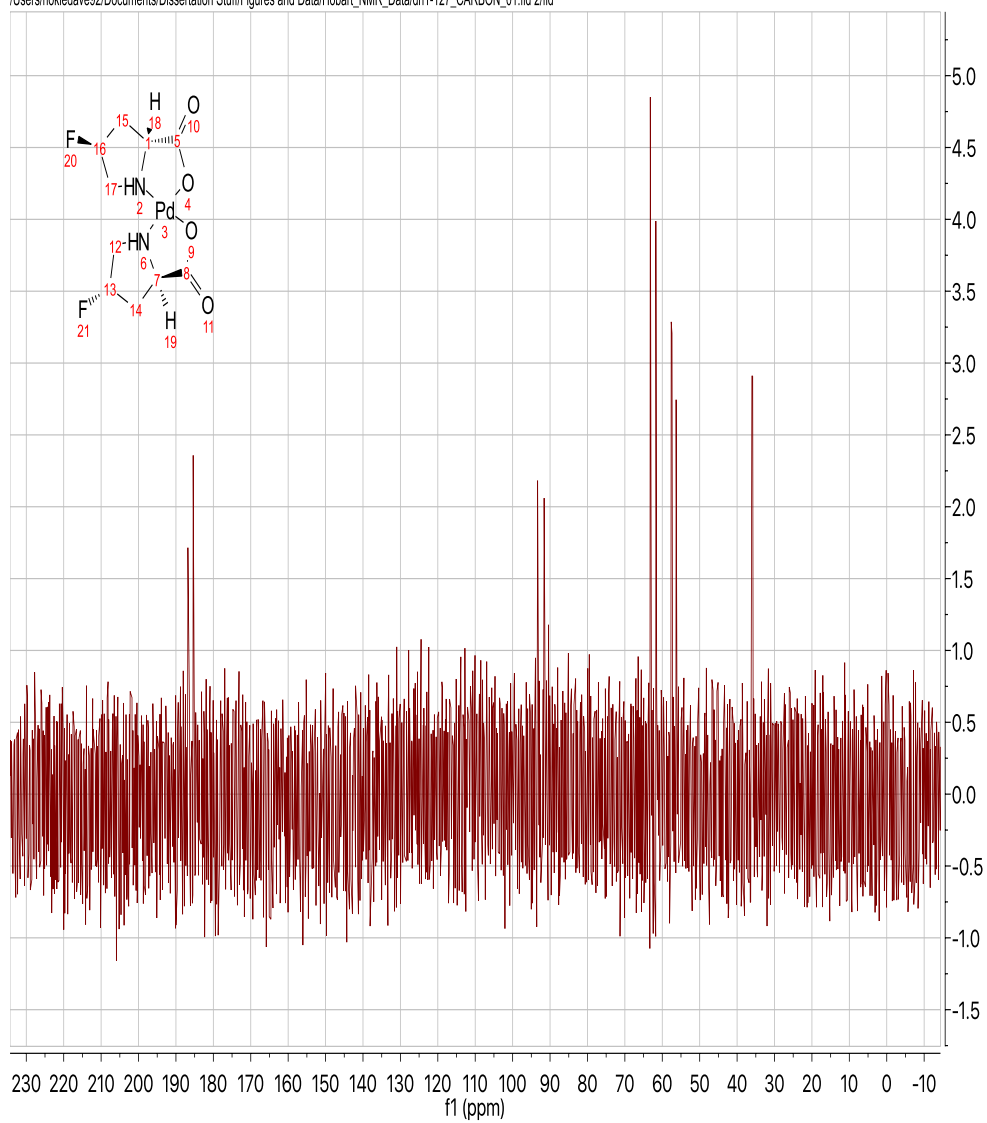Microanalysis of cis-bis(prolinato)palladium(II)

Compound 6

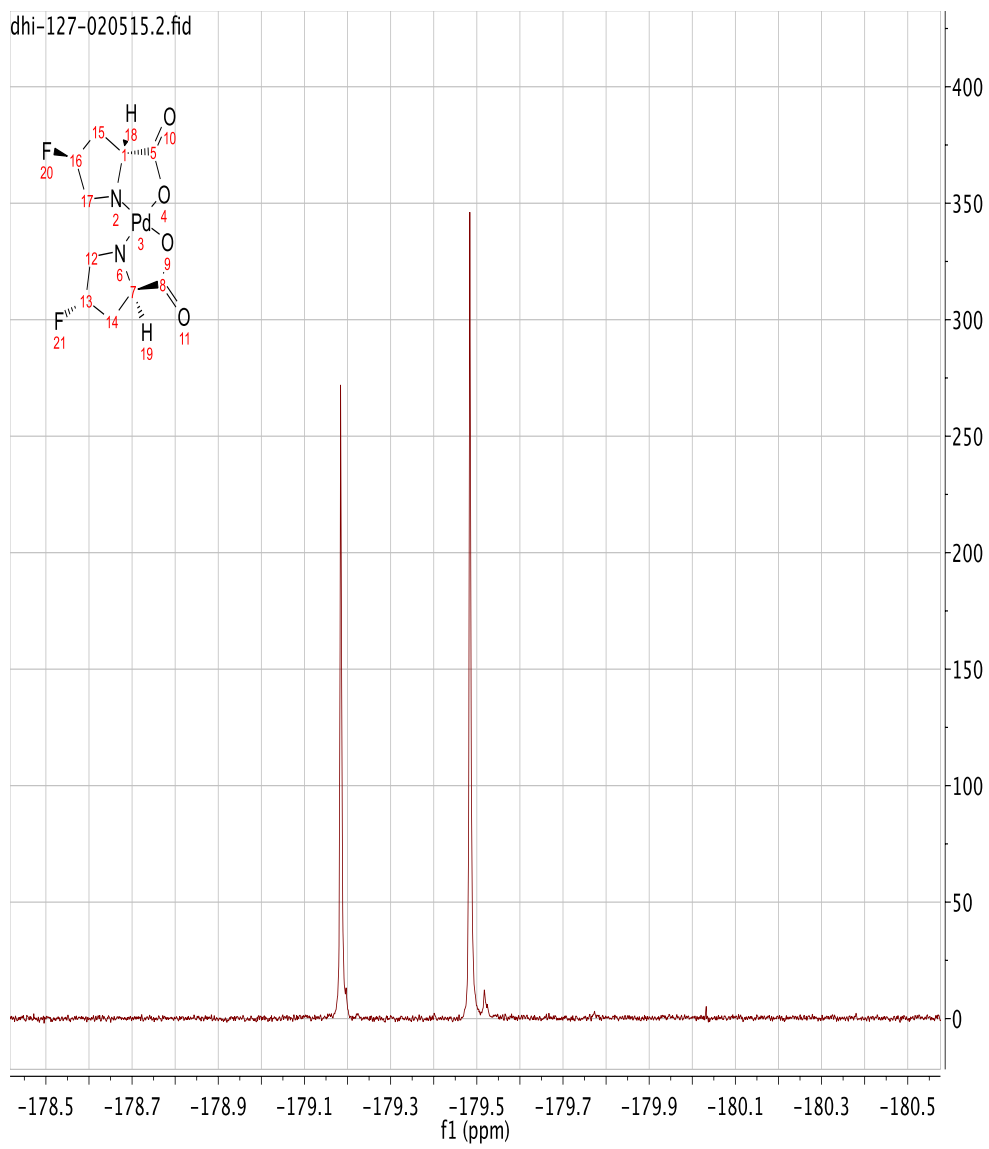*cis*-bis(*trans*-4-fluoroprolinato)palladium(II)
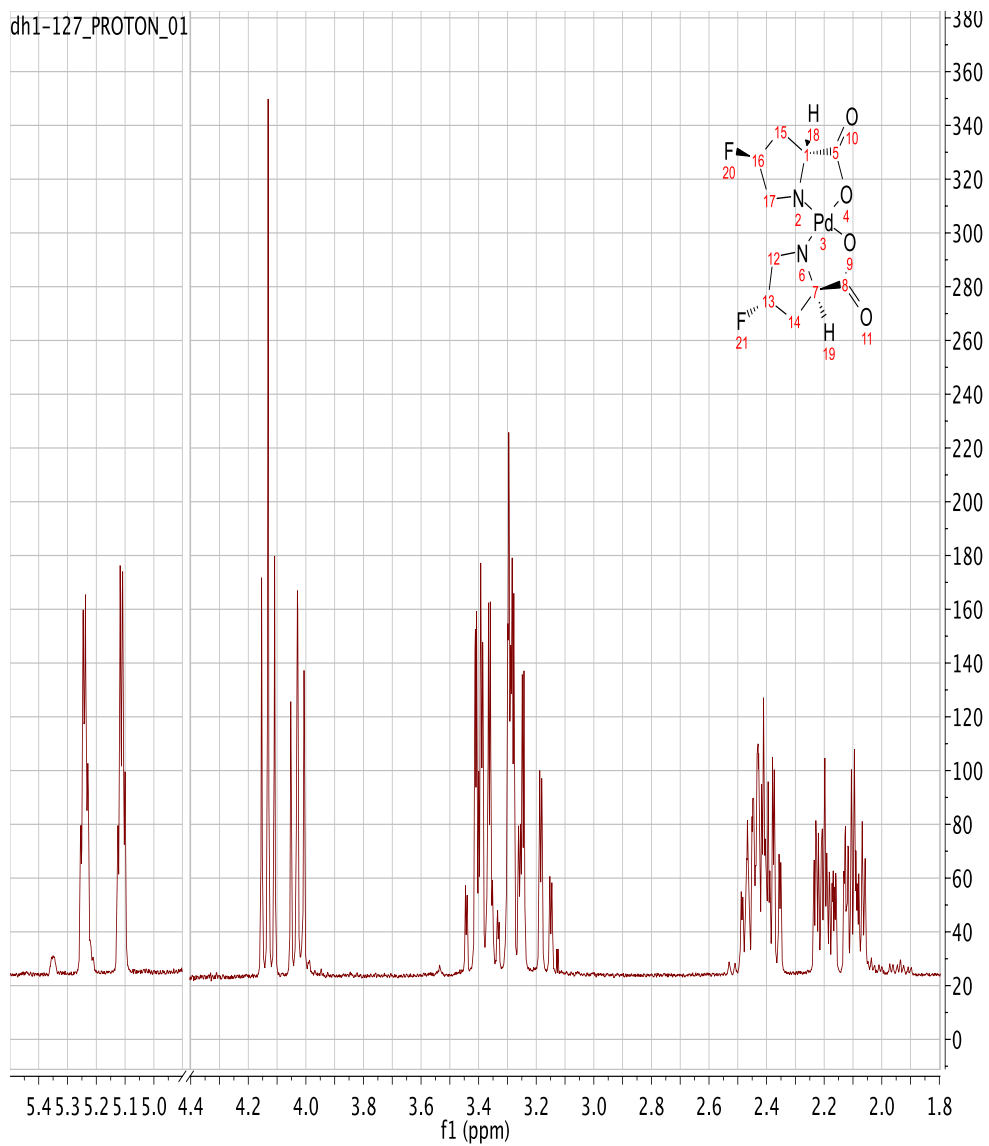
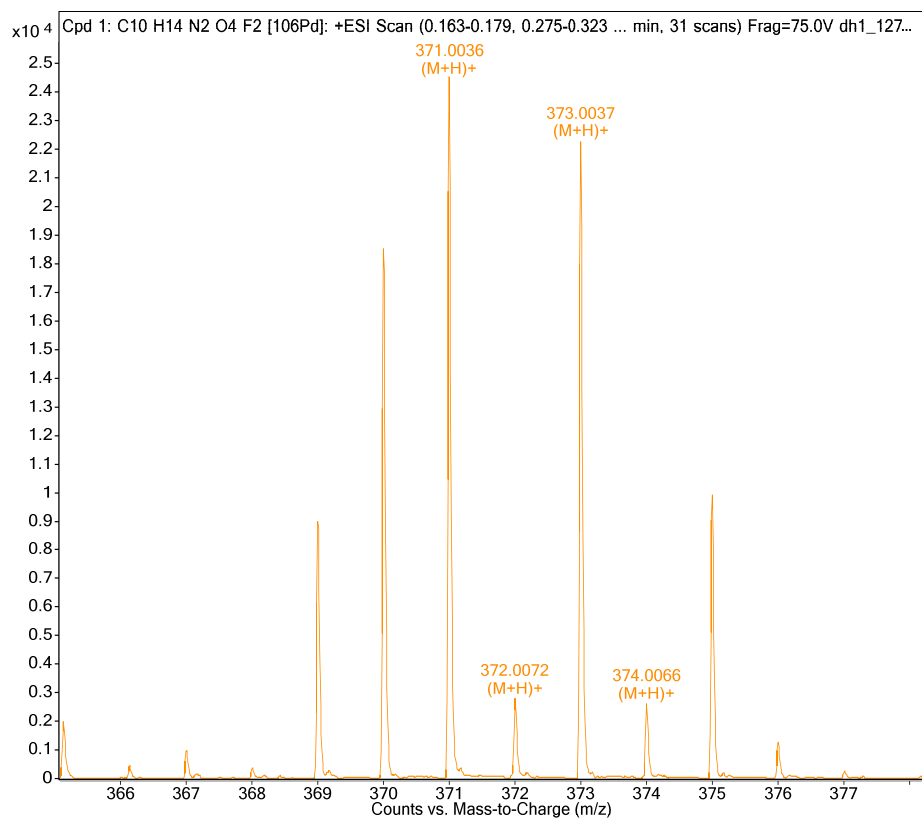^{1}H NMR spectrum of cis-bis(trans-4-fluoroprolinato)palladium(II)

^{13}C NMR spectrum of cis-bis(trans-4-fluoroprolinato)palladium(II)

^{19}F NMR spectrum of cis-bis(trans-4-fluoroprolinato)palladium(II)

Cpd 1: C10 H14 N2 O4 F2 [106Pd]: +ESI Scan (0.163-0.179, 0.275-0.323 ... min, 31 scans) Frag=75.0V dh1_127...

HRMS of cis-bis(trans-4-fluoroprolinato)palladium(II)

Atlantic Microlab, Inc.

Sample No. dh1-127

6180 Atlantic Blvd. Suite M
Norcross, GA 30071
www.atlanticmicrolab.com

Professor/Supervisor: Merola

PO# / CC#. P2343956

Company/School Virginia Tech

Dept. Chemistry

Address Hahn Hall North

City, State, Zip Blacksburg, VA 24061

Name Dave Hobart   Date 01/08/2013

Phone (540) 231-4713

Element	Theory	Found				
C	32.40	32.99	32.91	Single ☒ Duplicate ☐		
H	3.81	3.92	4.03	Elements Present: C, H, N, O, F, Pd		
N	7.56	7.53	7.53	Analyze for: C, H, N		
				Hygroscopic ☒ Explosive ☐ M.P. _____ B.P. _____		
		NO CHARGE FOR DUPLICATES		To be dried: Yes ☒ No ☐ Temp. RT Vac. best Time 1 hr		
				Rush Service ☐ Rush service guarantees analyses will be completed and results available by 5 PM EST on the day the sample is received by 11 AM.		
				Include Email Address or FAX # Below		
				dhobart@vt.edu		

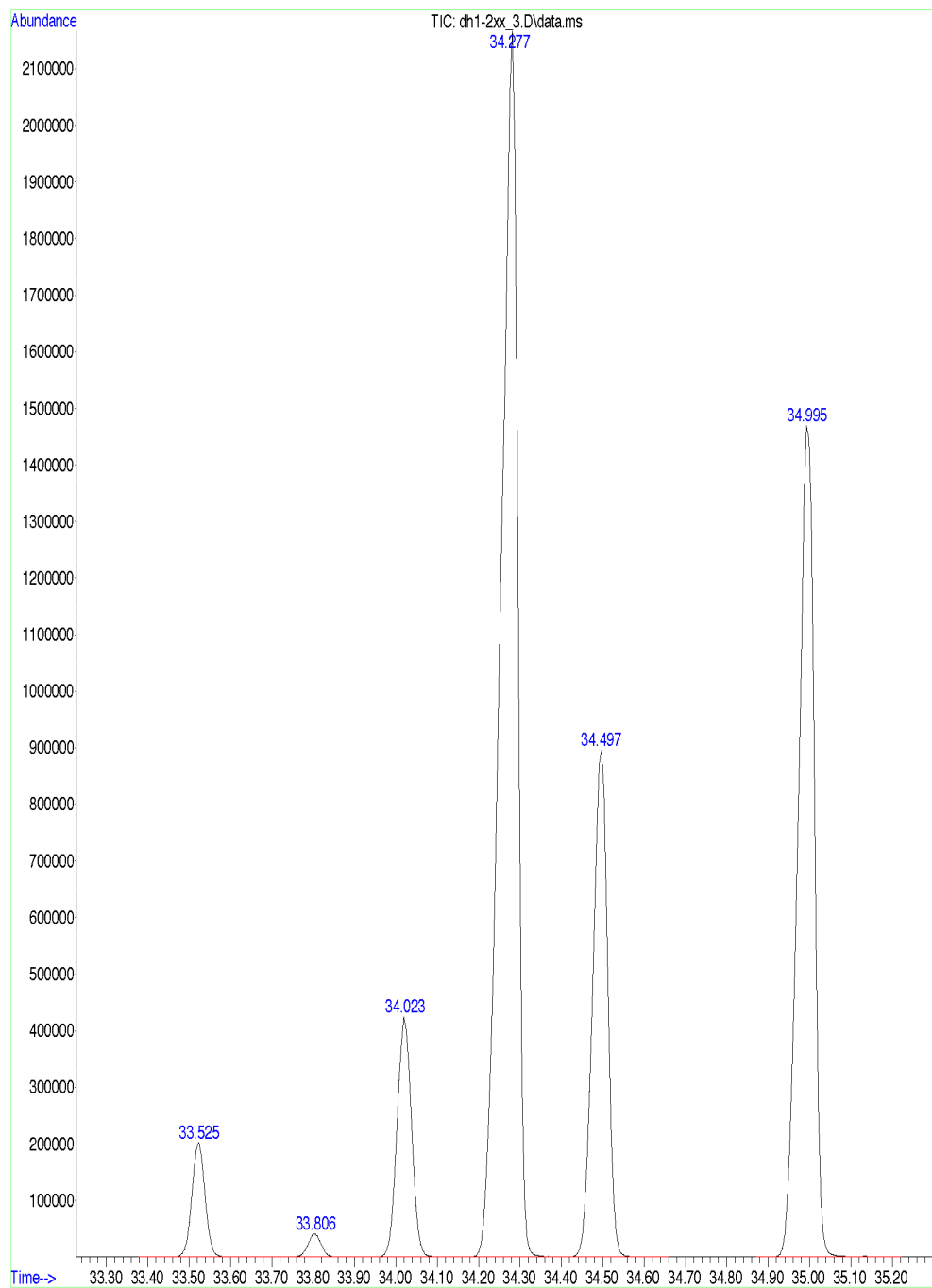Date Received   JAN 0 9 2013   Date Completed   JAN 10 2013

Remarks: bis-fluoroproline Pd(II)

Microanalysis of cis-bis(trans-4-fluoroprolinato)palladium(II)

GC Traces of the Oxidative Coupling
of Phenylboronic Acid to Methyl Tiglate
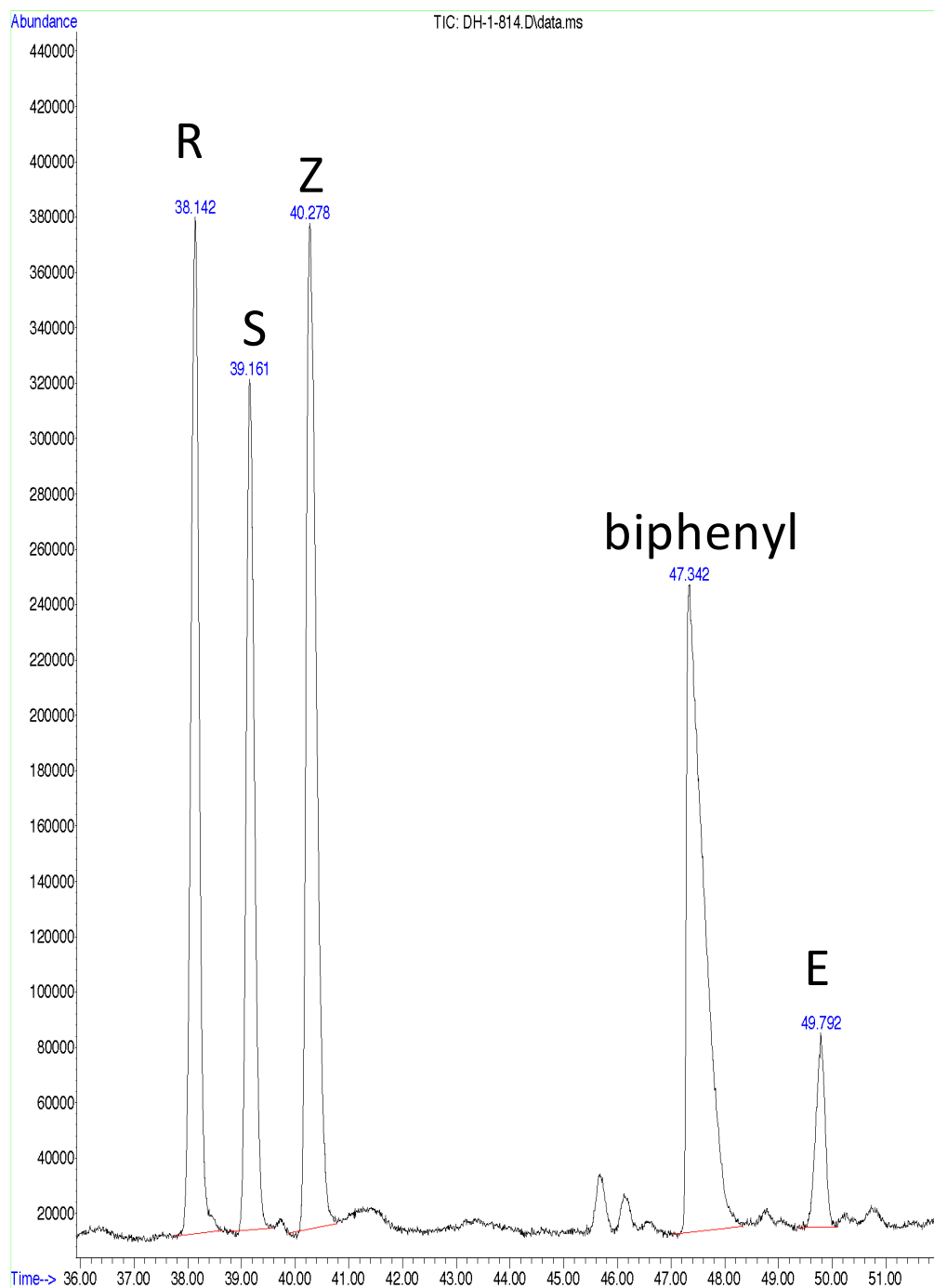
Typical GC-MS trace of the oxidative coupling of phenylboronic acid with methyl tiglate. Peaks R, S, Z, E have masses of 190.2 amu.

Typical GC-MS trace of the second oxidative coupling products of phenylboronic acid with methyl tiglate. Peaks shown have masses of 266.3 amu.
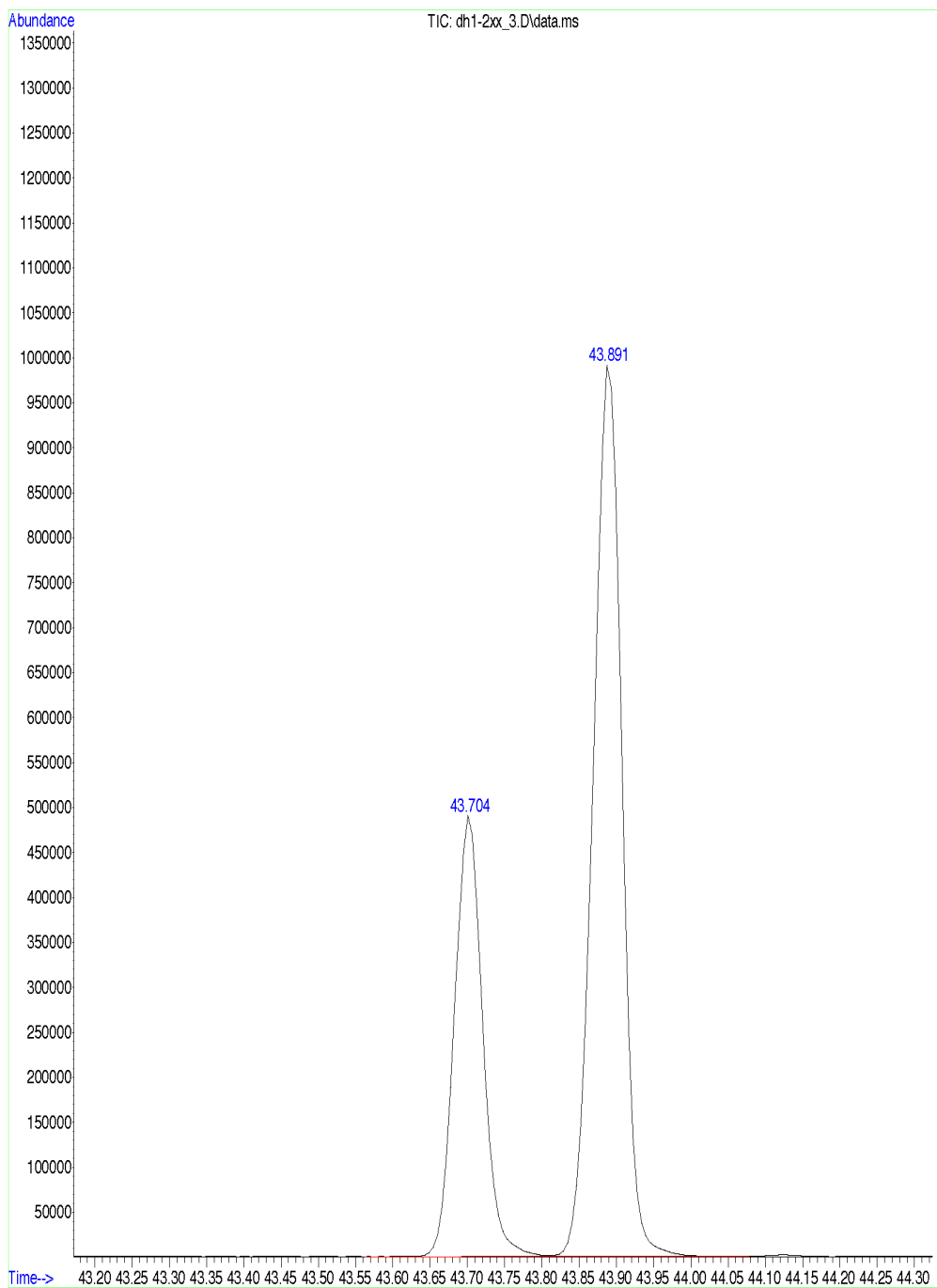
Typical GC-MS trace of the third oxidative coupling products of phenylboronic acid with methyl tiglate. Peaks shown have masses of 342.4 amu.